JOURNAL OF POLYMER SCIENCE: PART A VOL. 1, PP. 833–841 (1963)

Polymer NMR Spectroscopy. VII. The Stereochemical Configuration of Polytrifluorochloroethylene*

G. V. D. TIERS and F. A. BOVEY, *Central Research Department, Minnesota Mining & Manufacturing Company, St. Paul, Minnesota*

The structure of polytrifluorochloroethylene has not been established in detail. Kaufman[1] reported that the x-ray fiber diagram of the crystalline polymer indicates a hexagonal cell for which $a_0 = 6.5$ A. and $c_0 = 35$ A.; Ermolina et al.[2] reported the same dimensions, while Liang and Krimm[3] found a fiber repeat distance of 43 A. The very long fiber repeat distance suggests that the chains are present in the crystal as helices turning through 360° every 14–16 monomer units, the pitch of the helix possibly varying somewhat with the thermal history of the sample. It is inferred that the structure is very similar to that of polytetrafluoroethylene, which has been well established as a zigzag, the plane of which is twisted so as to give a repeat distance of 16.8 A. or 6.5 monomer units.[4] The high melting point (approx. 215°C.) and high attainable degree of crystallinity characteristic of high molecular weight polytrifluorochloroethylene would lead one to assume that its chains must have a high degree of stereochemical regularity. In this paper we present evidence, based on the high resolution NMR spectra of polytrifluorochloroethylene solutions, which strongly indicates that in fact the stereochemical configuration of the chain is very irregular, although not strictly random or "atactic."

EXPERIMENTAL

Polymer Preparation

Polymerizations of trifluorochloroethylene (Matheson Co., Inc.) were carried out in solution. Approximately 2.4 g. (1.5 ml. at −78°C.) portions of the monomer were transferred on a vacuum bench to thick-walled glass ampules containing 5 ml. of carbon tetrachloride. These ampules were then sealed under vacuum. In two ampules, 100 mg. of benzoyl peroxide was included. In these, polymerization was carried out at 50 and at 100°C. for 16 hr. Two other ampules, containing no initiator, were exposed to Co^{60} gamma radiation (0.49 Mrad in 6.5 hours) at 25°C. and at approximately −10°C. (salt–ice bath). In all cases, the polymer precipitated

* Contribution No. 221.

from solution as formed, giving a turbid appearance to the contents of the ampules. Molecular weights were not measured but were probably much lower than that of commercial polytrifluorochloroethylene (KEL-F, a product of Minnesota Mining and Manufacturing Co.). This was desirable, as the polymers were easier to dissolve; there is no reason to believe that the stereochemical configuration of the chains were thereby affected. After polymerization had occurred, the contents of the ampules were poured into methanol (approx. 100 ml.); the polymers were filtered out on fritted glass filters and dried at 50°C. *in vacuo* for 16 hr.

A further sample of polytrifluorochloroethylene was kindly supplied by Dr. R. Seffl (Commercial Chemicals Dept., Minnesota Mining & Manufacturing Co.); this was prepared in solution in a trifluorochloroethylene "trimer" having the structure $Cl(CF_2CFCl)_3Cl$ at 120°C., with the use of 2 mole-% of di-*tert*-butyl peroxide as initiator.

Sample Preparation

The polymer solutions for NMR spectral measurements were prepared by weighing 0.100 g. of polymer into the 5 mm. o.d. Pyrex NMR tubes; 0.5 ml. of solvent was then added and the tubes sealed under approximately 400 mm. of nitrogen pressure. The tubes were then heated to approximately 140°C. in a glycerine bath, with occasional shaking, until a uniform solution was obtained. In earlier work, *o*-chlorobenzotrifluoride (Hooker Electrochemical Co.) was employed as solvent, but it was later found that 3,3′-bistrifluoromethylbiphenyl[5] (prepared in this laboratory by R. I. Coon) gave spectra of improved resolution. The results discussed in this paper were obtained in this solvent.

Spectral Measurements

A Varian V-4300-2 40.00 Mcycle/sec. spectrometer equipped with a Varian heated probe, field homogeneity control unit, Hewlett Packard 522-B frequency counter, and Varian recorder was employed. The polymers were not soluble in trichlorofluoromethane (which in any case would have been difficult to handle at elevated temperatures), and therefore neither ϕ^* nor ϕ values[6] could be obtained directly. All polymer spectra were recorded at 150 ± 2°C. in order to maintain solubility and to improve the spectral resolution. The spectra of the model compounds (see below and next section) in 3,3′-bistrifluoromethylbiphenyl solution were also recorded at this temperature, as it was found that there was a marked shift of their spectral peaks with temperature. The spectral peak positions of polymer and model compounds were compared directly, the CF_3 peak of the solvent being used as an internal reference standard. Approximate ϕ^* values were arrived at by comparison with the peak position of a 10% solution of trichlorofluoromethane in 3,3′-bistrifluoromethylbiphenyl at 150°C.

The model compounds *meso*- and *dl*-$CF_2ClCFClCF_2CFClCF_2Cl$ were

prepared in this laboratory by photochemical chlorination of the olefin $CF_2ClCFClCF_2CF{=}CF_2$, in the manner already described elsewhere.[7,8]

Peak areas were evaluated by sweeping the spectrum at a rate of 4.6 cycles/sec./cm. and then measuring the areas of the component peaks with a planimeter.

EXPERIMENTAL RESULTS

In Figure 1*a* is shown the spectrum of polytrifluorochloroethylene in 3,3′-bistrifluoromethylbiphenyl at 150°C. The peak positions are expressed in parts per million (ppm) with respect to the CF_3 groups of the solvent, taken as 63.8ϕ*. The large peak at the left is that of the solvent;

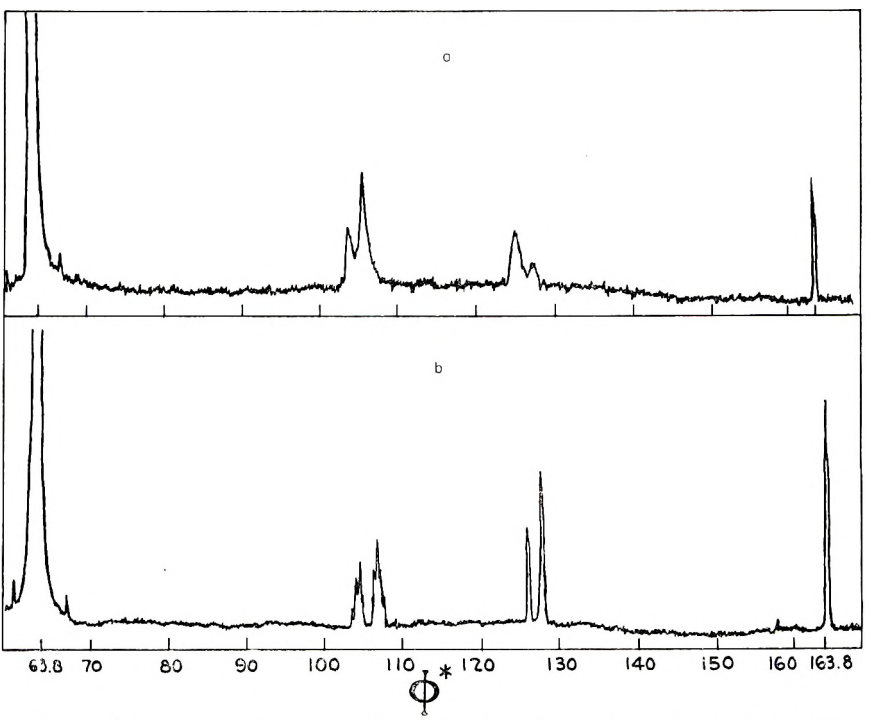

Fig. 1. NMR spectra of (*a*) polytrifluorochloroethylene, 100 mg. in 0.5 ml. of 3,3′-bistrifluoromethylbiphenyl at 150°C.; (*b*) *meso* and racemic $CF_2ClCFClCF_2CFClCF_2Cl$, 10% solution in 3,3′-bistrifluoromethylbiphenyl at 150°C.

the peak at the right is its sideband at 4000 cycles/sec. (100 ppm). The polymer spectrum consists of two "doublets" having unequal components. Those at lower field, separated by 1.8 ppm, correspond to CF_2 chain units, while those at higher field, separated by 2.2 ppm, correspond to CFCl units. The spectra for the polymers prepared at −10, 50, 100, and 120°C. are identical in appearance to Figure 1*a*. The ratio of the two components of the CF_2 resonance is 1:2 within experimental error (approximately ±5% of the ratio) for all polymers, and is thus inde-

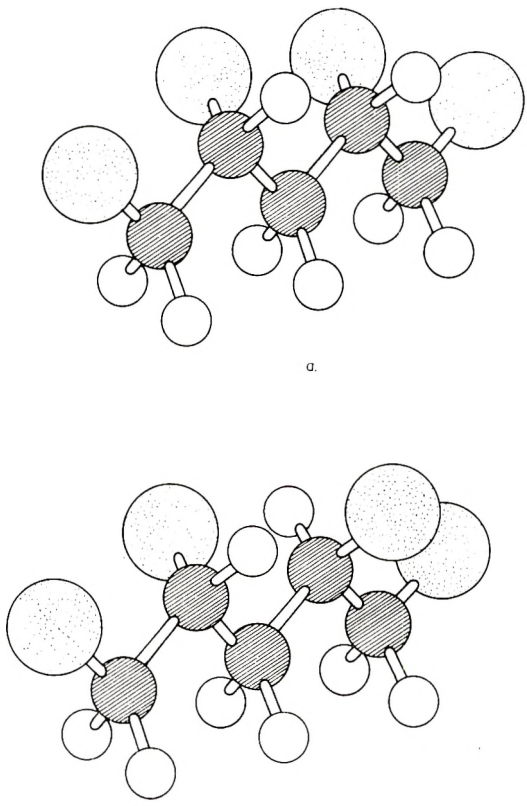

Fig. 2. $CF_2ClCFClCF_2CFClCF_2Cl$ (*a*) *meso* isomer; (*b*) racemic isomer

pendent of the temperature of polymerization. The ratio of the two components of the CFCl resonance also appears to be temperature-independent, but this conclusion is less certain because of the uncertainty in the measurement of these smaller peak areas.

In order to shed further light on this result, the spectra of the model compounds *meso*- and *dl*-$CF_2ClCFClCF_2CFClCF_2Cl$ were obtained. When chlorine is added to the double bond of the *dl*-olefin $CF_2ClCFClCF_2$-$CF{=}CF_2$, the *dl* (racemic) and *meso* pentanes are obtained in nearly equal amounts.[8] The spectrum of the mixture as a 10% solution in 3,3′-bistrifluoromethylbiphenyl at 150°C. is shown in Figure 1*b*. This spectrum includes only the resonances of the CF_2 and CFCl groups; the CF_2Cl end groups appear as a triplet at lower field, and are not included because there is no corresponding resonance in the polymer spectrum. In Figure 2 are shown pictorial representations of the *meso* and racemic pentanes in planar zigzag form, in order to make clear the relationship of the models to possible chain structures. It will be seen that, as pointed out previously,[9] the *meso* form corresponds to the isotactic polymer configuration, whereas the racemic form corresponds to the syndiotactic configuration. In the

racemic isomer, the two central fluorine atoms are geometrically and magnetically identical; they therefore do not split each other's resonance, but are each coupled identically to the four terminal fluorine atoms and to the two nearest neighboring fluorine atoms. The former coupling is much stronger (17.3 cycles/sec.) than the latter (3–5 cycles/sec. est.), and in the expanded spectrum (obtained with a 50% CCl_3F solution of the isomers at 25°C.), the racemic CF_2 resonance appears as a clear quintuplet, and can thus be identified. It appears as the peak at higher field of the two CF_2 peaks in Figure 1*b*, but the resolution here is only barely adequate to show the quintuplet structure. In the *meso* isomer, the two central fluorine atoms are nonidentical and split each other to an AB-type quartet.[8–13] In the present case, the coupling of the fluorine nuclei (J_{AB} is probably about 280 cycles/sec.[13]) is substantially greater than their chemical shift difference, and so the central peaks of the quartet appear closely spaced (16.0 cycles/sec. separation in CCl_3F at 25°C.), and the outer peaks are so weak that they cannot be seen.[7] There is again a quintuplet multiplicity associated with each of the central peaks of the AB pattern, and therefore the resonance is complex. It appears (poorly resolved) as the lower of the two CF_2 resonance regions in Figure 1*b*. From the analysis of the spectrum it is found[8] that one of the two central fluorine atoms is coupled to the neighboring fluorine nuclei with a J of 3.4 cycles/sec. and to the terminal fluorine nuclei with a J of 14.3 cycles/sec.; for the other central fluorine, the corresponding couplings are 5.1 and 17.1 cycles/sec., respectively.

The CFCl peaks, which appear as singlets in Figure 1*b*, are found to be complex, closely spaced multiplets when examined under high resolution.[8] They have not been fully analyzed. Comparison of peak areas in the spectra of *dl–meso* mixtures which had been partially fractionated by vapor-phase chromatography showed that the peak at higher field is that of the *meso* isomer, and is thus associated with the CF_2 peak at lowest field. This assignment was confirmed by spin decoupling studies.[8]

The assumption that the polymer spectra and structure correspond to those of the model compounds rests essentially on the approximate correspondence of peak positions. As indicated in the Experimental section, it is important that the spectra be compared at approximately the same temperature, as there is a marked dependence of the peak positions upon temperature. For the polymer at 150°C., the peak positions, in ϕ^* values with respect to the solvent as $+63.8\phi^*$, are: 104.2, 106.0, 125.6, and 127.8. At 25°C., the solvent peak position was found to be $+63.2\phi^*$, and the model compound peak positions were: 106.3, 108.8, 126.6, and 128.9, deviating substantially from the polymer positions. When the model compound spectra are observed at 150°C., there is a marked "down-field" shift, which brings the ϕ^* values into much closer correspondence with those of the polymer: 104.1, 106.2, 126.2, and 127.7. There appear to be some small relative changes as well, particularly for the *meso* compound, for the appearance of its AB-type CF_2 resonance is distinctly temperature-dependent. The most likely explanation for this behavior is that it arises from

changes in the relative populations of the internal-rotation energy levels, which correspond to changes in the time-averaged conformational structures of the molecules.

DISCUSSION

Comparison with the model spectra strongly suggests that in the CF_2 resonance region of the polymer spectrum, the peak at $104.2\phi^*$ represents CF_2 groups which are between monomer units in isotactic dyads, i.e., *dd* or *ll*, whereas the peak at $106.0\phi^*$ represents those CF_2 groups which are located between *dl* or *ld* configurations, i.e., in syndiotactic dyads. As before,[9] we designate the fraction of (or probability of forming) CF_2 groups which are located between *dl* or *ld* configurations as the fraction P_r of racemic units; the fraction lying between *dd* or *ll* units, i.e., the probability of forming *meso* CF_2 units, we shall designate as P_m. If the propagation is governed by a single value of σ, the probability of isotactic monomer placement,[9] then:

$$P_m = \sigma = P_i^{1/2}$$

and

$$P_r = 1 - \sigma = P_s^{1/2}$$

where P_i and P_s are as before[9] the probabilities of occurrence of isotactic and syndiotactic monomer triads, respectively. For an "atactic" or random chain, $P_m = P_r$, and the CF_2 peaks should be of equal area. We have seen that in fact P_m/P_r is not unity but is approximately 0.50 and is independent of the polymerization temperature. From this it follows that the difference in enthalpies of activation for isotactic propagation,

$$\Delta H_i^{\ddagger} - \Delta H_s^{\ddagger} = \Delta(\Delta H_p^{\ddagger}) = 0$$

within experimental error. For the difference in entropies of activation

$$\begin{aligned} \Delta S_i^{\ddagger} - \Delta S_s^{\ddagger} &= \Delta(\Delta S_p^{\ddagger}) \\ &= R\ln(k_i/k_s) + \Delta(\Delta H_p^{\ddagger})/T \\ &= R\ln P_m/P_r = -1.38 \text{ e.u.} \end{aligned}$$

k_i and k_s being the rate constants for isotactic and syndiotactic propagation, respectively. These findings are in marked contrast to those for polymethyl methacrylate;[14] for polymethyl methacrylate it is found that isotactic propagation requires about 775 cal. greater enthalpy of activation than syndiotactic propagation, but that there is no difference in the entropies of activation. Evidently, in trifluorochloroethylene propagation, a preference for syndiotactic placement is dictated entirely by steric hindrance, whereas in methyl methacrylate propagation steric hindrance plays little or no role, the preference for syndiotactic placement probably being due primarily to interaction of polar groups.

If trifluorochloroethylene propagation is indeed governed by a single σ, then, regardless of temperature:

$$P_i = 0.11$$
$$P_h = 0.45$$
$$P_s = 0.44$$

P_h being the probability of occurrence of a heterotactic[9] triad of monomer units. If the resonance in the CFCl region were analogous to that in the α-methyl region of the polymethyl methacrylate spectrum, one would expect to see two nearly equal peaks for h and s triads together with a much smaller one for i triads. In fact, only two peaks can be observed. From the assignments deduced for the model compounds, the smaller of these peaks (having approximately $^1/_5$ the area of the other peak) would be attributed to CFCl groups of monomer units in isotactic configurations. The larger peak must then represent an (unresolved) combination of the CFCl resonances for the central monomer units in h and s triads. However, the model compounds are probably less reliable as a basis for assignment of the CFCl resonances than for the assignment of the CF_2 resonances, and so no definite conclusion can be drawn as yet. If, in fact, the propagation cannot be described by a single σ, the calculated values of P_r and P_m are still valid, but the calculated value of $\Delta(\Delta S_p^{\ddagger})$ can be only approximate.

One may speculate that the multiple CF_2 and CFCl resonances may arise from the occurrence of some head-to-head as well as head-to-tail monomer units. Naylor and Lasoski[15] have interpreted the NMR spectrum of polyvinylidene fluoride as indicating the presence of about 10% of head-to-head units. It is difficult to believe, however, that head-to-head units could occur in polytrifluorochloroethylene with the frequency which this explanation would demand. Such an explanation would also require the assumption that the polytrifluorochloroethylene chain is nearly completely either isotactic or syndiotactic, for otherwise a large multiplicity of peaks arising from chain irregularity would be expected to appear, and the polymer spectrum would be more complex than is observed. There is no question as to the correct interpretation of the CF_2 resonance in the racemic and *meso* model compounds, and we believe that a corresponding interpretation of the polymer spectrum is by far the more plausible. However, a study of head-to-head model compounds would be required to establish this point with certainty.

Polytrifluorochloroethylene appears to be one of that very limited group of vinyl polymers which are capable of readily crystallizing despite a high degree of stereochemical irregularity. This is probably to be attributed chiefly to the relatively great stiffness of its chains. Polyvinyl alcohol appears to be another example.[16] Polyvinyl chloride is crystallizable if prepared at very low temperature, and is then largely syndiotactic,[17,18] but as normally prepared it crystallizes only with difficulty and is probably much more nearly random. It is, of course, conceivable that isotactic and syndiotactic polytrifluorochloroethylene chains are formed side by side,

and that therefore the polymer is more regular than the NMR spectrum indicates. But it seems extremely unlikely that the polymerization could take this course in the solution system employed, even though the polymer precipitates in the course of the reaction, and the system is therefore not strictly homogeneous.

Note added in proof: We have since shown[19] that low-temperature polyvinyl chloride is *not* syndiotactics but instead is largely random.

We are indebted to Dr. Raymond Seffl and Mr. Samuel Smith for samples and for valuable discussions, to Mr. R. B. Calkins for the careful operation of the NMR spectrometer and to Mrs. Katherine LaCroix for the preparation of polymers and sample tubes.

References

1. Kaufman, H. S., *J. Am. Chem. Soc.*, **75**, 1477 (1953).
2. Ermolina, A. V., G. S. Markova, and V. A. Kargin, *Kristallografiya*, **2**, 623 (1957).
3. Liang, C. Y., and S. Krimm, *J. Chem. Phys.*, **25**, 563 (1956).
4. Bunn, C. W., and E. R. Howells, *Nature*, **174**, 549 (1954).
5. Pettit, M. R., and J. C. Tatlow, *J. Chem. Soc.*, **1954**, 1071.
6. Filipovich, G., and G. V. D. Tiers, *J. Phys. Chem.*, **63**, 761 (1959).
7. Miller, W. T., Jr., W. Frass, and P. R. Resnick, *J. Am. Chem. Soc.*, **83**, 1767 (1961).
8. Tiers, G. V. D., to be submitted.
9. Bovey, F. A., and G. V. D. Tiers, *J. Polymer Sci.*, **44**, 173 (1960).
10. Hahn, E. L., and D. E. Maxwell, *Phys. Rev.*, **88**, 1070 (1952).
11. Pople, J. A., W. G. Schneider, and H. J. Bernstein, *High Resolution Nuclear Magnetic Resonance*, McGraw-Hill, New York, 1959, pp. 119–123, p. 292.
12. Wiberg, K. B., and H. W. Holmquist, *J. Org. Chem.*, **24**, 578 (1959).
13. Tiers, G. V. D., *Proc. Chem. Soc.*, **1960**, 389.
14. Bovey, F. A., *J. Polymer Sci.*, **46**, 59 (1960).
15. Naylor, R. E., and S. W. Lasoski, Jr., *J. Polymer Sci.*, **44**, 1 (1960).
16. Bunn, C. W., *Nature*, **161**, 929 (1948).
17. Krimm, S., A. R. Berens, V. L. Folt and J. J. Shipman, *Chem. & Ind. (London)*, **1958**, 433, 1512.
18. Grisenthwaite, R. J., and R. F. Hunter, *Chem. & Ind. (London)*, **1958**, 719.
19. Bovey, F. A., and G. V. D. Tiers, *Chem. & Ind. (London)*, **1962**. 1826.

Synopsis

The NMR spectrum of polytrifluorochloroethylene in 3,3′-bistrifluoromethylbiphenyl solution at 150°C. consists of two doublets having unequal components. Those at lower field correspond to CF_2 chain units, while those at higher field correspond to CFCl units. In the CF_2 doublet, the weaker component (at lower field) is found to have half the area of the stronger (at higher field), for polymers prepared over a 120°C. range of polymerization temperatures. By comparison to the spectra of the model compounds *meso*- and *dl*-$CF_2ClCFClCF_2CFClCF_2Cl$, the peaks of which closely coincide with those of the polymer when both are compared at 150°C., it is concluded that of the two CF_2 peaks in the polymer spectrum, the weaker one represents CF_2 groups which are between monomer units in isotactic dyads whereas the stronger one represents CF_2 groups which are between monomer units in syndiotactic dyads. It follows that in trifluorochloroethylene propagation, syndiotactic dyad formation is twice as probable as isotactic dyad formation. This preference for syndiotactic placement corresponds to an activation entropy for isotactic propagation 1.38 e.u. more negative than that for syndiotactic propagation; there is no difference in the activation enthalpies. This behavior is in

contrast to that previously found for methyl methacrylate propagation; here, preference for syndiotactic placement is entirely dictated by a greater activation enthalpy for isotactic placement.

Résumé

Le spectre de résonance magnétique nucléaire du polytrifluorochloroéthylène en solution dans le 3,3′ bis-trifluorométhylbiphényle à 150° est constitué de deux "doublets" ayant des composantes inégales. Ceux à champ plus faible correspondent aux unités de chaîne CF_2, tandis que ceux à champ plus élevé correspondent aux unités CFCl. On a constaté que la composante plus faible (à champ plus faible) dans le "doublet" de CF_2 a une surface deux fois plus petite que la composante plus forte (à champ plus élevé) pour les polymères préparés au-dessus de 120° comme température de polymérisation. En comparant les spectres des composés de référence *méso* et *dl*-$CF_2ClCFCl$-$CF_2CFClCF_2Cl$, dont les pics coïncident étroitement avec ceux du polymère si tous les deux sont comparés à 150°, on peut conclure que des deux pics de CF_2 obtenus dans le spectre de polymère, le pic le plus faible représente les groupes CF_2, qui sont entre les unités monomériques dans les diades isotactiques, tandis que les pics plus forts représentent les groupes CF_2 qui se trouvent entre les unités monomériques dans les diades syndiotactiques. Par conséquent, lors de la propagation du trifluorochloroéthylène la probabilité de formation de diades syndiotactiques est deux fois plus grande que celle de diades isotactiques. Cette préférence pour l'arrangement syndiotactique correspond à une entropie d'activation pour la propagation isotactique de 1.38 e.u. plus négative que celle de la propagtion syndiotactique; il n'y a pas de différence dans les enthalpies d'activation. Ce comportement est en contraste avec celui trouvée préalablement pour la propagation du méthacrylate de méthyle; ici la préférence pour l'arrangement syndiotactique est gouverné entièrement par une plus grande enthalpie d'activation pour l'arrangement isotactique.

Zusammenfassung

Das NMR-Spektrum von Polytrifluorchloräthylen in 3,3′-Bis-trifluoromethylbiphenyllösung bei 150°C besteht aus zwei "Dubletts" mit ungleichen Komponenten. Diejenigen bei niedrigerem Feld entsprechen den CF_2-Kettenbausteinen, während diejenigen bei höherem Feld den CFCl-Bausteinen entsprechen. Bei Polymeren, die in einem Polymerisationstemperaturbereich von 120° hergestellt wurden, besitzt die schwächere Komponente (bei niedrigerem Feld) im CF_2-Dublett den halben Flächeninhalt der stärkeren (bei höherem Feld). Durch Vergleich mit den Spektren der Modellverbindungen *meso*- und *d,l*-$CF_2ClCFClCF_2CFClCF_2Cl$, deren Maxima bei einem Vergleich bei 150° eng mit denen des Polymeren zusammenfallen, kommt man zu dem Schluss, dass von den beiden CF_2-Maxima im Polymerspektrum das schwächere von CF_2-Gruppen zwischen Monomerbausteinen in isotaktischen Dyaden herrührt, während das stärkere CF_2-Gruppen zwischen Monomereinheiten in syndiotaktischen Dyaden repräsentiert. Daraus folgt, dass beim Wachstum von Trifluorchloräthylen die Bildung syndiotaktischer Dyaden doppelt so wahrscheinlich als die Bildung isotaktischer Dyaden ist. Die Bevorzugung der syndiotaktischen Anordnung entspricht einer um 1,38 cal/grad stärker negativen Aktivierungsentropie für das isotaktische Wachstum als für das syndiotaktische Wachstum; bei den Aktivierungsenthalpien besteht kein Unterschied. Dieses Verhalten steht im Gegensatz zu dem früher beim Methylmethacrylatwachstum festgestellten; hier ist die Bevorzugung der syndiotaktischen Anordnung zur Gänze durch eine grössere Aktivierungsenthalpie für die isotaktische Anordnung bedingt.

Received November 6, 1961

JOURNAL OF POLYMER SCIENCE: PART A VOL. 1, PP. 843–848 (1963)

Polymer NMR Spectroscopy. VIII. The Influence of the pH of the Polymerization Medium on the Stereochemical Configuration of Polymethacrylic Acid

F. A. BOVEY,* *Central Research Department, Minnesota Mining & Manufacturing Company, St. Paul, Minnesota*

Katchalsky and Blauer reported[1] that the rate of polymerization of methacrylic acid in aqueous solution at 75°C., initiated by hydrogen peroxide, decreases with increasing pH, becoming virtually zero at pH 5.5. The pK_a of the monomer was reported to be 4.36, and it would therefore be over 90% dissociated at pH 5.5; they concluded that the rate of polymerization is proportional to the concentration of undissociated monomer and that the methacrylate anion does not undergo polymerization. Pinner[2] found, however, that when potassium persulfate is employed as initiator, polymerization occurs at pH values as high as 13.0. Blauer[3] observed that with 2,2′-bisazoisobutyronitrile as initiator, the rate at pH 6–7 was only about $^1/_{10}$ of that at pH 4, but that it then increased somewhat at pH 8–11 and finally decreased once more at pH values above 12. It appears that the result obtained by Katchalsky and Blauer may have been due to failure of the initiating system at higher pH. It appears possible that the monomer and hydrogen peroxide may have reacted, and that the initiating efficiency of the resulting permethacrylic acid became nearly nil above pH 5.5 as a result of dissociation. The pH of half-dissociation of polymethacrylic acid depends strongly on its concentration, being about 6.3 at a base molar concentration of 0.1M.[4] (The apparent pK_a is near this value, but because the electrostatic work function is appreciable and varies with pH, an exact assignment of pK_a cannot be made. The apparent pK_a of the polymer depends on its stereochemical configuration, isotactic polymer being about 0.3 unit weaker than "atactic"—probably actually predominantly syndiotactic—polymer.[5]) In the pH range above 7.5–8.0, both the growing chain and the monomer are nearly completely ionized. Coulombic repulsions may be expected to retard both the propagation and termination steps, and therefore to have opposing effects on the polymerization rate. Blauer's results indicate that the ionized monomer propagates the reaction much more slowly than the unionized form even when attacked by growing chain radicals which are substantially undissociated. Above pH 8, the retardation of termination becomes important, and the polymerization rate increases.

* Present address: Bell Telephone Laboratories, Inc., Murray Hill, N. J.

The degree of dissociation of the monomer and polymer might be expected to have a significant effect on the stereochemical configuration of the growing chain. The terminal monomer unit at the growing end of a polymer radical is probably unable to maintain asymmetry, as we have indicated previously;[6] when reaction occurs with a monomer molecule, this terminal monomer unit must decide whether to assume an isotactic or syndiotactic configuration with respect to the penultimate monomer unit. In methyl methacrylate polymerization, syndiotactic addition tends to be favored, because the assumption of the isotactic configuration requires approximately 800 cal. greater activation enthalpy.[7] It appears reasonable to suppose that when both the monomer and the growing polymer radical are negatively charged, as in methacrylic acid polymerization at high pH, coulombic repulsion will tend to favor one mode of addition over the other. In this paper, it is shown that under these conditions syndiotactic addition is favored to a greater extent than in methacrylic acid polymerization at low pH or in methyl methacrylate polymerization.

EXPERIMENTAL

Polymer Preparation

Solutions of 5 g. of methacrylic acid (m.p. 16°C., Monomer-Polymer Laboratories, Inc., Philadelphia, Pa.) were prepared in 20 ml. portions of deionized water containing 250 mg. of potassium persulfate as initiator and 50 mg. of sodium mercaptoacetate to control the molecular weight of the polymer and prevent the formation of gels during polymerization and excessive solution viscosities in the NMR measurements. The pH of a methacrylic acid solution of this concentration (approx. 2.3*M*) is 2.0. Higher pH values were obtained by addition of sodium hydroxide. Measurements of pH were carried out at 25°C. with a Radiometer TTT1A pH meter. Polymerizations were carried out in ampules at 50°C. for periods ranging from 1 hr. at pH 2 to 48 hr. at the higher pH values. Polymer yields varied from nearly quantitative at lower pH values to 50% or less at pH 6 and above. The ampules were swept with prepurified nitrogen before sealing, but considerable induction periods were observed in several cases.

The polymers were precipitated in acetone, and dried *in vacuo* for 16 hr. at 75°C. All polymers, with the exception of that prepared at pH 2, were then redissolved to form approximately 5% solutions in deionized water, acidified to pH 2 with HCl, dialyzed for 16 hr. against water with the use of Visking $^5/_8$ in. diameter cellulose sausage casing, and finally recovered and dried by lyophilization. They were then methylated with diazomethane by the method of Katchalsky and Eisenberg.[8]

Titrations of methacrylic acid and polymethacrylic acid were carried out with the Radiometer TTT1A pH meter in conjunction with a Radiometer SBR 2b Titrigraph.

Spectral Measurements

The polymethyl methacrylate samples resulting from the above procedures were dissolved in chloroform (Matheson, Coleman, and Bell Spectroquality grade), a concentration of 100 mg. of polymer in 0.5 ml. of solvent being employed. The solvent contained 2% of tetramethylsilane as internal reference standard,[9] although peak positions were not required and are not reported in this paper. A Varian V-4300-2 40 Mcycle/sec. spectrometer equipped with a Varian heated probe, Varian field homogeneity control unit, Hewlett Packard 522-B frequency counter, and Varian recorder was employed. Spectra were obtained at a temperature of 90 ± 1°C. The relative areas of the three peaks at 8.78τ, 8.95τ, and 9.09τ, corresponding to the α-methyl protons of central monomer units in isotactic, heterotactic, and syndiotactic triads, were measured as previously described.[6] The measured values of i, h, and s, the relative proportions of isotactic, heterotactic, and syndiotactic monomer triads, were reproducible within ±0.007–0.008.

EXPERIMENTAL RESULTS AND DISSCUSION

It is assumed that the free-radical polymerization of methacrylic acid is governed by a single value of σ when only one species of polymer radical and only one species of monomer are present, as at low or high pH. If this is the case, then the probability of formation of a syndiotactic triad of monomer units along the chain is given by:[6]

$$P_s = (1 - \sigma)^2$$

From the observed proportion of such triads, s, estimated by measuring the ratio of the area of the 9.09τ peak to the total area of the α-CH_3 resonance, we can calculate k_i/k_s, the apparent ratio of the rate of isotactic propagation to the rate of syndiotactic propagation:

$$k_i/k_s = \sigma/(1 - \sigma) = s^{-1/2} - 1$$

In Figure 1, k_i/k_s is plotted as a function of the initial pH of the polymerization medium. (Since the polymer is a considerably weaker acid than the monomer, there is an appreciable increase in pH during polymerization; this may be as much as 1 pH unit in the region 6–7, but decreases at higher and lower pH values. Because conversion to polymer is incomplete above pH 5, this effect is not large; but nevertheless the "average" pH during the reaction is perhaps as much as 0.5 unit higher than the initial value in the middle range of pH.) It can be seen that with increasing pH, there is a distinct tendency to favor the syndiotactic mode of propagation; k_i/k_s is nearly twice as great when uncharged polymer radicals and uncharged monomer react as when both are negatively charged. The difference between the free energies of activation for isotactic and syndiotactic propagation, $\Delta F_i‡ - \Delta F_s‡$, calculated from k_i/k_s, is approximately 0.9 kcal. at pH 2.0 and 1.3 kcal. at pH 10.0. It appears reasonable to interpret

the additional 0.4 kcal. free energy requirement at high pH as arising from a greater coulombic repulsion in the activated state for isotactic placement than in the activated state for syndiotactic placement. The ionic strength of the polymerization medium is very high (of the order of 2) at high pH; it would therefore appear that an even more marked effect of pH on k_i/k_s could be expected in media of lower dielectric constant and decreased ionic strength.

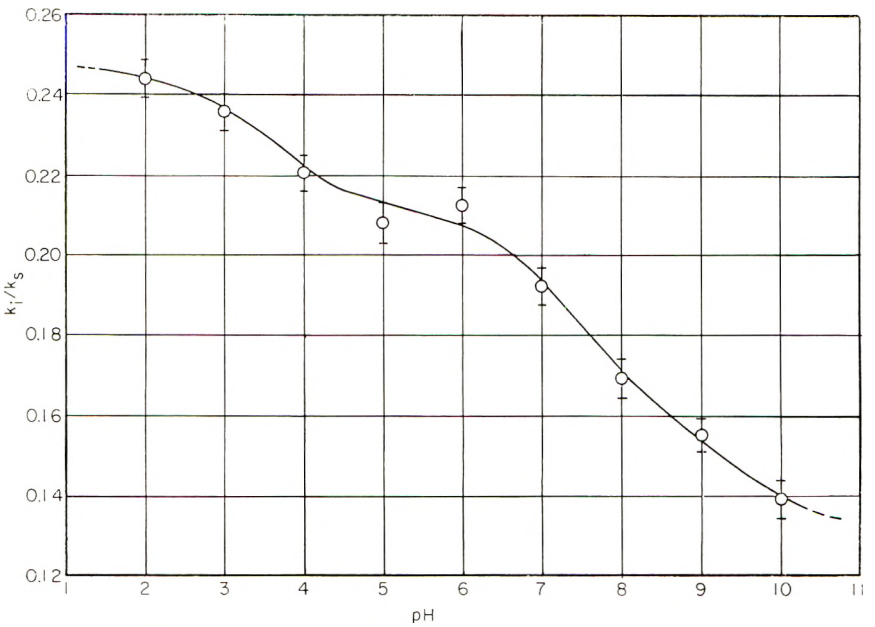

Fig. 1. The effect of pH on the ratio of isotactic to syndiotactic propagation rates k_i/k_s in the polymerization of methacrylic acid in aqueous solution.

The apparent pK_a of methacrylic acid at 2.3M concentration is 4.18 by our measurements; we find the pH of half-dissociation of polymethacrylic acid to be approximately 6.2 in this concentration range, a value in approximate agreement with that reported by Katchalsky and Spitnik[4] for 0.1M polymethacrylic acid. The concentrations of both monomer and polymer vary of course throughout the reaction. In the middle pH range, both pH and ionic strength therefore vary during the reaction. For this reason, it is difficult to express exactly the degree of dissociation of the monomer and of the growing polymer radical, even assuming, with Katchalsky and Blauer,[1] that the latter is in electrochemical equilibrium with its surroundings. Despite these difficulties, however, it seems permissible to conclude from Figure 1 that propagation is influenced by the dissociation of the monomer even when the polymer radicals are undissociated, but that the largest effect occurs when both are dissociated.

In the middle pH range, three propagation reactions are contributing in varying proportions to the overall polymerization:

$$P\cdot + M \rightarrow P\cdot$$

$$P\cdot + M^- \rightarrow P\cdot$$

$$P\cdot^- + M^- \rightarrow P\cdot^-$$

where P· and M represent the growing polymer chain and the monomer, respectively. In this range, therefore, the interpretation of the reaction in terms of a single value of σ is not strictly correct, although interpretation in terms of an average σ appears to be permissible, for it is found that at each pH the relative proportions of *i*, *h*, and *s* units fall on the theoretical parabolic curves[6] within the probable experimental error.

The author is indebted to Dr. G. V. D. Tiers for stimulating discussions; to Mr. R. B. Calkins for the careful operation and maintenance of the NMR spectrometer; to Mrs. Katherine LaCroix for the preparation of polymer samples and NMR tubes; and to Mr. R. I. Coon for carrying out the methylation of the polymethacrylic acid samples.

References

1. Katchalsky, A., and G. Blauer, *Trans. Faraday Soc.*, **47**, 1360 (1951).
2. Pinner, S. H., *J. Polymer Sci.*, **9**, 282 (1952).
3. Blauer, G., *J. Polymer Sci.*, **11**, 189 (1953).
4. Katchalsky, A., and P. Spitnik, *J. Polymer Sci.*, **2**, 432 (1947).
5. Loebl, E. M., and J. J. O'Neill, *J. Polymer Sci.*, **45**, 538 (1960).
6. Bovey, F. A., and G. V. D. Tiers, *J. Polymer Sci.*, **44**, 173 (1960).
7. Bovey, F. A., *J. Polymer Sci.*, **46**, 59 (1960).
8. Katchalsky, A., and H. Eisenberg, *J. Polymer Sci.*, **6**, 145 (1951).
9. Tiers, G. V. D., *J. Phys. Chem.*, **62**, 1151 (1958).

Synopsis

It is shown that when methacrylic acid is polymerized in an aqueous system, the stereochemical configuration of the polymer, deduced by observation of the high resolution NMR spectra of polymethyl methacrylate samples prepared by methylation, is markedly influenced by the pH of the system. Syndiotactic propagation is favored at higher pH, presumably because coulombic repulsion between negatively charged monomer and negatively charged growing polymer radicals increases the free energy of activation for isotactic monomer placement.

Résumé

On montre que si l'acide méthacrylique est polymérisé dans un système aqueux, la configuration stéréochimique du polymère, déduite par observation du spectre de résonance magnétique nucléaire à haute résolution des échantillons de polyméthacrylate de méthyle préparés par méthylation, est fortement influencée par le pH du système. La propagation syndiotactique est favorisée aux valeurs de pH plus élevées, probablement parce que la répulsion coulombienne entre les monomères et les radicaux polymériques en croissance, chargés négativement, augmente l'énergie libre d'activation pour l'arrangement isotactique des monomères.

Zusammenfassung

Es wird gezeigt, dass bei der Polymerisation von Methacrylsäure in einem wässrigen System die sterische Konfiguration des Polymeren, wie sie aus den Hochauflösungs-NMR-spektren der durch Methylierung hergestellten Methylmethacrylatproben abgel-

eitet werden kann, durch das pH des System merklich beeinflusst wird. Bei höherem pH wird syndiotaktisches Wachstum begünstigt, wahrscheinlich dadurch bedingt, dass die coulombsche Abstossung zwischen negativ geladenem Monomeren und negativ geladenen wachsenden Polymerradikalen die freie Artivierungsenergie für isotaktische Anordnung des Monomeren vergrössert.

Received December 13, 1961

JOURNAL OF POLYMER SCIENCE: PART A VOL. 1, PP. 849–861 (1963)

Polymer NMR Spectroscopy. IX. Polyacrylamide and Polymethacrylamide in Aqueous Solution

F. A. BOVEY* and G. V. D. TIERS, *Central Research Department, Minnesota Mining & Manufacturing Company, St. Paul, Minnesota*

The structure and behavior of polyacrylamide and polymethacrylamide in aqueous solution appears to have received comparatively little study. In particular, it is not known whether there is intramolecular hydrogen bonding between the amide groups, nor is there any information concerning the rates and mechanisms of amide group rotation and proton exchange. In this paper, we have therefore applied nuclear magnetic resonance to the study of these questions. Our measurements give no support to the supposition that extensive intramolecular hydrogen bonding occurs, although they do not conclusively rule it out. It is shown that amide proton exchange with the solvent is catalyzed by both acid and base, but that amide group rotation is catalyzed by neither; these processes do not, therefore, proceed by way of a common intermediate as has been claimed for small-molecule amides.

EXPERIMENTAL

Polymer Preparation

Acrylamide was obtained from the American Cyanamid Co. Polymerizations were carried out at 50°C. (water bath) in sealed, evacuated glass ampules containing 5 g. of monomer, 20 ml. of deionized water, and 0.050 g. of potassium persulfate. Substantially complete conversion to polymer was obtained in less than 3 hr. The polymers were precipitated in about 10 volumes of acetone in order to free them from any residual monomer and were dried *in vacuo* for 16 hr. at 75°C. The NMR spectra revealed some residual acetone (small peak at 7.80 τ') but this was not sufficient to influence the results. In order to control molecular weight and prevent gelation and excessive solution viscosity, sodium mercaptoacetate (Matheson, Coleman, and Bell, practical grade) was included in the system. Polymer preparations were carried out with 0.005, 0.010, 0.050, and 0.100 g. of this substance as a chain transfer agent. The molecular weights of the polymers (see Table II) were determined by viscosity measurements in

* Present address: Bell Telephone Laboratories, Inc., Murray Hill, N. J.

1.0M sodium nitrate solutions at 30°C., the relationship[1] of eq. (1) being used.

$$[\eta]_{30°C.} = 3.73 \times 10^{-4} \bar{M}_w^{0.66} \quad (1)$$

Sample Preparation

Polymer solutions for NMR spectral measurements were prepared by dissolving 0.100 g. of polymer in 0.5 ml. of water, previously adjusted to the proper pH, in a small vial. One per cent (5 mg.) of DSS (sodium 2,2-dimethyl-2-silapentane-5-sulfonate)[2,3] was added to each solution to serve as an internal reference standard. To buffer the polymer solutions in the pH region 8–9, 0.1M borate buffers (boric acid plus sodium hydroxide) were employed. For pH 9 and above, unbuffered sodium hydroxide solutions were employed. In the pH region 4–5, 0.1M phosphate buffers (NaH_2PO_4 plus hydrochloric acid) were used. More strongly acid solutions were prepared with hydrochloric acid without buffering. The pH determinations were carried out with a Radiometer TTT1 pH meter. All solutions and NMR tubes were stored at about 5°C. between measurements in order to minimize hydrolysis and imidization.

Polymer solutions were transferred to 5 mm. o.d. Pyrex NMR tubes, which were evacuated and then sealed under about 400 mm. of nitrogen pressure in order to prevent boiling at elevated temperatures.

Spectral Measurements

A Varian V-4300-2 40.00 Mcycle/sec. spectrometer, equipped with a Varian heated probe, field homogeneity control unit, Hewlett Packard 522-B frequency counter and Varian recorder, was employed. In the spectra, the peak for the methyl groups of the sodium 2,2-dimethyl-2-silapentane-5-sulfonate [$(CH_3)_3Si(CH_2)_3SO_3Na$] reference appears at the extreme right and its position is taken[3] as +10.000 ppm. Peak position values on this scale are termed τ'-values, to distinguish them from those referred to tetramethylsilane;[3] the latter is not sufficiently soluble in water to serve as a reference. τ' values and peak separations are determined by linear interpolation in these spectra.

EXPERIMENTAL RESULTS AND INTERPRETATION

The Polyacrylamide Spectrum

In Figure 1a is shown the spectrum of polyacrylamide of molecular weight 138,000 (polymer no. 3 in Table II) in pH 4.5 phosphate buffer at 25.0°C. The large central peak is that of water. To the right of the water peak appears the broad peak for the backbone protons, with a maximum (methylene group) at 8.30 τ' and a shoulder (α-hydrogen) at approximately 7.9 τ'; there appears here also the small spike at 7.80 τ' due to residual acetone in the polymer. To the left of the water peak appear the two amide peaks, which are of chief interest for our present purpose. These peaks are of

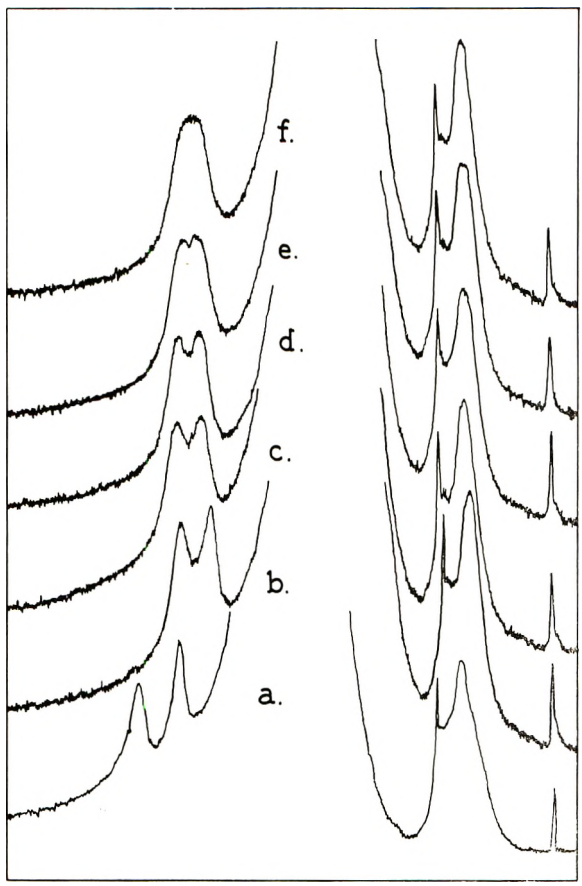

Fig. 1. NMR spectrum of polyacrylamide in aqueous solution (0.100 g. in 0.5 ml. water) at pH 4.5 (0.1*M* phosphate buffer): (*a*) 25.0°C.; (*b*) 60.0°C.; (*c*) 65.0°C.; (*d*) 67.5°C.; (*e*) 68.5°C.; (*f*) 70.0°C.

equal area and width, and at 25°C. appear at 2.26 and 3.01 τ', a separation ($\delta\nu$) of 30 cycles/sec. As a comparison, the single peaks for peptide hydrogens in nonaromatic dipeptides, in trifluoroacetic acid solution, appear at about 1.6–2.2 τ;[4] the centers of the broad NH resonances for formamide, acetamide, and isobutyramide in aqueous solution were observed in this laboratory to occur at about 1.9 τ', 1.9 τ', and 3.0 τ', respectively.

The amide peaks for the polymer are much narrower (only about 10–12 cycles/sec. in width at half-height) than those normally observed for unsubstituted amides. The resonance due to protons attached to N^{14} might be expected to be a triplet, consisting of equal peaks with an approximately 50 cycles/sec. separation, because of interaction with the three spin states of N^{14} ($I = 1$). This has been observed for rigorously dried liquid ammonia,[5] for alkylamines in acid solution,[6,7] and for pure liquid formamide, acetamide, and *N*-methylacetamide at elevated temperatures.[8] This triplet is collapsed to a singlet when fairly rapid exchange of the

N^{14}—H protons with each other is possible.[5-8] Collapse to a singlet will also be observed if the electric quadrupole moment of the N^{14} nucleus is coupled particularly effectively to the tumbling motions of the molecule. Most amides at moderate temperatures show a broad singlet NH_2 resonance for the latter reason.[8] Some *N*-substituted amides, including many glycyl dipeptides, show a relatively narrow (about 6–10 cycles/sec.) singlet absorption, apparently because the molecular electric field gradient at the N^{14} nucleus is particularly strong in these compounds.[9] The coupling of the nitrogen nucleus to the motions of the molecular framework is evidently more effective when the motions are relatively slow.[8] The segmental motion of a polyacrylamide chain would be expected to be considerably slower than the tumbling of a small-molecule analog, such as acetamide, under equivalent conditions. We believe that this is the reason for the marked narrowing of the N^{14}—H resonance in the polymer spectrum; in the absence of such special circumstances (i.e., for all peaks not broadened by electric quadrupole effects) the slower motions of polymer chains necessarily result in a broadening of the resonance peaks.[10] In support of this explanation, we have observed that the amide proton resonance of acetamide can be caused to appear as two much narrower peaks, (closely resembling those of aqueous polyacrylamide) by the simple expedient of using as the solvent a 50:50 (by volume) mixture of glycerol and water, the viscosity being thus made six times that of water.

The doublet resonance of the amide protons of the polymer (and of small molecule amides in viscous solvents) arises from the restricted rotation of the amide group about the C—N bond. Because of this restricted rotation, the two amide protons are chemically and magnetically distinct, with the one in the *trans* position to the carbonyl group probably appearing at higher field.[11] Being magnetically different, they might, by analogy to the CH_2 group, be expected to be mutually coupled with a J of approximately 15 cycles/sec. if the H—N—H angle were close to the tetrahedral value observed for ammonia and amino groups. The resultant splitting of the resonance would be seen readily as an AB quartet pattern[12,13] instead of the observed doublet. It is clear that any coupling of the protons must be much smaller than 15 cycles/sec. We interpret this as indicating that the H—N—H bond angle, rather than being that of a normal amino group, instead tends to approximate the H—C—H bond angle in a vinyl group. It is known that the coupling of these vinyl protons is of the order of only 0–3.5 cycles/sec.[14] This finding appears to give additional direct support to the suggestion of Pauling[15] that the structure of amides should not be represented in the conventional manner, but rather as:

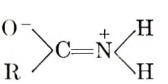

The spectrum of doubly irradiated formamide[11] (in which the N^{14} nucleus is uncoupled from these protons and their nonequivalence can be seen) appears to be in agreement with the present observation.

Amide Group Rotation

The two amide proton resonances are seen as separate peaks at temperatures near 25°C. because the rate of rotation of the amide group is so slow that the residence time t for a proton at each of the two observable sites is at least an order of magnitude greater than $1/(2\pi\delta\nu)$ i.e., at least 0.05 sec.[11] As the temperature is raised, the apparent separation of the peak maxima becomes less until at 70°C. they blend into a single broadened peak. In Figures 1*b*, c, *d*, *e*, and *f* are shown the NH_2 resonance at 60.0, 65.0, 67.5, 68.5 and 70°C., respectively. In Table I, the measured apparent peak maxima separations $\delta\nu_{obs}$ are tabulated, together with the ratios $\delta\nu_{obs}/\delta\nu$ and the first-order rate constant $1/t$ for amide group rotation, obtained from the curves given by Gutowsky and Holm.[17] In deriving these rate constants, it was assumed that T_2 for these protons was not substantially less than 0.1 sec. (reasonable in view of the observed values for other polymers[10,18]) and that therefore the curve corresponding to $T_2\delta\omega = \infty$ could be used without serious error (Figure 1 of reference 17).

TABLE I

Temperature Dependence of Apparent Peak Maxima Separations $\delta\nu_{obs}$ and Calculated First-Order Rate Constants $1/t$ for Rotation of the Amide Groups in an Aqueous Solution of Polyacrylamide (0.100 g./0.5 ml. solvent; Mol. Wt. 138,000; Buffered at pH 4.50)

Temperature, °C.	$\delta\nu_{obs}$, cycles/sec.	$\delta\nu_{obs}/\delta\nu$	$1/t$, sec.$^{-1}$
25.0	30.0	1	—
60.0	23.2	0.77	85
65.0	18.4	0.61	106
67.5	14.9	0.50	115
68.5	10.8	0.36	124
70.0	Single peak		—

These data allow the calculation of an activation energy of 10.5 ± 1 kcal. for the amide group rotation. By measurement of the collapse of the *N*-methyl doublets, Gutowsky and Holm[17] obtained values of 7 ± 3 kcal. for *N*,*N*-dimethylformamide and 12 ± 2 kcal. for *N*-methylacetamide, the neat liquids rather than aqueous solutions being employed. The value for the polymer is within this range and it therefore appears that the rotation of its amide groups does not require the cooperation of neighboring groups along the chain (e.g., intramolecular hydrogen bonding) as this would be expected to require a markedly larger activation energy.

Proton Exchange

Exchange of protons between the polymer amide groups and water should be a moderately rapid process. Berger et al.[19] measured the rate of exchange of water protons with *N*-methylacetamide by observation of the collapse of the *N*-methyl proton doublet and concluded that the direct

exchange with the H_2O molecule as such is quite slow, but that exchange via H_3O^+ and OH^- is rapid; for the reaction

$$CH_3CONHCH_3 + OH^- \overset{k_1}{\rightleftharpoons} (CH_3CONCH_3)^- + H_2O$$

the rate constant $k_1 = 5.2 \times 10^6$ l./mole sec., while for

$$CH_3CONHCH_3 + H_3O^+ \overset{k_2}{\rightleftharpoons} (CH_3CONH_2CH_3)^+ + H_2O$$

they found $k_2 = 3.8 \times 10^2$ l./mole sec.; it is assumed that both charged intermediates are very rapidly attacked by water to regenerate the *N*-methylacetamide. The pH of minimum exchange rate was found to be about 5. From experiments to be detailed below it has been found that the pH of minimum exchange for polyacrylamide should be about 4.5, which is the pH of the solution employed for the amide group rotation studies. It

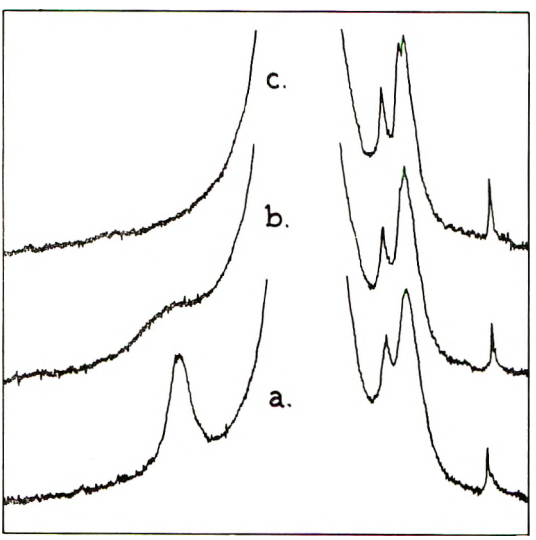

Fig. 2. NMR spectrum of polyacrylamide in aqueous solution (0.100 g. in 0.5 ml. water) at pH 4.5 (0.1*M* phosphate buffer): (*a*) 128.5°C.; (*b*) 136.0°C.; (*c*) 142.0°C.

is to be expected that, at a sufficiently high temperature, exchange between the polymer amide groups and water will result in a coalescing of the amide peak with that of the water. Such coalescing is in fact observed, but because of the large molar excess of water (approximately 20-fold) the peak maxima do not appear to move together; rather, the amide peak broadens, decreases in height, and finally disappears. As can be seen from curves *a*, *b*, and *c* of Figure 2, its disappearance is complete at 142°C. These observations serve to emphasize the true nature of the "doublet collapse" phenomenon: the observed motion of the peaks toward each other is actually only apparent and is caused by a decrease in their height, accompanied by the growth of a third peak between them. When one peak is very much larger than the other, the smaller peak merely disappears, with

little or no apparent motion.[20] Actually, in the present system the amide resonance moves from 2.63 τ' at 25°C. (average position of the doublet components) to 3.20 τ' at 128.5°C.; this motion is "real" and is caused by a decrease in the degree of hydrogen bonding of the amide groups. The resonance for water is known[3,21] to move upfield with increasing temperature for the same reason; this was observed qualitatively in the present experiments, but was not measured accurately.

On cooling the tube to 25°C., the amide doublet reappears unchanged, indicating that the phenomena observed at higher temperatures are reversible and not due to imidization or hydrolysis of the amide groups, although both may occur to a minor extent.

When the peaks are of unequal magnitude, the analytical expression describing the signal shape as a function of exchange rate becomes very complex and unwieldly, and requires experimental data exceedingly difficult to obtain.[17,20] For this reason, no attempt is made in this paper to calculate exactly the exchange rate between water and polyacrylamide. It may be assumed, however, that when the amide peak has disappeared, the *average* residence time of the proton at both sites (i.e., water and amide group; the residence time at each site is proportional to the concentration of that site) will be no greater than $1/(2\pi\delta\nu)$, or roughly 10^{-3} sec.

Effect of pH

It is evident from these experiments that amide group rotation and proton exchange in polyacrylamide are separate reactions, neither being the rate-determining process for the other. This conclusion is further strengthened by studies in which the pH was varied over a wide range. From the experiments already described, it is clear that at pH 4.5 the proton exchange rate is considerably slower than the rotation of the amide group. In Figure 3 are shown the spectra of polyacrylamide solutions at 24.5°C. and pH 8.0, 8.3, 8.5, 8.7, 9.0, and 10.0. Spectra were also obtained at pH 11.0 and 12.0; these are indistinguishable from the spectrum at pH 10.0. In Figure 4 are shown the spectra in 0.1*N* HCl (pH 1.20), and in 0.5 and 1.0*N* HCl; in the last two the pH was not measured. From the results of Berger et al. with *N*-methylacetamide,[19] it may be assumed that the polymer amide groups are protonated to some extent in the most acid solutions and that therefore the hydronium ion concentration is somewhat less than it would be in the absence of the polymer.

From Figures 3 and 4, it is evident that proton exchange between polyacrylamide and water is catalyzed by both acid and base. The amide resonance decreases in intensity and has nearly disappeared at pH 9 and in 0.1*N* HCl. At pH 10 and higher and in 1*N* HCl it has disappeared entirely. As long as it is visible, however, it remains a doublet, and the separation remains at 30 cycles/sec. Thus, our results provide no evidence that amide group rotation is catalyzed by acid or by base. Since both proton peaks disappear together, it may be concluded that both protons exchange equally rapidly with water. If one of the protons in each amide group (or

in a substantial fraction of the amide groups) were intramolecularly hydrogen-bonded to a neighboring carbonyl group, the other being hydrogen-bonded to a water molecule, it would be expected that the rates of proton exchange with water would differ markedly, the proton hydrogen-bonded to water being exchanged more rapidly. It is well known that the peptide protons of native proteins and polypeptides in α-helical configuration

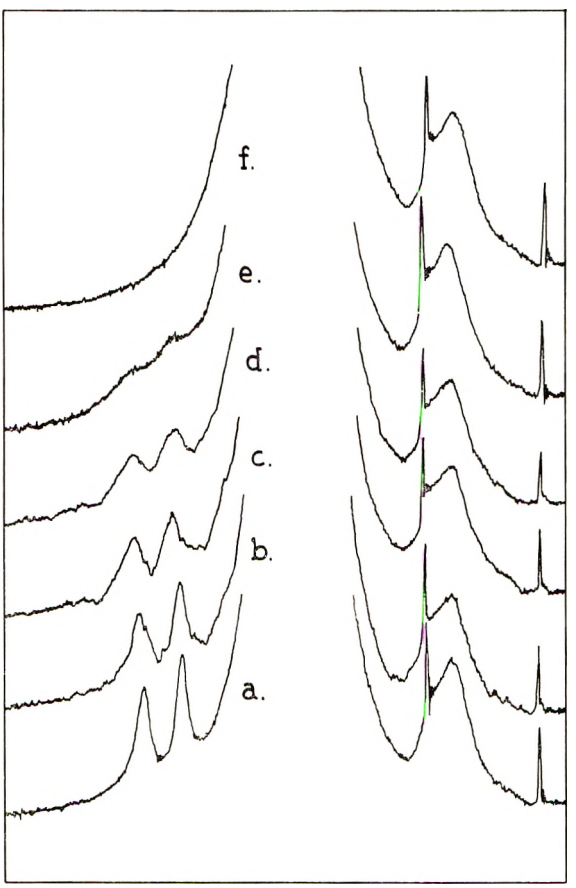

Fig. 3. NMR spectrum of polyacrylamide in aqueous solution (0.100 g. in 0.5 ml. water) at 25°C.: (*a*) pH 8.0; (*b*) pH 8.3; (*c*) pH 8.5; (*d*) pH 8.7; (*e*) pH 9.0; (*f*) pH 10.0.

exchange much more slowly with solvent D_2O than the denatured or random coil forms,[22] presumably because in the α-helix such exchange requires the momentary rupture of a cooperative system of intramolecular hydrogen bonds between the peptide groups. Our present evidence, therefore, does not appear to favor the existence of extensive intramolecular hydrogen bonding in aqueous polyacrylamide.

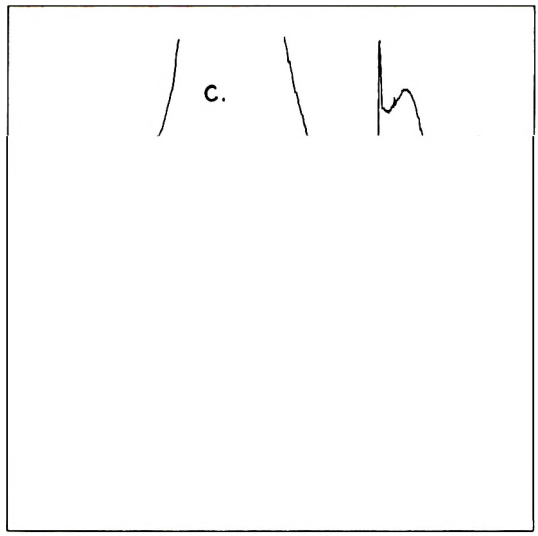

Fig. 4. NMR spectrum of polyacrylamide in aqueous solution (0.100 g. in 0.5 ml. water) at 25°C.: (*a*) 0.1*N* HCl (pH 1.2); (*b*) 0.5*N* HCl; (*c*) 1.0*N* HCl.

DISCUSSION

Berger et al.[19] have observed that proton exchange in *N*-methylacetamide is rather weakly catalyzed by hydronium ion and that under very strongly acid conditions the *N*-methyl doublet reappears, indicating that exchange has actually been retarded. They also observed that in the spectrum of *N*,*N*-dimethylacetamide (in which proton exchange cannot occur) the *N*-methyl doublet, which results from a slight chemical shift difference between the *N*-methyl groups combined with restricted rotation about the C—N bond, collapses in acidic solution at nearly the same pH (between 1.0 and 1.6) as the doublet collapse in *N*-methylacetamide, arising from proton exchange. They concluded that in acidic solution an *O*-protonated and an *N*-protonated form of the amide may both exist. The *N*-protonated form should permit both exchange and free rotation about the C—N bond, as previously pointed out by Phillips,[23] since its double-bond character is destroyed:

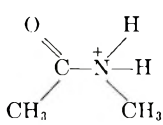

whereas in the *O*-protonated form both free rotation and exchange are presumably prevented:

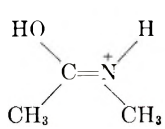

The *N*-protonated form is assumed to be produced relatively slowly and to exist only in small concentration, whereas the *O*-protonated form is believed to predominate in strongly acidic solution.[24] The reaction yielding the *N*-protonated form is believed to be the rate-determining step in both proton exchange and amide group rotation. This last conclusion is not necessarily valid for *N*-methylacetamide, however. In this case, rotation cannot be observed separately from exchange. The comparison to the behavior of *N*,*N*-dimethylacetamide is not conclusive, because the latter should be considerably more basic and would be expected to be protonated on nitrogen to a much larger extent under equivalent conditions. It thus cannot be regarded as demonstrated that proton exchange and rotation about the C—N bond proceed by way of a common intermediate. In polyacrylamide it is clear that this is not the case, for each process can be observed separately and under appropriate conditions each can be made to occur much more rapidly than the other. Under all conditions employed in our experiments, amide group rotation is apparently uncatalyzed. In polyacrylamide, proton exchange is even more weakly catalyzed by hydronium ion than in *N*-methylacetamide, an acid concentration about ten times greater being required to cause the amide peak to disappear than is required to cause collapse of the *N*-methyl doublet in the latter. This is probably primarily due to the yet weaker basicity of the unsubstituted amide group.

The amide–amide hydrogen bond is moderately strong; estimates, mostly based on measured degrees of dimerization in inert solvents, are in quite close agreement, and indicate a heat of formation of approximately 3.7 ± 0.3 kcal. for several different unsubstituted and *N*-substituted amides.[25,28] In aqueous solutions of amides, however, we are in effect dealing with the reaction:

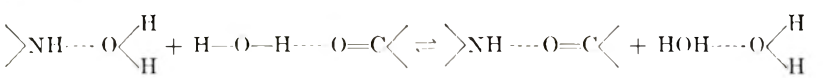

Intramolecular (or intermolecular) hydrogen bond formation in aqueous solutions of amides[28] will be favored if the bonds on the right side of the equations are stronger than those on the left. Schellman[26] has calculated that for the formation of the dimer of urea in aqueous solutions: ΔF° = 1990 cal., ΔH° = −2090 cal., ΔS° = −13.7 e.u., and that the heat of formation of a single urea–urea hydrogen bond does not exceed −1500 cal., the exact value depending on the number of bonds assumed to exist in the dimer. The stability of an intramolecularly hydrogen-bonded polymeric structure in aqueous solution will, of course, depend strongly on the entropy of formation; even assuming no strain in the structure, such intramolecular bonds cannot play a prominent role (i.e., the structural features dependent on such hydrogen bonding cannot be stable) if the entropy of formation per bond is more negative than about −4 to −5 e.u. For a polypeptide chain in aqueous solution, the stabilizing energy of the peptide–peptide hydrogen bonds is probably only of the order of RT. The α-helical structure tends to be stabilized because the formation of a break in the helix involves the

rupture of at least three peptide hydrogen bonds and a relatively small gain in configurational entropy.[27] In the polyacrylamide chain, intramolecular hydrogen bonds would not have to break cooperatively, and our results suggest that the gain in configurational entropy per hydrogen bond is greater than for an α-helix.

Effect of Molecular Weight

By means described in the experimental section, acrylamide was polymerized to yield products of four different molecular weights, as shown in Table II. Solutions of these polymers were prepared at pH 8 (borax buffers) and their NMR spectra observed. All spectra appeared the same despite the considerable variation in solution viscosity. Thus neither solution viscosity nor molecular weight as such has an appreciable influence on the spectra.

TABLE II
Molecular Weights of Polyacrylamide Prepared with Sodium Mercaptoacetate as Chain Transfer Agent

Polymer no.	Wt. sodium mercaptoacetate, mg.	$[\eta]$ in 1.0N $NaNO_3$ solution	$\bar{M}_w$
1	5	1.42	2.57×10^5
2	10	0.96	1.48×10^5
3	50	0.90	1.38×10^5
4	100	0.18	1.12×10^4

Polymethacrylamide

It was found that methacrylamide polymers prepared as described in the experimental section for polyacrylamide showed no amide hydrogen peak in aqueous solution at 25°C. and pH 4.0. This might be attributable to a very rapid exchange with solvent protons, but as this appeared unlikely another explanation was sought. It was found that polymethacrylamide prepared in the presence of 500 mg. of sodium mercaptoacetate exhibited an amide hydrogen doublet very similar to that of polyacrylamide, although with somewhat broader peaks. In the spectra of all methacrylamide polymers, the α-methyl peak was abnormally broadened. It is suggested that in these more hindered and therefore stiffer chains, the reorientation of the polymer molecules, and hence of the amide groups, is very slow; thus their NMR peaks undergo the usual "dipolar" broadening.[10] Only in chains of very low molecular weight does the reorientation rate become comparable to that of polyacrylamide chains.

Note added in proof: Since submission of this manuscript, an interesting study of hydrogen bonding between peptide groups in aqueous solutions has been completed and published.[28] It was concluded that such bonds probably do not stabilize macromolecular configurations significantly.

We are greatly indebted to Dr. Kenneth D. Kopple of the University of Chicago for bringing to our attention the existence of the "doublet" NH peak in aqueous polyacrylamide solutions, which he had observed in connection with another investigation. The careful NMR work was done by Mr. R. B. Calkins, and the polymer preparations by Mrs. Katherine LaCroix. We thank Mr. G. W. Morneau for the molecular weight determinations.

References

1. American Cyanamid Co. Bulletin MDD-9236, *Cyanamer P 26 Acrylamide Copolymer; Cyanamer P 250 Polyacrylamide*, June, 1959, p. 6.

2. Tiers, G. V. D., and R. I. Coon, *J. Org. Chem.*, **26**, 2097 (1961).

3. Tiers, G. V. D., and A. Kowalsky, paper presented to the Division of Physical Chemistry, 137th National Meeting, American Chemical Society, Cleveland, Ohio, 1960; Abstracts, p. 17R, currently being prepared for publication.

4. Bovey, F. A., and G. V. D. Tiers, *J. Am. Chem. Soc.*, **81**, 2879 (1959).

5. Ogg, R. A., *Discussions Faraday Soc.*, **17**, 215 (1954); *J. Chem. Phys.*, **22**, 560 (1954).

6. Tiers, G. V. D., unpublished experiments.

7. Grunwald, E., A. Loewenstein, and S. Meiboom, *J. Chem. Phys.*, **27**, 630 (1957).

8. Roberts, J. D., *J. Am. Chem. Soc.*, **78**, 4495 (1956).

9. Tiers, G. V. D., and F. A. Bovey, *J. Phys. Chem.*, **63**, 302 (1959).

10. Bovey, F. A., G. V. D. Tiers, and G. Filipovich, *J. Polymer Sci.*, **38**, 73 (1959).

11. Piette, L. H., D. J. Ray, and R. A. Ogg, *J. Mol. Spectroscopy*, **2**, 66 (1958).

12. Jackman, L. M., *Applications of Nuclear Magnetic Resonance Spectroscopy in Organic Chemistry*, Pergamon Press, New York, 1959, p. 89.

13. Pople, J. A., W. G. Schneider, and H. J. Bernstein, *High Resolution Nuclear Magnetic Resonance*, McGraw-Hill, New York, 1959, p. 119.

14. Jackman, L. M., *op. cit.*, p. 85.

15. Pauling, L., *The Nature of the Chemical Bond*, 2nd Ed., Cornell Univ. Press, Ithaca, N. Y., 1948, p. 207.

16. Pople, J. A., W. G. Schneider, and H. J. Bernstein, *op. cit.*, p. 218 et seq.

17. Gutowsky, H. S., and C. H. Holm, *J. Chem. Phys.*, **25**, 1228 (1956).

18. McCall, D. W., and F. A. Bovey, *J. Polymer Sci.*, **45**, 530 (1960).

19. Berger, A., A. Loewenstein, and S. Meiboom, *J. Am. Chem. Soc.*, **81**, 62 (1959).

20. Charman, H., D. Vinard, and M. M. Kreevoy, *J. Am. Chem. Soc.*, **84**, 347 (1962).

21. Bovey, F. A., *Nature*, **192**, 324 (1961).

22. Linderstrøm-Lang, K., Symposium on Peptide Chemistry, Mar. 30, 1955, Special Publication No. 2, The Chemical Society, London, 1955, pp. 1–24.

23. Roberts, J. D., *Nuclear Magnetic Resonance*, McGraw-Hill, New York, 1959, p. 70.

24. Fraenkel, G., A. Loewenstein, and S. Meiboom, *J. Phys. Chem.*, **65**, 700 (1961); G. Fraenkel and C. Niemann, Proc. Natl. Acad. Sci., U. S., **44**, 688 (1958).

25. See G. C. Pimentel and A. L. McClellan, *The Hydrogen Bond*, W. H. Freeman, San Francisco, 1960, p. 361.

26. Schellman, J. A., *Compt. rend. trav. lab. Carlsberg, Ser. chim.*, **29**, 223 (1955).

27. Schellman, J. A., *Compt. rend. trav. lab. Carlsberg, Ser. chim.*, **29**, 230 (1955).

28. Klotz, I. M., and J. S. Franzen, *J. Am. Chem. Soc.*, **84**, 3461 (1962).

Synopsis

The NMR spectrum of polyacrylamide in aqueous solution exhibits a doublet resonance in the amide proton region, in contrast to the broad singlet shown by most small-molecule amides. This is attributed to the relatively slow reorientation rate of the polymer segments, permitting effective coupling of the electric quadrupole moment of the N^{14} nucleus to the motions of the molecular framework. This, in turn, narrows the

amide resonance to such a degree that the two protons can be discriminated. By observation of the collapse of this doublet, the rate of rotation of the amide groups can be measured; at pH 4.5 this rotation requires an activation energy of 10.5 ± 1 kcal. and is more rapid than proton exchange between the amide group and water. Rotation is not catalyzed by acid or base, whereas exchange is catalyzed by both and becomes more rapid than rotation at high and low pH. The two amide protons exchange at equal rates; if intramolecular hydrogen bonding of amide groups is present, it has no apparent retarding effect on proton exchange. These results are discussed in terms of possible protonated intermediates.

Résumé

Le spectre NMR du polyacrylamide, en solution aqueuse, présente un doublet de résonance dans la région du proton de l'amide, par opposition au large singulet observé pour la plupart des petites molécules d'amides. On attribue ce phénomène à la vitesse relativement lente de réorientation des segments polymériques, permettant un couplage effectif du moment quadripolaire électrique du noyau N^{14} aux mouvements du squelette moléculaire. Ceci diminue la résonance de l'amide à un degré tel que les deux protons peuvent être distingués. Par observation de la disparition de ce doublet, on peut mesurer la vitesse de rotation des groupes amides, à pH 4.5; cette rotation exige une énergie d'activation de 10.5 ± 1 kcal et est plus rapide que l'échange de proton entre le groupe amide et l'eau. La rotation n'est pas catalysée par les acides et les bases, tandis que l'échange est catalysé par ceux-ci et devient plus rapide que la rotation à des valeurs élevées et faibles du pH. Les deux protons de l'amide échangent à vitesse égale; si le lien hydrogène intramoléculaire est présent, il n'en résulte pas d'effet de retardement sur l'échange de proton. On discute ces résultats en termes d'intermédiaires protonés possibles.

Zusammenfassung

Das NMR-Spektrum von Polyacrylamid in wässriger Lösung zeigt im Gegensatz zu dem breiten Singulett der meisten niedermolekularen Amide eine Dublett-Resonanz im Amidprotonen-Bereich. Diese Erscheinung wird auf die verhältnismässig niedrige Reorientierungsgeschwindigkeit der Polymersegmente zurückgeführt, die eine effektive Kopplung des elektrischen Quadrupolmoments des N^{14}-Kernes mit den Bewegungen des Molekülgerüstes erlaubt. Dadurch wird wieder die Amidresonanz so weit verengt, dass die beiden Protonen unterschieden werden können. Durch Beobachtung des Zusammenfallens dieses Dubletts kann die Rotationsgeschwindigkeit der Amidgruppen gemessen werden; bei pH 4,5 erfordert die Rotation eine Aktivierungsenergie von 10,5 ± 1 kcal und verläuft rascher als der Protonenaustausch zwischen der Amidgruppe und Wasser. Die Rotation wird weder durch Säuren noch durch Basen katalysiert, während der Austausch durch beide katalysiert wird und bei hohem und niedrigem pH schneller als die Rotation wird. Die beiden Amidprotonen tauschen mit gleicher Geschwindigkeit aus; eine eventuell bestehende intramolekulare Wasserstoffbindung hat offensichtlich keinen verzögernden Einfluss auf den Protonenaustausch. Eine Diskussion der Ergebnisse unter Berücksichtigung möglicher protonierter Zwischenprodukte wird gegeben.

Received February 9, 1962

JOURNAL OF POLYMER SCIENCE: PART A VOL. 1, PP. 863–876 (1963)

Polyamides Containing Phosphorus. I. Preparation and Properties*

JOSEPH PELLON and W. G. CARPENTER, *Chemical Research Department, Central Research Division, American Cyanamid Company, Stamford, Connecticut*

INTRODUCTION

Phosphorus chemistry related to trivalent phosphorus (phosphines) has been greatly expanded in recent years. It was of interest to extend this into the polymer field by introducing trivalent phosphorus into a polymer backbone structure and studying the resultant structural effects. While polymers containing other phosphorus groups are known,[1,2] phosphine units had not previously been incorporated into well-defined polymer systems. The present study deals with the preparation and characterization of polyamides containing phosphine (C—P—C) and related oxide (C—P(=O)—C) or sulfide (C—P(=S)—C) groups in their backbone structure.

Polyesters and polyamides derived from bis(*p*-carboxyphenyl)-phosphine oxides

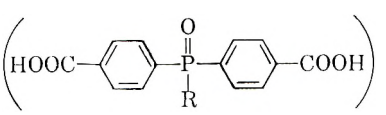

have previously been prepared by Korshak, Frunze and co-workers[3–7] and others.[8–9] Efforts to prepare polymers of the class considered here by less conventional routes have also been described.[10–14]

* Presented in part at the International Symposium on Inorganic Polymers, Nottingham, England, July 1961.

EXPERIMENTAL

Materials

Phosphorus-Containing Monomers. The monomers bis(3-aminopropyl)-phenylphosphine, b.p. 140–150°C./1 mm., n_D^{25} = 1.5722; bis(3-amino-propyl)-*n*-octylphosphine, b.p. 155–163°C./0.5 mm., n_D^{25} = 1.4948, anal. theory, C 64.62, H 12.69, P 11.92, N 10.77; found C 64.23, H 12.85, P 11.85, N 10.88, and bis(3-aminopropyl)-isobutylphosphine, b.p. 94°C./0.2 mm., n_D^{25} = 1.5014, anal. theory, C 58.52, H 12.25, P 15.19, N 13.73; found, C 58.52, H 12.46, P 14.89, N 13.63 were prepared by the free radical-initiated (azobisisobutyronitrile) addition of allylamine to the appropriate phosphine. Bis(2-cyanoethyl)phenylphosphine[15] was similarly prepared from phenylphosphine and acrylonitrile. Bis(3-aminopropyl)phenylphosphine oxide, b.p. 290–302°C./0.45, n_D^{25} = 1.5690 was prepared by hydrogen peroxide oxidation of bis(3-aminopropyl)phenylphosphine. Bis(2-cyanoethyl)phenylphosphine sulfide, m.p. 74–75°C., anal. theory, C 58.07, H 5.34, P 12.50, N 11.29, S 12.90; found C 57.77, H 5.41, P 12.47, N 11.28, S 12.63 was obtained by treatment of bis(2-cyanoethyl)phenylphosphine with sulfur. Bis(3-aminopropyl)methylphosphine oxide, 165–166°C./0.2 mm., n_D^{25} = 1.5098, anal. theory, C 47.19, H 10.67, P 17.41, N 15.73; found, C 46.57, H 11.93, P 16.94, N 15.86 was prepared from bis(2-cyanoethyl)-methylphosphine[16] by first oxidizing the phosphine with hydrogen peroxide in acetic acid followed by catalytic reduction of the nitrile groups with Raney cobalt in ethanol. 3-Aminopropyl-4-aminobutylmethylphosphine oxide, b.p. 186–188°C./0.5 mm., n_D^{25} = 1.5060, anal. theory, C 49.98, H 11.01, N 14.58, P 16.11; found C 49.93, H 11.01, N 14.11, P 15.46, was similarly prepared. Bis(2-carboxyethyl)phenylphosphine oxide, m.p. 203.5–205°C. anal. theory, C 53.33, H 5.55, P 11.48; found C 53.17, H 5.85, P 11.35 was prepared directly from bis(2-cyanoethyl)phenylphosphine by hydrolysis with sodium hydroxide in aqueous solution. Bis-(2-carboxyethyl)methylphosphine oxide, m.p. 161–163°C., anal. theory, C 40.39, H 6.25, P 14.90; found C 33.50, H 5.70, P 15.87 was similarly prepared from bis(2-cyanoethyl)methylphosphine. Bis(*p*-carboxyphenyl)-phenylphosphine oxide, m.p. 334–336°C. was prepared by the method of Morgan and Herr.[17]

Coreactants. The following chemicals were used as received: hexamethylenediamine, piperazine, sebacic acid, dimethyl oxalate, and terephthalic acid (Distillation Products Ind.); decamethylenediamine and 3-methyladipic acid (Aldrich Chemical Co.); bis(carboxyethyl)sulfide (Evans Chemetics Ind.); 3,3′-(methylimino)-bispropylamine (American Cyanamid Co.); *m*-cresol and formic acid (J. T. Baker Chem. Co.). Heptamethylenediamine (m.p. 28°C., b.p. 74–76°C./2 mm.) was kindly supplied by Dr. P. Paré of this laboratory.

Polymer Synthesis

Preparation of Polyamides from the amine salt or equivalent amounts of diamine and diacid components[18] was carried out in 30 × 1.8 cm. tubes

formed by closing one end of a length of Fischer-Porter glass piping. These tubes were sealed during the first stage of the polymerization either by using a special stainless steel screw-type closure[19] or preferably by a high pressure, three-way valve (Fischer-Porter Co.). Polymerizations were carried out under deaerated conditions. In a typical preparation 2 g. of the salt of adipic acid and bis(3-aminopropyl)phenylphosphine were placed in a tube which was then deaerated and sealed. The initial polymerization stage involved heating for 2 hr. at 200°C. in a Wood's metal bath having a Thermocap temperature controller. Polymerization was completed by an additional heating period of 2 hr. at 250°C., during which time the pressure was reduced to a few millimeters.

The polyamide obtained, poly-bis(3-aminopropyl)phenylphosphine adipamide, is a hard, clear, colorless to faint yellow polymer having an $[\eta]^{30°}_{HCOOH}$ in the range of 2 to 3.

ANAL. Calc.: C; 64.6%; H, 8.08%; N, 8.38%; P, 9.28%. Found: C, 63.25%; H, 8.29%; N, 8.86%; P, 9.10%.

It is soluble in formic acid, cresol, dimethylformamide, dimethyl sulfoxide, and aqueous alcohol and has a softening temperature at 70–80°C. It readily forms fibers and films, shows good metal bonding characteristics and is considerably less flammable than nylon 66.

In a typical polyamide preparation starting with a diamine and a phosphorus-containing dinitrile,[20] 2 g. (9.3 mmole) of bis(2-cyanoethyl)phenylphosphine, 1.08 g. (9.3 mmole) of hexamethylenediamine and 2.68 g. (32.2 mmole) of water were placed in a glass tube which was then inserted in an autoclave. After deaeration the autoclave was heated for 20 hr. at 200°C. At the end of this heating period, the autoclave was allowed to cool and liberated ammonia slowly vented. Polymerization was completed by further heating for 2 hr. at 255°C. at autogeneous pressures and finally 2 hr. at 255°C. at reduced pressure.

Polymer Characterization

Reduced and intrinsic viscosities were determined in Cannon-Ubbelodhe dilution viscometers. Adhesive tests were performed on test blocks of $^1/_2$ in.^{2} circular contact area. Metal blocks were cleaned with carborundum paper (#400/w), washed with acetone, and immersed in cleaning solutions: aluminum blocks were immersed for 10 min. in dichromate solution, steel for 2 min. in a mixture of nitric acid, hydrochloric acid, and formaldehyde, and copper dipped into nitric acid. After rinsing and air-drying, the blocks were heated on a hot plate to temperature sufficient to melt the polymer. Polymer was melted onto the blocks which were then pressed together under minimum pressure to insure proper spreading and joint formation. After conditioning (>24 hr. at 23°C., 50% R.H.) the force required to rupture the joint (in tension) was measured on the Baldwin tester. In a few designated cases the samples were conditioned 24 hr. at 23°C. over Drierite. In most cases, a minimum of three deter-

TABLE I
Summary of Physical Data on Phosphorus Polyamides and Related Materials

No.	Coreactant	Appearance	Reduced viscosity, dl./g.[a]	Softening temp., °C.[b]	Flow temp., °C.	Density, g./cc.[c]
	A. Adipic acid polyamides					
1	$H_2N(CH_2)_6NH_2$	Hard, tough, white, opaque	1.53	220	268	1.13
2	$H_2N(CH_2)_7NH_2$	Hard, tough, off-white, opaque	0.94	—	245	1.104
3	$\phi P(CH_2CH_2CH_2NH_2)_2$	Hard, tough, transparent, colorless	2.64	72	200	1.16
4	$n\text{-}C_8H_{17}P(CH_2CH_2CH_2NH_2)_2$	Soft, tough, white, opaque	0.87	135	160–170	1.08
5	$i\text{-}C_4H_9P(CH_2CH_2CH_2NH_2)_2$	Hard, tough, transparent, colorless	1.5	100–110	120	—
6	$\phi P(CH_2CH_2CH_2NH_2)_2$ (O)	Soft, tough, transparent, straw yellow	1.35	100	125–160	—
7	$CH_3P(CH_2)_3NH_2$ / $(CH_2)_4NH_2$ (O)	Hard, tough, transparent, colorless, tends to become tacky in air	0.91	70–80	145–147	1.15
8	$CH_3P(CH_2CH_2CH_2NH_2)_2$ (O)	Hard, tough, transparent, slightly yellow	1.20	90–100	165	1.2
9	$CH_3N(CH_2CH_2CH_2NH_2)_2$	Hard, brittle, transparent, slightly brown	0.36	70–75	105–110	1.11–1.12
	B. Hexamethylenediamine polyamides					
10	$HOOCCH_2CHCH_2CH_2COOH$ / CH_3	Hard, tough, white opaque	1.12	170	230–235	1.094
11	$\phi P(CH_2CH_2CN)_2$ (S)	Transparent, greenish solid	0.30	42–48	52–95	—
12	$\phi P(CH_2CH_2CN)_2$	Hard, transparent, dark colored	0.17	65–70	87–130	—

13	$\phi P(CH_2CH_2COOH)_2$	Hard, tough, translucent, colorless	0.4	50–60	120–155	—
14	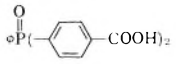	Hard, tough, transparent, colorless	$[\eta]^{0.42}_{\text{cresol}}$	228	Never free flowing	—
15	$CH_3P(CH_2CH_2COOH)_2$	Hard, brittle, transparent, yellow	0.50	68–72	100–140	—
16	$S(CH_2CH_2COOH)_2$		0.46	203–205	215–216	—
	C. Bis(3-aminopropyl)phenylphosphine polyamides					
17	$HOOC(CH_2)_8COOH$	Hard, tough, transparent, colorless	0.83	37	50–60	1.102
18	$CH_3OOCCOOCH_3$	Hard, brittle, transparent, straw yellow	0.42	74–75	80–100	1.208
19	NH_2CNH_2	Hard, brittle, transparent, colorless	0.70	84	105	1.174
20		Hard, tough, translucent, straw yellow	1.47	135	165–240	—
	D. Miscellaneous					
21	$n\text{-}C_8H_{17}P(CH_2CH_2CH_2NH_2)_2 + CH_3OOCCOOCH_3$	Soft, tough, transparent, yellow	0.33	40–42	65–70	1.086
22	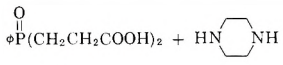	Hard, brittle, translucent, colorless	0.33	95–105	155–190	—
	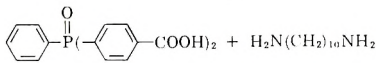	Hard, tough, transparent colorless	$[\eta]^{0.43}_{\text{creso}}$	175 195	210 270	—
24	$CH_3P(CH_2CH_2CH_2NH_2)_2 + HOOC(CH_2)_8COOH$	Hard, tough, transparent, pale yellow	0.63	35–40	60–100	

[a] Reduced viscosity in formic acid at 30°C. and 0.1% concentration.

[b] Initial softening of polymer under mild probing on a Fisher John's melting point apparatus.

[c] Gradient density technique.

TABLE II
Polymer Solubilities

No.[b]	Monomers	Stability[a]											
		Chlorobenzene	Hexane	Acetone	Acetonitrile	Water	Chloroform	Ethanol (2B)	5% HCl	Dimethylformamide	C-7 Fluoroalcohol	Cresol	Formic acid
1	Hexamethylenediamine + adipic acid	—	—	—	—	—	—	—	—	—	—	+2	+3
2	$H_2N(CH_2)_7NH_2$ + adipic acid	—	—	—	—	—	—	—	—	—	—	+3	+3
3	$\phi P(CH_2CH_2CH_2NH_2)_2$ + adipic acid	—	sw	—	—	—	—	+	+3	+2	—	+	+3
4	n-$C_8H_{17}P(CH_2CH_2CH_2NH_2)_2$ + adipic acid	sw	—	—	—	—	+3	—	sw	+1	+1	+1	+3
5	i-$C_4H_9P(CH_2CH_2CH_2NH_2)_2$ + adipic acid	—	—	+2	—	sw	—	—	+2	sw	—	+2	+2
6	$\phi P(CH_2CH_2CH_2NH_2)_2$ + adipic acid	—	—	—	—	sw	sw	+3	+2	+1	+2	+2	+3
7	$CH_3P(O)(CH_2)_3NH_2$ + adipic acid	—	—	—	—	+2	—	+2	+2	—	+2	+2	+3
8	$CH_3P(O)(CH_2CH_2CH_2NH_2)_2$ + adipic acid	—	—	—	—	+3	—	+1	+3	—	+2	+2	+3
9	$CH_3N(CH_2CH_2CH_2NH_2)_2$ + adipic acid	—	—	—	—	+3	+3	+3	+3	+1	+2	+2	+3
10	Hexamethylenediamine + $HOOCCH_2CH(CH_3)CH_2CH_2COOH$	—	—	—	—	—	—	—	—	—	+3	+3	+3

13	Hexamethylenediamine + $\phi P(CH_2CH_2COOH)_2$ (O)	—	—	—	sw	sw	sw	+2	sw	+2	+2	+2	+2
14	Hexamethylenediamine + $\phi P(\phi COOH)_2$ (O)	—	—	—	—	—	—	sw	—	+2	+1	+1	sw
16	Hexamethylenediamine + $S(CH_2CH_2COOH)_2$	—	—	—	—	—	—	—	—	+1	sw	+2	+3
17	$\phi P(CH_2CH_2CH_2NH_2)_2$ + sebacic acid	—	—	—	—	—	sw	—	sw	—	+3	+3	+3
18	$\phi P(CH_2CH_2CH_2NH_2)_2$ + $CH_3OOCCCOCH_3$	—	—	—	sw	—	+2	—	+3	+3	+2	+2	+3
19	$\phi P(CH_2CH_2CH_2NH_2)_2 + H_2NC(=O)NH_2$	—	—	—	—	—	sw	sw	+3	+3	+3	+3	+3
20	$\phi P(CH_2CH_2CH_2NH_2)_2$ + HOOC–C$_6$H$_4$–COOH	—	—	—	—	—	—	sw	sw	+2	—	+2	+2
21	n-$C_8H_{17}P(CH_2CH_2CH_2NH_2)_2$ + $CH_3OOCCOOCH_3$	—	—	—	+2	—	+3	—	+3	+1	+3	+3	+3
22	HN(C$_4$H$_8$)NH + $\phi P(=O)(CH_2CH_2COOH)_2$	—	—	—	sw	sw	+3	+1	+3	+3	+2	+2	+3
23	Decamethylenediamine + $\phi P(=O)(\phi COOH)_2$	—	—	—	—	—	sw	sw	—	+3	+2	+2	sw

[a] Code: (+3) immediately soluble (2–3 hr.); (+2) soluble on standing 24 hr.; (+1) soluble on heating; (sw), swollen; (—) insoluble even after heating.

[b] Numbering system is not consecutive but corresponds to that of Table I.

minations was made on each polymer, and the scatter of the results was about 20%. Tensile and flexural strength data were determined with an Instron tester by slightly modified ASTM test procedures. Thermogravimetric analysis was determined by heating samples in air at a rate of 10°C./min.

RESULTS AND DISCUSSION

Experimental Results

Successful polyamide preparations are listed in Table I. Several previously known polyamides not containing phosphorus were prepared for

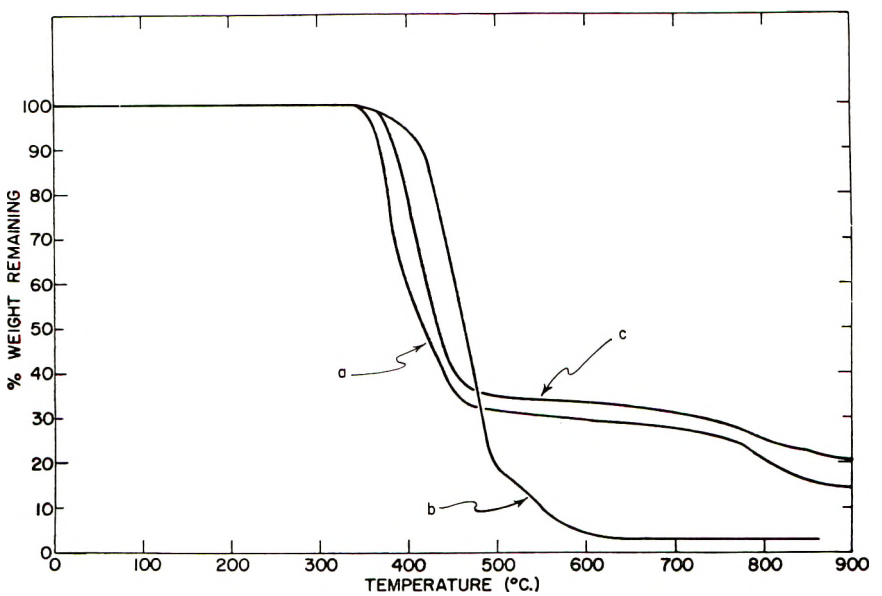

Fig. 1. Comparison of thermogravimetric behavior of polyamides: (*a*) polyamide from $\phi P(CH_2CH_2CH_2NH_2)_2$ + $HOOC(CH_2)_4COOH$; (*b*) polyamide from $NH_2(CH_2)_6NH_2$ + $HOOC(CH_2)_4COOH$; (*c*) polyamide from $\phi P(CH_2CH_2CH_2NH_2)_2$ + $HOOC(CH_2)_4COOH$.

comparative purposes and are included in the table. Solubility data are summarized in Table II. A thermogram comparison of nylon 66 with polyamides containing a phosphine and a phosphine oxide group is given in Figure 1.

Polymer Preparation

Several alternate synthetic routes are available for the preparation of polyamides.[21] A number of these were tried during the course of this work. Bulk polymerization with diacid and diamine components was

found to be the preferred method. Solution polymerization in cresol, either in the regular manner or by the technique described by Batzer et al.,[22] gave materials which tended to be yellow in color and had lower intrinsic viscosities. Several attempts at interfacial polymerizations[23] with bis-(3-aminopropyl)phenylphosphine and various diacyl halides gave only poor yields of polymer with low solution viscosity.

In contrast to the corresponding dinitriles, phosphine diacids, RP-$(R'COOH)_2$, are not easily prepared. For this reason direct polyamide synthesis from phosphorus-containing dinitriles was attempted. This technique gave polymers with reasonably high solution viscosities. However, in a direct comparison of the polymerization of bis(2-cyanoethyl)-phenylphosphine oxide or bis(2-carboxyethyl)phenylphosphine oxide with hexamethylenediamine, the diacid route gave better results.

As summarized in Table I, this study has resulted in the preparation of a new series of well-defined polymers containing phosphine units in their backbone structure. Furthermore the previously known series of polyamides containing aromatic phosphine oxide units[3-6] $[—C_4H_4—\overset{\overset{O}{\|}}{P}(R)—C_4H_4—]$ has been extended by us to include methylene phosphine oxide units $[—CH_2\overset{\overset{O}{\|}}{P}(R)CH_2—]$.

Polymer Properties

Softening Temperature and Density. The data presented in Table I indicate that the phosphorus-containing polyamides generally are transparent, light-colored materials. In contrast to regular nylons, they are amorphous and soften at relatively low temperatures. Further analysis of structural effects on softening behavior is presented in the second publication of this series.[24].

The phosphorus polyamides have higher densities than regular nylons (compare polymers 3, 7, and 8 with polymer 2 in Table I). This is somewhat unexpected in view of their amorphous state. The increased density apparently reflects a greater density for the individual polymer chains.

Solubility. Polymer solubility data have been summarized in Table II. The phosphine and phosphine oxide polyamides were found to exhibit a range of solubilities much greater than that of regular nylons. This range of solubility extends from formic acid and cresol, in which virtually all polyamides are soluble to various other less acidic polar solvents. Individual polymers, for example, were found to be soluble in dimethylformamide, ethanol, water, chloroform, and 5% HCl. The greater range of solubility for the phosphorus polyamides over nylons 66 and 76 is due in part to the amorphous character of the phosphorus polyamides. It is known for example that *N*-substituted hydrocarbon polyamides also have greater solubility as a result of reduction of the polar interactions of the

amide linkages. The solubility of the phosphine polyamides in dilute hydrochloric acid is due to the basicity of the phosphorus atom. Similarly, the water solubility of the methylphosphine oxide polyamides results from the tendency of phosphine oxides to form hydrates.[25] Extended solubility range is also exhibited by the amine-containing polyamide.

It was discovered by Dr. B. L. Williams of this laboratory that solutions of poly(bis-3-aminopropylphenylphosphine adipamide) [designated ϕP-66] in formic acid showed a loss in reduced viscosity on standing. A 1% solution of ϕP-66 in formic acid having an initial reduced viscosity of 1.2 (0.1% solution, 30°C.) gave a reduced viscosity of 0.60 after standing at room temperature for 200 hr. The other phosphine polyamides listed in

TABLE III
Adhesive Bond Strengths

Polymer designation	Tensile, psi			Lap shear tension on aluminum, psi	Impact (Izod) on aluminum, ft. lb./in.
	Aluminum	Steel	Copper		
Nylon 66[a]	9700	9900	10,900	3800	0.33
Nylon 610[a]	8300	7700	9,000	3100	0.15
ϕP-66[b]	6500	6200	6,400	4100	0.21
$CH_3P(=O)$-76[c]	5500 (9000)[d]	(5300)[d]	(7000)[d]	(3500)[d]	0.48

[a] Special samples obtained from duPont.

[b] Polyadipamide from $\phi P(CH_2CH_2CH_2NH_2)_2$.

[c] Polyadipamide from $CH_3P(=O)(CH_2)_3NH_2)(CH_2)_4NH_2$.

[d] Dry storage conditions.

Table I showed a similar loss of viscosity to varying (lesser) degrees except for the bis(3-aminopropyl)phenylphosphine polyamides of urea (polymer 19) and dimethyl oxalate (polymer 18). (Numbers in parentheses here and in the following discussion refer to the number given the polymer in the tables.) On the other hand, nylon 66 (polymer 1) and the polyamides containing phosphine oxide, amine (polymer 9) and sulfide linkages (polymer 15) were stable in formic acid. The reason for the apparent instability of the phosphine polyamides in acid has not yet been determined. However, the change in viscosity has been studied sufficiently so that the possibility of a simple deaggregation process was eliminated.

Adhesion. Among the advantages generally claimed in the patent literature for introducing phosphorus into a polymer is improved metal bonding characteristics. It was, therefore, of interest to compare the

adhesive behavior of the phosphorus polyamides with that of regular nylons. Results are given in Table III. It was found that the polyamides generally have high metal adhesive bond strengths. Furthermore the bond strengths are not greatly altered by the introduction of the phosphorus groups. This could result from a masking of the interfacial characteristics of the phosphorus groups by the amide groups. It could also indicate that the bond strengths are not sensitive to the interfacial forces.

TABLE IV
Comparison of Polyamide Mechanical Properties[a]

Polymer	Tensile strength, psi	Elongation, %	Flexural strength, psi	Flexural modulus $\times 10^{-5}$, psi
Nylon 66	10,500[b]	90[b]	—	4
Nylon 610	7,000[b]	90[b]	—	2.6
ϕP-66	5,900	3	13,800	3.7

[a] Except where otherwise indicated these data were obtained by standard methods used in this laboratory.
[b] Data of Floyd.[26]

Mechanical Properties. Comparison of mechanical properties of nylon 66 and nylon 610 with ϕP-66 (see Table IV) shows no major differences except in terms of percentage elongation at the break point.

TABLE V
Thermal Gravimetric Analysis of Adipic Acid Polyamides (Heating in Air)

No.	Comonomer	T_{10}, temp. at 10% weight loss	Total weight loss, %
1	$H_2N—(CH_2)_6NH_2$	415	97
2	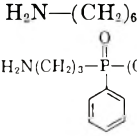	385	80
3	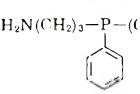	370	85
4	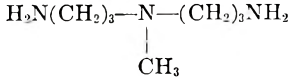	335	79

Adhesive and mechanical test data would seem to indicate minor direct effect by P or P=O. In generalizing on the fiber properties of silicon-containing polyamides, Speck[27] also states that "in general the polyamides

had properties which appeared to be little different from those of their carbon analogs" (although the data on the carbon analog were not disclosed). Low elongation (5%) was also observed for the silicon-containing polymers.

Thermal Stability. The results of thermal stability tests are summarized in Table V in terms of the temperature at which 10% weight loss occurred. The differences between nylon 66 (polymer 1), ϕP-66 (polymer 2), and ϕP-66 (polymer 3) were found to be small. On the other hand CH_3N-66 (polymer 4) was significantly less stable. Lack of thermal stability can account in part for the difficulty of preparing CH_3N-66 polymers of high intrinsic viscosity. A similar lower thermal stability (relative to nylon 66) was noted by Frunze and Korshak[28] for the sulfur-containing polyamides, particularly in the case where an $-SO_2-$ linkage was involved. The authors considered the lower C—S bond strength (61.5 kcal./mole while C—C bond is 80 kcal./mole) to be responsible.

We wish to acknowledge a major contribution from Mrs. K. Loeffler and Miss D. Nenortas in synthesizing the phosphorus monomers. In addition, we are indebted to Mr. D. Wilson and other members of the Chemical Engineering Department as well as Dr. M. Grayson, Dr. M. Rauhut, Miss H. Currier, and Mrs. P. Keough for their contributions in the form of monomers or intermediates. The collaboration of Dr. A. F. Lewis on the adhesive and mechanical behavior work is also acknowledged.

References

1. Childs, A. F., and H. Coates, *J. Oil Colour Chemists Assoc.*, **42**, 612 (1959).
2. Gefter, E. L., *Organophosphorus Monomers and Polymers*, Academy of Sciences of the U.S.S.R., Moscow, 1960.
3. Korshak, V. V., *J. Polymer Sci.*, **31**, 319 (1958).
4. Frunze, T. M., V. V. Korshak, V. V. Kurashev, G. S. Kolesnikov, and B. A. Zhubanov, *Izvest. Akad. Nauk S.S.S.R. Otdel. Khim. Nauk*, **1958**, 783 (1958).
5. Frunze, T. M., V. V. Korshak, and V. V. Kurashev, *Vysokomolekulyarnye Soedineniya*, **1**, 670 (1959).
6. Frunze, T. M., V. V. Korshak, L. V. Kozlov, and V. V. Kurashev, *Vysokomolekulyarnye Soedineniya*, **1**, 677 (1959).
7. Vinogradova, S. V., V. V. Korshak, G. S. Kolesnikov, and B. A. Zhubanov, *Vysokomolekulyarnye Soedineniya*, **1**, 357 (1959).
8. Morgan, P. W., U.S. Pat. 2,646,420, assigned to duPont (1953).
9. Petrov, K. A., and V. V. Parshina, *Zhur. Obshchei Khim.*, **30**, 1342 (1960).
10. Korshak, V. V., G. S. Kolesnikov and B. A. Zhubanov, *Izvest. Akad. Nauk S.S.S.R. Otdel. Khim. Nauk*, **1958**, 618 (1958).
11. (a) H. Niebergall, German Patents 1,086,896, 1,086,897 (1960); (b) Monsanto Chemical Company, Australian Application 60,743/60 (filed March 24, 1960).
12. McCormack, W. B., U.S. Pat. 2,671,077, assigned to duPont (1954).
13. Errede, L. A., and W. A. Pearson, *J. Am. Chem. Soc.*, **83**, 954 (1961).
14. Bloomfield, P. R., paper presented at the International Symposium on Inorganic Polymers, Nottingham, England, July 1961.
15. Mann, F. M., and I. T. Miller, *J. Chem. Soc.*, **1952**, 4453 (1952).

16. Grayson, M., P. Keough, and G. Johnson, *J. Am. Chem. Soc.*, **81**, 4803 (1959).
17. Morgan, P. W., and B. C. Herr, *J. Am. Chem. Soc.*, **74**, 4526 (1952).
18. Coffman, D. D., G. J. Berchet, W. R. Peterson, and E. W. Spanagel, *J. Polymer Sci.*, **2**, 306 (1947).
19. Antony, P. Z., *J. Chem. Educ.*, **36**, 489 (1959).
20. Greenewalt, C. H., U.S. Pat. 2,245,129, assigned to duPont (1941); German Pat. 745,029.
21. Schildknecht, C. E., *Polymer Processes*, Interscience, New York, 1956, p. 239.
22. Batzer, H. von, H. Holtschmidt, F. Wiloth, and B. Mohr, *Makromol. Chem.*, **7**, 82 (1951).
23. Morgan, P. W., and S. L. Kwolek, *J. Chem. Educ.*, **36**, 182 (1959).
24. Pellon, J., *J. Polymer Sci.*, to be published.
25. Kosolapoff, G. M., *Organophosphorus Compounds*, Wiley, New York, 1950, p. 112.
26. Floyd, D. E., *Polyamide Resins*, Reinhold, New York, 1958, p. 12.
27. Speck, S. B., *J. Org. Chem.*, **18**, 1689 (1953).
28. Frunze, T. M., and V. V. Korshak, *Vysokomolekulyarnye Soedineniya*, **1**, 293 (1959).

Synopsis

This study has for the first time provided a series of high molecular weight polymers having trivalent phosphorus in the backbone structure (as phosphine-containing polyamides) and has extended the series of phosphine oxide polyamides beyond the previously disclosed bis(carboxyphenyl)phosphine oxide types. It was found that bulk polymerization rather than solution or interfacial procedures was the preferred method of preparing these materials. The phosphorus polyamides generally were found to be amorphous, relatively low softening materials having an extended solubility range. Most polyamides containing trivalent phosphorus slowly degrade in formic acid solution. A comparison of the thermal stability, adhesive bond strengths, and mechanical behavior of typical polyamides containing phosphine or phosphine oxide groups in their backbone structure to those of analogous regular nylons disclosed no major differences.

Résumé

Cette étude a pour la première fois fourni une série de polymères de haut poids moléculaire renfermant du phosphore trivalent dans la chaîne (comme des polyamides renfermant du phosphore) et la série des polyamides oxyde de phosphore a été étendue au dela des types de bis(carboxyphényl)oxyde de phosphore découvert antérieurement. On a trouvé que la polymérisation en masse était la méthode la plus adéquate de préparation de ces matériaux plutôt que le procédé en solution ou d'interface. On a trouvé que les polyamides de phosphore étaient généralement amorphes, les matériaux à point de ramollissement relativement bas ayant un domaine étendu de solubilité. La plupart des polyamides contenant du phosphore trivalent se dégradent lentement dans une solution d'acide formique. Une comparaison de la stabilité thermique, des forces d'adhésion et du comportement mécanique entre des polyamides typiques renfermant des groupes phosphorés ou des groupes oxydes de phosphore dans leur chaîne et les nylons analogues réguliers ne montrent pas de différences majeures.

Zusammenlassung

In der vorliegenden Arbeit werden zum ersten Mal eine Reihe hochmolekularer Polymerer mit dreiwertigem Phosphor in der Hauptkette (als phosphinhältige Polyamide) beschrieben und die Reihe Mer Phosphinoxydopolyamide über die früher endeckten Bis-(Carboxyphenyl)-phosphinoxydtypen hinaus erweitert. Es wurde gefunden, dass die Polymerisation in Substanz für die Herstellung dieser Materialien besser geeignet ist als Lösungs- oder Grenzflächenverfahren. Die Phosphorpolyamide

waren allgemein amorphe Stoffe mit relativ niedrigem Erweichungspunkt und einem weiten Löslichkeitsbereich. Die meisten Polyamide mit dreiwertigem Phosphor wurden in ameisensaurer Lösung langsam abgebaut. Ein Vergleich der thermischen Beständigkeit, der Klebefestigkeit und des mechanischen Verhaltens von typischen Polyamiden mit Phosphinoder Phosphinoxydgruppen in der Hauptkette mit denen des analogen regulären Nylons ergab keine growen Unterschiede.

Received October 23, 1961
Revised December 12, 1961

JOURNAL OF POLYMER SCIENCE: PART A VOL. 1, PP. 877–893 (1963)

Study of the Rate of Heterogeneous Polymerization of Methyl Acrylate in Aqueous Solution

TILAK GUHA* and SANTI R. PALIT,
Indian Association for the Cultivation of Science, Calcutta, India

Introduction

Water is a moderate solvent for some vinyl monomers, such as methyl methacrylate, methyl acrylate, acrylonitrile, and vinyl acetate, but is a poor solvent for the polymers. During the solution polymerization of these monomers in an aqueous medium, the polymers separate in the form of an insoluble phase and make the process typically heterogeneous in nature. The physical state of the insoluble phase is initially colloidal, and it changes via a coarse latex to a compact precipitate on increasing progressively the ionic strength of the medium. We have observed in the case of methyl methacrylate that the rate of polymerization in this system strongly depends on the physical state of the insoluble phase.[1] Similar dependence has been observed in the case of methyl acrylate polymerisation also. The present paper reports the results for the latter and discusses the possible reasons for a dependence of the kinetics of heterogeneous vinyl polymerization in aqueous medium on the physical state of the separated polymer phase.

EXPERIMENTAL

The monomer, methyl acrylate (obtained from the N.C.L. Poona, India), was freed from the inhibitors by the usual procedure of washing with dilute alkali and was fractionated before use in a stream of oxygen-free nitrogen. A water-soluble redox pair, potassium persulfate ($K_2S_2O_8$) and sodium hyposulfite ($Na_2S_2O_4$), both of analytical reagent quality (supplied by E. Merck), was used for the polymerization. All experiments were carried out in an atmosphere of nitrogen in a flask system which was a slightly modified form of that used by Baxendale et al.[2] The percentage conversion of the monomer was determined by weighing the polymer formed at different intervals. The polymer was coagulated out from a known volume of the latex by adding to it a small quantity of saturated sodium chloride solution followed by hydrochloric acid. The polymer was filtered in a

* Present address: Chemical Engineering Department, Birmingham University, England.

sintered-glass crucible, washed with hot water, and dried at 50°C. *in vacuo*, and weighed.

In typical experiments the percentage polymerization with time was recorded (*a*) with various ratios of persulfate and hyposulfite, the concentration of one (either of the persulfate or of hyposulfite) being kept constant (*b*) with different percentages of organic emulsifiers and inorganic electrolytes, (*c*) with different monomer concentrations, and (*d*) with the addition of different organic solvents into the system. The molecular weight of the polymer was measured by determining the intrinsic viscosity value $[\eta]$ of the polymer dissolved in benzene. The coagulation value of the latex was measured in each experiment to acquire some idea regarding the degree of dispersion and stability of the dispersed phase with progress of polymerization under different conditions. A known volume of an aqueous solution of an electrolyte of gradually diluted strength was added to a known volume of the latex of approximately 2% solid content and the liminal strength of the electrolyte expressed in millimoles/liter was recorded as the coagulation value of the latex.

RESULTS

Effect on Rate of Initiator Concentration

Figures 1 and 2 show two sets of typical results of polymerization of methyl acrylate in a dilute aqueous solution (2%) initiated by systematic variation of the concentration of one of the redox pair keeping the other constant. In Figure 1 the concentration of persulfate has been varied from 0.01% to 1.0% that of hyposulfite being kept constant at 0.01%; in Figure 2 the hyposulfite concentration has been varied from 0.01% to 1.0%, and persulfate is fixed at 0.01%. The initial rates have been calculated from the slopes at the origin of these plots. In heterogeneous polymerization, however, the rate at the stage when sufficient amount of polymer has separated in the form of an insoluble phase is worth studying. The percentage yield of polymer after 30 min. of polymerization has been used to represent such a rate in an indirect way. In Figure 3 the initial rate as well as the per cent yield after 30 min. of polymerization have been plotted against the square root of the product of redox pair concentrations. From the figures it is evident that the initial speed of polymerization is enhanced on increasing the concentration of either of the redox pair. The deceleration in a given run, however, starts earlier on increasing the concentration of the initiators beyond 0.1% as a result of which the plots of yield versus time at higher catalyst concentrations cross those at lower catalyst concentrations. This peculiar retardation of the rate by higher initiator concentrations is also evident from Figure 3, where the per cent yield after 30 min. of polymerization suffers a fall on increasing the initiator strength in the medium. Another observation which has been made in parallel with the rate measurement at various ratios of the redox initiators is a loss in the colloidal insoluble phase, initially separating in the medium, with higher

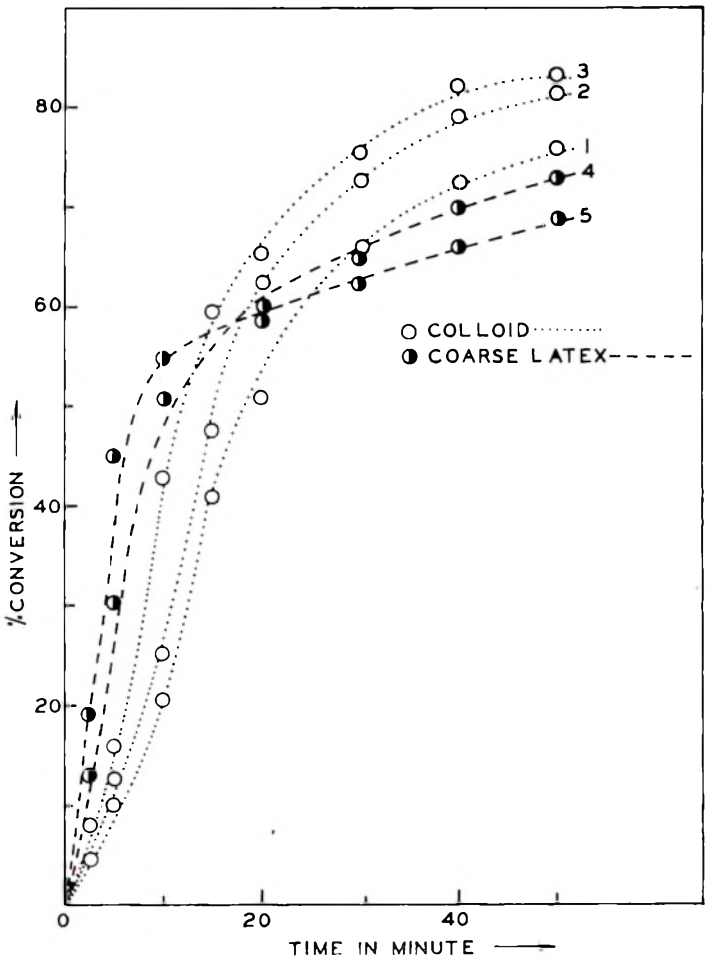

Fig. 1. Conversion vs. time plot for 2% aqueous methyl acrylate solution at fixed concentration of hyposulfite (0.01%) and varying concentration of persulfate: (*1*) 0.01%; (*2*) 0.05%; (*3*) 0.10%; (*4*) 0.50%; (*5*) 1.0%.

concentrations of the initiators. Table I reports the coagulation values of the latex measured at different intervals and the average rate of the heterogeneous polymerization, represented by the per cent yield after 30 min. of polymerization.

It is evident from the results that a high average rate of polymerization is in parallel with the production of a stable sol. Increase of the initiator concentration effects a coagulation of the latex with the attendant fall in the rate. A few experiments have been carried out in which a fresh quantity of initiator is added into the system at different stages of the polymerization. Figure 4 shows the typical results obtained by adding a given volume (15 ml. to 200 ml. of polymerizing medium) of 1% $K_2S_2O_8$ solution near the start and at the middle of the polymerization. It is evident that fresh addition of the initiator near the beginning of the polymerization, en-

TABLE I
Monomer: Methyl Acrylate (2%); Activator: Sodium Hyposulfite (0.01%)

Catalyst (persulfate), %	Yield at 30 min. polymerization, %	Coagulation value of the latex, mmoles/l. of $MgSO_4$ at different intervals.		
		5 min.	15 min.	30 min.
0.01	67	20	15	10
0.05	72	27	14	6
0.10	76	25	10	3
0.50	68	22	10	2
1.00	64	16	7	1.5

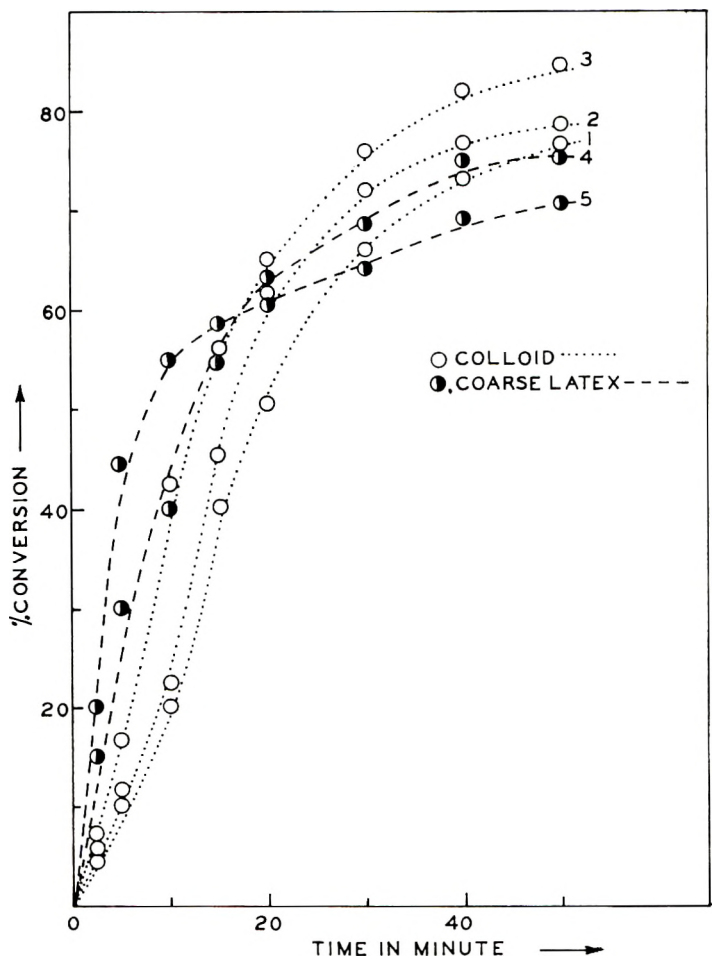

Fig. 2. Conversion vs. time plot for 2% aqueous methyl acrylate solution at fixed concentration of persulfate (0.01%) and varying concentration of hyposulfite: (*1*) 0.01%; (*2*) 0.05%; (*3*) 0.10%; (*4*) 0.50%; (*5*) 1.0%.

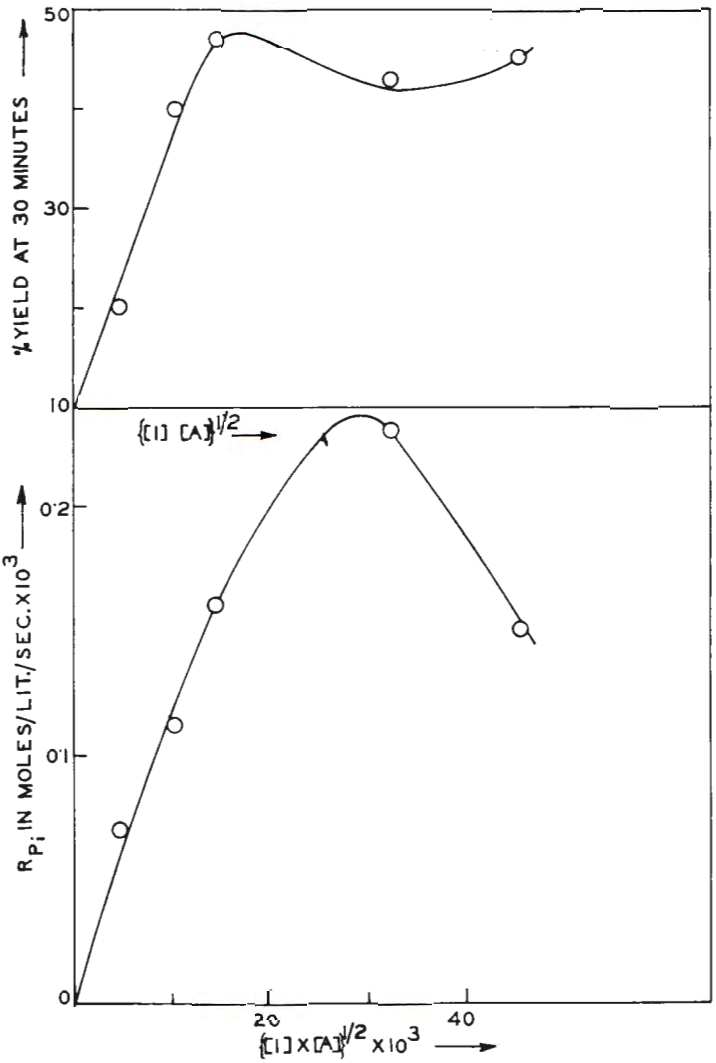

Fig. 3. Plot of initial rate and yield after 30 min. polymerization vs. square root of the product of redox pair concentration.

hances the rate, whereas the addition at the middle stage does not increase the rate but shows on the other hand a slight depressing action on it.

Effect on Rate of Neutral Electrolytes and Emulsifiers

Addition of neutral salts has been found by a few investigators[3] to depress the rate of a redox polymerization in an aqueous medium. A similar effect has also been observed in this case too. Figure 5 shows the typical results obtained by adding increasing quantity of an electrolyte, such as sodium chloride, into a polymerization initiated by 0.01% $K_2S_2O_8$ and 0.01% $Na_2S_2O_4$. It is evident that the rate of polymerization increases first

on slight addition of the electrolyte, falls off rapidly on further increase of electrolyte concentration, and eventually rises again in the region of very high salt concentration (~1.0%). A parallel examination on the physical nature of the medium has revealed that on addition of a small amount of salt the insoluble phase becomes more dispersed but rapidly coarsens to a thick latex on increasing the salt concentration and eventually coagulates to a

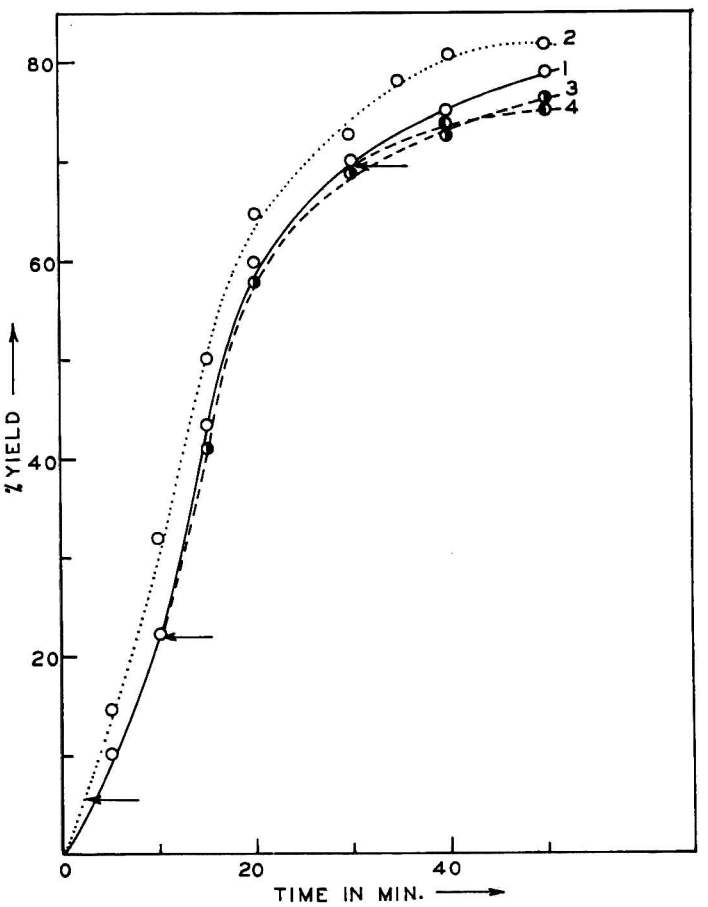

Fig. 4. Conversion vs. time plots on fresh addition of initiator (persulfate) at intermediate stages of polymerization: (*1*) blank; (*2*) initiator added near the start; (*3*) initiator added at 10 min. polymerization; (*4*) initiator added at 300 min. polymerization.

precipitate when the salt concentration reaches 1.0%. Thus the yield of polymer is high when the insoluble polymer phase remains as a stable colloid, becomes lower on the conversion of the colloid to a coarse latex, and rises again on the precipitation of the latex. A similar observation was made in the case of methyl methacrylate polymerization in aqueous medium by the same redox system.[1]

Organic emulsifiers, when added even in a very small amount below their critical micelle concentration, are known to increase the rate of a heterogeneous polymerization in an aqueous medium.[2,3] The effect has been

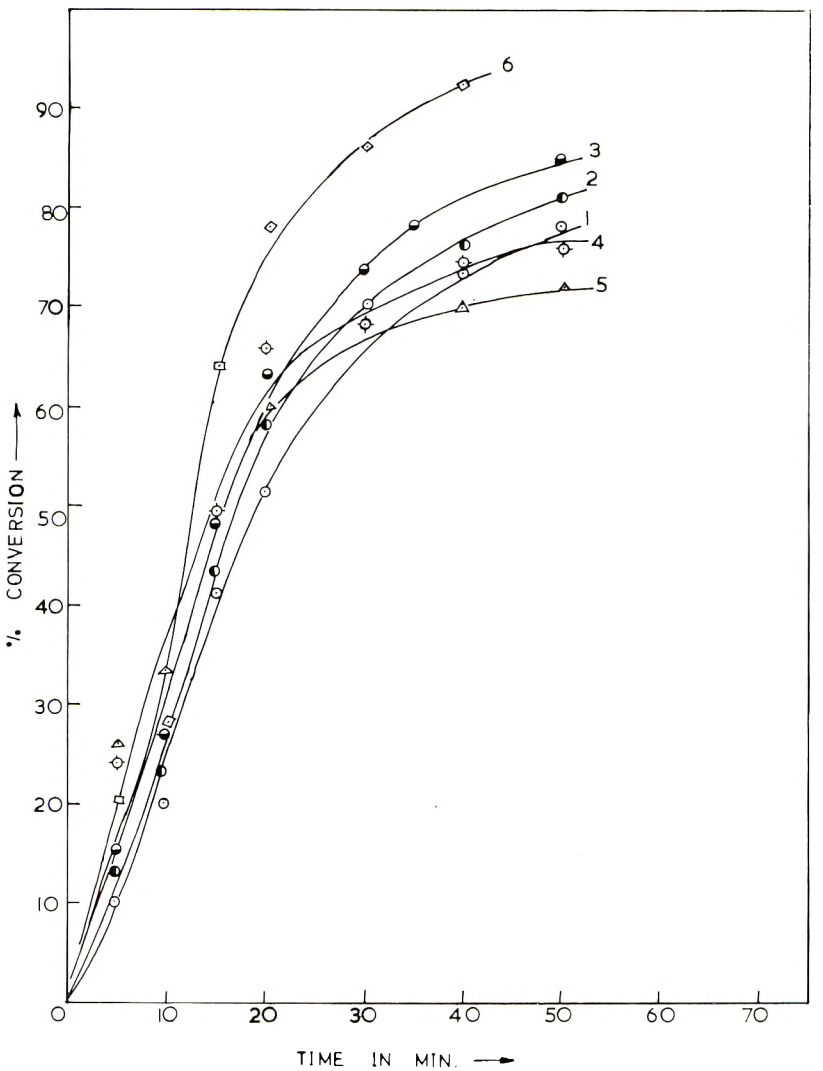

Fig. 5. Conversion vs. time plots at varying concentrations of NaCl in the medium in a polymerization initiated by 0.01% persulfate and 0.01% hyposulfite: (*1*) blank (colloid); (*2*) 0.005% NaCl (colloid); (*3*) 0.01% NaCl (colloid); (*4*) 0.1% NaCl (thick latex); (*5*) 0.5% NaCl (thick latex); (*6*) 1.0% NaCl (precipitate).

found to be the same in this case too. Very low concentration (0.005%) of Cetavalon increases the yield of polymer to 80% in 50 min. of polymerization from the normal yield of 60% without it, the catalyst concentration being 0.01% $K_2S_2O_8$ and 0.5% $Na_2S_2O_4$.

Effect on Rate of Monomer Concentration

At fixed concentrations of the persulfate and hyposulfite, the concentration of the dissolved monomer has been varied from 0.65% to 5.0% at 35°C. The percentage polymerization after 30 min. reaction has been plotted against the initial monomer concentration in the system at different ratios of persulfate and hyposulfite and is shown in Figure 6.

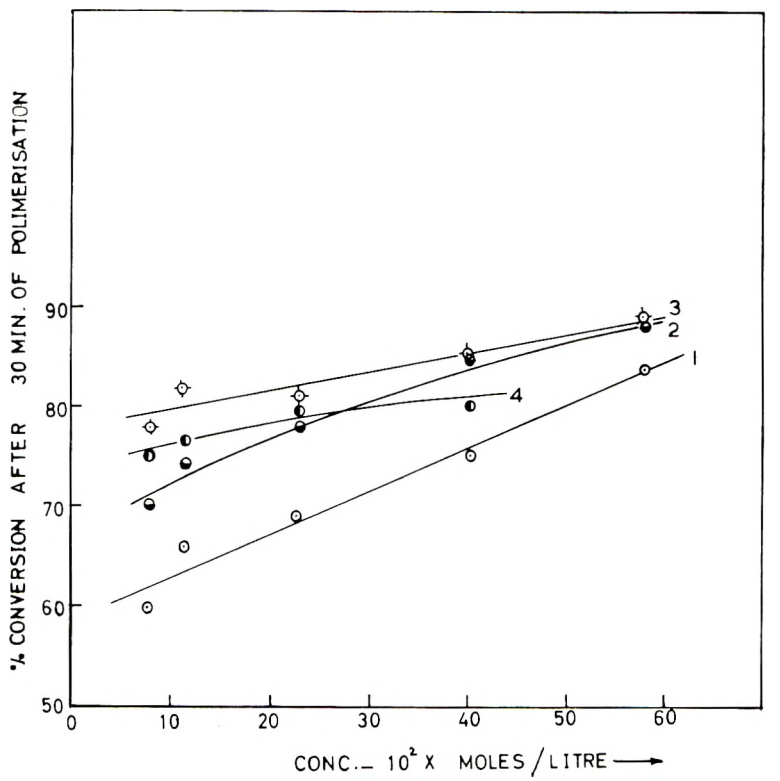

Fig. 6. Conversion after 30 min. polymerization vs. monomer concentration in solution in a polymerization with fixed concentration of hyposulfite (0.01%) and varying concentration of persulfate: (*1*) 0.01%; (*2*) 0.05%; (*3*) 0.5%; (*4*) 1.0%.

It will be evident that at a low concentration of the initiators the polymerization rate depends more or less linearly on the concentration of the dissolved monomer. Increase of the ratio of the redox components reduces the degree of dependence of the rate on the monomer concentration.

The physical state of the insoluble phase has been observed to be highly dense in the region of high monomer and high catalyst concentrations. The coagulation value of the latex rapidly falls off from 15 mmoles/l. to nearly 5 mmoles/l. of $MgSO_4$ at a monomer concentration of 5% and initiator ratio of 0.1% $K_2S_2O_8$:0.01% $Na_2S_2O_4$.

Effect on Rate of Organic Solvents

The heterogeneous polymerization has been observed to be peculiarly sensitive to the presence of a small quantity of organic solvent in the medium when the insoluble phase exists as a fine colloid. Much higher amount of the same solvents is required to show any effect when the phase is a thick latex or a coagulum.

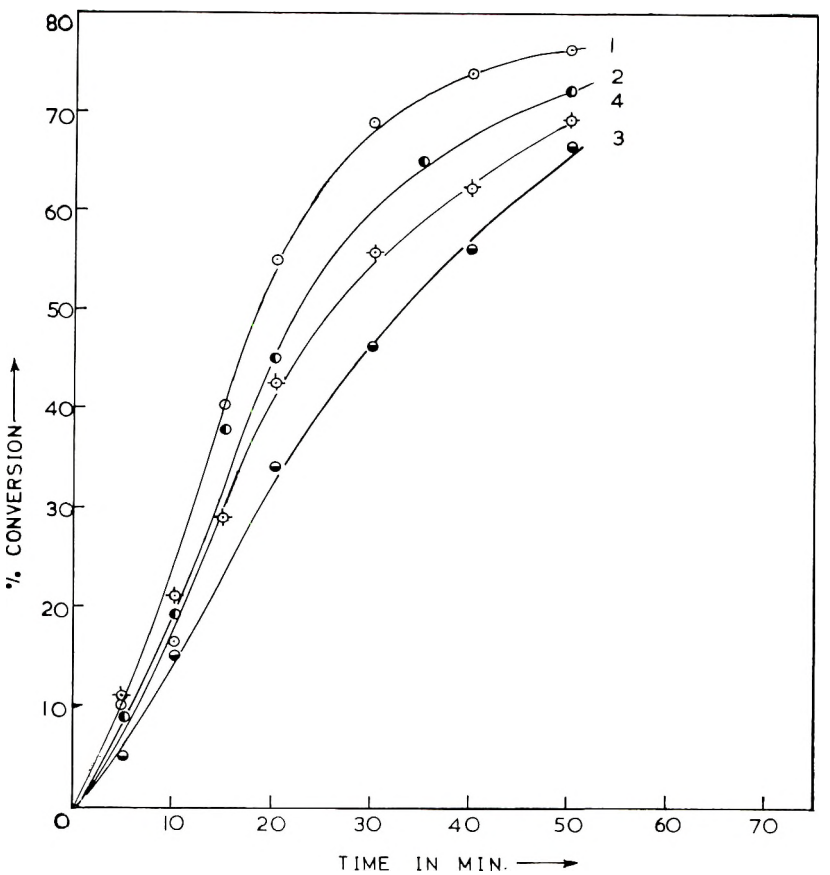

Fig. 7. Effect of different solvents on concentration vs. time in a polymerization initiated by 0.01% persulfate and 0.01% hyposulfite: (*1*) blank; (*2*) ethylene glycol, 3% (v/v); (*3*) dimethylformamide, 3% (v/v); (*4*) benzene, 3% (v/v).

Thus we have seen that addition of 5% by volume of a solvent such as ethanol or ethylene glycol, which have more affinity for the aqueous phase than the polymer phase, dimethylformamide, which has affinity both for water and the vinyl polymer, and benzene which has affinity mostly for the insoluble organic phase in the aqueous medium, remarkably depress the rate. Dimethylformamide, however, is more active rate retarder than the alcoholic solvents, and benzene starts to affect the rate only when a sufficient quantity of insoluble polymer has accumulated in the medium.

Figure 7 shows the results obtained on adding the different solvents to a polymerization intiated by 0.01% $K_2S_2O_8$ and 0.01% $Na_2S_2O_4$.

Molecular Weight and Rate of Polymerization

The intrinsic viscosity [η] of the polymer in benzene has been used as an indication of the molecular weight in this study. It has been observed that [η] of the polymer falls only slightly on increasing the initiator concentration in the medium till the insoluble phase exists as a stable colloid in the medium. In a thick latex phase, the [η] drops appreciably on increasing the initiator concentration. At a fixed initiator concentration, addition of a small quantity of a neutral salt increases the polymer molecular weight in parallel with the polymerization rate but both the rate and molecular weight drop off rapidly on progressive increase in the salt concentration. Tables II and III report typical results.

TABLE II
Monomer: Methyl Acrylate (2%); Temperature: 35°C.; $Na_2S_2O_4$: 0.01%

$K_2S_2O_8$, %	Coagulation value of the latex after 20 min. polymerization, mmoles/l. $MgSO_4$	[η], cc./gm.
0.005	10	2.4
0.008	12	2.3
0.010	15	2.2
0.030	14	1.9
0.050	12	1.7
0.080	10	1.5
0.100	8	1.3
0.500	5	1.1

TABLE III
Monomer: Methyl Acrylate (2%); $K_2S_2O_8$: 0.01%; $Na_2S_2O_4$: 0.01%

NaCl, %	Yield after 30 min. polymerization, %	[η], cc./gm.
—	68	2.2
0.005	72	2.4
0.010	74	2.8
0.050	79	2.9
0.100	69	2.5
0.500	65	2.0

Heterogeneous Polymerization of Methyl Acrylate and Methyl Methacrylate

On comparing the polymerization characteristics of methyl acrylate and methyl methacrylate in a dilute aqueous solution initiated by the redox initiator $K_2S_2O_8/Na_2S_2O_4$ it has become evident that methyl acrylate polymerizes faster than methyl methacrylate in this system at the same

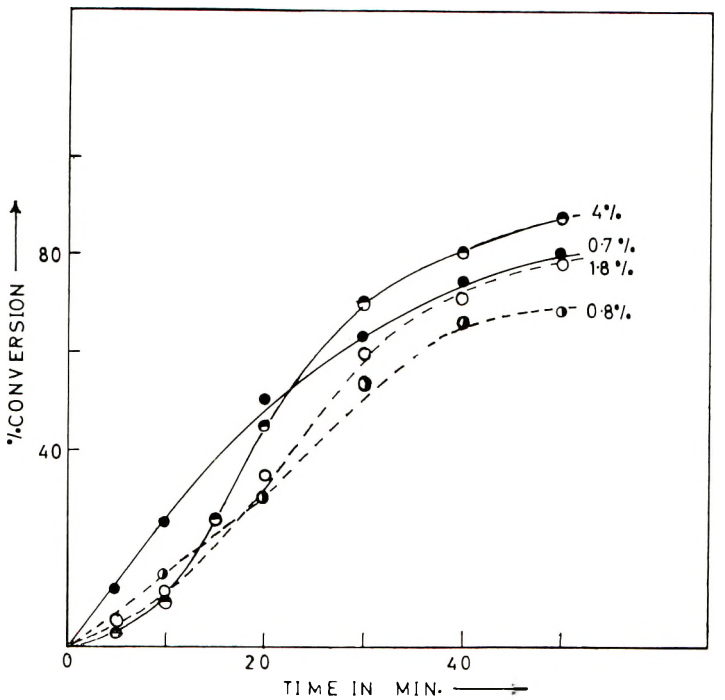

Fig. 8. Conversion vs. time plots for polymerization of methyl acrylate and methyl methacrylate initiated by 0.01% persulfate and 0.01% hyposulfite: (○), (◑) methyl methacrylate; (◓), (●) methyl acrylate.

monomer and initiator concentration. Figure 8 shows the results of the comparative study. It has also been observed in this context that the insoluble phase of poly(methyl acrylate) (PMA) remains as a more stable colloid in the aqueous medium over a wide range of the redox pair concentrations than that of poly(methyl methacrylate) (PMMA). In fact, the stability of the latter as a dispersed phase in aqueous medium is so low that the coagulation value can be measured by sodium sulfate, whereas for poly(methyl acrylate) the coagulation value is too high with sodium sulfate and a bivalent salt such as magnesium sulfate should preferably be used.

TABLE IV

		Coagulation value of the latex after 20 min. polymerization	
$K_2S_2O_8$, %	$Na_2S_2O_4$, %	PMMA, mmole/l. Na_2SO_4	PMA, mmole/l. $MgSO_4$
0.01	0.01	2.6	15
0.03	0.01	2.3	
0.05	0.01	1.9	12
0.10	0.01	Ppt.	10
0.30	0.01	Ppt.	8

Table IV reports the coagulation values of the latex produced in the two cases at different ratios of the redox pair.

DISCUSSION

From the above survey it is thus evident that the polymerization kinetics of methyl acrylate in aqueous medium are influenced by the physical state of the insoluble polymer phase. It may be quite possible, as has been pointed out by Breitman,[4] that the change in the number and size of the insoluble particles accompanying the variation of the physical state of the separated phase effects the changes in the polymerization kinetics. A stable colloid consisting of fine particles in large number, well protected from undergoing coagulation by a strong interface, is an ideal insoluble phase to give rise to the kinetics of an emulsion polymerization.[5] A thick latex may be supposed to consist of particles large in size and small in number, evidently due to coagulation among the fine particles of the initial colloid. Increase in size permits the coexistence of more than one radical in a suspended particle and effects a transition to the kinetics of a suspension polymerization. The overall rate falls partly due to this transition and partly due to smaller number of radicals in the system because of the interparticle coagulation.[6] When precipitation takes place, the increase in rate and molecular weight may be due to the production of "trapped" radicals in the system.[7]

On the basis of the above view, the effects of the initiators, coagulants, emulsifiers, monomers, and organic solvents on the polymerization rate may be explained in the following way.

Rate Dependence on Initiators, Coagulants, and Peptizers

Enhancement of the initial rate by increase in the concentration of either of the redox pair is due to the existence of the reaction locus in the aqueous phase at the start of the polymerization. The faster the rate of radical production, the higher will be the rate of the dissolved monomer consumption. A square root dependence of the initial rate on the product of ($S_2O_8^=$) and ($S_2O_4^=$) indicates a bimolecular reaction between the redox components as the initiation step and a bimolecular reaction among the growing radicals as the termination step.[8] Rapid deceleration of the polymerization rate, at early stages, in the region of high concentrations of the redox initiators may be due to progressively increased coagulation of the dispersed phase onto which the polymerization locus shifts after sufficient accumulation of the insoluble polymer in the medium. This coagulating action of the initiators at high concentration may be expected, because they are typical electrolytes themselves as well as the products of their redox reaction, viz., K_2SO_4, Na_2SO_4 etc. Electron microscopic study of the latex in such a heterogeneous polymerization initiated by the $ClO_3^-/SO_3^=$ redox pair has shown the increase in particle size of the insoluble phase on increasing the initiator concentration.[9] When added fresh at an inter-

mediate stage of a polymerization, the initiators do not increase the reaction rate when the insoluble phase is a stable colloid; rather, it slightly depresses the rate (Fig. 4). This indicates the absence of the reaction locus in the aqueous phase and the independence of the reaction rate localized in the insoluble colloidal phase, of the rate of radical production in the external aqueous phase.[10] The slight rate-depressing action of the fresh charge of catalyst is due to its coagulating influence on the colloidal particles.

Addition of electrolytes, such as NaCl, increases the ionic strength in the medium. The result will be a loss of dispersion stability of the colloid, which is evidently charge stabilized in the medium, and the rate will fall because of the decrease in number and increase in size of the suspended particles. Added emulsifiers will stabilize the fine particles and hence keep the rate and molecular weight high.[11]

Rate Dependence on Monomer

The rate dependence on monomer in a heterogeneous polymerization is determined by the distribution of the polymerization locus in the medium and the relative concentration of the monomer at the different loci. In the case of this monomer, methyl acrylate, the locus of polymerization may exist either in water or in the insoluble polymer phase because the monomer has affinity for both of them. The extent to which the locus is distributed between the two phases depend on the relative affinity of the monomer for the two as well as on the rate of partition of the monomer between the phases. Initially, the monomer is present homogeneously distributed in the aqueous phase and the polymerization locus exists in it. As soon as the polymer separates as an insoluble phase, there is started a competition between itself and the aqueous phase for the monomer. When the insoluble phase is a stable colloid, the size of the polymer particles is very fine, and the rate of diffusive transfer of the monomer to the insoluble particles is consequently low. As a result, the locus of polymerization shifts slowly from the aqueous phase to the insoluble phase, and it may be possible for a simultaneous existence of two loci in the medium in a sol-phase polymerization. The homogeneous aqueous phase polymerization will depend on the dissolved monomer concentration as usual. The heterogeneous polymer-phase polymerization will also depend on the monomer concentration, probably because of the following reason. The stable colloid consisting of a large number of fine particles will contain a large number of free radicals (nearly half the number of particles). The rate of monomer consumption in the colloidal phase will be very high, as a result of which the rate of monomer diffusion to this phase may become the rate-controlling step. Thus, the polymerization in either of the two loci, aqueous phase and the colloidal polymer phase, being monomer-dependent, the overall rate of polymerization in the region of low monomer and initiator concentrations depends on the monomer concentrations in the medium. In the region of high monomer concentration, the locus of polymerization rapidly shifts to

the insoluble phase where the degree of monomer dependence of the rate is relatively less. When the initiator concentration is increased, the colloidal phase of the insoluble polymer becomes an unstable latex consisting of a small number of large size particles. The rate of diffusive transfer of the monomer dissolved in the aqueous phase to the suspended large particles becomes high, and this favors a faster shift of the polymerization locus to the dispersed phase. The rate of monomer consumption at the latter, however, will not be high because of the smaller number of radicals present in the unstable latex phase. Consequently, the rate will not depend on the transfer rate of monomer to the insoluble phase, and as the latter is well loaded with the monomer, the rate shows a very small dependence on the monomer concentration (nearly zero order) in the region of high initiator concentration.

Effect of Organic Solvents

The retardation of the rate by solvents which are polymer precipitants like water, such as ethanol or glycol, seems difficult to explain. It is, however, known that addition of low molecular weight alcohols or ketones having strong affinity for water to a hydration-stabilized organic colloid (lyophilic) in an aqueous medium reduces the thickness of the stabilizing hydration layer and makes the colloid unstable. The colloidal stability of insoluble poly(methyl acrylate) in aqueous medium is usually very high, and a hydration stabilization of this organic phase may be supposed in view of the less sensitivity of this colloid to a wide range of electrolyte concentration (Table IV). Ethanol or glycols may therefore be supposed to reduce the rate of the sol-phase polymerization by affecting the dispersion stability of the colloidal phase in the aqueous environment. It is worth mentioning in this context that these alcoholic solvents have been observed not to affect the rate of polymerization of methyl methacrylate in aqueous solution.[12] This, in our view, is due to the small influence of water in stabilizing the colloid of poly(methyl methacrylate). The stability of the dispersed phase of this polymer is due to the adsorbed ions in solution and this is also evident from the sensitivity of the colloid to the electrolyte concentration in the medium (Table IV). Low molecular weight hydroxylic organic solvents will not affect the stability of such charged, stabilized hydrophobic colloids and hence very little affect the rate of polymerization in such a phase.

Solvents such as dimethylformamide and benzene have strong affinity for the polymer. In heterogeneous polymerizations where the polymer separates as a solid precipitate, addition of polymer solvents reduces the rate.[7] This is because of the decrease in "trapped" radical concentration in the medium. The solvent reduces the strength of the physical barrier of the solid aggregates to the bimolecular termination of the occluded radicals. This mechanism, however, may not hold good in this system where the insoluble polymer particles are suspended, and hence the state of aggregation is very loose. It may be supposed, however, that these solvents

soluble in the polymer compete with the monomer for the separated polymer phase. They may act as diluents in lowering the monomer activity in the dispersed phase and hence lower the rate of polymerization located in the polymer phase.

Polymerization of Methyl Acrylate and Methyl Methacrylate

The heterogeneous polymerization of methyl acrylate in aqueous medium is faster than that of methyl methacrylate. The higher colloidal stability of poly(methyl acrylate) in water may be the possible reason. Table IV shows the wide range of the initiator concentrations possible to maintain in the medium without affecting the physical state of the dispersed polymer phase in the case of methyl acrylate. The greater hydrophilic/hydrophobic ratio in the structure of poly(methyl acrylate) than that of poly(methyl methacrylate) may account for the higher stability of the former as a colloid; in addition to charge stabilization, a hydration layer may impart stability to the suspended particles of poly(methyl acrylate).

Conclusion

It appears, thus, that the rate of heterogeneous polymerization of a vinyl monomer in aqueous medium is not only determined by the relative affinity of the monomer for the polymer and the aqueous phase but also by the physical state of insoluble polymer phase. The latter depends on the polarity and structure of the polymer. If the physical state of the polymer phase is too sensitive to external conditions and varies on a slight change of the latter, the kinetics may appear to be highly anomalous. Usually an insoluble polymer whose monomer is soluble in water, varies from a colloid via a coarse latex to a compact precipitate. Accordingly, it may be possible to encounter in such a system the kinetics of an emulsion polymerization, a homogeneous "suspension" polymerization, or that of a typical "explosive" polymerization.

References

1. Palit, S. R., and T. Guha, *J. Polymer Sci.*, **34**, 243 (1959).
2. Baxendale, J. H., M. G. Evans, and J. K. Kilham, *Trans. Faraday Soc.*, **42**, 668 (1946).
3. Thomas, W. M., E. H. Gleason, and G. Mino, *J. Polymer Sci.*, **24**, 43 (1957).
4. Breitman, L., discussion in *J. Polymer Sci.*, **34**, 250 (1959).
5. Smith, W. V., and R. H. Ewart, *J. Chem. Phys.*, **16**, 592 (1948).
6. Evans, M. G., *J. Chem. Soc.*, **1947**, 266.
7. Bamford, C. H., and A. D. Jenkins, *Proc. Roy. Soc. (London)*, **A228**, 220 (1955).
8. Roskin, E. S., *Zhur. Priklad. Khim.*, **30**, 1030 (1957).
9. Stannett, V., *J. Polymer Sci.*, **21**, 343 (1951).
10. Bovey, F. A., I. M. Kolthoff, A. I. Medalia, and E. J. Meehan, *Emulsion Polymerization*, High Polymer Series, Vol. IX, Interscience, New York–London, 1955, p. 198.
11. Allen, P. W., *J. Polymer Sci.*, **31**, 206 (1958).
12. Guha, T., D. Phil. thesis, Calcutta University (1960).

Synopsis

Study of the heterogeneous polymerization of methyl acrylate in dilute aqueous solution in a redox-initiated system consisting in $Na_2S_2O_4$–$K_2S_2O_8$ reveals the fact that the initial rate of polymerization increases with the increase in concentration of either of the redox pair. The rate, however, suffers a rapid deceleration in the course of polymerization in the region of high concentrations of the catalysts. At a low concentration of the initiators, addition of a small quantity of neutral electrolyte increases the rate, which falls off rapidly on further increase of the electrolyte concentration. Addition of emulsifiers in a concentration less than their critical micelle concentration in water remarkably increases both the rate and the molecular weight. The rate of polymerization depends more or less linearly on monomer concentration when the concentration of the initiators is low in the medium. A monomer dependence tending to zero order is found when the catalyst concentration is high. Water-soluble alcohols and glycols lower the rate when the insoluble phase in the heterogeneous polymerization is a stable colloid. Solvents such as dimethylformamide and benzene, which have strong affinity for the polymers produced in the medium, also reduce the rate. The peculiarities in the rate of this heterogeneous polymerization seem to be connected with the physical state of the insoluble polymer phase. The latter depends mainly on the ionic strength of the aqueous medium. At a low concentration of electrolytes, which may be either a neutral salt or water soluble electrolytic initiators such as $K_2S_2O_8/Na_2S_2O_4$, the insoluble phase is a stable colloid which changes via an unstable latex to a coarse precipitate on progressive increase of the electrolyte concentration in the medium. It appears that a kinetics similar to that of an emulsion polymerization operates when the insoluble phase is a stable colloid, suspension polymerization kinetics hold good when the insoluble phase is an unstable latex, and the kinetics of a typical "explosive" polymerization is the mechanism when the insoluble phase precipitates.

Résumé

L'étude de la polymérisation hétérogène de l'acrylate de méthyle en solution aqueuse diluée par un système initiateur redox consistant en $Na_2S_2O_4$–$K_2S_2O_8$ met en lumière le fait que la vitesse initiale de polymérisation augmente avec l'augmentation de concentration de l'un ou l'autre composant du système redox Toutefois la vitesse subit une décélération rapide dans le cours de la polymérisation dans la région des concentrations élevées en catalyseur. A basse concentration en initiateur, l'addition de petites quantités d'éléctrolyte neutre augmente la vitesse qui retombe rapidement quand on augmente ensuite la concentration en électrolyte. L'addition d'emulsifiant en concentration inférieure à leur C.M.C. dans l'eau, augmente remarquablement et la vitesse et le poids moléculaire. La vitesse de polymérisation dépend de façon plus ou moins linéaire de la concentration en monomère lorsque la concentration en initiateur est faible dans le milieu. On a trouvé une dépendance du monomère tendant vers un ordre zéro lorsque la concentration en catalyseur est élevée. Les alcools solubles dans l'eau et les glycols abaissent la vitesse lorsque la phase insoluble dans la polymérisation hétérogène est un colloïde stable. Des solvants tels que le diméthylformamide et le benzène, qui possèdent une forte affinité pour les polymères produits dans le milieu, diminuent également la vitesse. Les particularités au cours de la vitesse de cette polymérisation hétérogène semblent être en relation avec l'état physique de la phase polymérique insoluble. Celui-ci dépend surtout de la force ionique du milieu aqueux. A basse concentration en électrolyte, qui peut être soit un sel neutre, soit un initiateur électrolytique soluble dans l'eau comme $K_2S_2O_8/Na_2S_2O_4$, la phase insoluble est un colloïde stable qui passant par un latex instable devient un précipité grossier par augmentation progressive de la concentration en électrolyte dans le milieu. Il semble qu'une cinétique semblable à celle d'une polymérisation en émulsion se produit lorsque la phase insoluble est un colloïde stable; une cinétique de polymérisation en suspension convient bien lorsque la phase insoluble est un latex instable at la cinétique d'une polymérisation typiquement "explosive" semble être le mécanisme lorsque la phase insoluble précipite.

Zusammenfassung

Die Untersuchung der heterogenen Polymerisation von Methylacrylat in verdünnter wässriger Lösung mit einem Redoxstartersystem, das aus $Na_2S_2O_4$–$K_2S_2O_8$ bestand, ergab, dass die Anfangspolymerisationsgeschwindigkeit mit zunehmender Konzentration eines jeden der beiden Bestandteile des Redoxpaares zunimmt. Im Bereich hoher Katalysatorkonzentrationen nimmt jedoch die Geschwindigkeit im Verlauf der Polymerisation rasch ab. Bei einer kleinen Starterkonzentration erhöht der Zusatz einer geringen Menge eines neutralen Elektrolyten die Geschwindigkeit, die bei weiterer Erhöhung der Elektrolyten die Geschwindigkeit, die bei weiterer Erhöhung der Elektrolytkonzentration rasch abfällt. Ein Zusatz von Emulgatoren in einer kleineren Konzentration als der C.M.C. in Wasser erhöht bemerkenswerterweise sowohl die Geschwindigkeit als auch das Molekulargerwicht. Ist die Starterkonzentration im Medium gering, so hängt die Polymerisationsgeschwindigkeit mehr oder weniger linear von der Monomerkonzentration ab. Bei hoher Katalysatorkonzentration wird eine Monomerabhängigkeit gefunden, die gegen nullte Ordnung geht. Wasserlösliche Alkohole und Glykole verringern die Geschwindigkeit, wenn die unlösliche Phase bei der heterogenen Polymerisation ein stabiles Kolloid ist. Lösungsmittel wie Dimethylformamid und Benzol mit grosser Affinität für die in dem Medium gebildeten Polymeren setzen ebenfalls die Geschwindigkeit herab. Die Eigentümlichkeiten der Geschwindigkeit dieser heterogenen Polymerisation scheinen mit dem physikalischen Zustand der unlöslichen Polymerphase in Beziehung zu stehen. Dieser hängt hauptsächlich von der Ionenstärke des wässrigen Mediums ab. Bei geringer Konzentration an Elektrolyten, die entweder ein Neutralsalz oder wasserlösliche elektrolytische Starter wie $K_2S_2O_8/Na_2S_2O_3$ sein können, ist die unlösliche Phase ein stabiles Kolloid, bei fortschreitender Zunahme der Elektrolytkonzentration im Medium wandelt sie such über einen instabilen Latex in einen groben Niederschlag um. Ist die unlösliche Phase in stabiles Kolloid, so scheint eine Kinetik ähnlich der einer Emulsionspolymerisation wirksam zu sein, ist sie ein instabiler Latex, so besteht die Kinetik einer Suspensionspolymerisation und fällt die unlösliche Phase aus, so entspricht der Mechanismus der Kinetik einer typischen "explosiven" Polymerisation.

Received December 5, 1961

JOURNAL OF POLYMER SCIENCE: PART A VOL. 1, PP. 895–919 (1963)

Gas Transmission in Irradiated Polyethylene*

HARRIS J. BIXLER, ALAN S. MICHAELS, and MORRIS SALAME,
Department of Chemical Engineering, Massachusetts Institute of Technology, Cambridge, Massachusetts

INTRODUCTION

Previous investigations in this laboratory[1–3] have considered the effect of mode of polymerization and heat treatment on the morphology of press molded polyethylene film and sheet. Although x-ray diffraction and electron microscopy were used for contrast and comparison, attention has been focussed primarily on the indirect information about the polymer microstructure derived from the solubility and diffusion of small gas molecules in polyethylene. These latter quantities are of practical significance in characterizing the gas barrier properties of a polymer film.

To extend the use of gas solubility and diffusion in probing the interior of polymers, irradiated polyethylene was chosen for study. At the time this work was undertaken, only two previous investigations[4,5] had been reported on the effect of ionizing irradiation on the gas barrier properties of polyethylene. The major conclusions of these investigators were that the crosslinking induced by irradiation brought about a reduction in the permeability of polyethylene to gases, and a threshold radiation dose ($\sim 10^7$ roentgens) was necessary to have any measurable effect on permeability.

These results have been supported by the present work. The observation has again been made, however, that study of the permeability alone in this field is inadequate and that separate examination of the solution and diffusion processes is necessary to elucidate the effect of polymer morphology on the flow process.

A more recent study[6] has considered the effect of gamma-radiation on the moisture vapor permeability of polyethylene. In many respects this work was very similar to our own. A similar polyethylene was used, the irradiation was by Co^{60} in air, and the diffusion and solubility constants were separated from the permeability constant. A decrease in the diffusion constant of water vapor at 25°C. was observed with increasing irradiation dose. A marked increase in the solubility constant was also observed, leading to an increase in the permeability of polyethylene to water vapor with increasing irradiation dose. Bent[7] observed a similar effect on the permeability of irradiated polyethylene to organic liquids.

* Presented at the XVIIIth International Congress of Pure and Applied Chemistry, Montreal, Canada, August 1961.

Increased crosslinking with increased dose was suggested as one reason for the behavior of the diffusion constant in Chmutov's work.[6] Increased polarity of the polymer due to the incorporation of oxygen was said to account for increased water solubility. These findings parallel very closely those to be presented below so that further comparison with this work will be made in the discussion. Chmutov also suggests that radiation results in reduction in crystallinity in polyethylene which in turn reduces the diffusion constants. This latter effect has in no way been supported by the work from this laboratory.

If the steady-state and unsteady-stage diffusion of a gas can be described by Fick's laws with a constant diffusion coefficient and the equilibrium solubility of the gas in the polymer obeys Henry's law, the integrated expression for steady-state diffusion is given by

$$\bar{P} = Dk \tag{1}$$

where $\bar{P}$ is the flux rate per unit pressure gradient and is referred to as the permeability constant, D is the diffusion constant, and k is the solubility or Henry's law constant. Barrer[8] should be consulted for a detailed development of eq. (1). For homogeneous amorphous polymers, the significance of the parameters in eq. (1) is entirely analogous to their significance in normal liquids. In partially crystalline polymers, such as polyethylene, the meaning of the above factors when expressed on a total polymer basis has only recently become partially understood.

Michaels and Parker[1] and, more recently, Michaels and Bixler[2] have shown that the process of dissolution in polyethylene is confined to the noncrystalline regions of the polymer. The volume fraction of this amorphous material has been most successfully determined from density measurements where the amorphous and crystalline polymer are assumed to have characteristic densities. Except for a slight effect on the density of the amorphous phase, the mode of polymerization was found not to alter the solubility of a gas per unit volume of amorphous polymer. Molecular weight and method of sample preparation were found also to exert no unusual influence on the thermodynamics of gas dissolution in the amorphous polymer. These factors indicated that

$$k = \alpha k^* \tag{2}$$

where k is the solubility constant based on total polymer, k^* is based on amorphous polymer, and α is the amorphous volume fraction determined from density measurements.

This simple two-phase model for solubility was found to hold over a fairly wide temperature range (5–55°C.) as long as the effect of temperature on α and the thermodynamic mixing process of a gas with a liquid were considered. The relationship

$$k = k_0 e^{-\Delta H/RT} \tag{3}$$

where k_0 is a constant, ΔH is the apparent heat of solution, R is the gas

constant, and T is absolute temperature, was found to apply in all systems studied. ΔH is not simply the heat of solution of the gas with the amorphous polymer, but must include a contribution from any crystalline melting which occurs in the temperature range of investigation. In general, the crystallites in linear polyethylene have been found to be stable in the above temperature range, while those in branched polyethylene are detectably unstable even between 5 and 10°C.

The above authors also studied the diffusion process in polyethylene and found that this polymer behaves like a dispersion of highly anisometric impenetrable crystallites in penetrable amorphous polymer. These crystallites impede the flow of gas by constricting the available passageways for flow. Since diffusion of gases is an activated process in polymers, i.e.,

$$D = D_0 e^{-E_D/RT} \tag{4}$$

where D_0 is a constant and E_D is the apparent activation energy, the crystallites also impede the flow of gas by altering the activation process through their crosslinking action. The effect of crosslinking on the activation process could either be to alter the size of the activation zone and thus the entropy of activation, or it could directly increase the activation energy by chain restriction. To account for these two impedance factors the following expression has evolved:

$$D = D^*/\tau\beta \tag{5}$$

where D^* is the diffusion constant in amorphous polyethylene, τ is the geometric impedance factor accounting for pore constriction, and β is the chain immobilization factor accounting for the crosslinking action of crystallites. Natural rubber has been assumed to be a completely amorphous homolog of polyethylene giving experimental values of D^* so that values of τ and β can be determined indirectly.

Values of τ have been related to the degree of anisometry of crystallites and to the mode of polymer synthesis. Values of β have been related to the size of the gas molecule and the volume fraction of amorphous polymer.

In the present paper the diffusion, solubility, and permeability constants of helium, nitrogen, methane, and propane have been studied in irradiated and unirradiated branched polyethylene over the temperature range 0–55°C. In an attempt to ascertain the effect of the irradiation on the polymer morphology, the above model will be used for analysis of the diffusion and solubility constants. The total gamma-radiation dose from a Co^{60} source to which the samples were subjected was 10^8 roentgens at a dose rate of 1.34×10^6 r/hr. The samples were irradiated from both sides in air.

PROCEDURE

The time-lag method was used throughout this study to determine diffusion and permeability constants. The apparatus, experimental technique, and manipulation of the data obtained from the time-lag measurements

TABLE I
Properties of Polyethylene Films

Film no.	Description	Branching index[a]	Crosslink index[b]	Carbonyl content[c]	$\overline{M}_n$	$\overline{M}_w$	Density, g./cc.[d]	Volume fraction amorphous polymer, α	Thickness, cm.
A3U1	DuPont Alathon 3 NC-10 high pressure polyethylene	2.4	0	None	31,000	600,000	0.9154	0.56	0.0231
A3U2	"	2.4	0	None	31,000	600,000	0.9183	0.54	0.0699
A3I1	Same as above but irradiated: 10^8 r at 1.34×10^6 r/hr.	—	3.7	5.3	—	—	0.9311	0.55	0.0230
A3I2	"	—	3.7	1.7	—	—	0.9268	0.55	0.0697

[a] Pendant methyl groups/100 C atoms.
[b] Crosslinks/1000 C atoms.
[c] Carbonyl/1000 C atoms.
[d] At 25°C.

have been well documented by Barrer.[8] In this laboratory the apparatus is so constructed that an initially evacuated film is subjected to a constant upstream pressure of 5–900 mm. Hg for the gas under study. The pressure build-up in an initially evacuated reservior downstream of the film is measured as a function of time on an unheated McLeod gage calibrated from 0.01 to 20 μ. With respect to the upstream pressure, this downstream pressure can be considered equal to zero. The use of an unheated McLeod gage with the gases in question has been carefully considered and has been reported elsewhere.[9] The diffusion constants have been determined from the unsteady-state portion of the flow process from the time lag, and the permeability constants have been determined directly from the flow rate into the downstream reservoir after a steady state has been reached. Temperature control of the sample was maintained by a constant temperature (± 0.1°C.) water bath.

Solubility constants were indirectly obtained from eq. (1). The applicability of this technique in the present work is considered in the discussion.

Commercially cast films of Alathon 3, NC-10 supplied by E. I. du Pont de Nemours and Co., Inc. were used throughout this work. The characteristics of Alathon 3, NC-10, a high pressure polyethylene, are included in Table I. Both the irradiated and unirradiated films were transmitted to this laboratory by Dr. R. C. Giberson from the Hanford Atomic Products Operation at Richland, Washington, where Dr. Giberson was performing a separate study of the oxidation of polyethylene in a gamma-radiation field.[10]

Two nominal film thicknesses (0.023 and 0.070 cm.) were used for both irradiated and unirradiated samples. These films were quite uniform in thickness, showing a maximum deviation 0.001 cm. from the mean of fifteen to twenty measurements made over the film area to be exposed in the time-lag apparatus.

For a fixed diffusion constant, the measured time lag is inversely proportional to the square of the film thickness. Diffusion constants in this work ranged from approximately 10^{-8} to 10^{-5} cm.^{2}/sec., so it should be clear that the two film thicknesses used were not entirely satisfactory for maximum accuracy over the entire range of study. For the very short time lags ($\sim$1 min.), the accuracy of the diffusion constants are probably no better than $\pm 25\%$ due to the large effect of a small absolute error in the time lag. For the very long time lags ($\sim$50 min.), the permeability constants are subject to a similar error due to the magnified effect of an otherwise inconsequential leak rate into the downstream reservoir. However, most of this work was performed in a much more favorable region with respect to system parameters so that for an "average" run the 95% confidence limits on the permeability and diffusion constants were $\pm 6\%$. Since the solubility constants were derived from measured diffusion and permeability constants by eq. (1), they are subject to greater error. Again, for an "average" run, the 95% confidence limits were $\pm 9\%$.

The gases used in this study had a minimum purity of 99% as obtained from commercial suppliers. Except for drying the gases over calcium sulfate before introducing them into the time-lag apparatus, no further attempt at purification was made.

RESULTS AND DISCUSSION

Significance of Flow Parameters in Irradiated Films

Before proceeding with a presentation and analysis of the experimentally determined values of the permeability, diffusion and solubility constants in irradiated polyethylene, the significance of these parameters must be considered. In particular, the applicability of Fick's laws of diffusion where gas solubility in the polymer is used as a driving force for permeation must be evaluated. Sufficient, although not in all cases necessary, conditions for attaching the usual significance to the quantities $\bar{P}$, D, and k as determined from time-lag measurements are: (*a*) the diffusion constant is independent of gas concentration and position in the films; (*b*) the gas solubility is directly proportional to pressure and the solubility constant is independent of position in the film. The authors[2,3] have previously shown that press-molded films of polyethylene fulfill these conditions for the gases, pressures, and temperatures under study. Random distribution of impenetrable crystallites on a macroscopic scale (where a distribution of crystallite size and shape exists) and chemical homogeneity of the amorphous phase are all that is required.

For polyethylene films irradiated in air, three and possibly four alterations in polymer morphology, topology, and chemistry occur, all of which can affect gas transmission properties. The polymer chains become crosslinked. From the work of Miller et al.,[11] there are about four crosslinks per thousand chain carbon atoms formed for an irradiation dose of 10^8 roentgens. Chain scission could also occur, but in polyethylene there is no evidence of this to any measureable extent. The probability of a free radical at the ends of a fractured chain combining with hydrogen atoms is much smaller than the probability of recombination or reaction with a free radical on an adjacent chain.

The crystallinity could be reduced by the disrupting effect on lattice spacing due to crosslinking within the crystallites. Charlesby[12] argues that this is the case even at 10^8 roentgens, but the evidence in this work would tend to refute destruction of crystallinity at this low dosage.

Oxidation, when the irradiation is carried out in air, and introduction of unsaturation are the principal chemical changes. The infrared spectra of samples of the irradiated (A3I1) and unirradiated (A3U1) films used in this work showing these chemical changes appear in Figure 1. The general reduction in the infrared transmission above 8 μ is probably an indication of lost chain mobility due to crosslinking in the irradiated sample.

How would these changes be expected to affect gas sorption and flow properties? Crosslinking resulting in restricted chain mobility should re-

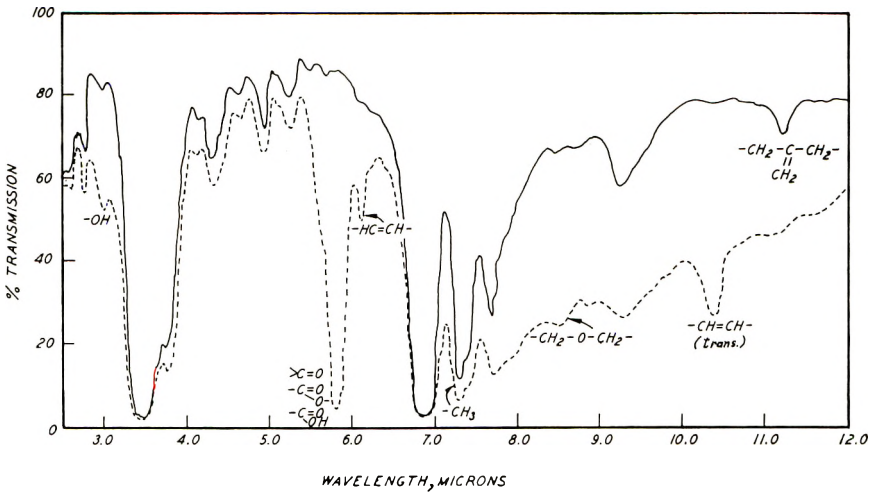

Fig. 1. Infrared spectra of polyethylenes: (——) A3U1; (--) A3I1.

duce the diffusion constants. Since the molecular gas solubility is so low ($<10^{-4}$ molecules/CH_2 unit) the effect of crosslinking on solubility due to contraction of the polymer should be negligible. Crystallinity changes (both in quantity and size and shape of crystallities) should alter diffusion and solubility constants as pointed out in the introduction. Chemical changes should alter the solubility through changes in the cohesive energy density of the polymer. Although the energy of activation for gas diffusion in a polymer should be proportional to its cohesive energy density,[2] the effect of crosslinking on the diffusion process might be thought to overshadow the chemical effects.

To satisfy the conditions prescribed above for usual interpretation of time-lag data, the processes of crosslinking, oxidation, and unsaturation, and/or crystallite degradation must take place at random through the polymer. The crosslinking and chemical changes need occur only at random in the amorphous polymer, since flow is limited to this phase.

For the photon energy of Co^{60} (1.17 and 1.33 M.e.v.), the sample thickness and dose rate were small enough and the total dose large enough to assure random and uniform crosslinking through the polymer.[12] The degree of oxidation (expressed in terms of carbonyl content) was not uniform throughout the film. Before considering the effect of nonuniform carbonyl content in detail, it should be pointed out that the irradiation conditions and film thicknesses were such that the process of crosslinking and chemical change were probably occurring independently.[13] Therefore, even though the carbonyl content was not uniform, the crosslink density was in all likelihood essentially uniform.

Giberson,[10] studying the same films reported here, has shown that carbonyl formation is probably controlled by oxygen diffusion. The carbonyl concentration is a maximum at the film surfaces and goes through a minimum at the film centerline. Since the boundary conditions for

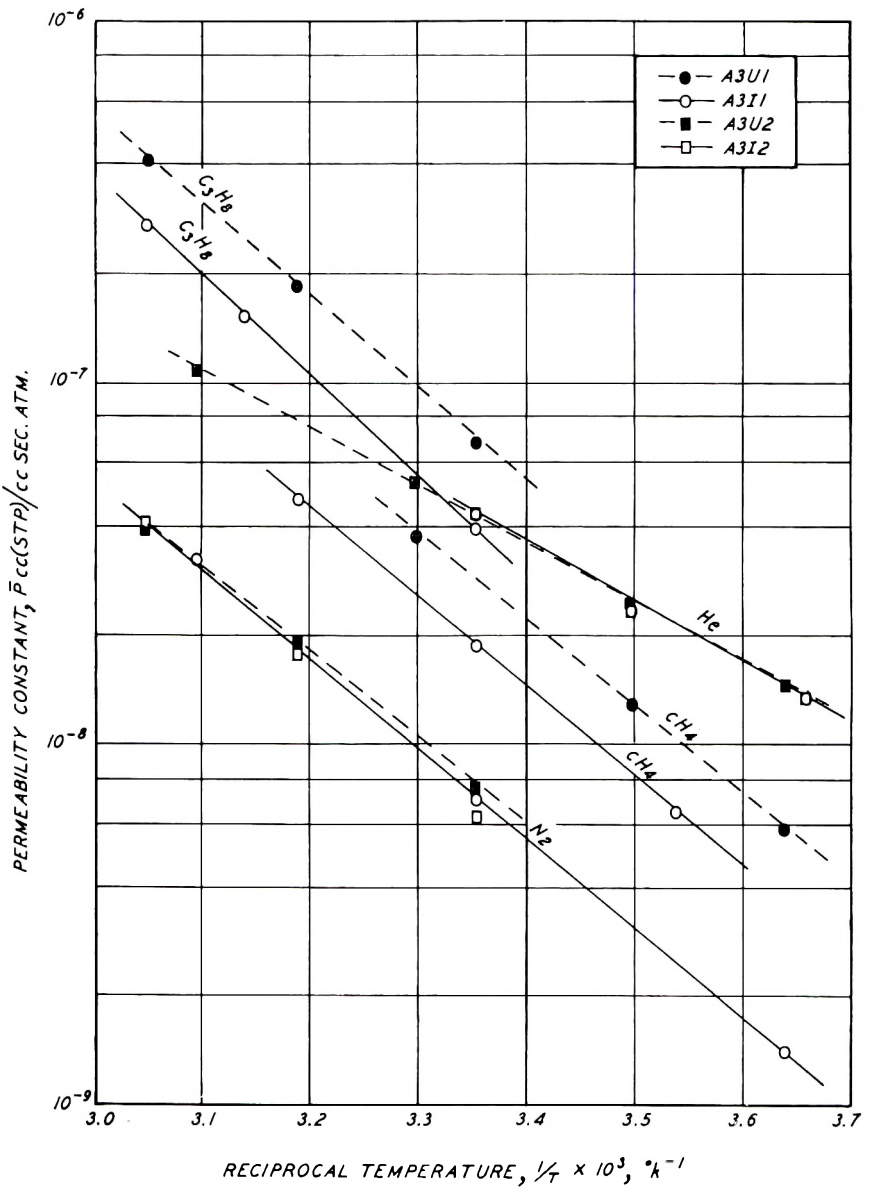

Fig. 2. Permeability constants in polyethylenes.

oxidation are independent of film thickness, the surface carbonyl concentration should be independent of film thickness at the same total irradiation dose and dose rate. For the films A3I1 and A3I2, the optical density at 5.8 μ (HC = O, C = O, OC = O) were approximately the same and equal to 1.40. This corresponds to 8.1×10^{-6} moles of carbonyl/cm.^{2}. Therefore, the average carbonyl concentration per cubic centimeter was inversely proportional to the film thickness. Giberson's work has shown

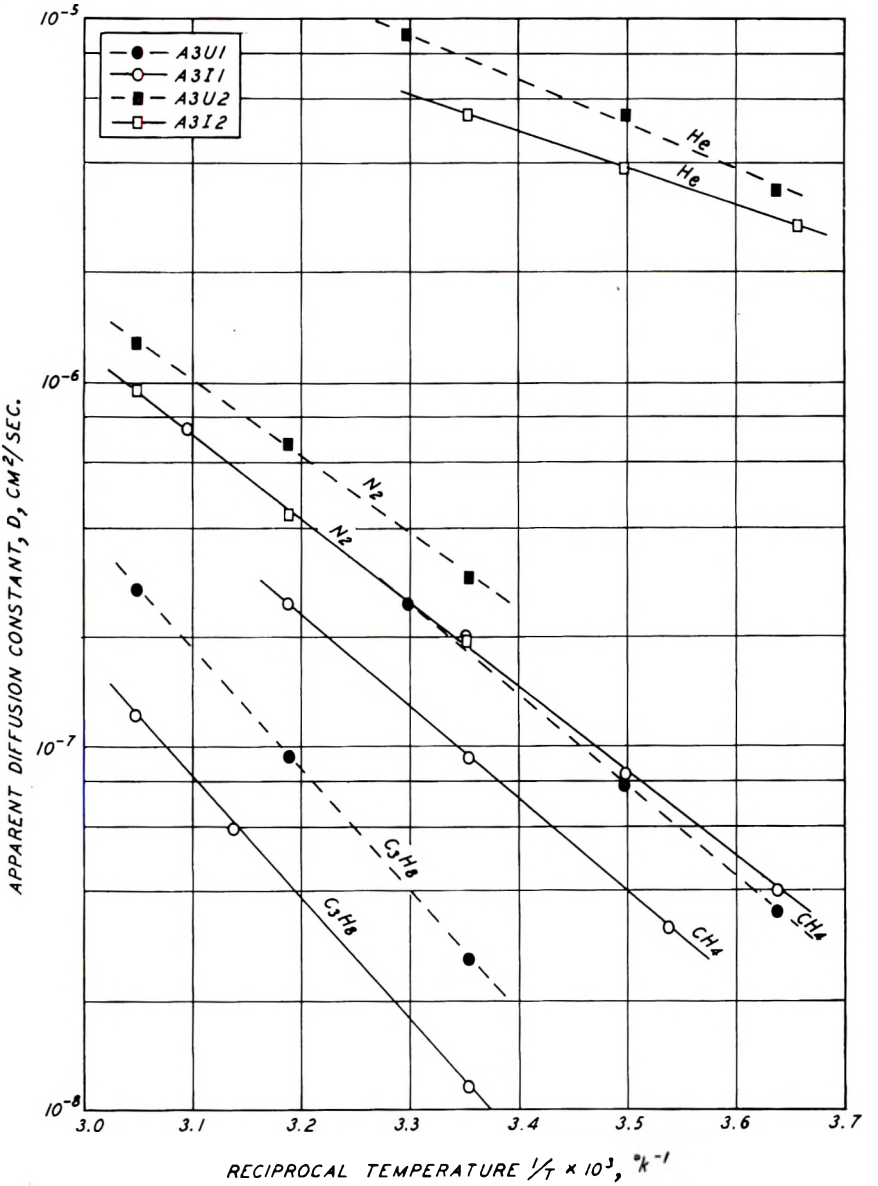

Fig. 3. Diffusion constants in polyethylenes.

that there is a sharp decrease in optical density for carbonyl for films thinner than 0.023 cm. and essentially no change for films thicker than 0.030 cm.

In light of nonuniform carbonyl distribution, two possible conditions could exist within the films which bear on the interpretation of the time-lag data. Competitive reactions to form carbonyl and unsaturation could occur giving rise to essentially uniform, but higher, cohesive energy density

in the irradiated films. This fulfills conditions (*b*) above. Comparison of gas solubilities in polyvinyl acetate[14] and natural rubber[2] with amorphous polyethylene[2] indicate both carbonyl and unsaturation could increase gas solubility constants in polyethylene.

A second condition could be that a gradient of the chemical composition affecting solubility does exist. Under these circumstances there is no assurance that the apparent diffusion and solubility constants will retain their usual significance. For a gradient in chemical composition it is entirely possible that a linear concentration gradient is no longer established through the film at steady-state permeation, thus invalidating the significance of the time lag. Even if a linear gradient is established, the solubility constants determined from time-lag data need not be identical to the values obtained from equilibrium sorption experiments.

This condition of a gradient in chemical composition of a polymer film would be a fruitful subject for separate investigation. No direct experimental evidence of nonuniformity of the equilibrium sorption capacity of the polymer was obtained in this investigation. Insufficient polymer was available to measure the solubility constants by the static sorption technique developed in this laboratory.[15] A comparison of static sorption with time-lag measurements would aid in clarifying the effect of a nonuniform carbonyl content. A study similar to that made by Giberson[10] on carbonyl formation should be made on unsaturation to determine whether or not the distribution is uniform when oxidation is also occurring.

Having introduced the possibility that the normal diffusion expression could be negated as a result of a nonuniform distribution of chemical changes, we shall proceed on the assumption that such negation has not occurred. Certain experimental facts tend to support this assumption. Chief among these were a lack of pressure dependence of any of the flow parameters for any of the gases studied in one particular film, and identical results within experimental error for all three flow parameters for nitrogen in both A3U1 and A3U2. This identity of results was observed over the entire temperature range of the investigation (see Figs. 2 and 3).

Experimental Results

The experimental results are presented in Figures 2 and 3. The basis for the correlation in these figures is eq. (4) and a combination of eqs. (1), (3), and (4) which yields

$$\bar{P} = \bar{P}_0 e^{-E_{\bar{P}}/RT} \tag{6}$$

and

$$E_{\bar{P}} = E_D + \Delta H \tag{7}$$

where $E_{\bar{P}}$ is referred to as the activation energy for permeation. Smoothed parameters based on these correlations are presented in Table II.

TABLE II
Values of D, $\bar{P}$, E_D, and $E_{\bar{P}}$ at 25°C.

Gas	Film	$D \times 10^7$, cm.²/sec.	$\bar{P} \times 10^7$, cc.(STP)/ cm. sec. atm.	E_D, kcal./ g.-mole	$E_{\bar{P}}$, kcal./ g.-mole
He	A3U2	77.0	0.43	5.6	7.4
He	A3I2	54.0	0.44	4.7	7.7
N_2	A3U2	2.90	0.078	9.7	10.6
N_2	A3I1, A3I2	1.90	0.070	10.5	11.5
CH_4	A3U1	1.80	0.280	11.3	10.9
CH_4	A3I1	0.95	0.190	11.5	11.5
C_3H_8	A3U1	0.26	0.69	15.1	11.7
C_3H_8	A3I1	0.117	0.39	15.3	12.6

The permeability constants are presented for their limited practical value in describing the gas barrier properties of films irradiated under the present conditions. It can be seen from Figures 2 and 3 that significant changes in irradiated polyethylene could go unnoticed if permeability constants alone were measured. Although Bent[7] and Chmutov[6] have observed an increase in permeability constants for organic liquids and water in irradiated polyethylene, no such increase has been observed here. Apparent solubility and diffusion constants must be considered separately to understand this anomaly. Henceforth the analyses of the data will be

for gas solubility in a microcrystalline polymer. Values of α were obtained from the relationship

$$\alpha = \frac{v_a(v - v_c)}{v(v_a - v_c)} \tag{8}$$

where v_a and v_c are the specific volumes of the amorphous and crystalline phase, respectively, and v is the specific volume of the sample. v was determined in a density gradient column. As in past publications from this laboratory, v_c and v_a are taken as 1.003 and 1.171 cm.^{3}/g., respectively, at 25°C. The calculated values of k for the unirradiated samples in this work are included in Table III. Except for methane, the agreement is within the experimental accuracy of the data. The high value for methane remains unexplained considering the consistency of the methane data otherwise.

The apparent heats of solution in the unirradiated films are very similar to those previously reported for a linear polyethylene and about 0.5 kcal. more negative than those obtained on a similar branched polyethylene. This indicates no crystalline melting in the temperature interval studied. Although the thermal history of the films used here is not accurately known, this behavior would not be expected for a branched polyethylene. These results may be more apparent than real, since the accuracy of the heats of solution is at best ± 0.5 kcal.

Irradiated Films. For the irradiated films the values of k are 40% higher for all gases. Although a decrease in crystallinity due to irradiation could bring about this uniform increase in solubility, it appears that no destruction of crystallites has occurred. X-ray analysis has shown that the weight fraction of crystalline (and amorphous) material remains unchanged by irradiation. However, according to eq. (2) it is the volume fraction and not weight fraction of amorphous material which characterizes the sorptive capacity of polyethylene. Since

$$x_a = \frac{v - v_c}{v_a - v_c} \tag{9}$$

where x_a is the weight fraction of amorphous material, v_a and/or v_c must be altered by irradiation to retain x_a constant. Table I shows that the polymer density ($1/v$) increases upon irradiation. No direct experimental work in this investigation allows a conclusive determination of whether v_a, v_c, or both are affected by the radiation.

Since crystallites represent a uniform low energy arrangement of molecules, there is no reason to believe that irradiation would affect v_c without altering the crystalline content of the film. If irradiation effects are restricted to the amorphous regions of the polymer, then v_a might be expected to change. Crosslinking and unsaturation should cause a densification of the amorphous material. Likewise, replacement of hydrogen by oxygen in the polymer should result in densification. Keeping x_a constant and equal to 0.52 leads to an average value of v_a at 25°C. equal to 1.144

after irradiation. This increased density of the amorphous phase is in fair agreement with the value extrapolated from the dilatometric data presented by Charlesby[12] on pile-irradiated polyethylene above the crystalline melting point. Due to the nature of the system parameters, this new value of v_a in conjunction with the irradiated sample densities has little effect on α. For all practical purposes the volume fraction of amorphous material is unaltered by irradiation.

The increased gas solubilities may stem from the chemical changes in the polymer. According to Michaels and Bixler, gas solubilities in amorphous polyethylene are described quite well by the relationship

$$\ln k^* \bar{V} = 0.026\epsilon/\bar{k} - (1 + \chi) \tag{10}$$

where $\bar{V}$ is the partial molal volume of the gas in polyethylene, $\epsilon/\bar{k}$ is the force constant in the Lennard-Jones potential field equation, and χ is the mixing parameter related to the heat of dilution. This equation assumes the sorption process to be one of the condensation of the gas and subsequent mixing of the liquid with the polymer. The Flory-Huggins mixing equation was used to describe the latter process, while the integrated Clausius Clapyron equation was used to describe the former process. Michaels and Bixler did not attempt to evaluate χ or $\bar{V}$ but simply plotted $\ln k^*$ against $\epsilon/\bar{k}$ and obtained a good linear correlation. The uniform increase in the solubility constants after irradiation would, of course, continue to validate this correlation.

Both $\bar{V}$ and χ are dependent on the cohesive energy density of the polymer. Prausnitz[16] has shown that the partial molal volume of a gas in a liquid decrease with increasing cohesive energy density of the liquid. On the other hand

$$\chi \sim (\delta_p - \delta_g)^2 \tag{11}$$

where δ_p and δ_g are the square root of the cohesive energy density of the polymer and gas, respectively. Since δ_p is about 8.0 $(\text{cal./cc.})^{1/2}$ for unirradiated polyethylene, χ increases with increasing cohesive energy density of the polymer for all gases studied here. Therefore, heats of dilution should be somewhat greater in the irradiated polymer and from eq. (10) the solubility constants would be expected to decrease. A more important factor appears to be the partial molal volume. A decrease in $\bar{V}$ leads to an increase in the solubility constant. This behavior has been observed in natural rubber and partially hydrogenated polybutadiene.[2] The cohesive energy densities of these amorphous polymers are greater than polyethylene, and the gas solubility constants were higher by 50% and 25%, respectively. It is not possible at this writing to determine the cohesive energy density of the irradiated polymer with accuracy through the use of eq. (10), but in comparison with the sorption behavior of natural rubber it would appear that a value of 8.3–8.4 would be suitable.

Chmutov[6] in his work measured the solubility of water vapor in irradiated polyethylene but did not determine the value in an unirradiated

sample of the same material. However, Myers et al.[17] have determined the solubility constant of water vapor in a polyethylene of similar density. At 25°C. Myers found the solubility constant to be 2.5×10^{-6} g. H_2O/cc. mm. Hg while Chmutov found the solubility constant to be 18.0×10^{-6} g. H_2O/cc. mm. Hg at 25°C. after irradiation with Co^{60} to a total dose of 10^8 roentgens. Both polymers had a density of approximately 0.92 g./cc. before irradiation. This sevenfold increase is much greater than that observed in the present work. The ability of water to form hydrogen bonds with the carbonyl formed upon irradiation of the polyethylene in air may account for this very marked increase in solubility.

Apparent Heats of Solution

The apparent heats of solution in the irradiated polymer are on the average about 0.5 kcal./g.-mole greater (more positive) than in the unirradiated polymer. Since any crystalline melting in the temperature range of this investigation would be included in ΔH, the possibility of reduced stability of crystallites after irradiation must be included along with any effect of the increase of cohesive energy density of the polymer on ΔH. Densification of the amorphous phase due to crosslinking could conceivably induce sufficient stress in the polymer to reduce the stability of the crystallites. It will be shown in the next section where the apparent diffusion constants are considered that this does not appear to occur. Using the same thermodynamic model as used in developing eq. (10), Michaels and Bixler[2] found that the true heats of solution should be given by

$$\Delta H = 0.59\chi - 0.0156\epsilon/\bar{k} \text{ kcal./g.-mole} \tag{12}$$

A plot of ΔH in the unirradiated films versus $\epsilon/\bar{k}$ is shown in Figure 4. Values of $\epsilon/\bar{k}$ are included in Table IV. From this plot,

TABLE IV
Gas Parameters

Gas	$\epsilon/\bar{k}$, °K.	d, A.[a]
He	10	2.2
N_2	94	3.7
CH_4	148	4.1
C_3H_8	284	5.8

[a] Method of determination given by Michaels and Bixler.[3]

$$\Delta H = 2.4 - 0.20\epsilon/\bar{k} \text{ kcal./g.-mole} \tag{13}$$

which is in fair agreement with the relationship,

$$\Delta H = 2.7 - 0.164\epsilon/\bar{k} \text{ kcal./g.-mole} \tag{14}$$

reported by Michaels and Bixler for Alathon 14, a polyethylene similar to Alathon 3.

For the irradiated samples (also shown in Figure 4)

$$\Delta H = 3.0 - 0.20\epsilon/\bar{k} \text{ kcal./g.-mole} \tag{15}$$

Since it has already been argued that χ would increase due to incorporating carbonyl and unsaturation in the irradiated polymer, the observed effect of irradiation on ΔH is thermodynamically consistent.

In summary, it appears that the major effect of irradiation on the sorptive properties of polyethylene stems from the chemical changes. The effect of these chemical changes on the thermodynamic properties of the

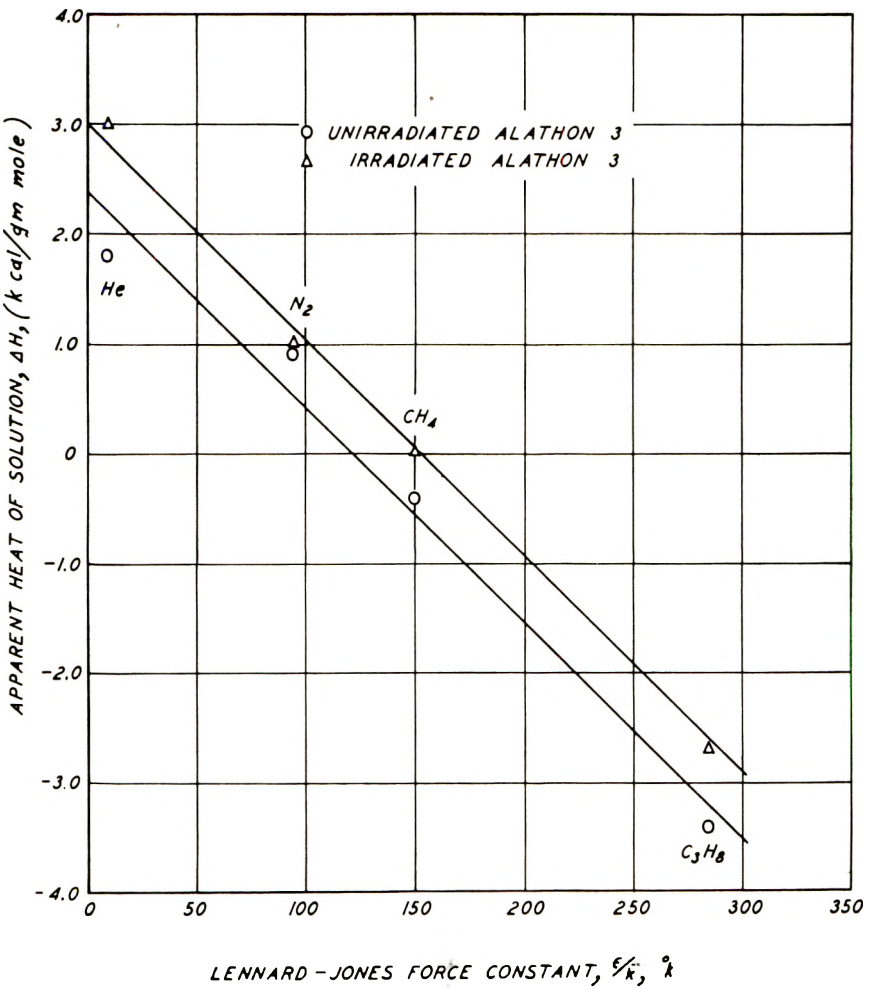

Fig. 4. Correlation of apparent heats of solution of Alathon 3: (○) unirradiated; (△) irradiated.

polymer are sufficient to account for the increased solubility of gases in the polymer and the more positive heats of solution. The change in density of the polymer after irradiation appears to stem simply from a densification of the amorphous phase with no attendant reduction in crystallinity or stability of crystallites.

Diffusion Constants

Irradiation Films: General Considerations. Referring to Table II, there are two major effects of irradiation on the diffusion constants in polyethylene. Irradiation reduces the diffusion constants, and the per cent reduction increases with increasing molecular size. The energies of activation for diffusion show only a slight increase with radiation. No marked size dependency for the diffusing molecule is observed. The reported reduction in the activation energy for helium is doubtful due to the difficulty in obtaining reasonable time lags over a significant temperature range.

These results parallel the results of Barrer and Skirrow[18] for lightly sulfur-crosslinked natural rubber in comparison with the work of Michaels and Bixler[3] on unvulcanized natural rubber. The diffusion results for nitrogen, methane, and propane in a rubber containing 2.7% sulfur compared with unvulcanized natural rubber are almost identical to a similar comparison between the results in irradiated and unirradiated Alathon 3.[3] Ascribing the effect of irradiation on the diffusion process to crosslinking, therefore, seems reasonable.

From eq. (4) it can be seen that D_0 and/or E_D must change for the diffusion constant to be lower in the irradiated polymer at constant temperature. Using the model of Brandt[19] whereby the activation energy for diffusion is the energy required for symmetrical separation of two chain segments, Michaels and Bixler[3] have shown that to a first approximation in polyethylene,

$$E_D \sim Sd_p[d - (\phi^{1/2}/2)]\delta_p^2 \tag{16}$$

where S is the length of a chain segment involved in a diffusion step, ϕ is the free volume per unit length of a CH_2 group, d_p is the chain diameter, d is the diffusion diameter of the gas molecule, and δ_p^2 is the cohesive energy density.

From the theory of absolute reaction rates,[20] D_0 is given by:

$$D_0 = e\lambda^2(\bar{k}T/h)\, e^{\Delta S^*/R} \tag{17}$$

where λ is the length of a successful diffusion step, $\bar{k}$ is Boltzmann's constant, h is Planck's constant, and ΔS^* is the entropy of activation.

If it is assumed that D_0 is unaltered by irradiation, then the experimental values of D in Table II would indicate that E_D should be 0.2 kcal./g.-mole higher in the irradiated film for helium. This incremental increase in E_D should be progressively higher for the larger gas molecules. An incremental increase of 0.5 kcal./g.-mole would be required for propane. These incremental increases in E_D fall within the precision limits on the data, so it is impossible to ascertain conclusively whether or not the experimental values of E_D reflect these changes. An increase in E_D is consistent with eq. (16), however, since an increase in the cohesive energy density and decrease in the amorphous free volume has been argued in conjunction with the solubility data.

In general, where an "activated" process involves the participation of a large number of degrees of freedom to achieve the activated state there is a porportional increase in the activation entropy with increasing activation energy. Qualitatively, this indicates that the larger the activation energy the larger the number of degrees of freedom over which this energy is most likely to distribute itself. This relationship is usually observed for gases diffusing in amorphous polymers. The parameters E_D, λ, and ΔS^* are, however, mean values for an Avogadro's number of diffusion steps. For individual diffusion steps there is undoubtedly a spectrum of energies, entropies, and diffusion step lengths which give rise to the mean experimental values. In a completely amorphous matrix of macromolecules this spectrum may be fairly broad. If the amorphous polymer chain segments are gradually restricted in their mobility via crystallization and/or crosslinking, the first change to be observed with respect to the diffusion process may be the loss of availability of some low energy diffusion sites. There may be no significant change in the measured value of E_D accompanying this process. Depending on the activation energy distributions, a significant reduction may occur in the probability that gas molecules will find regions in the polymer where there exist conditions favorable for a diffusion step. This would result in a reduction in the activation entropy without a compensating change in the activation energy.

If the restraints on the polymer chains are heterogeneously distributed on a molecular scale, the above argument seems even more reasonable. Such a heterogeneous distribution would more conclusively remove certain regions in the amorphous polymer from probable participation in a successful diffusion step. Mild irradiation probably induced this small-scale heterogeneity. In fact, the low carbonyl concentrations encountered in this work may lead to a similar heterogeneity in favorable diffusion zones. Thus, in the irradiated films it is felt that there is no significant reduction in E_D but a reduction in D_0 causing the reduced apparent diffusion constants. If appears that a similar condition may exist in lightly crosslinked rubber vulcanizates.[18]

This argument may be better illustrated by considering what would happen if the crosslinking in irradiated polyethylene was so heterogeneously distributed that small fragments of highly crosslinked polymer were formed. Assume the fragments to be impenetrable to gas molecules and that these fragments are widely dispersed compared to the mean activation zone size. Clearly, under these conditions E_D should not be affected, but the diffusion constants would be reduced through the loss of available sites in polymer for diffusion and a probable increase in mean diffusion path length through the polymer. Although this degree of heterogeneity is not expected in the present films, it is this type of reduction in diffusion constants that is being considered. It should be pointed out that the impedance factors in the model depicted by eq. (5) have been developed by the above line of reasoning.

In concluding this discussion it would be well to point out that a high cross-

link density should result in an appreciable increase in both E_D and ΔS^*. If the average distance between crosslinks is less than the average zone size in the absence of crosslinks, then a greater energy of activation must be distributed over a larger number of degrees of freedom to give rise to a successful diffusion step. The latter condition results from the fact that isolated segments of the polymer chain can no longer move independently and any chain motion must disturb a large number of units in the network polymer. This situation has been observed in highly crosslinked rubber vulcanizates.[18]

Unirradiated Films: Comparison with Previous Study. Consider the diffusion process in light of the microporous model depicted by eq. (5). As outlined above, this model has been proposed to account for the effects of crystallinity on the diffusion process in the amorphous phase of polyethylene. The interpretation of the diffusion data in the unirradiated films is fairly straightforward with respect to this model. It is assumed that τ is the impedance offered to a helium molecule in traversing the amorphous phase due simply to the irregular diffusion path imposed by impenetrable crystallites. If it is further assumed that in a 50% crystalline film the mean distance between crystallites is larger than the size of the activation zone; β is essentially equal to 1.0. In light of the above arguments, β is related to probability that crystallites in polyethylene will significantly alter the spectrum of E_D and ΔS^* values that would be encountered in the absence of crystallites. A value of β equal to 1.0 indicates that no significant change is expected to occur for the small helium molecule. Therefore τ for helium is given by the ratio of D in completely amorphous polyethylene to the experimental value in Alathon 3.

From the experimental value of D in unvulcanized natural rubber for the former ($D^* = 2.16 \times 10^{-5}$ cm.^{2}/sec.), a value of τ equal to 2.8 is obtained. This is in excellent agreement with the value predicted from the relationship of Michaels and Bixler[3] for branched polyethylenes:

$$\tau = \alpha^{-1.88} \tag{18}$$

The definitions of τ and β are seen to be highly arbitrary; although thus defined, τ does represent the minimum impedance that would be encountered by a gas molecule of any size due only to the geometry of the amorphous regions as a result of the presence of crystallites. The utility of τ rests in its ability to give some insight into the shape of crystallites in polyethylene. For instance, from the analysis presented in the previous paper, the mean axial ratio of the crystalline lamellae (assumed to be disks) in the unirradiated samples in this work is about 20/1 as determined from τ. Crystallities of this shape are consistent with light-scattering and electron microscopy data.

Values of β calculated in the above manner have been correlated in polyethylenes by the relationship

$$\ln \beta = \gamma[d - (\phi^{1/2}/2)]^2 \tag{19}$$

where γ is a constant expected to be dependent on α and the size and shape of crystallites. Analytical dependence of γ on these quantities has not been fully determined. Values of β obtained from the unirradiated films are correlated in accordance with eq. (19) in Figure 5, from which γ was found to equal 0.045.

According to eq. (16), a linear correlation of E_D with $[d - (\phi^{1/2}/2)]$ should be obtained. It should be borne in mind that the values of E_D for a branched polyethylene will contain a contribution from crystalline

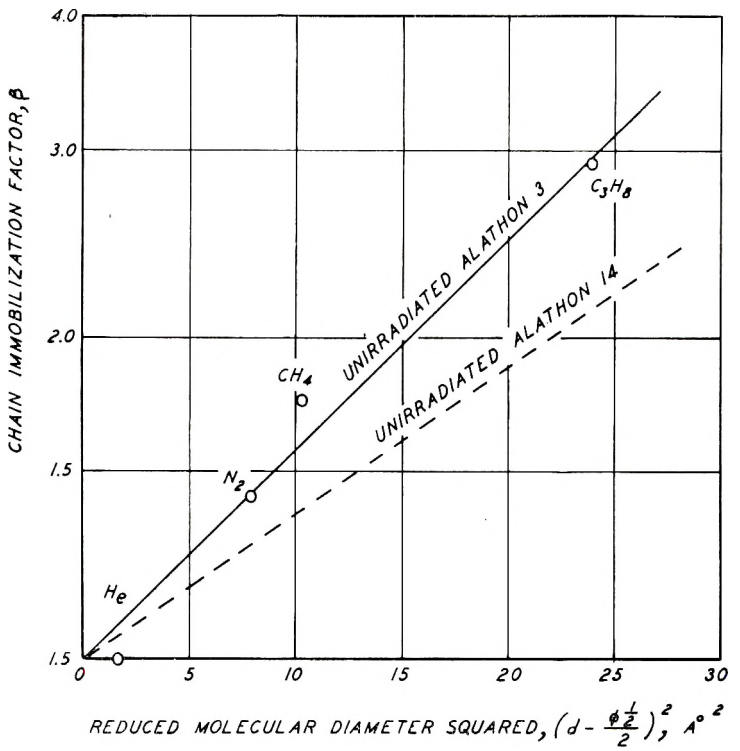

Fig. 5. Effect of gas molecular size on chain immobilization factor.

melting as this affects the parameters τ and β. An energy contribution of this type is not implicit in the model for eq. (16). For polyethylene, $\phi^{1/2}/2$ equals 0.9 A. in the unirradiated films, and values of d are included in Table IV. Figure 6 shows the correlation which is certainly as good as could be expected considering the assumptions involved. The line in this figure is given by

$$E_D = 2.5[d - (\phi^{1/2}/2)] + 2.1 \text{ kcal./g.-mole} \quad (20)$$

The data for Alathon 3 differ in two respects from the data previously presented for a similar branched polyethylene (Alathon 14, $\alpha = 0.57$). In

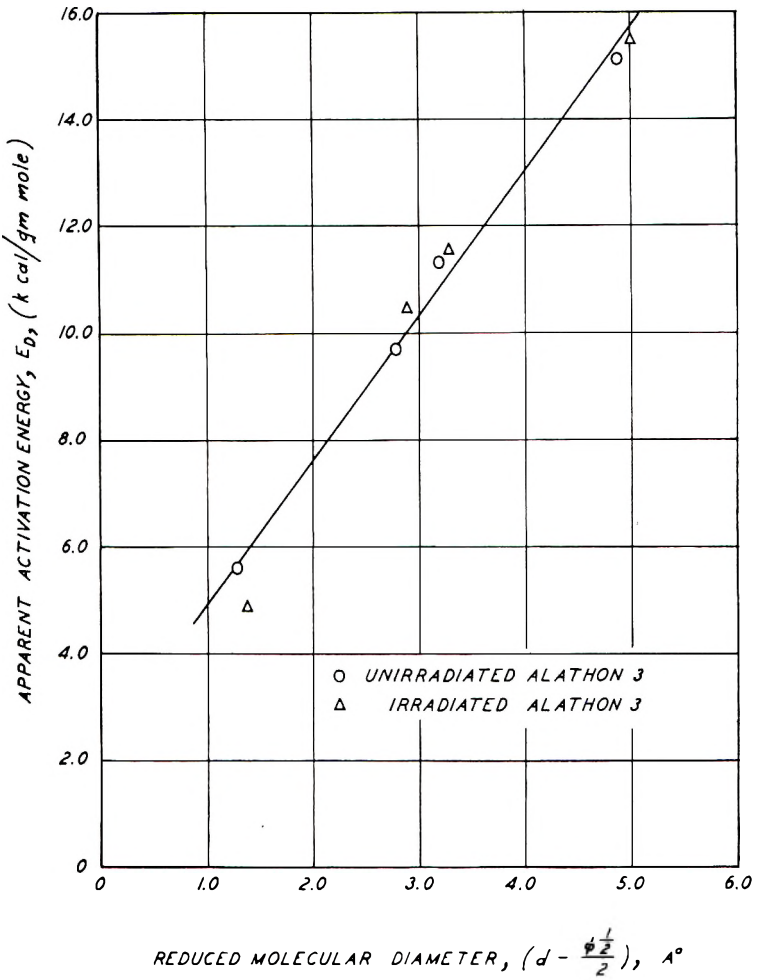

Fig. 6. Correlation of apparent activation energies for Alathon 3: (O) unirradiated; (△) irradiated.

that polymer γ was equal to 0.031 and the apparent energies of activation for diffusion were given by

$$E_D = 1.8[d - (\phi^{1/2}/2)] + 4.6 \text{ kcal./g.-mole} \quad (21)$$

The slightly smaller value of α for the Alathon 3 would not be expected to give this significantly greater molecular size dependence of diffusion parameters. A key to the difference came from an x-ray diffraction analysis which indicated some orientation of crystallites. The Alathon 3 films were extruded, while the Alathon 14 samples were press-molded. From the agreement in the values of τ, the orientation was not sufficient to either alter the crystallite shape or to cause preferred alignment of crystallites. It may have been sufficient to decrease the mobility of the amorphous chain segments as indicated by the increased molecular size dependence

of γ and E_D. Smaller, more thermally stable crystallites resulting in a reduction in the mean intercrystalline spacing could also account for this behavior. The increased thermal stability implied from the apparent heats of solution could result from increased crystallite perfection. Nothing in a comparison of the properties of Alathon 3 versus Alathon 14 suggests this behavior, however.

Irradiated Films: Application of Microporous Model. It appears futile to attempt to differentiate between τ and β in the irradiated films. The crystallinity appears to be unaltered by irradiation, so it is tempting to say that τ is again equal to 2.8. In other words, a helium molecule diffusing through the irradiated polymer would, on the average, traverse a micropore of amorphous polymer geometrically similar to a pore in the unirradiated polymer. A moment's reflection will indicate that this assumption is probably invalid. One properly positioned crosslink could effectively block a region between two crystallites to helium flow that would otherwise be readily accessible to this small gas molecule. Thus, crosslinking resulting from irradiation could alter the geometric impedance factor, τ.

In spite of the fact that τ and β cannot be logically separated to retain the significance attributed to them in the microporous model, the product $\tau\beta$ can be calculated. A small correction to the values of D^* allowing for the fact that the amorphous phase is denser after irradiation has been neglected. The analogy between diffusion constants in natural rubber and amorphous polyethylene is not sufficiently exact to warrant attempting such a correction.

The interpretation of the effect of crosslinking on β in the irradiated films should be similar to the interpretation ascribed to β in a microcrystalline polymer. The chain mobility in irradiated polyethylene should be limited by both crystallites and chemical crosslinking. Since τ has been assumed to be independent of gas molecular size, the product $\tau\beta$ in the irradiated films should have the same gas molecular size dependence as β alone. Figure 7 is a plot of ln $\tau\beta$ versus $[d - (\phi^{1/2}/2)]^2$, and a reasonable correlation is observed. Due to the densification of the amorphous phase, a slightly reduced value of $\phi^{1/2}/2$ (0.8 A) has been used. The slope of this line is 0.071, indicating the higher gas size dependency as already noted. It appears from the correlation in Figure 7 that τ cannot be appreciably less than 4.0, indicating a significant increase upon irradiation. It appears as if crosslinking has converted some regions in the amorphous polymer that were previously merely a "tight" fit for helium into regions which are now impassable with any reasonable activation energy.

It has already been noted that the experimental values of E_D are not appreciably affected by irradiation. These values of E_D are included in Figure 6, again for a value of $\phi^{1/2}/2$ equal to 0.8 A. With respect to the microporous model this would indicate that no significant crystalline melting is occurring in the temperature range of the investigation over and above that which was occurring in the unirradiated films. This is addi-

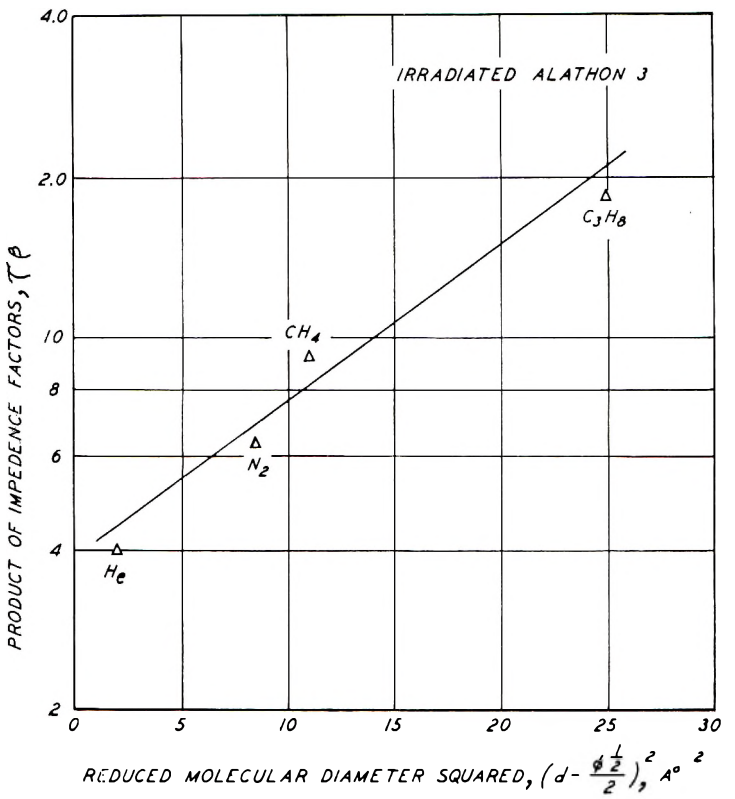

Fig. 7. Effect of gas molecular size on product of impedance factors for irradiated Alathon 3.

tional support for the argument that the values of ΔH in the irradiated polymer are more positive due to changes in chemical composition of the film and not due to additional crystalline melting.

Chmutov[6] found an even more marked reduction in the diffusion constant of water in irradiated polyethylene. At 25°C., D was found to be 0.6×10^{-7} cm.^{2}/sec. Comparing this value with a value of 2.9×10^{-7} cm.^{2}/sec. reported by Myers[17] for a similar unirradiated polymer indicates a fivefold reduction for an irradiation dose at 10^8 roentgens. This seems like an excessive reduction in comparison with the present work, but without a knowledge of the exact thermal histories of the films of Chmutov and Myers the comparison cannot be carried too far. Since Chmutov's[6] films may have suffered from the same gradient in chemical composition noted earlier in this paper, caution should be exercised in attaching undue significance to his apparent values of D. The effect of a gradient in carbonyl content would probably be much more serious than in the case of nonpolar gas transmission.

In summary, the apparent solubility constants are higher by an equivalent fraction for all non polar gases consistent with the chemical composi-

tional changes occurring upon irradiation in air. The apparent diffusion constants are lower after irradiation, the fractional decrease being greater, the larger the molecules. In light of the suggested model for gas transmission in polyethylene this behavior is consistent with reduced chain mobility due to crosslinking in the amorphous phase. Although all aspects of this work appear to be internally consistent, the possible effects of a gradient in chemical composition through the films cannot be overlooked. Fick's laws as applied to the time lag method of measuring gas transmissional parameters are probably not applicable if a significant gradient in chemical composition does exist through a polymer film.

This paper represents a continuation of work in this laboratory sponsored by grants-in-aid from the National Science Foundation (Grant No. G-11144) and the Polymer Chemicals Division of W. R. Grace and Company. The polymer samples were supplied by Dr. R. C. Giberson from the Hanford Atomic Products Operation at Richland, Washington. Dr. Giberson's personal transmittal of pertinent information from time to time to this laboratory is gratefully acknowledged. The x-ray analyses of the polymer films performed by Dr. George Ashby of the Washington Research Laboratories of W. R. Grace and Company were invaluable in interpreting the present results. Similarly, the infrared analyses performed by Dr. W. A. Patterson of the Cryovac Division of W. R. Grace and Company were most helpful.

References

1. Michaels, A. S., and R. B. Parker, Jr., *J. Polymer Sci.*, **41**, 53 (1959).
2. Michaels, A. S., and H. J. Bixler, *J. Polymer Sci.*, **50**, 393 (1961).
3. Michaels, A. S., and H. J. Bixler, *J. Polymer Sci.*, **50**, 413 (1961).
4. Sobolev, I., J. A. Meyer, V. Stannett, and M. Szwarc, *J. Polymer Sci.*, **17**, 417 (1955).
5. Myers, A. W., C. E. Rogers, V. Stannett, and M. Szwarc, *Tappi*, **39**, 734 (1956).
6. Chmutov, K., and E. Finkel, *Zhur. Fiz. Khim.*, **33**, 93 (1959).
7. Bent, H. A., *J. Polymer Sci.*, **24**, 387 (1957).
8. Barrer, R. M., *Trans. Faraday Soc.*, **35**, 628 (1939).
9. Bixler, H. J., A. S. Michaels, and R. B. Parker, Jr., *Rev. Sci. Instr.*, **31**, 1155 (1960).
10. Giberson, R. C., *J. Phys. Chem.*, **66**, 463 (1962).
11. Miller, A. A., E. J. Lawton, and J. S. Balivit, *J. Phys. Chem.*, **60**, 599 (1956).
12. Charlesby, A., *Atomic Radiation and Polymers*, Pergamon Press, London, 1960.
13. Alexander, P., and D. Toms, *J. Polymer Sci.*, **22**, 343 (1956).
14. Meares, P., *Trans. Faraday Soc.*, **54**, 40 (1958).
15. Michaels, A. S., and R. B. Parker, Jr., *J. Phys. Chem.*, **62**, 1604 (1958).
16. Prausnitz, J. M., *A.I.Ch.E. Journal*, **4**, 269 (1958).
17. Myers, A. W., J. A. Meyer, C. E. Rogers, V. Stannett, and M. Szwarc, to be published.
18. Barrer, R. M., and G. Skirrow, *J. Polymer Sci.*, **3**, 549 (1948).
19. Brandt, W. W., *J. Phys. Chem.*, **63**, 1080 (1959).
20. Glasstone, S., K. J. Laidler, and H. Eyring, *The Theory of Rate Processes*, McGraw-Hill, New York, 1941.

Synopsis

The transmission of helium, nitrogen, methane and propane was studied in samples of a high pressure, branched polyethylene (46% crystalline) irradiated to a dose in air of 10^8 roentgens from a Co^{60} source. By using a time-lag apparatus the permeability,

diffusion, and solubility constants were measured in the temperature range 0–55°C. These data were compared with those obtained in samples of the above polymer before irradiation. Infrared analysis indicates that oxidation, unsaturation, and crosslinking had resulted from irradiation of the polymer. Because of a possible gradient in chemical composition through the irradiated films, the usual analysis of the time-lag data may not have been applicable to the present work. The apparent diffusion and solubility constants were, however, qualitatively consistent with the anticipated effects of the chemical and physical changes resulting from irradiation. The apparent solubility constants were uniformly higher by 40% in the irradiated film as compared to the values in the unirradiated films. No reduction in crystallinity was observed upon irradiation, so this increase was ascribed to the effect of chemical composition changes. A thermodynamically consistent increase in the apparent heats of solution was also observed. The apparent diffusion constants were lower in the irradiated samples with the fractional reduction increasing with gas molecular diameter. The reduction for helium was 30%, while that for propane was 54%. The apparent energies of activation for diffusion showed no significant change upon irradiation. Arguments are presented to indicate that the reduced apparent diffusion constants apparently arose from the mild crosslinking which had occurred in the amorphous phase. Comparisons are made between the gas transmission data obtained in the unirradiated samples with those for other high pressure, branched polyethylenes studied in this laboratory in light of a simple model for gas flow in the crystalline-amorphous matrix.

Résumé

On a étudié la passage d'hélium, d'azote, de méthane et de propane dans des échantillons de polyéthylène (46% cristallin) obtenus sous haute pression, irradiés par une dose 10^8 roentgens provenant de Co^{60}. Les constantes de perméabilité, de diffusion et de solubilité ont été mesurées à des températures allant de 0 à 55°C. Ces données furent comparées avec celles obtenues sur des échantillons du polymère ci-dessus avant irradiation. Les analyses infra-rouges montrent que l'irradiation du polymère provoque une oxydation, une insaturation et une réticulation. Etant donné que les films irradiés présentent un gradient possible dans la composition chimique, les analyses usuelles pourraient ne pas être applicables dans le présent travail. Les constantes de diffusion et de solubilité apparentes furent néanmoins qualitativement en accord avec les effets prévus et occasionnés par les variations chimiques et physiques tels qu'ils résultent de l'irradiation. Les constantes de solubilité apparente sont uniformément plus élevés de 40% pour des films irradiés comparées aux valeurs de films non-irradiés. Aucune réduction de cristallinité n'a été observée après irradiation, de sorte que cette augmentation était due à une variation dans la composition chimique. On a égalemet observé une augmentation pour la chaleur de solution apparente. Les constantes apparentes de diffusion pour des films irradiés avient une valeur inférieure, cette diminution étant fonction du diamètre de la molécule du gaz. La diminution pour l'hélium était de 30% tandis que pour le propane elle était de 50% inférieure. Les énergies apparentes d'activation pour la diffusion ne montraient aucune variation significative après irradiation. Les arguments présentés semblent indiquer qu'une diminution des constantes de diffusion provient de la réticulation qui a lieu dans la phase amorphe. On a comparé les résultats obtenus sur la transmission de gaz à travers des films de polyéthylène non irradiés avec ceux d'autres films obtenus sous haute pression, et constitutés de polyéthylène ramifiés qui ont été étudiés dans ce laboratoire en vue d obtenir un modèle simple pour étucier le passage du gaz è travers une matrice cristalline-amorphe.

Zusammenfassung

Der Durchtritt von Helium, Stickstoff, Methan und Propan wurde an Proben von verzweigtem Hochdruckpolyäthylen (46% kristallin) untersucht, das in Luft mit einer Dosis von 10^8 Röntgen aus einer Co^{60}-Strahlungsquelle bestrahlt worden war. Unter

Verwendung eines Apparats zur Messung der Durchbruchszeit wurden die Permeabilitäts-, Diffusions- und Löslichkeitskonstanten im Temperaturbereich von 0° bis 55°C gemessen. Die Ergebnisse wurden mit den an unbestrahlten Proben der genannten Polymeren erhaltenen verglichen. Die Infrarotuntersuchung zeigte, dass die Bestrahlung des Polymeren zur Oxydation, Bildung von Doppelbindungen und Vernetzung führt. Wegen eines möglichen Gradienten der chemischen Zusammensetzung in den bestrahlten Filmen ist die gewöhnliche Auswertung der Durchbruchszeitdaten auf die vorliegende Arbeit vielleicht nicht anwendbar. Die scheinbaren Diffusions- und Löslichkeitskonstanten standen aber qualitativ mit den erwarteten, durch die Bestrahlung bedingten Effekten der chemischen und physikalischen Veränderungen im Einklang. Die scheinbaren Löslichkeitskonstanten waren bei den bestrahlten Filmen einheitlich um 40% höher als bei den unbestrahlten. Da keine Änderung der Kristallinität durch die Bestrahlung beobachtet wurde, wurde diese Zunahme dem Einfluss von Veränderungen in der chemischen Zusammensetzung zugeschrieben. Eine thermodynamisch konsistente Zunahme der scheinbaren Lösungswärme wurde ebenfalls beobachtet. Die scheinbaren Diffusionskonstanten waren für bestrahlte Proben geringer, wobei die relative Abnahme mit dem Moleküldurchmesser des Gases grösser wurde. Die Abnahme betrug für Helium 30%, für Propan 54%. Die scheinbare Aktivierungsenergie der Diffusion zeigte bei Bestrahlung keine grössere Veränderung. Es werden Gründe dafür angeführt, dass die Verminderung der scheinbaren Diffusionskonstanten offenbar auf eine geringe Vernetzung in der amorphen Phase zurückzuführen ist. Die an unbestrahlten Proben erhaltenen Gasdurchlässigkeitsdaten wurden mit den an anderen verzweigten Hochdruckpolyäthylenen erhaltenen verglichen, die in diesem Laboratorium anahnd eines einfachen Modells für den Gasfluss in der kristallin-amorphen Matrix untersucht worden waren.

Received September 5, 1961

JOURNAL OF POLYMER SCIENCE: PART A VOL. 1, PP. 921–927 (1963)

Depolarization Measurements of Polymer Solutions at High Dilutions. Part II

V. KALPAGAM and M. RAMAKRISHNA RAO, *Department of Inorganic and Physical Chemistry, Indian Institute of Science, Bangalore, India*

Introduction

The importance of measuring the depolarization ratios and the valuable information these ratios give in the case of polymer solutions have been discussed in an earlier paper.[1] Apart from these depolarization ratios the individual components which make up these ratios also give us an idea of the geometry and the behavior of the polymer molecules in solutions.

The V_v component in macromolecular solutions generally constitutes all of the transversely scattered light. Therefore it is justifiable to discuss it as though it were the total scattered light. According to the predictions of Doty,[2] the ratio V_v/C in a good solvent should decrease sharply at first with increasing concentration and level off at higher concentrations, while in a poor solvent it should be more or less independent of concentration.

It has been demonstrated by the reciprocity theorem[3] that H_v and V_h must necessarily be equal. Therefore, it is sufficient to consider the component H_v alone instead of H_v and V_h. Due to increased intermolecular and intramolecular contacts existing in poor solvent media, the average configuration of the polymer molecules will be altered somewhat, which in turn changes the anisotropy. The molecules coil up to make available the larger number of contacts required; hence, H_v/C or V_h/C should decrease with increasing concentration. However, in a good solvent, as long as the solution is dilute, there will be no change in the anisotropy of the molecules, as a consequence of which H_v/C or V_h/C should be independent of concentration. These are the theoretical conclusions drawn by Doty.[2]

In view of the interesting results obtained in the depolarization measurements of the poly(vinyl acetate) system these studies were extended to the poly(methyl methacrylate) system in a good solvent as well as in a critical consolute mixture in order to confirm the validity of earlier conclusions. In addition to this, the analysis of the individual components V_v and H_v for the systems studied were carried out to elucidate further the geometry of the molecules at high dilutions.

Experimental

For the depolarization measurements the Brice-Phoenix Universal type 1000 D light-scattering photometer[4] and the differential amplifier described elsewhere[1] were used.

The fractions of poly(vinyl acetate) used in this investigation were the same as those used in the previous investigation.[1] The fractions of poly(methyl methacrylate) were prepared as follows. The monomer methyl methacrylate was first distilled under vacuum to remove the inhibitors and was then bulk polymerized at 40 ± 0.25°C. with the use of various concentrations of the catalyst, benzoyl peroxide, to obtain different molecular weight ranges, the conversion being kept well below 20% to obtain linear polymer molecules.[5] Various fractions were obtained from those polymer samples by subjecting them to fractional precipitation.

The solutions employed for this investigation were rendered dust-free as before.[1] The depolarization measurements were taken at 90°, for the various solutions, for vertically, horizontally, and unpolarized light at the wavelength 4360 A.

Results and Discussion

The graphs of ρ_u, ρ_v, and ρ_h plotted against the concentration C (in grams/100 ml.) for poly(methyl methacrylate) in methyl ethyl ketone and a critical consolute mixture of methyl ethyl ketone and isopropanol (1:1 by volume) are shown in Figure 1, while Table I gives the corresponding data.

TABLE I

Fraction	System	Polymer concn., C, g./ml.	ρ_u	ρ_v	ρ_h Experimental	ρ_h Calculated	At infinite dilution
M_5F_7	Poly(methyl	0.00043	0.012	0.005	1.25	0.87	0.80
(M_w = 0.57	methacrylate)–	0.00067	0.010	0.004	1.43	0.69	
× 10^6)	methyl ethyl	0.00093	0.011	0.005	1.43	0.94	
	ketone	0.00131	0.009	0.005	1.56	0.98	
		0.00184	0.008	0.004	2.11	1.01	
$M_{15}A_4$		0.00016	0.146	0.097	0.95	1.52	
(M_w = 0.4		0.00108	0.065	0.026	1.04	0.64	
× 10^6)		0.00144	0.022	0.011	1.08	1.02	0.90
		0.00194	0.015	0.006	1.27	0.72	
		0.00228	0.011	0.006	1.33	1.02	
		0.00294	0.013	0.005	1.45	0.75	
$M_{15}A_4$	Poly(methyl	0.00115	0.119	0.061	0.98	0.94	
(M_w = 0.4	methacrylate)–	0.00148	0.105	0.056	0.99	0.99	
× 10^6)	critical con-	0.00158	0.090	0.046	0.98	0.97	0.93
	solute mixture	0.00282	0.040	0.019	0.97	0.88	
		0.00308	0.041	0.019	0.96	0.84	

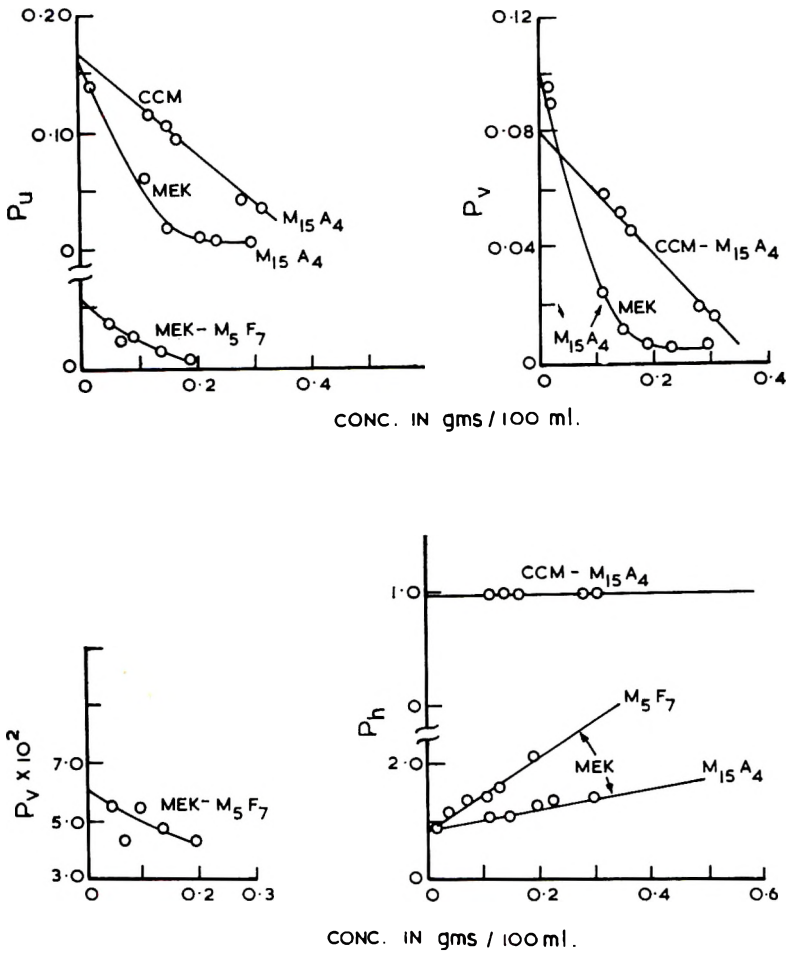

Fig. 1. Plots of depolarization ratios ρ_u, ρ_v, and ρ_h of poly(methyl methacrylate) (PMM) in methyl ethyl ketone (MEK) and critical consolute mixture (CCM), as functions of concentration C.

The trends of the plots of the depolarization ratios ρ_u, ρ_v, ρ_h for the poly(methyl methacrylate)–methyl ethyl ketone system confirm our earlier observations for the poly(vinyl acetate)–methyl ethyl ketone and poly-(vinyl acetate)–ethyl acetate systems. The observed decrease in the ρ_u and ρ_v values with increasing concentration can be attributed to the fact that the types of interactions predominant in the high and low dilution regions are the solute–solvent and solute–solute types, respectively. As in the poly(vinyl acetate) systems, the ρ_h values for this system also decrease with decreasing concentration.

In the case of poly(methyl methacrylate)–critical consolute mixture (PMM–CCM) the behavior of the depolarization ratios is different. From the figure it is seen that both ρ_u and ρ_v for the fraction $M_{15}A_4$ in the critical consolute mixture decrease with increasing concentration. The critical

concentration region, above which the curves were flattening up (thereby showing that the anisotropy of the molecules does not alter any further) is absent for this system. The constancy of the ρ_u, ρ_v graphs above a certain concentration indicates that the solute–solute interactions, on account of which the polymer molecules tend to become less and less anisotropic are being balanced by the solute–solvent interactions which try to alter the shape or anisotropy of the molecules; hence, the anisotropy of the molecules becomes constant above a certain critical concentration. In the case of the critical consolute mixture, however, since solute–solvent interactions are absent, the effect is due only to the solute–solute interactions, as a result of which the molecules are trying to become less and less anisotropic. ρ_h values are also seen to be independent of concentration for this system.

In a critical consolute mixture the solute–solvent interaction is zero. A steady decrease in ρ_u, ρ_v values with increasing concentration appears to be due to the effect of anisotropy alone for the ρ_h values at these concentrations are constant which in turn indicates the constancy of size. In the case of a critical consolute mixture the root-mean-square radius of the polymer molecule will be the same as that of the unperturbed coil $(\bar{r}_0^2)^{1/2}$. Hence there is no variation in the ρ_h values.

The ρ_h values are higher than unity for the poly(methyl methacrylate)–methyl ethyl ketone system and are less than one in the critical consolute mixture. As such, the ρ_h values calculated from Krishnan's reciprocity theorem[3] vary widely from the experimentally determined values in methyl ethyl ketone, but in the critical consolute mixture the agreement between the two sets of values is very good. Therefore this confirms our previous conclusion[1] that the reciprocity theorem holds good only for those polymer solutions where ρ_h is unity or less than unity.

Figures 2–4 show the plots of the individual components V_v/C and H_v/C for the systems poly(vinyl acetate)–methyl ethyl ketone, poly(vinyl acetate)–ethyl acetate, poly(methyl methacrylate)–methyl ethyl ketone and poly(methyl methacrylate)–critical consolute mixture. Actually the components V_v and H_v of the different samples are expressed as the fraction of solvent readings such as

$$V_v = (V_{v_s} - V_{v_0})/V_{v_0}$$

and

$$H_v = (H_{v_s} - H_{v_0})/H_{v_0}$$

where the subscripts v_s and v_0 correspond to the solution and solvent readings, respectively.

From Figures 2–4, it is seen that V_v/C decreases with increasing concentration in all the systems studied except in the system poly(methyl methacrylate)–critical consolute mixture. In some cases the curves tend to become constant above a concentration of about 0.1% or so.

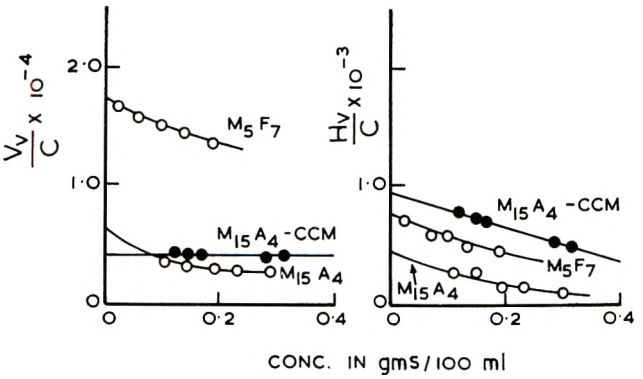

Fig. 2. Plots of the individual components V_v/C and H_v/C of the depolarization measurements of poly(methyl methacrylate) (PMM) in (○) methyl ethyl ketone (MEK) and (●) critical consolute mixture (CMM), as functions of concentration C.

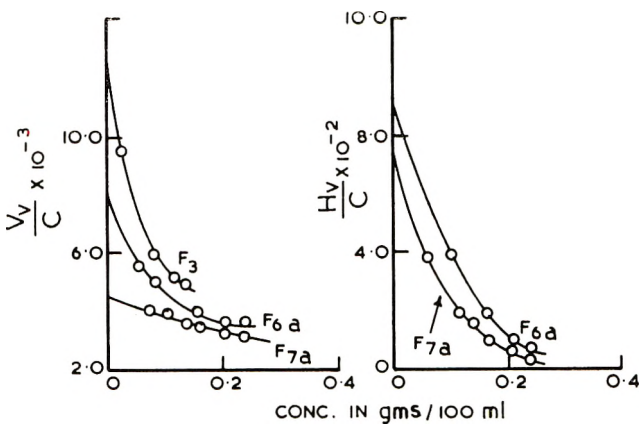

Fig. 3. Plots of the individual component V_v/C and H_v/C of the depolarization measurements of poly(vinyl acetate) (PVA) in ethyl acetate as functions of concentration C

As mentioned already, the V_v component in macromolecular solutions constitutes practically all of the transversely scattered light. As the intensity of the scattered light will be more in the case of a higher molecular weight fraction, V_v and V_v/C will be higher for a higher molecular weight fraction. These predictions are confirmed by the plots obtained in this investigation.

As the solvent power is decreased, the intensity of the scattered light decreases, as a result of which V_v and hence V_v/C also decrease. In the case of the poly(methyl methacrylate)–critical consolute mixture it is seen that the V_v/C curve runs parallel to the concentration axis, thereby indicating that V_v/C is independent of the concentration.

A study of Figures 2–4 shows that H_v/C values also decrease with increasing concentration for all the systems studied. In some cases it is seen that the H_v/C values tend to become constant above a certain concen-

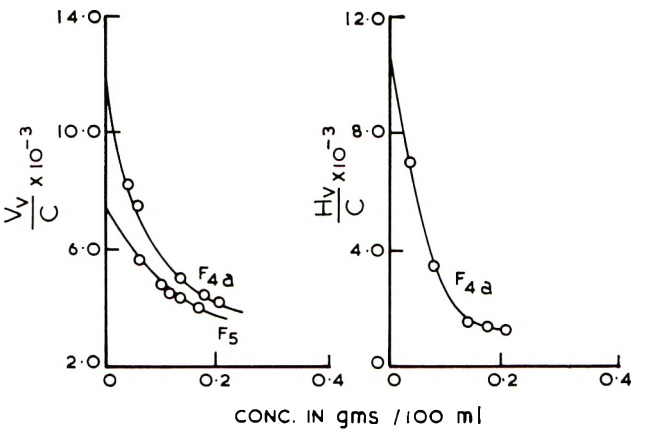

Fig. 4. Plots of the individual components V_v/C and H_v/C of the depolarization measurements of poly(vinyl acetate) (PVA) in methyl ethyl ketone as functions of concentration C.

tration. H_v is related to the anisotropy of the polymer molecule. The explanation given for the behavior of the ρ_u and ρ_v plots holds good even in the case of V_v/C and H_v/C graphs.

According to the predictions of Doty,[2] H_v/C should decrease continuously with increasing concentration in the case of poor solvents and remain independent of concentration in good solvents. However, in the present investigation it is seen that, in the case of the good solvent, H_v/C decreases with increasing concentration and in some cases tends to become constant above a certain critical concentration. In the case of the critical consolute mixture, however, the H_v/C values decrease steadily with increasing concentration, contrary to Doty's prediction.

The authors gratefully acknowledge the encouragement and advice tendered by Dr. S. Bhagavantam and Prof. M. R. A. Rao during the course of this investigation.

References

1. Kalpagam, V., and M. Ramakrishna Rao, *J. Polymer Sci.*, **A1**, 517 (1963).
2. Doty, P., *J. Polymer Sci.*, **3**, 750 (1948).
3. Krishnan, R. S., *Proc. Indian Acad. Sci.*, **1A**, 717 (1935).
4. Brice, B. A., M. Halwer, and R. Speiser, *J. Opt. Soc. Am.*, **40**, 768 (1950).
5. Wheeler, O. L., S. L. Ernest, and R. N. Orozier, *J. Polymer Sci.*, **8**, 409 (1952).

Synopsis

Depolarization measurements of transversely scattered light were determined for well fractionated samples of poly(methyl methacrylate) in methyl ethyl ketone and a critical consolute mixture of methyl ethyl ketone and isopropanol (1:1 by volume). ρ_u and ρ_v in methyl ethyl ketone decrease with increasing concentration and tend to become constant above a certain critical concentration, while in the critical consolute mixture, the values decrease steadily with increasing concentration. The ρ_h values increase with increasing concentration in methyl ethyl ketone, while in the critical consolute mixture they are independent of concentration; this indicates that the size does not change in critical consolute mixture. The individual components H_v and V_v are analyzed for the

poly(vinyl acetate) and poly(methyl methacrylate) systems studied by plotting H_v/C and V_v/C versus concentration. The observed discrepancies from Doty's predictions are explained.

Résumé

Des mesures de dépolarisation de la lumière diffusée transversalement ont été effectuées sur des échantillons bien fractionnés de polyméthacrylate de méthyle en solution dans la méthyl-éthyle-cétone et dans un mélange critique de méthyle-éthyle-cétone et d'isopropanol (1:1 en volume). Les valeurs de ρ_u et de ρ_v obtenues dans le méthyle-éthyle-cétone diminuent lorsque la concentration agumente et tendent vers une constante au dessus d'une certaine concentration critique, tandis que dans le cas de l'emploi du mélange critique, ces valeurs diminuent d'une façon régulière lorsque la concentration augmente. Les valeurs de ρ_h augmentent avec l'augmentation de la concentration lorsqu'on emploie la méthyle-éthyle-cétone, tandis que dans le cas du mélange critique, elles sont indépendantes de la concentration, ce qui indique que la dimension n'est pas altérée dans la mélange critique. Les composantes individuelles H_v et V_v ont été analysées et étudiées dans le cas de l'acétate de polyvinyle et du polyméthacrylate de méthyle en portant H_v/C et V_v/C en fonction de la concentration. On explique les différences observées par rapport aux prédictions de Doty.

Zusammenfassung

Die Depolarisation des Streulichtes wurde an gut fraktionierten Polymethylmethacryllatproben in Methyläthylketon und in einem kritischen Lösungsmittelgemisch von Methyläthylketon und iso-Propanol (Volumsverhältnis 1:1) bestimmt. Die ρ_u und ρ_v-Diagramme in Methyläthylketon fielen mit steigender Konzentration ab und strebten oberhalb einer bestimmten kritischen Konzentration einem konstanten Wert zu, während im kritischen Lösungsmittelgemisch die Werte beständig mit steigender Konzentration abnahmen. Die ρ_h-Werte steigen in Methyläthylketon mit zunehmender Konzentration an, während sie im kritischen Lösungsmittelgemisch unabhängig von der Konzentration sind, was zeigt, dass sich die Grösse im kritischen Lösungsmittelgemisch nicht ändert. Eine Analyse der individuellen Komponenten H_v und V_v wird für Polyvinylacetat- und Polymethylmethacrylatsysteme anhand einer Auftragung der H_v/C- und V_v/C-Kurven gegen die Konzentration gegeben. Die beobachteten Abweichungen von dem nach Doty zu erwartenden Verhalten können erklärt werden.

Received November 28, 1961

JOURNAL OF POLYMER SCIENCE: PART A VOL. 1, PP. 929–942 (1963)

Viscosities of Dilute Solutions of Polymethyl Methacrylate

W. R. MOORE and R. J. FORT, *Polymer Research Laboratories, Department of Chemical Technology, Bradford Institute of Technology, Bradford, Yorkshire, England*

Introduction

Investigations of the factors affecting dilute solution viscosities of polymethyl methacrylate seem to have been mainly concerned with the effects of variations in solvent and molecular weight of polymer. Daoust and Rinfret[1] reported values of intrinsic viscosity $[\eta]$ and the Huggins constant k' for an unfractionated sample in thirteen solvents and attempted to correlate them with the solubility parameter and polarity of the solvent. Values of the constants K and a in the expression

$$[\eta] = KM^a \tag{1}$$

where M is the molecular weight, have been given by a number of authors.[2–8] In most cases, values for a particular solvent and temperature are in reasonable agreement, although somewhat different values have been given for acetone as solvent.[4–8] Bischoff and Desreux,[4] Chinai et al.,[5] and Billmeyer and De Than[7] give K and a values for several solvents.

Kawai and Ueyama[9] measured intrinsic viscosities of fractions in acetone at temperatures at 25–40°C. and found a maximum value of $[\eta]$ for each fraction at about 30°C. Few other studies of the effects of temperature variations seem to have been made. This paper is concerned with viscosities of dilute solutions of polymethyl methacrylate fractions in six solvents at temperatures between 25 and 60°C. Effects of variations in solvent, molecular weight, and temperature on $[\eta]$, k', and other parameters are considered. Similar studies have recently been made on dilute solutions of polyvinyl acetate.[10] Polymethyl methacrylate chains are said to be somewhat stiffer than those of polyvinyl acetate,[1] and it was thought that this difference might be reflected in viscosity–temperature relationships.

Experimental

Two unfractionated samples, both of low conversion and with molecular weights estimated from viscosity measurements to be approximately 100,000 and 500,000, were fractionated by stepwise addition of hexane to 1% solutions in benzene. Hexane was added with stirring at 25°C. until

a moderate turbidity developed and the liquid warmed to 35°C., at which temperature the turbidity disappeared. The solution was cooled slowly to 25°C. and allowed to stand at this temperature overnight. The supernatant liquid was decanted from the gel which formed. The gel was dissolved in acetone and the polymer precipitated by pouring the acetone solution into excess water. The polymer was well washed with water and dried at 80°C. for 24 hr. Further hexane was added to the supernatant to obtain a second fraction and the whole process repeated twice in the case of the higher molecular weight sample and four times in the case of the lower. The fractions obtained were redissolved in benzene to give 1% solutions and refractionated to give 8 subfractions from the higher molecular weight sample and 11 from the lower. Of all these, six, designated H1C, H3A, H3B, L1A, L3A, and L5B, were of sufficient quantity to be used in further work. The number-average molecular weight $\bar{M}_n$ of each was determined osmotically in benzene at 25 ± 0.005°C. in Pinner-Stabin osmometers[11] statically. Cellophane membranes were used and no diffusion of polymer was detected.

Benzene, toluene, chloroform, *s*-tetrachloroethane, acetone, and *n*-amyl methyl ketone were used as solvents. The best available grades were further purified and fractionally distilled just before use. The pairs of aromatic hydrocarbons, chlorinated hydrocarbons, and ketones were chosen as examples of different solvent types and solvent power.

Viscosities of the pure solvents and of solutions in the concentration range 0.25–1.0 g./dl. at 20°C. were measured in capillary viscometers of such dimensions that shear effects were negligible. Kinetic energy corrections were made where applicable. Viscosities were measured at temperatures in the range 25–60°C., except in the cases of chloroform and tetrachloroethane, where the range was 25–53°C. and of acetone the range for which was 25–46°C. The temperature was varied in steps of 7°C. in each case, with the use of a water bath of which the temperature could be varied and maintained to within 0.05°C. of any temperature within the range used. Solutions were filtered before use. Intrinsic viscosities were obtained by extrapolation of linear plots of η_{sp}/c against c, where η_{sp} is the specific viscosity and c the concentration, by the method of least squares. Concentrations were corrected for thermal expansion. The flow times of solutions of the highest molecular weight fraction in tetrachloroethane at 53°C. were found to decrease slightly when successive measurements were made. This indicates degradation of polymer and this may also have occurred, to a lesser extent, with other fractions and at lower temperatures in tetrachloroethane.

Results

Plots of π/c against c, where π is the osmotic pressure, for the fractions in benzene at 25°C. are shown in Figure 1. The plots are linear and values of $\bar{M}_n$ obtained by extrapolation to zero c by the method of least squares are

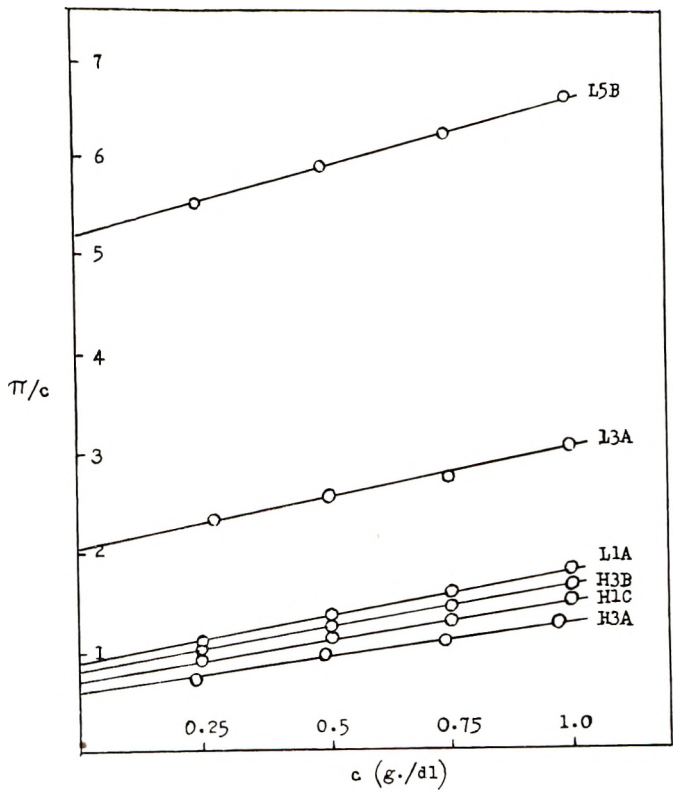

Fig. 1. π/c vs. c plots for fractions in benzene at 25°C.

given in Table I, which also includes values of the second virial coefficient A_2 and of the polymer-solvent interaction parameter χ_1.

TABLE I
Data for Fractions in Benzene at 25°C.

Fraction	$\bar{M}_n$	$A_2 \times 10^4$, (cc./g.^{2})	χ_1
H3A	406,000	2.93	0.463
H1C	325,000	3.07	0.461
H3B	314,000	3.45	0.456
L1A	297,000	3.69	0.453
L3A	122,000	4.04	0.448
L5B	48,000	5.32	0.433

Figure 2 shows plots of η_{sp}/c against c for the fractions of highest and lowest molecular weight at the highest and lowest temperatures used with each solvent. These are typical of results for other fractions and at other temperatures. Intrinsic viscosities for all fractions at each temperature in each solvent are given in Table II. Values of the Huggins constant k' for fraction H3B in all the solvents at temperatures from 25 to 46°C.

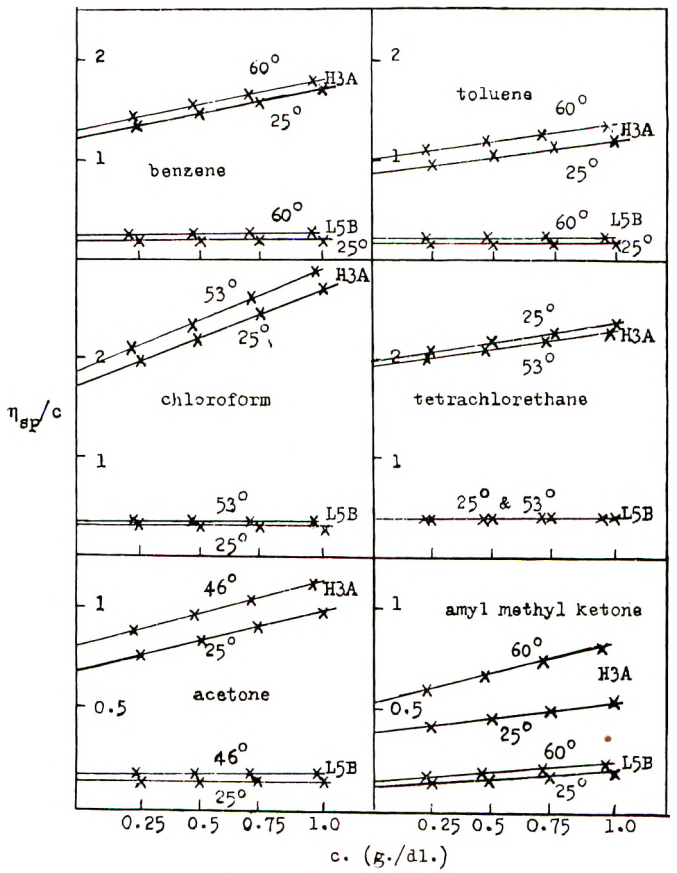

Fig. 2. Typical plots of η_{sp}/c vs. c.

are given in Table III. Table IV gives values of k' for all fractions in each solvent at 25°C. Values in Tables III and IV may be regarded as typical of those for other fractions and temperatures, respectively.

Discussion

The values of A_2 in Table I decrease with increasing molecular weight and those of χ_1 increase, as theory[12] predicts. The χ_1 value of 0.448 at a molecular weight of 122,000 may be compared with 0.429 given by Schulz and Doll[13] for a fraction of molecular weight 124,000 in benzene.

For each fraction and temperature the values of $[\eta]$ follow the order: amyl methyl ketone < acetone < toluene < benzene < chloroform < tetrachloroethane. Daoust and Rinfret[1] give the same order for the last four solvents, and it appears to be one of increasing solvent power as estimated from χ_1 values.[13] Acidic hydrogen atoms of the chlorinated hydrocarbons will interact strongly with basic carbonyl groups of the polymer causing solvation and increasing solvent power beyond that expected from considerations of solubility parameters alone. The solubility parameter of

TABLE II
Values of $[\eta]$

Solvent	Temp., °C.	η for various fractions					
		H3A	H1C	H3B	L1A	L3A	L5B
Benzene	25	1.23	1.04	0.80	0.66	0.39	0.22
	32	1.24	1.06	0.81	0.68	0.40	0.23
	39	1.25	1.07	0.82	0.69	0.41	0.23
	46	1.28	1.09	0.84	0.70	0.42	0.24
	53	1.30	1.11	0.86	0.72	0.42	0.24
	60	1.29	1.13	0.85	0.70	0.41	0.23
Toluene	25	0.87	0.76	0.60	0.49	0.29	0.18
	32	0.89	0.77	0.61	0.50	0.30	0.18
	39	0.91	0.79	0.61	0.51	0.30	0.18
	46	0.93	0.80	0.62	0.52	0.30	0.19
	53	0.95	0.82	0.63	0.54	0.31	0.19
	60	0.98	0.85	0.65	0.55	0.32	0.19
Chloroform	25	1.72	1.44	1.14	0.93	0.53	0.30
	32	1.74	1.46	1.16	0.94	0.54	0.29
	39	1.76	1.48	1.18	0.95	0.55	0.29
	46	1.79	1.51	1.20	0.97	0.56	0.30
	53	1.82	1.55	1.23	1.00	0.58	0.29
Tetrachloroethane	25	1.96	1.56	1.19	0.97	0.54	0.37
	32	1.96	1.56	1.18	0.98	0.55	0.37
	39	1.95	1.55	1.18	0.97	0.55	0.37
	46	1.94	1.55	1.18	0.97	0.53	0.37
	53	1.93	1.55	1.18	0.97	0.55	0.37
Acetone	25	0.69	0.63	0.49	0.41	0.25	0.14
	32	0.73	0.65	0.51	0.43	0.27	0.15
	39	0.76	0.68	0.53	0.44	0.28	0.15
	46	0.79	0.71	0.55	0.45	0.29	0.16
Amyl methyl ketone	25	0.38	0.40	0.31	0.26	0.18	0.13
	32	0.42	0.44	0.34	0.27	0.19	0.14
	39	0.46	0.47	0.37	0.29	0.20	0.14
	46	0.51	0.51	0.39	0.31	0.21	0.15
	53	0.53	0.54	0.42	0.33	0.22	0.15
	60	0.52	0.52	0.39	0.30	0.21	0.12

TABLE III
Values of k' for Fraction H3B

Solvent	k' at various temperatures			
	25°C.	32°C.	39°C.	46°C.
Benzene	0.36	0.34	0.33	0.32
Toluene	0.45	0.44	0.43	0.46
Chloroform	0.39	0.38	0.38	0.35
Tetrachloroethane	0.29	0.31	0.31	0.31
Acetone	0.52	0.51	0.49	0.48
n-Amyl methyl ketone	0.86	0.79	0.69	0.64

TABLE IV
Values of k' at 25°C.

Solvent	k' for various fractions					
	H3A	H1C	H3B	L1A	L3A	L5B
Benzene	0.32	0.33	0.36	0.41	0.38	0.29
Toluene	0.43	0.39	0.45	0.46	0.61	0.57
Chloroform	0.34	0.34	0.39	0.34	0.35	0.31
Tetrachloroethane	0.13	0.25	0.29	0.31	0.40	0.43
Acetone	0.61	0.65	0.52	0.59	0.60	0.85
n-Amyl methyl ketone	1.27	0.57	0.86	1.48	0.86	2.23

TABLE V
Values of K

Solvent	$K \times 10^5$					
	25°C.	32°C.	39°C.	46°C.	53°C.	60°C.
Benzene	6.15	6.46	6.74	6.81	6.52	4.46
Toluene	8.12	7.70	7.24	7.00	6.63	6.60
Chloroform	5.81	5.24	5.02	4.89	3.90	
Tetrachloroethane	12.8	12.6	12.5	12.4	12.2	
Acetone	6.59	6.51	6.40	6.18		
n-Amyl methyl ketone	50.6	41.1	35.0	24.3	7.12	10.4

TABLE VI
Values of a

Solvent	$a \pm 0.02$					
	25°C.	32°C.	39°C.	46°C.	53°C.	60°C.
Benzene	0.76	0.75	0.75	0.75	0.76	0.79
Toluene	0.71	0.71	0.72	0.72	0.73	0.73
Chloroform	0.79	0.80	0.80	0.80	0.82	
Tetrachloroethane	0.73	0.73	0.73	0.73	0.73	
Acetone	0.71	0.71	0.72	0.72		
n-Amyl methyl ketone	0.51	0.53	0.55	0.57	0.69	0.65

polymethyl methacrylate has been estimated to be 9.1 $(\text{cal./cc.})^{1/2}$ at 25°C., and considerations of solubility parameter may account for the greater solvent power of the aromatic hydrocarbons as compared with that of the ketones. Polarization of the aromatic hydrocarbons by the carbonyl groups of the polymer and subsequent fairly strong interaction is another possibility.

The variation of k' with solvent at any temperature is generally the reverse of that of $[\eta]$, smaller values being associated with better solvents.[14] Where comparison is possible, the values are similar to those of Daoust and Rinfret.[1] The high values obtained with amyl methyl ketone may be

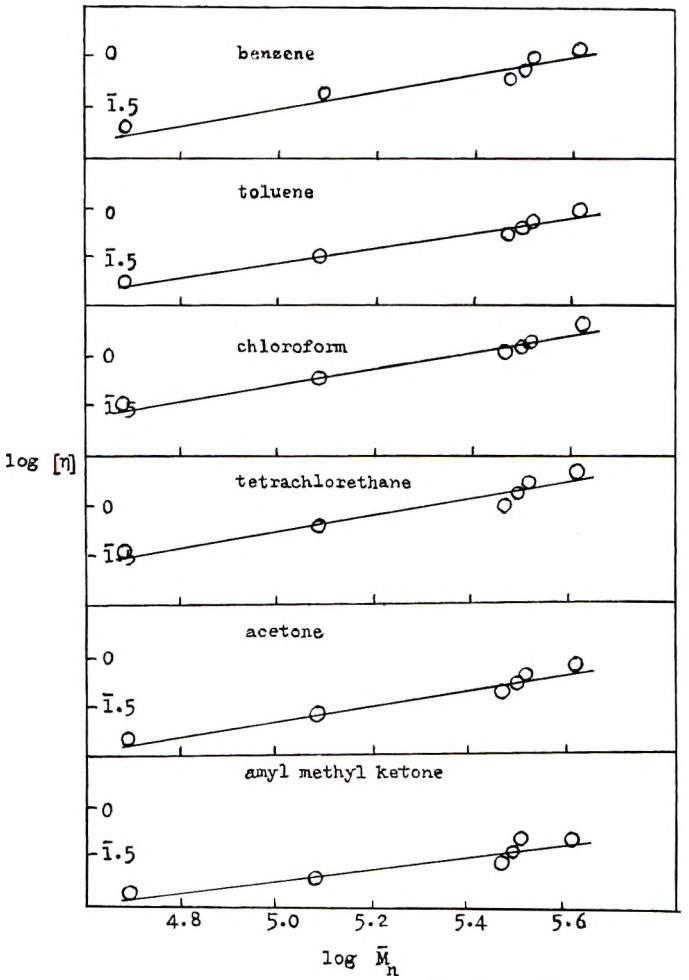

Fig. 3. Plots of log $[\eta]$ vs. log $\bar{M}_n$.

a consequence of association of polymer in this solvent which is the poorest of those used. High values of k' have been noted in cases of association of cellulose derivatives.[15]

Figure 3 shows plots of log $[\eta]$ against log $\bar{M}_n$ at 25°C. Similar plots are obtained at other temperatures. It is perhaps unfortunate that three of the fractions are of similar $\bar{M}_n$ and the points for these show some scatter, presumably because of somewhat different molecular weight distributions. Values of the constants K and a in eq. (1), obtained by the method of least squares, are given in Tables V and VI. In spite of the scatter, values for chloroform are in reasonable agreement with those of other workers,[2–5] as are those for acetone with the values given by Billmeyer and De Than[7] and by Bischoff and Desreux.[4] Values for benzene at 25°C. agree with those cited by Flory.[16]

The exponent a may be regarded as a measure of chain extension, which would appear to be greatest in chloroform which gives values of a at or near the theoretical limit of 0.8 for flexible chains. It might perhaps have been expected that tetrachloroethane which, for each fraction, generally gives the largest values of $[\eta]$, would also give the largest values of a. Degradation is a possible reason for the lower values and it is also possible that solvation, rather than chain extension, is responsible for the larger values of $[\eta]$. Similar results have been obtained with polyvinyl acetate.[10]

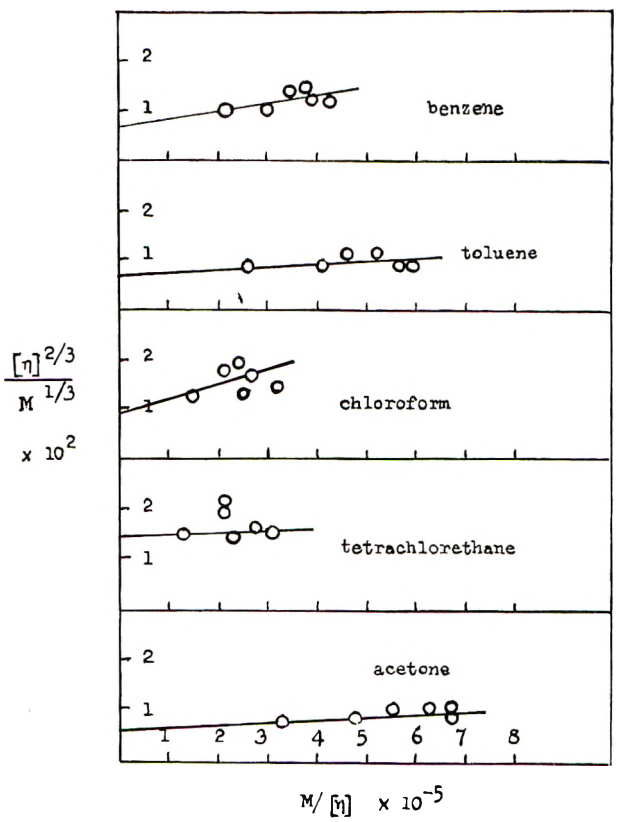

Fig. 4. Typical plots of $[\eta]^{2/3}/M^{1/3}$ vs. $M/[\eta]$ at 25°C.

In other cases, values of a tend to follow the order of solvent power. The value of a for n-amyl methyl ketone at 25°C. is close to 0.5, suggesting that this temperature is near the theta temperature for this solvent. Association of polymer is likely, however, and if this occurs correlation of a values with chain extension is hardly valid. Values of a generally tend to be greater than for polyvinyl acetate.[10] This may be due to differences in solvent power, but differences in chain stiffness[1] may also contribute.

Table IV shows that the values of k' for the fractions in each solvent are rather scattered. The reason for this is not clear. Similar results have been obtained with polyvinyl acetate.[10]

TABLE VII
Values of K' and α

Solvent	Temp., °C.	α H3A	H1C	H3B	L1A	L3A	L5B	$K' \times 10^4$
Benzene	25	1.35	1.33	1.22	1.16	1.13	1.09	7.3
	32	1.39	1.37	1.28	1.23	1.19	1.15	6.9
	39	1.40	1.40	1.30	1.25	1.21	1.16	6.7
	46	1.47	1.44	1.33	1.26	1.23	1.19	6.4
	53	1.48	1.47	1.38	1.32	1.27	1.23	5.9
	60	1.45	1.45	1.35	1.29	1.24	1.18	6.2
Toluene	25	1.21	1.21	1.09	1.09	1.05	1.04	7.3
	32	1.22	1.22	1.10	1.09	1.05	1.05	7.3
	39	1.23	1.23	1.11	1.10	1.06	1.05	7.3
	46	1.24	1.23	1.11	1.11	1.06	1.05	7.3
	53	1.25	1.24	1.12	1.11	1.07	1.06	7.3
	60	1.25	1.25	1.13	1.13	1.08	1.07	7.3
Chloroform	25	1.44	1.41	1.31	1.24	1.19	1.15	9.1
	32	1.47	1.43	1.34	1.26	1.21	1.16	8.7
	39	1.50	1.47	1.36	1.29	1.25	1.18	8.2
	46	1.53	1.50	1.40	1.32	1.27	1.21	7.8
	53	1.57	1.55	1.44	1.35	1.31	1.21	7.4
Tetrachloro-ethane	25			1.12	1.06	1.04	1.01	15.0
	32			1.12	1.07	1.04	1.02	14.9
	39			1.12	1.07	1.04	1.02	14.9
	46			1.13	1.07	1.05	1.02	14.5
	53			1.14	1.08	1.06	1.04	14.1
Acetone	25	1.28	1.30	1.22	1.17	1.15	1.11	4.9
	32	1.28	1.30	1.22	1.17	1.16	1.11	5.0
	39	1.29	1.30	1.22	1.16	1.15	1.10	5.3
	46	1.30	1.31	1.23	1.17	1.16	1.11	5.3

According to Flory,[17] the variation of $[\eta]$ with molecular weight and solvent is also given by:

$$[\eta] = \Phi (\bar{r}_0^2/M)^{3/2} M^{1/2} \alpha^3 = K' M^{1/2} \alpha^3 \qquad (2)$$

where Φ is a universal constant, $\bar{r}_0^2$ the mean square unperturbed end-to-end chain distance, and α a swelling or expansion factor which varies with the solvent having larger values in thermodynamically good solvents and a value of unity in a theta solvent in which the chains adopt their unperturbed configuration. Values of K' may be obtained from plots of $[\eta]^{2/3}/M^{1/3}$ against $M/[\eta]$ which should be linear with intercepts equal to $K'^{2/3}$. The points in such plots, as shown in Figure 4, are rather scattered particularly in the cases of chloroform and tetrachloroethane. Similar scatter has been obtained in other cases.[5,10,18] In evaluating the intercepts by the method of least squares, the points for the two highest molecular weight fractions in tetrachloroethane were not included, as these are seen to differ

from those for other fractions, perhaps because of degradation. Values of K' are given in Table VII. Those for amyl methyl ketone are not included in view of the probable association in this solvent. Values of α, obtained from those of K' and $[\eta]$ by use of eq. (2), are also given in Table VII. The values of K' and α must be regarded as approximate and probably only indicative of trends. This is not only because of the scatter shown in Figure 4. Recent work[19-22] has suggested refinements of the original treatment[17] and that the exponent of α in eq. (2) may be somewhat less than 3.

Values of K' are similar to those for other flexible polymers[23-25] but they seem, at a given temperature, to vary with the solvent. Chinai et al.[5] obtained a value of 9×10^{-4} for polymethyl methacrylate at 25°C. which appeared to be independent of the solvents (chloroform, methyl ethyl ketone, toluene, and a theta solvent) which were used. The value obtained with chloroform at 25°C. agrees with this and the different values for benzene and toluene might result from uncertainties arising from the scatter shown in Figure 4. This seems, perhaps, to be less likely in the cases of tetrachloroethane and acetone and the higher and lower values respectively obtained with these solvents might be due to variations in $\bar{r}_0^2$ with solvent. According to Flory,[17] such variations should be small. It is possible, however, that in cases involving solvation differences in $\bar{r}_0^2$, and hence of K', may arise from specific influences of solvent molecules on the disposition of a chain bond relative to its predecessor in the chain. It may be significant that values of K' are greatest with the two solvents, chloroform and tetrachloroethane, in which solvation is believed to occur. Solvation, perhaps by steric effects, may prevent chains adopting the unperturbed configuration obtained in less polar solvents.

Temperature coefficients of $[\eta]$ are similar to those for other flexible polymers, tending to increase with molecular weight, as theory[17] predicts, and to decrease with increasing solvent power. Temperature coefficients are positive in all cases but that of tetrachloroethane but maxima at about 53°C. are observed with benzene and amyl methyl ketone. Maxima near 30°C. with acetone[9] as solvent are not observed. While benzene, toluene, acetone, and amyl methyl ketone may be regarded as poor solvents with which positive temperature coefficients of $[\eta]$ might be expected, those for chloroform, a good solvent, are perhaps surprising. Small negative temperature coefficients are obtained with tetrachloroethane. Degradation might be a contributory factor. Kawai and Ueyama[9] have suggested that the temperature at which $[\eta]$ is a maximum is that at which the chains are most expanded and the values of α for benzene agree with this view. In the case of amyl methyl ketone, association, which should vary with temperature, may in some way lead to a maximum. The reason for the absence of maxima with acetone at about 30°C. is not clear.

k' decreases with increase of temperature, suggesting increasing solvent power, in all cases but that of tetrachloroethane and, possibly, toluene. k' seems to be little affected by temperature in the case of toluene and

increases with temperature in that of tetrachloroethane. Values of the exponent a in eq. (1) increase with temperature in all cases but that of tetrachloroethane. The increases are small, except in the case of amyl methyl ketone, where it is possible that decreasing association of polymer may account for the marked increases in the value of a. The values of a for tetrachloroethane appear to be independent of temperature although, again, degradation, which is more likely at higher temperatures, may possibly account for this. K decreases with increase of temperature in all cases but that of benzene, and the decrease is marked with amyl methyl ketone. Positive temperature coefficients of a imply increasing chain extension with increase of temperature.

K' decreases with increase of temperature in the cases of benzene, chloroform, and tetrachloroethane, seems to be independent of temperature with toluene, and increases with temperature in the case of acetone. Decreases might be expected, since hindrance to free rotation should decrease with increasing temperature and cause a reduction in the value

TABLE VIII

Solvent	Fraction	$d(\log [\eta])/dT \times 10^3$	$3d(\log \alpha)/dT$ 3/2 $\times 10^3$	$d[\log(\bar{r}_0^2/M)]/dT \times 10^3$
Benzene	H3A	1.15	4.4	−3.15
	H1C	1.00	4.65	−3.65
	H3B	1.1	5.7	−4.6
	L1A	1.35	6.0	−4.65
	L3A	1.15	5.4	−4.25
	L5B	1.35	5.6	−4.25
Toluene	H3A	1.5	1.2	0.3
	H1C	1.4	1.2	0.2
	H3B	1.1	1.35	−0.25
	L1A	1.45	1.35	0.1
	L3A	1.2	1.05	0.15
	L5B	0.7	1.0	−0.3
Chloroform	H3A	0.9	4.0	−3.1
	H1C	1.15	4.4	−3.25
	H3B	1.1	4.4	−3.2
	L1A	1.15	3.95	−2.8
	L3A	1.4	4.5	−3.1
Tetrachloroethane	H3B	−0.1	0.8	−0.9
	L1A	0.0	0.9	−0.9
	L3A	0.0	0.9	−0.9
	L5B	0.0	1.5	−1.5
Acetone	H3A	2.8	1.0	1.8
	H1C	2.5	0.6	1.9
	H3B	2.4	0.5	1.9
	L1A	1.9	0.0	1.9
	L3A	3.1	0.55	2.55
	L5B	2.75	0.0	2.75

of $\bar{r}_0^2$. α increases with increase of temperature in all cases, the increases being small in the cases of tetrachloroethane and acetone. The dependence of α on temperature is complex, involving the reciprocal of temperature, $\bar{r}_0^2$, and heat and entropy parameters.[17]

From eq. (2), since Φ and M are independent of temperature,

$$d(\log [\eta])/dT = {}^3/_2\, d[\log(\bar{r}_0^2/M)]/dT + 3d(\log \alpha)/dT \qquad (3)$$

Both log $[\eta]$ and log α are approximately directly proportional to temperature, and values of $d(\log [\eta])/dT$ and $3d(\log \alpha)/dT$ are given in Table VIII, together with those of ${}^3/_2\, d[\log(\bar{r}_0^2/M)]/dT$, obtained by difference. In the cases of chloroform and benzene, the values of ${}^3/_2\, d[\log(\bar{r}_0^2/M)]/dT$ are negative and smaller than those of $3d(\log \alpha)/dT$, so that the positive temperature coefficients of $[\eta]$ result from increase in α. The same is true in the case of toluene, where the values of ${}^3/_2\, d[\log(\bar{r}_0^2/M)]/dT$ are very small and of variable sign. These values are also negative for tetrachloroethane, but in this case they are of similar magnitude to those of $3d(\log \alpha)/dT$. With acetone the values of ${}^3/_2\, d[\log(\bar{r}_0^2/M)]/dT$ are positive and greater than those of $3d(\log \alpha)/dT$. In this case the variation of $[\eta]$ with temperature would seem to be largely due to that of $(\bar{r}_0^2/M)$ rather than to that of α as might be expected.[17] Somewhat similar results have been obtained with polyvinyl acetate[10] and with cellulose derivatives.[26,27] Positive temperature coefficients of $\bar{r}_0^2$ have been reported for polydimethylsiloxane.[28]

We are grateful for a Bradford City Research Scholarship to one of us (R. J. F.).

References

1. Daoust, H., and M. Rinfret, *J. Colloid Sci.*, **7**, 11 (1952).
2. Baxendale, J. M., M. G. Evans, and J. K. Kilham, *J. Polymer Sci.*, **1**, 466 (1946).
3. Baysal, B., and A. V. Tobolsky, *J. Polymer Sci.*, **9**, 171 (1952).
4. Bischoff, J., and V. Desreux, *J. Polymer Sci.*, **10**, 437 (1953).
5. Chinai, S. N., J. D. Matlack, A. L. Resnick, and R. J. Samuels, *J. Polymer Sci.*, **17**, 391 (1955).
6. Meyerhoff, G., and G. V. Schulz, *Makromol. Chem.*, **7**, 294 (1952).
7. Billmeyer, F. W., and C. B. De Than, *J. Am. Chem. Soc.*, **77**, 4763 (1955).
8. Kapur, S. L., *J. Sci. Indian Research*, **15B**, 239 (1956).
9. Kawai, T., and T. Ueyama, *J. Appl. Polymer Sci.*, **8**, 227 (1960).
10. Moore, W. R., and M. Murphy, *J. Polymer Sci.*, **56**, 519 (1962).
11. Pinner, S., and J. V. Stabin, *J. Polymer Sci.*, **9**, 575 (1952).
12. Flory, P. J., *Principles of Polymer Chemistry*, Cornell Univ. Press, Ithaca, N. Y., 1953, Chap. 12.
13. Schulz, G. V., and M. Doll, *Z. Elektrochem.*, **56**, 248 (1952).
14. Cragg, L. H., and R. H. Sones, *J. Polymer Sci.*, **9**, 585 (1952).
15. Moore, W. R., J. A. Epstein, A. M. Brown, and B. M. Tidswell, *J. Polymer Sci.*, **23**, 23 (1957).
16. Flory, P. J., *loc. cit.*, Chap. 7, p. 312.
17. Flory, P. J., *loc. cit.*, Chap. 14.
18. Berkowitz, J. B., M. Yamin, and R. M. Fuoss, *J. Polymer Sci.*, **28**, 69 (1958).
19. Kurata, M., W. H. Stockmayer, and A. Roig, *J. Chem. Phys.*, **33**, 151 (1960).
20. Kurata, M., and H. Yamakawa, *J. Chem. Phys.*, **29**, 311 (1958).

21. Schulz, G. V., and R. Kriste, Short Communications, International Symposium on Macromolecules, Weisbaden, 1959, II-B4.
22. Ohyanagi, Y., and M. Matsumoto, *J. Polymer Sci.*, **54**, 83 (1961).
23. Fox, T. G, and P. J. Flory, *J. Phys. & Colloid Chem.*, **53**, 197 (1949); *J. Am. Chem. Soc.*, **73**, 1909 (1951).
24. Krigbaum, W. R., and P. J. Flory, *J. Polymer Sci.*, **11**, 37 (1953).
25. Fox. T. G, and P. J. Flory, *J. Am. Chem. Soc.*, **73**, 1915 (1951).
26. Moore, W. R., and A. M. Brown, *J. Colloid Sci.*, **14**, 343 (1959).
27. Moore, W. R., and G. D. Edge, *J. Polymer Sci.*, **47**, 469 (1960).
28. Ciferri, A., *Trans. Faraday Soc.*, **57**, 846, 853 (1961).

Synopsis

Viscosities of dilute solutions of six fractions of polymethyl methacrylate in the molecular weight range of 48,000–400,000 have been obtained with benzene, toluene, chloroform, tetrachloroethane, and *n*-amyl methyl ketone as solvents at different temperatures in the range 25–60°C. There is evidence for association of polymer in amyl methyl ketone, and degradation in tetrachloroethane is possible at higher temperatures. Variations of $[\eta]$ and of k' with solvent agree generally with those observed by other workers. Where comparison is possible, values of K and a in the expression $[\eta] = KM^a$ are also in general agreement with other values. Values of K' in the Flory equation $[\eta] = K'M^{1/2}/\alpha^3$ may possibly vary with solvent, and it is suggested that in cases where solvation of polymer occurs, the chains may be prevented from adopting the unperturbed configuration adopted in less polar solvents. $[\eta]$ increases with increase of temperature in all cases but that of tetrachloroethane, but there appears to be a maximum value near 53°C. with both benzene and amyl methyl ketone. The variation of the exponent a with temperature is similar to that of $[\eta]$. In the cases of benzene and chloroform, the temperature coefficient of $[\eta]$ seems to be primarily due to changes in the value of the swelling factor α, but in other cases changes in the value of $(\bar{r}_0^2/M)$ are important, $\bar{r}_0^2$ being the mean square unperturbed end-to-end distance of the polymer chains.

Résumé

On a obtenu les viscosités à différentes températures entre 25° et 60° de solutions diluées de six fractions de polyméthacrylate de méthyle d'un poids moléculaire de l'ordre de 48.000 à 400.000. Comme solvants on a employé le benzène, le toluène, le chloroforme, le tétrachloréthane et la *n*-amyl-méthyl-cétone. On met en évidence une association de polymère dans l'amyl-méthyl-cétone; à température plus élevée, une dégradation est possible dans le tétrachloréthane. Les variations de $[\eta]$ et de k' avec le solvant correspondent généralement aux variations observées par d'autres auteurs. Généralement quand une comparaison est possible, les valeurs de K et a dans l'expression $(\eta) = KM^a$ correspondent aussi aux valeurs des autres chercheurs. Il est possible que les valeurs de K' dans l'équation de Flory varient selon le solvant. On suppose que quand les polymères se mettent en solution, les chaînes peuvent être empêchées de prendre la configuration non-perturbée qu'on obtient dans des solvants moins polaires. La valeur de $[\eta]$ augmente avec l'augmentation de température dans tous les cas sauf dans le cas du tétrachloréthane. Il semble exister toutefois un maximum vers 53°C dans le benzène et l'amyl-méthyl-cétone. La variation de l'exposant avec la température est similaire à celle de la valeur de $[\eta]$. Dans les cas du benzène et du chloroforme le coefficient de température de $[\eta]$ semble être principalement lié aux changements de la valeur du facteur de gonflement α Dans d'autres cas, les variations dans la valeur de $(\bar{r}_0^2/M)$ sont importantes, $\bar{r}_0^2$ étant la longueur quadratique moyenne non-perturbée de la chaîne polymérique.

Zusammenfassung

Die Viskosität verdünnter Lösungen von sechs Polymethylmethacrylatfraktionen im Molekulargewichtsbereich von 48000 bis 400000 wurde in Benzol, Toluol, Chloroform,

Tetrachloräthan und *n*-Amylmethylketon als Lösungsmittel bei verschiedenen Temperaturen im Bereich von 25° bis 60°C bestimmt. In Amylmethylketon scheint Assozization aufzutreten und in Tetrachloräthan ist bei höheren Temperaturen Abbau möglich. Die Abhängigkeit von $[\eta]$ und k' vom Lösungsmittel stimmt im allgemeinen mit den Beobachtungen anderer Autoren überein. Wo ein Vergleich möglich ist, stimmen auch die Werte von K und a in der Beziehung $[\eta] = KM^a$ allgemein mit anderen Werten überein. Die Werte von K' in der Flory-Gleichung $[\eta] = K'M^{1/2}\alpha^3$ hängen möglicherweise vom Läsungsmittel ab und es wird angenommen, dass bei Solvatation des Polymeren die Ketten nicht die ungestörte, in weniger polaren Lösungsmitteln vorhandene Konfiguration annehman können. $[\eta]$ steigt bei Temperaturzunahme in allen Fällen, ausser in Tetrachloräthan an, es scheint aber in Benzol und in Amylmethylketon ein Maximalwert nahe bei 53° aufzutreten. Die Temperaturabhängigkeit des Exponenten a ist ähnlich wie die von $[\eta]$. Im Falle von Benzol und Chloroform scheint der Temperaturkoeffizient von $[\eta]$ hauptsächlich durch Änderung des Expansionsfaktors α bedingt zu sein; in anderen Fällen ist aber die Änderung des Wertes von $(\bar{r}_0^2/M)$ von Bedeutung, wo r_0^{-2} das mittlere Quadrat des ungestörten End-zu-End-Abstandes der Polymerketten ist.

Received January 4, 1962

JOURNAL OF POLYMER SCIENCE: PART A VOL. 1, PP. 943–949 (1963)

Étude de l'Influence du Tetrahydrofurane sur la Radioreticulation du Chlorure de Polyvinyle

C. WIPPLER et R. GAUTRON, *Centre de Recherches de la Cie. de St. Gobain, Antony (Seine), France*

INTRODUCTION

Dans un travail antérieur,[1–3] nous avions montré que le rendement de la radioréticulation du chlorure de polyvinyle était considérablement augmenté si l'on gonflait ou dissolvait le polymère dans certains solvants organiques. Mais, nous n'avions jusqu'ici pu donner aucune explication théorique de ce phénomène. Pour tenter d'élucider son mécanisme, nous avons repris nos expériences en concentrant notre attention sur les solutions de chlorure de polyvinyle dans le tétrahydrofurane.

Le CPV récupéré après irradiation était analysé par de nombreuses méthodes tant chimiques que physico-chimiques: nous les décrirons brièvement. Les résultats actuels de nos expériences incitent à supposer que le tétrahydrofurane participe de façon active aux liaisons intermoléculaires. Dans ce cas, en effet, l'acide chlorhydrique qui est dégagé par le CPV lors de l'irradiation et qui attaque la molécule de tétrahydrofurane la transformerait en composés capables de réagir à leur tour avec les chaînes macromoléculaires.

CONDITIONS EXPERIMENTALES

Le CPV utilisé était un chlorure préparé industriellement par polymérisation en masse (C_1 de la Cie. de St.-Gobain). Ses seules impuretés étaient par conséquent les restes de catalyseurs. Sa masse moléculaire déterminée par diffusion de la lumière se situe à 117.000 ± 3.000 (dn/dc = 0,113 cm/g), la viscosité intrinsèque mesurée dans le tétrahydrofurane est de 82 ± cm³/g.

Les irradiations ont été effectuées avec une source de ^{60}Co à des intensités de l'ordre de 9.000 rads/heure. Le chlorure était dissous à raison de 1 g par 100 cc dans du THF et mis dans des ampoules scellées sans dégazage préalable.

La concentration choisie était suffisamment faible pour que, d'après nos études antérieures[2,3] le CPV reste soluble aux fortes doses d'irradiation utilisées.

Après irradiation les solutions étaient précipitées et lavées au méthanol, puis séchées sous vide en évitant tout chauffage.[4] Ensuite, nous avons

procédé à des mesures de masse moléculaire, à des mesures de viscosité, à une étude par spectrographie infra-rouge, à la microanalyse. Les variations de poids du polymère avant et après irradiation ainsi que les variations de l'indice de réfraction en fonction de la concentration ont également été déterminés.

RESULTAS EXPERIMENTAUX

Une grande partie des résultats de ces analyses a été consignée dans le tableau I.

TABLEAU I

Dose, MRad	M_p $\times 10^{-3}$	$[\eta]$cc/g	C, %	H, %	Cl, %	Complément à 100%
0	117	82	38,41	4,8	56,8	0
6,15	110	84	39,2	5,2	53,3	2,3
12,05	200	55	40,8	4,9	53	1,3
20,20	330	53	42,75	5,55	50	1,7
24	515	40	43,5	5,5	49,2	1,8
30	∞	∞	44,04	5,61	47,8	2,5

a. Masses moléculaires et Viscosités

Comme il fallait s'y attendre,[2,3] la masse moléculaire pour les produits irradiés à une dose de 20 à 24 Mr est trois à quatre fois plus élevée que celle du CPV initial alors que la viscosité intrinsèque est dûe à des réticulations entre chaînons d'une même molécule. Cette réticulation a, en effet, pour conséquence de réduire le volume apparent de la molécule.

Il est à remarquer que pour une dose de 30 Mrads, les liaisons intermoléculaires sont suffisamment nombreuses pour rendre le produit partiellement insoluble.

b. Spectres infra-rouges

Non moins intéressants sont les résultats obtenus par spectrographie infra-rouge. En effet, les spectres des CPV irradiés en solution diluée dans le THF possèdent des différences marquées avec le spectre du CPV témoin, différences qui peuvent se résumer ainsi:

modifications des bandes à 3,4 et 6,8 μ dues sans doute à l'augmentation des groupes CH_2; apparition d'une bande à 9,35 μ qui peut être attribuée à une liaison du type —C—O—C—; apparition d'une bande à 13,35 μ dûe aux liaisons CCl_2; diminution de la bande —C—Cl à 15,8 μ; apparition d'une très faible bande C=O.

Notons qu'aucune bande à 7,2 μ ne laisse supposer la formation de groupement méthyle.

c. Microanalyse

La perte de Cl par irradiation ressort évidemment des résultats de microanalyse. Il convient de noter que cette perte est de beaucoup supérieure à celle observée sur de la poudre de CPV pur. Corrélativement, on note une augmentation du pourcentage de carbone, mais nous verrons bientôt que cette augmentation ne peut pas s'expliquer par le seul départ de Cl_2 ou même de HCl. La différence entre 100 et la somme des pourcentages des autres éléments (dernière colonne tableau I) est dûe à la présence d'oxygène, mais elle englobe également toutes les imprécisions sur les dosages des autres éléments.

d. Perte de Poids

Il aurait été du plus haut intérêt de pouvoir déterminer la variation de poids du CPV avant et après l'irradiation. Malheureusement, cette détermination n'a pu se faire avec toute la précision souhaitable. Il est en effet inévitable qu'une partie du produit soit entrainé au cours des précipitations et lavages successifs. Un essai témoin sur du CPV non irradié nous a montré que dans ce cas les pertes sont de l'ordre de 6%. Nous aurions pu corriger les valeurs obtenues avec les CPV irradiés en tenant compte de ce pourcentage mais les produits irradiés, une fois précipités, ne se présentent pas sous le même aspect physique que le produit témoin de sorte qu'il nous parait osé d'admettre à priori que les entrainements sont du même ordre dans les deux cas.

e. Indice de Réfraction

Enfin, nous comptions préciser le mécanisme de l'effet d'irradiation en contrôlant la variation de l'incrément de l'indice de réfraction en fonction de la concentration (dn/dc). Mais nos espoirs ont été déçus. Il ne nous a pas été possible, en effet, d'obtenir des valeurs de dn/dc reproductibles. Nous nous sommes, en particulier, aperçus que l'indice de réfraction des solutions de CPV variait en fonction du temps. Nous n'avons trouvé, jusqu'ici, aucune explication à ce phénomène et préférons, dans ces conditions, ne pas faire intervenir ces résultats dans notre discussion.

DISCUSSION

De nombreuses hypothèses peuvent être envisagées au départ pour essayer d'expliquer l'influence du THF sur la radioréticulation du CPV. Nous n'en retiendrons que quatre. Nous soulignons qu'aucune de ces hypothèses ne fait appel à l'oxygène absorbé par les solutions. En effet, nous avions constaté à maintes reprises que le rendement de la radioréticulation était le même, aux erreurs d'expériences près, pour les solu-

tions irradiées en présence d'air, et pour les solutions soigneusement dégazées. Les quatre hypothèses retenues sons les suivantes.

(*1*) le THF n'intervient pas directement dans le produit final de réticulation. La réticulation est accompagnée du départ d'une molécule d'HCl. Les atomes de chlore et d'hydrogène appartiennent à deux molécules voisines, ou à deux parties voisines d' une même molécule

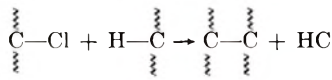

Nous exclurons ici la possibilité d'un départ en cascade de molécules d'HCl conduisant à la formation de doubles liaisons conjuguées. Cette hypothèse, généralement admise dans le cas de l'irradiation du CPV à l'état solide, explique la forte coloration du produit final. Or, la poudre de CPV récupérée après l'irradiation en solution dans le THF est parfaitement blanche, et rien dans le spectre infra-rouge ne laisse supposer qu'une telle réaction en chaîne ait lieu.

(*2*) Dans notre seconde hypothèse nous admettrons que la molécule de THF, après ouverture de son cycle sous l'action du chlore dégagé par le CPV et de l'irradiation, constitue le pont entre deux molécules de CPV, ou deux parties d'une même molécule de CPV

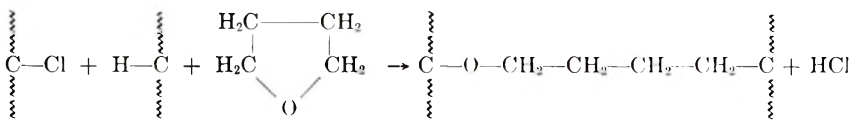

(*3*) La troisième hypothèse est très proche de la seconde, mais elle se fait avec l'élimination d'une molécule de Cl_2

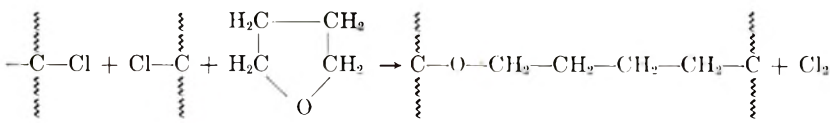

(*4*) La quatrième hypothèse, enfin, est basée sur une observation de Darimont.[5] Cet auteur a constaté que les solvants qui favorisaient la radioréticulation du CPV pouvaient donner sous irradiation des radicaux H—Ċ=O.

On peut alors se demander si la réaction de réticulation ne doit pas s'écrire:

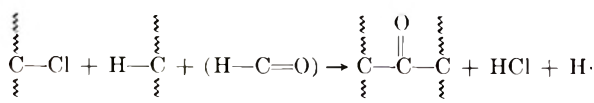

Reste alors à déterminer laquelle de ces hypothèses s'accorde le mieux avec les résultats expérimentaux. Dans ce but, nous avons reporté dans le tableau II les pourcentages de C, H, Cl, O calculés à partir des quatre hypothèses précédentes en faisant coïncider a priori les pourcentages de Cl avec les résultats obtenus par microanalyse. Dans la sixième colonne de

TABLEAU II

Dose Mrad		Valeurs calculés, % Hypothèse 1	Hypothèse 2	Hypothèse 3	Hypothèse 4	Valeurs expérimentales, %
6,15	C	41,7	40,5	40,7	40,2	39,2
	H	5,0	5,2	5,2	4,75	5,2
	Cl	53,3	53,3	53,3	53,3	53,3
	O	0	1,0	0,8	1,75	(2,3)
12,05	C	42	40,7	40,8	40,3	40,8
	H	5,0	5,2	5,2	4,7	4,9
	Cl	53	53	53,2	53	53
	O	0	1,1	0,8	2,0	(1,3)
20,20	C	44,8	42,5	42,9	42	42,75
	H	5,2	5,5	5,6	4,6	5,55
	Cl	50	50	50	50	50
	O	0	2,0	1,5	3,4	(1,7)
24	C	45,6	43,2	43,5	42,1	43,5
	H	5,2	5,5	5,65	4,65	5,5
	Cl	49,2	49,2	49,2	49,2	49,2
	O	0	2,1	1,7	4,05	(1,48)
30	C	46,9	44,0	44,5	42,6	44,04
	H	5,3	5,7	5,7	4,6	5,61
	Cl	47,8	47,8	47,8	47,8	47,8
	O	0	2,5	2,0	4,8	2,5

ce tableau nous avons inscrit les valeurs expérimentales. Nous avons mis entre parenthèses celles relatives à l'oxygène pour rappeler qu'elles sont obtenues indirectement par soustraction.

Il ressort de l'examen de ce tableau que l'hypothèse qui semble la mieux vérifiée est la seconde, suivie de très près par la troisième. La première et la quatrième conduisent à des valeurs calculées nettement différentes des valeurs expérimentales. Malgré tout, les écarts sont suffisamment faibles pour qu'il puisse persister un doute sur l'hypothèse à admettre.

Nous croyons, toutefois, pouvoir éliminer définitivement la première et la quatrième hypothèses en prenant en considération les résultats des analyses spectrales infra-rouge. En effet, aucune de ces hypothèses ne permet d'expliquer l'augmentation du nombre de groupes CH_2, ni l'apparition de liaisons du type —C—O—C. Remarquons cependant que l'apparition d'une bande dûe au groupe C=O serait en faveur de la quatrième hypothèse. Mais, d'une part, cette bande est très faible et, d'autre part, elle peut s'expliquer aisément par une légère oxydation du CPV sous l'influence du rayonnement.

Reste alors à faire un choix entre la deuxième et la troisième hypothèse. Nos préférences vont actuellement à la seconde tant parce que les valeurs des pourcentages calculées s'accordent un peu mieux avec l'expérience,

que parce que nous n'avons jamais observé de dégagement de chlore comme le voudrait la troisième hypothèse.

En calculant, enfin, le rendement radiochimique de réticulation, c'est-à-dire le nombre de ponts formés pour une énergie absorbée de 100 eV, on trouve $G = 81$ ponts/100 eV.

Ce rendement est considérablement plus élevé que celui (2,15) obtenu[1] à partir du point de gel des solutions plus concentrées en CPV. On pourrait évidemment arguer que cette dernière méthode ne tient compte que du nombre de ponts intermoléculaires et que la différence entre les deux valeurs est dûe aux ponts intramoléculaires. Il faudrait alors admettre qu'en solution concentrée il y a environ 40 fois plus de ponts intramoléculaires que de ponts intermoléculaires. Cette disproportion nous semble trop élevée.

CONCLUSION

Malgré les faits qui militent en faveur d'un mécanisme de participation directe de la molécule de THF à la radioréticulation du CPV en solution dans ce solvant, nous ne possédons actuellement aucune preuve permettant d'affirmer de façon sûre que les choses se passent bien ainsi. Dans l'état actuel des choses, nous estimons qu'une série d'expérience avec du THF marqué au ^{14}C pourrait nous donner la solution définitive de ce problème. Jusqu'ici, nous avons reculé devant le prix de telles expériences.

Références

1. Wippler, C., *J. Polymer Sci.*, **29**, 585 (1958).
2. Rougee, M., et C. Wippler, Symposium sur les macromolécules, Wiesbaden, Oct. 1959, IV C 12.
3. Wippler, C., *Nucleonics*, **18**, 68 (1960).
4. Gautron, R., et C. Wippler, *J. Chim. Phys.*, **18**, 754 (1961).
5. Darimont, H., Mémoire de licences-sciences chimiques, Liège, 1960.

Résumé

Dans ce travail nous avons essayé d'éclaircir le mécanisme de la réticulation du chlorure de polyvinyle irradié en présence de tétrahydrofurane. Tenant compte de nombreux résultats expérimentaux, nous sommes arrivés à la conclusion qu'il y a de très fortes chances que le pont qui relie deux molécules de CPV est constitué par une molécule de THF dont le cycle a été ouvert sous l'action combinée des radiations et du chlore ou de l'acide chlorhydrique dégagé par le CPV.

Synopsis

In this paper an attempt was made to explain the crosslinking mechanism of PVC, when irradiated in the presence of tetrahydrofurane. Taking into account several experimental results, a very likely conclusion seems to be that a bridge between two PVC molecules consists in a THF molecule, of which the ring has been opened by the combined effects of the irradiation and of the chlorine or hydrochloric acid evolved from the PVC.

Zusammenfassung

In der vorliegenden Arbeit wurde versucht, den Mechanismus der Vernetzung von Polyvinylchlorid bei Bestrahlung in Gegenwart von Tetrahydrofuran aufzuklären. Eine grosse Zahl von Versuchsergebnissen führte zu dem Schluss, dass eine grosse Wahrscheinlichkeit für die Bildung einer Vernetzung zwischen zwei PVC-Molekülen durch ein Molekül THF unter Ringöffnung unter dem gemeinsamen Einfluss der Strahlung und dem aus dem PVC entwickelten Chlor oder Chlorwasserstoff besteht.

Received December 19, 1961

JOURNAL OF POLYMER SCIENCE: PART A VOL. 1, PP. 951–964 (1963)

Syndiotactic Polyvinyl Formate and Derived Polyvinyl Alcohol

IRVING ROSEN, G. H. McCAIN, A. L. ENDREY and C. L. STURM,
Research Department, Diamond Alkali Company, Painesville, Ohio

INTRODUCTION

There are several reports in the literature on the preparation and polymerization of vinyl formate (VFo), but relatively little on the effect of polymerization conditions. The work on VFo has not been nearly so extensive as that with vinyl acetate. Probably the most comprehensive papers are those by Vansheĭdt and Chelpanova,[1] and Jordan and co-workers,[2] who investigated the effects of monomer purity and solvents on the polymer molecular weight.

A previous report from our laboratories on stereoregulating effects has shown that the low temperature polymerization of vinyl chloride enhances polymer syndiotacticity.[3] VFo also seemed a likely monomer from which to prepare syndiotactic polyvinyl formate (PVFo), and subsequently syndiotactic polyvinyl alcohol (PVA) by low temperature polymerization. This report presents the results of our studies along this line.

EXPERIMENTAL

VFo was prepared in good yield by the liquid-phase vinylation of anhydrous formic acid.[4] After a crude distillation, fractionation through a spinning band column yielded a highly purified monomer, b.p. 45.3–45.7°C., n_D^{22} 1.3856, which contained no low boiling impurities detectable by gas-phase chromatography.

The polymerizations were carried out under lamp grade nitrogen in a three-necked flask equipped with a stirrer, thermometer, gas inlet and outlet tubes, and reflux condenser. The preferred catalyst was ultraviolet light activation of azobisisobutyronitrile (AIBN) at a concentration of 1 mmole/mole of monomer. The conversions of monomer to polymer in the bulk polymerizations were usually in the range of 10 to 20%, and always less than 30%. Beyond this, heat transfer and temperature control become difficult. Low conversions were also advantageous, minimizing branching on the chain. The unreacted monomer was recovered by vacuum distillation. The polymer was purified by dissolution in $CHCl_3$, followed by precipitation in methanol or hexane. This was carried out twice. Reduced viscosities of the PVFo's were determined at 25.00 ± 0.01°C. on 0.1 g. samples in 100 ml. of $CHCl_3$.

The structure of the PVFo was investigated by means of infrared spectroscopy and x-ray diffraction. The infrared spectrum was obtained from a film cast on a KBr disk from a chloroform solution, with the use of a Perkin-Elmer Model 21 spectrometer (NaCl prism). Fiber-type diffraction patterns were obtained from films, with the use of nickel-filtered copper Kα radiation. The films studied were stretched 1000% at room temperature and annealed at 60°C.

PVFo was dissolved in dioxane and converted to PVA by alcoholysis with a solution of sodium methoxide in methanol and dioxane. The molecular weight of the PVA was estimated from the equation of Beresniewicz:[5]

$$[\eta] = 5.95 \times 10^{-4} \bar{M}_v^{0.63} \tag{1}$$

A plot of the viscosity of the PVFo in chloroform against that of the derived PVA in water showed that a linear relationship exists between these over the range studied, represented by eq. (2):

$$[\eta]_{\text{PVFo in CHCl}_3} = 0.69[\eta]_{\text{PVA in H}_2\text{O}} \tag{2}$$

The linearity indicates a small difference between the exponents of the Mark-Houwink equations for the two materials. Based on the assumption that the degree of polymerization ($\overline{DP}$) of the PVFo and derived PVA is the same, the eq. (3) was calculated from the Beresniewicz equation and used to estimate the $\overline{DP}$ of the PVFo:

$$[\eta] = 4.42 \times 10^{-3} \overline{DP}^{0.63} \tag{3}$$

To determine the Huggins viscosity constant and intrinsic viscosity of the PVA, viscosities were measured on 0.1–1% aqueous solutions at 25.00 ± 0.01°C. The inherent viscosity was plotted against concentration; extrapolation to zero concentration gave the intrinsic viscosity $[\eta]$. The Huggins constant k' was calculated from eqs. (4) and (5):

$$\eta_{\text{inh}} = [\eta] - k''[\eta]^2 C \tag{4}$$

$$k' = 0.5 - k'' \tag{5}$$

The 1,2-glycol content of the PVA was determined according to the method of Flory and Leutner[6] by degrading the polymer with periodic acid. From the molecular weights before and after degradation, the 1,2-glycol content was calculated.

The relative stereoregularity of the PVA was determined by the use of a PVA–iodine complex which was prepared by mixing 5 ml. of 1% aqueous PVA solution with 10 ml. of 0.02M I_2 + KI solution (1.27 g. I_2 + 1.5 g. KI/250 ml. solution). The mixture was allowed to stand for 1 min., then diluted to 100 ml.; further allowed to stand for 24 hr., diluted 2 to 5 with distilled water, and the optical density measured at 595 mμ with a Beckman spectrophotometer. The visible absorption spectrum of the iodine complex shows a maximum at 595 mμ.

By the given procedure for the preparation of complex solutions, the optical densities were measured and compared. In our early work, the absolute magnitudes of optical densities could not be reproduced, the variation apparently being associated with changes in the iodine solution. The relative order of optical densities, however, was always the same, provided that the iodine complexes were prepared at the same time. In subsequent determinations the optical densities were compared with the optical density of a conventional PVA complex, as standard, to enable comparison with previous determinations.

For the determination of swelling index and solubility, films were prepared by evaporating 5% aqueous solutions of the PVA's at room temperature. The films were cut into 1 in.^{2} pieces and additionally dried at 35°C. *in vacuo* overnight. After soaking, excess water was carefully wiped off and the film weighed. The film was then dried and reweighed. The swelling index was expressed as the weight of water imbibed per unit weight of polymer.

For the determination of density, films prepared by evaporating 1% aqueous solutions at room temperature were dried at 110°C./0.1 mm. for 18 hr. The density was determined by the flotation method in a carbon tetrachloride–benzene mixture. The density of the flotation medium was measured with a Mohr-Westphal balance.

Films were heat-treated by immersion in a silicone oil bath at 206–208°C. for 2 min. The water resistance was tested by immersing in boiling water for 1 min.

RESULTS

A. Polyvinyl Formate

As the polymerization temperature is raised from −20°C. to 30°C. there is a corresponding increase in the $\overline{DP}$ of the PVFo. This behavior is typical of a photochemically induced polymerization in which the molecular weight is controlled by chain termination rather than by chain transfer. Since chain termination is the principal process indicated, there is relatively little chain transfer to the polymer to form branched PVFo.

From the slope of the plot of the logarithm of the estimated $\overline{DP}$ of the PVFo against the reciprocal temperature (Fig. 1), the difference between the activation energy for propagation and termination $(E_p - E_t)/2$, was calculated to be 4.5 kcal./mole. This value is in good agreement with values obtained by other workers for the free radical-initiated polymerization of vinyl acetate, 4.4 and 4.7 kcal./mole.[7]

The infrared spectrum of VFo was obtained on 10% solutions in CCl_4 in the region from 4000 to 1080 cm.$^{-1}$ and in CS_2 from 1080 to 700 cm.$^{-1}$ (Fig. 2, top). The spectrum of VFo is quite similar to that of vinyl acetate for the comparable structural features. The major differences appear to be in a slight displacement of the carbonyl stretching from 1765 cm.$^{-1}$ in vinyl acetate to 1740 cm.$^{-1}$ in VFo, and the displacement of the

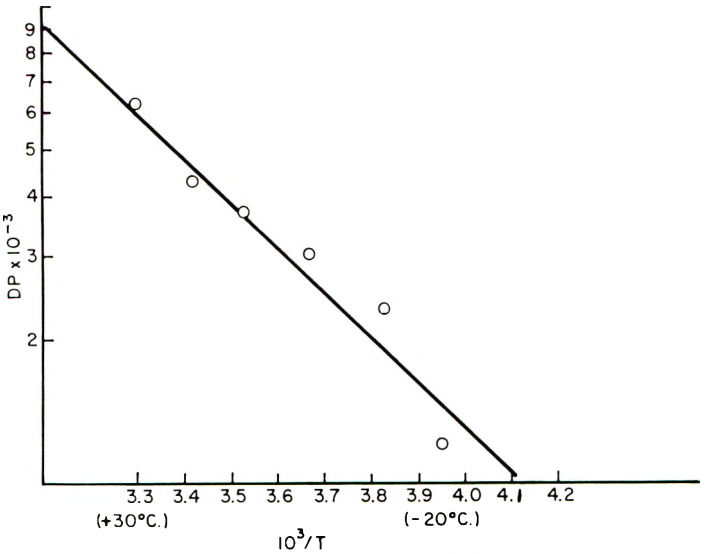

Fig. 1. Effect of polymerization temperature on $\overline{DP}$ of polyvinyl formate.

ester stretch from 1250 cm.$^{-1}$ to 1160 cm.$^{-1}$ in the formate. A weak unassigned absorption appears at 1365 cm.$^{-1}$ in the formate.

Comparison of the infrared spectra of the monomer and polymer (Fig. 2) shows that polymerization results in a minor shift in the C—H stretch absorption from 2950 cm.$^{-1}$ in the monomer to 2850 cm.$^{-1}$ in the polymer. The absorption bands in the monomer which are located at 1640, 937, and 872 cm.$^{-1}$ are associated with the double bond and disappear from the spectrum of the polymer. No difference was observed in the infrared spectra of polymers prepared at different polymerization temperatures.

The fiber x-ray diffraction patterns produced by the polymer prepared at 0°C. show the following (Fig. 3): three equatorial arcs with d spacings of 6.5 A. (very strong), 3.74 A. (weak), and 3.32 A. (weak); one set of diagonal arcs with d = 4.2 A. (moderately weak) corresponding to an axial translation (i.e., identity period of chain repeat distance) of 5.1 A.; a diffuse meridional arc with d = 2.68 A. These are interpreted as showing the presence of two kinds of crystallites. One, perhaps 10% of the sample, has a well developed three-dimensional structure including mean dimensions >250 A., both parallel and perpendicular to the fiber axis. The other, comprising ca. 25% of the sample, has good development perpendicular to the fiber axis (dimension >250 A.) and poor development parallel to the axis. Total crystallinity then is about 35%. The syndiotactic placements in the first type of crystallites must be nearly perfect, while those in the other type and also in the amorphous fraction are much more imperfect.

A similar interpretation of the fiber pattern produced by PVFo polymerized at 38°C. was not possible. In this instance, the pattern produced was too poor to yield any meaningful measurement. The only arcs found were equatorial, and no meridional arcs were detected, indicating the

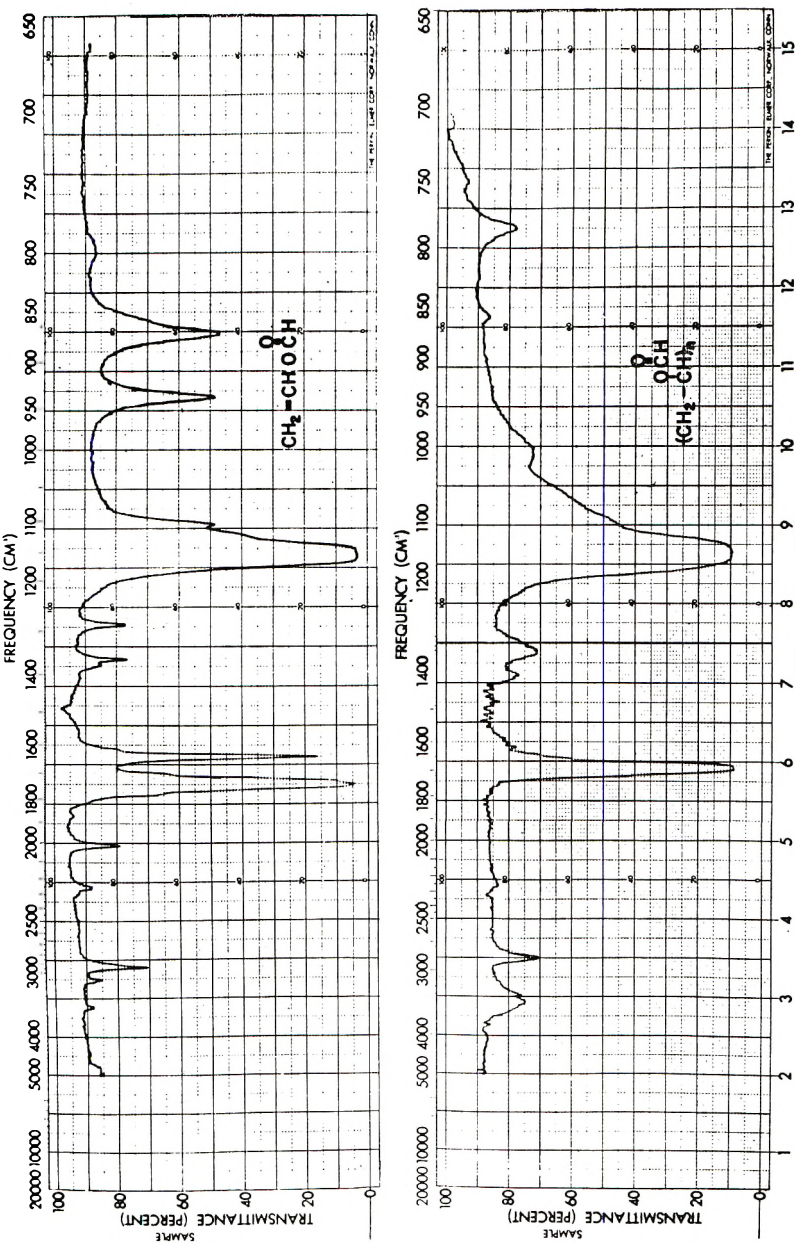

Fig. 2. Infrared spectra of (top) vinyl formate and (bottom) polyvinyl formate.

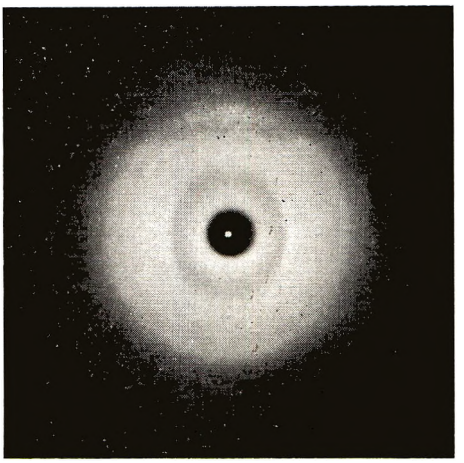

Fig. 3. X-ray pattern of oriented polyvinyl formate prepared at 0°C.

presence of only two-dimensional order with practically no order developing in a direction parallel to the fiber axis.

Two PVFo samples prepared at 0 and 38°C., of the same molecular weight, also demonstrated a different resistance to hot acetone vapor. The polymer prepared at 38°C. dissolved readily, while that prepared at 0°C. swelled and resisted dissolution for a much longer period of time. It is apparent from this study that a considerable difference in structure exists between the formates prepared at 0 and 38°C.

B. PVA Derived from Polyvinyl Formate

On the basis of the x-ray evidence, the low temperature polymerized PVFo appears to be the more syndiotactic. In order to establish further the increased stereoregularity of the PVFo polymerized at the lower temperatures, structural parameters of the derived PVA were compared with those of conventional and syndiotactic PVA (Table I).

As the polymerization temperature increases, one might expect the probability of branching on the polymer main chain to increase. The low conversions of monomer to polymer used in this work, however, tends to minimize the formation of such branches. In order to ascertain the presence or absence of branches, the Huggins viscosity constants k' of various polymers were compared. This constant is expected to increase with increasing degree of branching.[8] The method appears to be sensitive for long branches; for instance, amylose has a k' of 0.58, while amylopectin, which contains one long branch per molecule, has a k' of 1.47.[9] Although the method is insensitive for short branches, the measurement should indicate the relative total amount of branching present.

Polyvinyl acetate polymerized below −30°C. was shown to be predominantly linear,[10] therefore, PVA's derived from polyvinyl acetates polymerized at −30°C. appear to be suitable linear reference materials for comparison. Various PVA samples so prepared had Huggins constants

TABLE I
Structural Parameters of Various Polyvinyl Alcohols

Parent polyvinyl ester	Polymerization temp., °C.	PVA $[\eta]$	k'	Optical density of iodine–iodide complex	1,2-Glycol content, %	H_2O Soluble,[a] %	Swelling index[b]
Polyvinyl formate	38	0.88	—	0.85	—	—	—
	30	1.39	0.52	1.13	0.78	32	1.80
	20	1.34	0.54	1.46	—	13	1.30
	10	1.16	0.52	1.44	0.67	6	1.25
	0	0.95	0.56	1.74	0.53	5	1.18
	−10	0.78	0.57	1.83	—	4	1.14
	−20	0.46	0.52	1.89	0.46	—	—
	−35	1.09	0.56	—	0.31	—	—
Polyvinyl trifluoroacetate	60	1.25	0.56	1.67	0.94	5	1.60
	10	0.47	—	—	0.48	—	—
Polyvinyl acetate	60	0.97	0.54	0.67	1.25	100	2.90
	−30	0.66	0.50	0.91	0.50	100	2.6

[a] Solubility of film in water after one hour at 70°C.
[b] Measured at 30°C. in water.

in the range of 0.5–0.6, and it was concluded that a PVA with a Huggins constant in this range is linear. Huggins constants of the various experimental polymers were determined on their aqueous solutions. The results are shown in Table I. All the PVA's show Huggins constants between 0.5 and 0.6, therefore, all of the experimental polymers appear to be linear.

1,2-Glycol units in PVA occur as a result of head-to-head addition in the polymerization of the parent polyvinyl ester. The 1,2-glycol contents of PVA's obtained from various sources are shown in Table I. In agreement with previous data on other PVA samples,[6,11] the 1,2-glycol content of the PVA derived from PVFo increases as the polymerization temperature increases. The relationship between 1,2-glycol content Δ and absolute polymerization temperature for PVA prepared from PVFo is shown in Figure 4. From this relationship, the ratio of the frequency factors and the difference between the activation energies for head-to-head and head-to-tail addition can be calculated according to the equation:

$$\Delta = k'_p/k_p = (A'/A) \exp \{-(E' - E)/RT\}$$

where k'_p and k_p are rates of head-to-head and head-to-tail addition, respectively; A' and A are frequency factors for head-to-head and head-to-tail addition, respectively; and E' and E' are activation energies for head-to-head and head-to-tail addition, respectively.

The calculated activation energies are compiled in Table II, including data obtained for polyvinyl acetate and polyvinyl benzoate. The values appear to depend upon the steric and inductive effects of the ester groups.

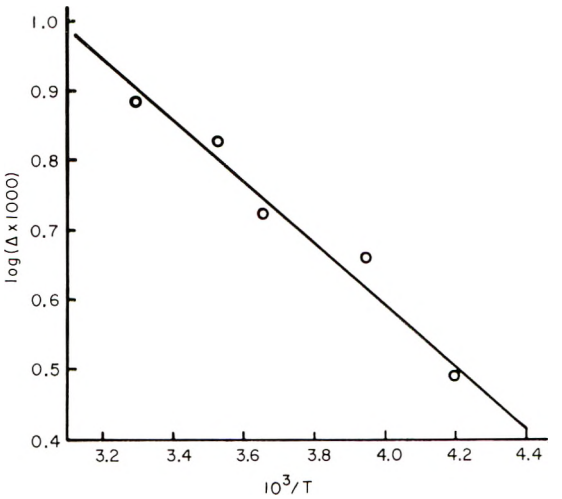

Fig. 4. Relationship between polymerization temperature and head-to-head addition (Δ) in polyvinyl formate.

Those aliphatic esters which have greater inductive effects require higher activation energies for head-to-head addition.

Recently, Imai and Matsumoto[12] showed that the iodine–iodide complexes of PVA's allow differentiation between various degrees of stereoregularity; for polymers of the same molecular weight the more stereoregular polymer shows a more bluish color. We had independently made similar observations, using a different procedure to prepare the complex. By employing the procedure described in the experimental section, polyvinyl alcohols prepared from polyvinyl acetate and polyvinyl chloroacetate showed blue-green colors, while those prepared from polyvinyl trifluoroacetate and polyvinyl formate showed blue to dark-blue colors and had higher optical densities. Thus, polyvinyl alcohols prepared from polyvinyl trifluoroacetate and polyvinyl formate appear to be more stereoregular. The optical densities of the complexes are given in Table I.

Both high and low molecular weight PVA prepared from polyvinyl trifluoroacetate and PVFo show relatively higher optical densities in the iodine–iodide complex. The optical density tends to increase with de-

TABLE II
Activation Energies for Head-to-Head Addition

Polymer	A'/A	E'-E, cal.	Reference
Polyvinyl acetate	0.10	1300	Flory and Leutner[6]
	0.103	1460	Imai and Maeda[11]
	0.10	1400	This work
Polyvinyl benzoate	0.15	1950	Imai and Maeda[11]
Polyvinyl formate	0.23	2000	This work
Polyvinyl trifluoroacetate	0.7	2800	This work

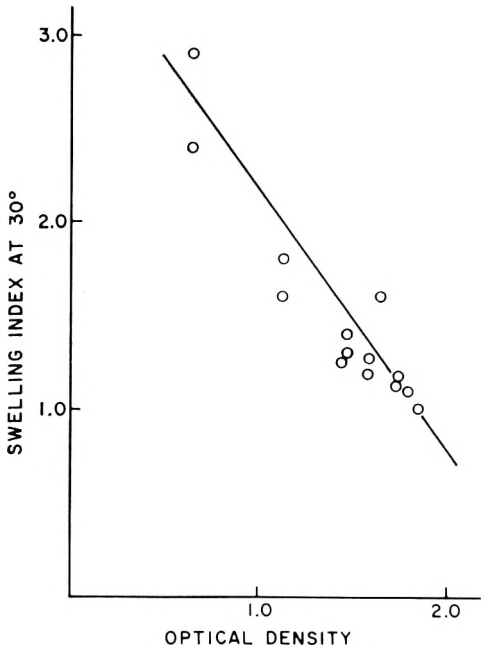

Fig. 5. Relationship between degree of swelling and optical density of iodine–iodide complex of PVA.

creasing polymerization temperature, showing that higher stereoregularity may be obtained by lowering the VFo polymerization temperature. One might be tempted to correlate high optical densities with low 1,2-glycol content. In agreement with the conclusions of Imai and Matsumoto,[12] however, we have also found that the optical density does not appear to be related to the 1,2-glycol content; rather it appears to be a true expression of stereoregularity. For example, PVA prepared from polyvinyl chloroacetate (1,2-glycol = 0.45%) and PVA prepared from polyvinyl acetate polymerized at −30°C. (1,2-glycol = 0.5%) show low optical densities in the complex, while PVA prepared from polyvinyl trifluoroacetate (1,2-glycol = 0.88–1.08%) shows a higher optical density.

In order to determine the degree of swelling, various PVA films were prepared by a uniform procedure to exclude variables of film preparation affecting film properties, and the degree of swelling and solubility determined in water at 30 and 70°C. Some results are shown in Table I. Films of PVA prepared from polyvinyl acetate show a relatively high degree of swelling and solubility, while PVA prepared from polyvinyl trifluoroacetate and PVFo shows a lower degree of swelling and solubility. In addition, PVA prepared from PVFo polymerized at relatively lower temperatures tends to show a lower degree of swelling and solubility. The scattered points of Figure 5 show decreased degree of swelling at 30°C. with increasing optical density, a relationship similar to that observed by Imai and Matsumoto.[12] Therefore, both degree of swelling and optical density of the

iodine complex appear to be good measures for estimating the relative order of stereo-regularity.

In order to decide whether or not higher stereoregularity resulted in higher crystallinity, various PVA films were prepared by a uniform procedure and the densities determined. A random variation in values was obtained in the range from 1.295 to 1.301, representing a variation of crystallinity between 35.5 and 44.5%.[13] This variation appears to be associated with small differences in the film preparation and does not appear to be significant. It appears that stereoregularity in polyvinyl alcohol does not result in higher crystallinity. This can be understood from the earlier work of Bunn,[14] who found that hydrogen atoms and hydroxyl groups, can be freely interchanged in the crystal lattice of polyvinyl alcohol and concluded that stereoregularity is not required for crystallization. An additional conclusion is that a change in the 1,2-glycol content does not result in a change of crystallinity, probably for the same reason that the change in stereoregularity does not. Because stereoregularity tends to increase while 1,2-glycol content tends to decrease with decreasing polymerization temperature, a previously reported[15] relationship between 1,2-glycol content and degree of swelling can just as well be attributed to stereoregularity. The same is probably true in part for the previously reported[16] decrease of the degree of swelling for PVA prepared from polyvinyl acetate with decreasing polymerization temperature, and which was originally attributed only to a decreased degree of branching.

Higher stereoregularity does not result in relatively higher crystallinity between the samples when the crystallinity is increased by heat treatment, but the relatively higher water resistance is retained. PVA films were heat-treated at 206–208°C. and then tested in boiling water. The solubility decreased in all cases, but the films of the conventional PVA became soggy and weak, while those prepared from polyvinyl trifluoroacetate and low temperature-polymerized PVFo remained fairly strong. Earlier, Sakurada reported[13] that swelling of PVA takes place primarily in the amorphous phase. Therefore, the higher water resistance of stereoregular PVA appears to be associated with the stereoregular structure in the amorphous phase. It is not yet clear how stereoregularity causes higher water resistance.

DISCUSSION

It is apparent from this study that a considerable difference in structure exists between PVFo's prepared at 0 and 35°C. PVFo polymerized at low temperatures is linear and in turn is hydrolyzed to a linear PVA. This PVA, however, is different from linear PVA prepared from polyvinyl acetate, in that it produces a more intense blue iodine complex and has greater water resistance. The same properties are obtained from syndiotactic PVA derived from polyvinyl trifluoroacetate.

As the PVFo polymerization temperature is decreased, the amount of head-to-head addition is also decreased. The amount of this type of addi-

tion present and the magnitude of the differences produced between the various polymerization temperatures is so small as to be negligible and does not appear to have much bearing on the observations relating to stereoregularity. The inductive effects in the various vinyl aliphatic esters seem to account for the differences in the amounts of head-to-head addition, either by a mechanism involving mutual repulsion or change in resonance stability.

The good correlation between the x-ray diffraction patterns of PVFo, the water resistance of the derived PVA, and the PVA iodine complex measurements is strong evidence that syndiotactic PVFo, and hence syndiotactic PVA, may be prepared by the free-radical polymerization of VFo at low temperatures.

In previous work from our laboratories, we showed how the stereoregularity (particularly syndiotacticity) of the free propagating species could be controlled by either a combination of inductive and steric effects, as in the case of the polyvinyl haloacetates,[17] or a temperature effect, as in the case of polyvinyl chloride.[3]

The formate group of VFo has a stronger inductive effect than an acetate group, but is not nearly as strong as the haloacetates. This may be seen in Table III, which lists the strengths of the various acids in these esters. Thus, it is not surprising that the room temperature polymerization of VFo results in only conventional polymer.

TABLE III
Dissociation Constants of Acid Portion of Vinyl Esters

Acid	K_A
Acetic acid	1.75×10^{-5}
Formic acid	1.70×10^{-4}
Chloroacetic acid	1.40×10^{-3}
Trifluoroacetic acid	5.00×10^{-1}

As the polymerization temperature is lowered, the growing polymer chain prefers the configuration requiring the least amount of activation energy. In the free-radical propagating species, the preferred configuration is syndiotactic.[18] In the case of VFo, there is a sufficient inductive effect to provide a difference in the activation energy for syndiotactic and isotactic placements which is significant at low polymerization temperatures. In the case of vinyl acetate, on the other hand, insufficient inductive effect is present to produce any noticeable differences, at least at temperatures down to −35°C. We have observed, as have others,[19] that VFo has a more rapid rate of polymerization than vinyl acetate. The greater number of syndiotactic placements in PVFo, therefore, cannot be attributed to a slower rate of polymerization with its consequent greater tendency toward stereoregulation. On the contrary, the more rapid polymerization and higher stereoregularity emphasize even more the stereoregulating strength of the formate group. The results show the greater influence of electro-

static over steric effects on controlling polymer regularity; the acetate group is larger than the formate group and yet exercises less control.

In conclusion, increased stereoregularity in polyvinyl esters can occur as a result of either decreased polymerization temperature or stereoregulating effect of the pendant ester group. Because PVA prepared from polyvinyl trifluoroacetate polymerized at 60°C. shows a higher stereoregularity by its degree of swelling and iodine complex than PVA prepared from PVFo polymerized at 30°C., the trifluoroacetyl group appears to have a somewhat stronger stereoregulating effect than the formate group. The stereoregulating effect of the acetyl group appears to be considerably less. These observations correlate well with the relative inductive strengths of the three groups.

References

1. Vansheldt, A. A., and L. F. Chelpanova, *Zhur. Obshchel Khim.*, **20**, 2353 (1950).
2. Jordan, E. F., Jr., W. E. Palm, D. Swern, L. P. Witnauer, and W. S. Port, *J. Polymer Sci.*, **32**, 33 (1958).
3. Fordham, J. W. L., P. H. Burleigh, and C. L. Sturm, *J. Polymer Sci.*, **41**, 73 (1959).
4. Owens, G. R., assigned to Monsanto, U. S. Pat. 2,329,644, September 14, 1943.
5. Beresniewicz, A., *J. Polymer Sci.*, **39**, 63 (1959).
6. Flory, P. J., and F. S. Leutner, *J. Polymer Sci.*, **3**, 880 (1948); *J. Polymer Sci.*, **5**, 267 (1950).
7. Matheson, M. S., E. E. Auer, E. B. Bevilacqua, and E. J. Hart, *J. Am. Chem. Soc.*, **71**, 2610 (1949); G. M. Burnett and H. W. Melville, *Proc. Roy. Soc. (London)*, **A189**, 456 (1947).
8. Cragg, L. H., and R. H. Sones, *J. Polymer Sci.*, **9**, 585 (1952).
9. Walker, O. J., Jr., and C. A. Winkler, *Can. J. Research*, **B28**, 298 (1950).
10. Burnett, G. M., M. H. George, and H. W. Melville, *J. Polymer Sci.*, **16**, 31 (1955).
11. Imai, K., and U. Maeda, *Kobunshi Kagaku*, **16**, 222 (1959).
12. Imai, K., and M. Matsumoto, *J. Polymer Sci.*, **55**, 335 (1961).
13. Sakurada, I., Y. Nukushina, and Y. Sone, *Ricerca Sci.*, **25A**, 715 (1955).
14. Bunn, C. W., and H. S. Peiser, *Nature*, **159**, 161 (1947); C. W. Bunn, *ibid.*, **161**, 929 (1948).
15. Motoyama, T., *Kunststoffe*, **50**, 33 (1960).
16. Ukida, J., R. Naito, and T. Kominami, *J. Chem. Soc. Japan, Ind. Chem. Sect.* **58**, 128 (1955).
17. Fordham, J. W. L., G. H. McCain, and L. E. Alexander, *J. Polymer Sci.*, **39**, 335 (1959).
18. Fordham, J. W. L., *J. Polymer Sci.*, **39**, 321 (1959).
19. Rostovskiĭ, E. N., S. N. Ushakov, and A. N. Barinova, *Izvest. Akad. Nauk S.S.S.R. Otdel. Khim. Nauk.*, **1958**, 59.

Synopsis

A study was made of the effect of polymerization temperature on the syndiotacticity of polyvinyl formate. Vinyl formate was polymerized with ultraviolet light initiation in the temperature range from −20 to +30°C. The value of $(E_p - E_t)/2$ obtained, 4.5 kcal./mole, is characteristic of those values obtained by other workers for the free radical-initiated polymerization of vinyl acetate. A linear relationship was found to exist between the viscosities of the polyvinyl formates and those of the derived polyvinyl alcohols. The degree of polymerization of polyvinyl formate may be calculated from the

equation: $[\eta] = 4.42 \times 10^{-3} \overline{DP}^{0.63}$. The low temperature polymerization of vinyl formate results in more syndiotactic polymer, as shown by x-ray diffraction. Polyvinyl formate obtained at more elevated polymerization temperatures did not demonstrate the same degree of order. No difference was found between the infrared spectra of the polyvinyl formates. The polyvinyl alcohol derived from polyvinyl formate polymerized at low temperatures (0 to −35°C.) exhibits water resistance and forms a colored iodine complex similar to that obtained with the syndioactic polyvinyl alcohol derived from polyvinyl trifluoroacetate. Conventional polyvinyl alcohol and that derived from polyvinyl acetate polymerized at −30°C. do not exhibit the same properties. Minor differences in the 1,2-glycol content in the various polyvinyl alcohols do not account for the differences in the observations. The amount of head-to-head addition in various vinyl aliphatic esters seems to be related to the inductive strength of the acid portion of the ester. No difference was found between the crystallinities of the various polyvinyl alcohols, as measured by film density. Heat treatment increases the crystallinities about the same amount, but the water resistance of the stereoregular materials remains higher. From the good correlation between the observations made on polyvinyl formate and the derived polyvinyl alcohol, it is concluded that syndiotactic polyvinyl formate, and hence syndiotactic polyvinyl alcohol, is obtained by the low temperature free radical-initiated polymerization of vinyl formate. Increased syndiotacticity is more readily obtained in polyvinyl formate than in polyvinyl acetate, indicating the greater influence of inductive effect compared with the steric effect in controlling stereoregularity during free-radical propagation.

Résumé

On a étudié l'effet de la température de polymérisation sur la syndiotacticité du formiate de polyvinyle. On a polymérisé le formiate de vinyle par initiation ultra-violette à des températures, variant de −20 à 30°C. La valeur obtenue de $(E_p - E_t)/2$, 4.5 Kcal/mole, est caractéristique pour ces valeurs obtenues par d'autres chercheurs pour la polymérisation de l'acétate de vinyle, initiée par un mécanisme radicalaire. On a trouvé un rapport linéaire entre les viscosités des formiates de polyvinyle et celles de ses alcools polyvinyliques dérivés. On peut calculer le degré de polymérisation suivant l'équation $[\eta] = 4.42 \times 10^{-3} \overline{DP}^{0.63}$. La polymérisation du formiate de vinyle à basse température produit un polymére plus fortement syndiotactique, ceci étant prouvé par diffraction aux rayons-X. Le formiate de polyvinyle obtenu à des températures plus élevées, n'a pas le même degré de tacticité. On n'a pas trouvé de différences entre les spectres infrarouges des formiates de polyvinyle. L'alcool polyvinylique dérivé du formiate de polyvinyle, polymérisé à basse température (0° à −35°C), résiste à l'eau et forme un complexe coloré avec l'iode, analogue à celui formé avec l'alcool polyvinylique syndiotactique, dérivé du trifluoroacétate de polyvinyle. L'alcool polyvinylique conventionnel et celui dérivé de l'acétate de polyvinyle, polymérisé à −30°C, n'ont pas les mêmes propriétés. Des différences minimes de taux de 1–2 glycol, dans les alcools polyvinyliques différents, n'expliquent pas les différences observées. Le pourcentage d'addition tête-à-tête dans différentes esters aliphatiques vinyliques semble être causé par la force inductive de la partie acide dans l'ester. On n'a pas trouvé des différences dans les cristallinités de différents alcools polyvinyliques, quand elles sont mesurées par densité de films. Le traitement à chaud augmente la cristallinité dans la même mesure mais la résistance-à l'eau des matériaux stéréoréguliers reste elevée. De l'existence d'une bonne corrélation, existant entre les observations sur le formiate de polyvinyle et l'alcool polyvinylique dérivé, on a conclu qu'on obtenait du formiate de polyvinyle syndiotactique et par suite de l'alcool polyvinylique syndiotactique par la polymérisation du formiate de vinyle à basse température, initié par un mécanisme radicalaire. Une syndiotacticité plus prononcée est obtenue d'une maniére plus aisée dans le cas du formiate de polyvinyle que dans celui de l'acétate de polyvinyle. Ceci indique une influence plus grande de l'effet inductif, comparé à l'effet stérique, sur la régulation de la tacticité pendant la propagation radicalaire.

Zusammenfassung

Eine Untersuchung des Einflusses der Polymerisationstemperatur auf die Syndiotaktizität von Polyvinylformiat wurde durchgeführt. Vinylformiat wurde bei Anregung mit Ultraviolettlicht im Temperaturbereich von −20 bis +30°C polymerisiert. Der für $(E_p - E_t)/2$ erhaltene Wert von 4,5 kcal/Mol stimmt mit den von anderen Autoren für die radikalische Polymerisation von Vinylacetat erhaltenen Werten überein. Eine lineare Beziehung wurde zwischen der Viskosität der Polyvinylformiate und der davon abgeleiteten Polyvinylakohole gefunden. Der Polymerisationsgrad von Polyvinylformiat kann aus der Gleichung $[\eta] = 4{,}42 \times 10^{-3}\ \overline{DP}^{0{,}63}$ berechnet werden. Die Tieftemperaturpolymerisation von Vinylformiat führt, wie die Röntgenbeugung zeigt, zu einem stärker syndiotaktischen Polymeren. Bei höherer Polymerisationstemperatur erhaltenes Polyvinylformiat zeigte nicht den gleichen Ordnungsgrad. Es bestand kein Unterschied zwischen den Infrarotspektren der Polyvinylformiate. Der aus bei tiefer Temperatur (0° bis −35°C) polymerisiertem Polyvinylformiat erhaltene Polyvinylalkohol zeigt Wasserbeständigkeit und bildet einen gefärbten Jodkomplex, der dem mit syndiotaktischem Polyvinylalkohol aus Polyvinyltrifluoracetat erhaltenen ähnlich ist. Konventioneller Polyvinylalkohol und der aus bei −30°C polymerisiertem Polyvinylacetat hergestellte zeigen diese Eigenschaften nicht. Geringe Unterschiede im 1,2-Glykolgehalt der verschiedenen Polyvinylakohole sind nicht für die beobachteten Unterschiede verantwortlich. Der Anteil an Kopf-Kopfaddition bei verschiedenen aliphatischen Estern scheint zur induktiven Stärke des Säureteiles des Esters in Beziehung zu stehen. Kein Unterschied bestand zwischen der durch die Dichte des Films gemessenen Kristallinität der verschiedenen Polyvinylalkohole. Wärmebehandlung erhöht die Kristallinität etwa um den gleichen Betrag, die Wasserbeständigkeit des sterisch regelmässigen Materials bleibt jedoch höher. Aus der guten Übereinstimmung zwischen den Beobachtungen an Polyvinylformiat und dem daraus gewonnenen Polyvinylalkohol wird der Schluss gezogen, dass durch radikalische Polymerisation von Vinylformiat bei tierfer Temperatur syndiotaktisches Polyvinylformiat, und damit auch syndiotaktischer Polyvinylalkohol erhalten wird. Erhöhte Syndiotaktizität wird bei Polyvinylformiat leichter erhalten als bei Polyvinylacetat, was für einen grösseren Einfluss des induktiven Effekts verglichen mit dem sterischen Effekt bei der Kontrolle der Stereospezifität während des radikalischen Wachstums spricht.

Received January 11, 1962

JOURNAL OF POLYMER SCIENCE: PART A VOL. 1, PP. 965–983 (1963)

Crystal Structure of a New Form of Polyoxymethylene

GIANALVISE CARAZZOLO and MARIO MAMMI, *Soc. Montecatini, Istituto Rierche e Applicazioni Resine, Castellanza, Varese, Italy, and Centro Nazionale di Chimica delle Macromolecole del C.N.R., Sezione di Padova, Italy*

Introduction

By means of a particular polymerization process, the Montecatini laboratory at the University of Padova, under the direction of Prof. Bezzi, has recently obtained a new type of polyoxymethylene which has not yet been described.

This new polymer of formaldehyde* has been examined at the Resins Research and Applications Institute at Castellanza from the point of view of its chemical, physic chemical, and applications properties. Here, also, studies were made which allowed the complete determination of its structure.

This material, which shall be called orthorhombic POM, because of the orthorhombic symmetry of its elementary cell, is clearly distinguishable from ordinary polyoxymethylene (hexagonal POM) by its density and the characteristics of its x-ray and infrared spectra (see Figs. 1–6).

X-Ray Diffraction Patterns

Owing to the difficulty of obtaining the spectra of fibers the entire examination of structure was based exclusively on the spectra of powders obtained with the Debye-Scherrer camera and high angle spectrogoniometer, using tubes with iron and copper anticathode (Figs. 1–4). It was possible in these spectra to observe over fifty reflections with intensity ratios varying from 1 to 1000. The intensities were measured by the areas of the peaks in the high angle goniometer spectra.

The intensity of each single peak (Table II) was taken as the mean of the values obtained with CuKα and FeKα radiation, after correction for the usual angular coefficients.

Elementary Cell and Space Group

As is known,[1–8] hexagonal POM has a hexagonal cell with $a = 4.46$ A. and $c = 17.3$ A. However, an orthorhombic elementary cell may be iso-

* A patent application has been filed (D.176, January 27, 1961) for the new product and for the process used in its preparation.

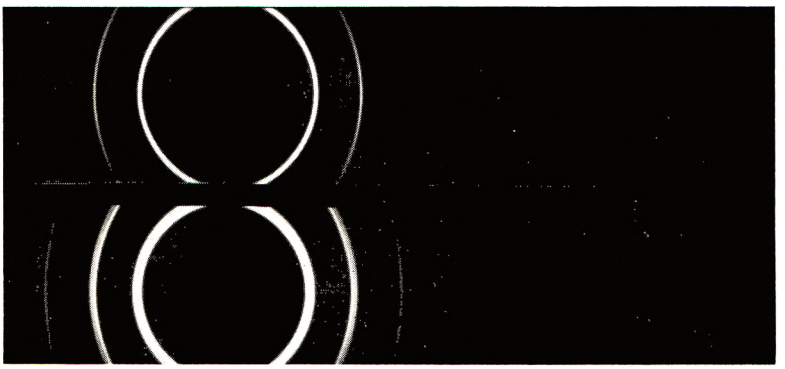

Fig. 1. Debye-Scherrer diagrams (FeKα radiation): (*a*) hexagonal POM; (*b*) orthorhombic POM.

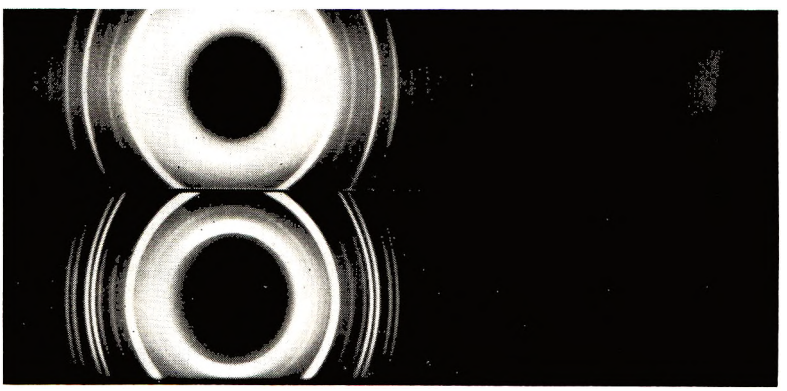

Fig. 2. Debye-Scherrer diagrams (CuKα radiation): (*a*) hexagonal POM; (*b*) orthorhombic POM.

lated in the same lattice with $a' = a = 4.46$ A., $b' = 2a \cos 30° = 7.72$ A., and $c' = c = 17.3$ A. (Fig. 7). To this lattice belong, among others, the following lattice planes.

$$d_{(110)} = d_{(020)} = 3.86 \text{ A.}$$

and

$$d_{(115)} = d_{(025)} = 2.58 \text{ A.}$$

These give rise in spectra of hexagonal POM to the two most intense reflections (2θ CuKα = 23° and 34.8°).

In the spectrum of orthorhombic POM the following spacing distances correspond to the four most intense reflections: 4.04 A., 3.83 A., 2.67 A., and 2.60 A. Examination of the experimental findings given above has led to the supposition that the same indices which correspond to the four most intense reflections in orthorhombic POM correspond also to the two main reflections in hexagonal POM. This hypothesis gives two possible structural solutions, corresponding to two different elementary

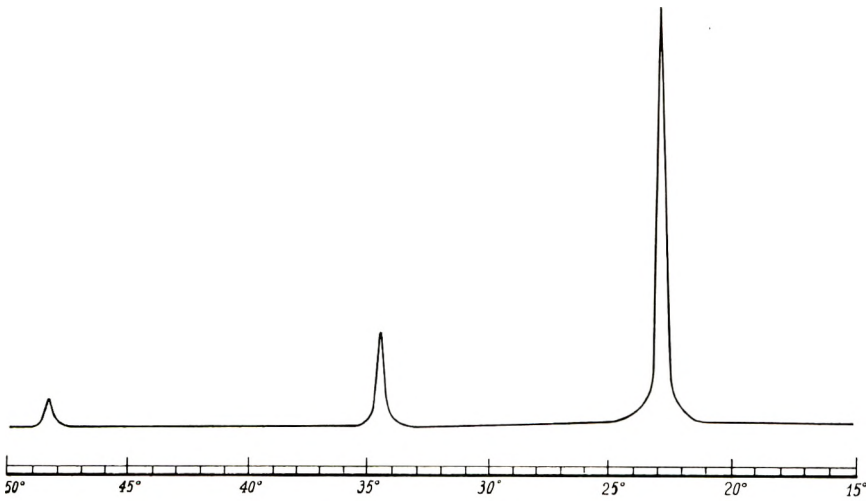

Fig. 3. Geiger spectrum (CuKα radiation) of hexagonal polyoxymethylene.

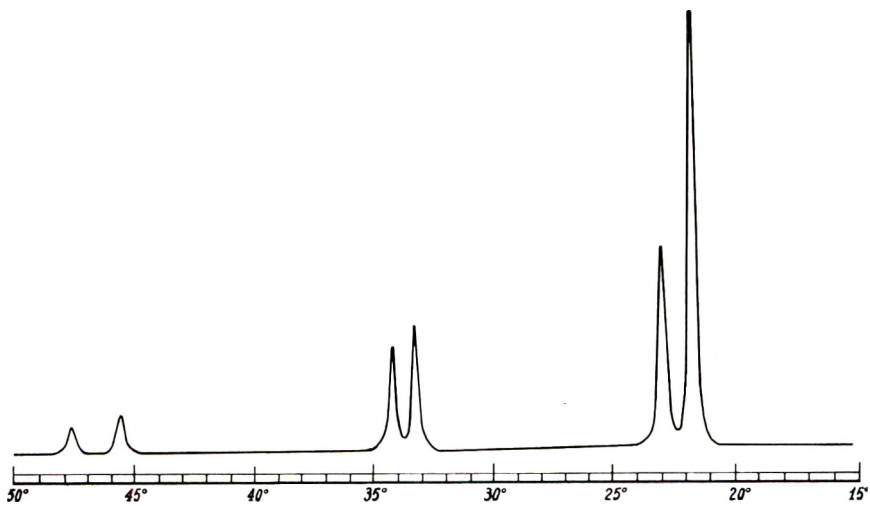

Fig. 4. Geiger spectrum (CuKα radiation) of orthorhombic polyoxymethylene.

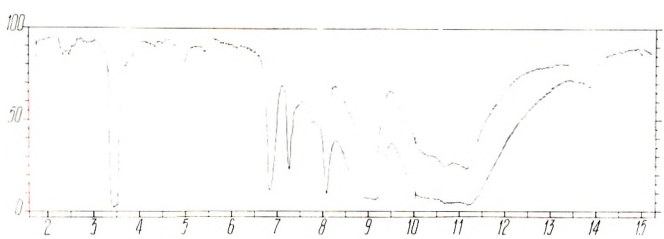

Fig. 5. Infrared spectrum of hexagonal polyoxymethylene.

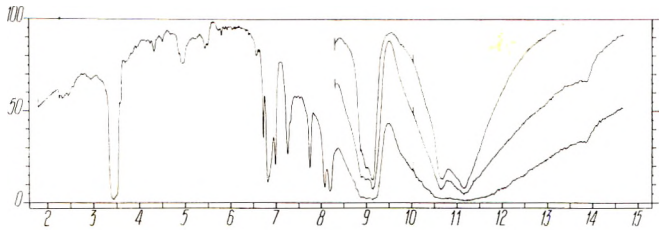

Fig. 6. Infrared spectrum of orthorhombic polyoxymethylene.

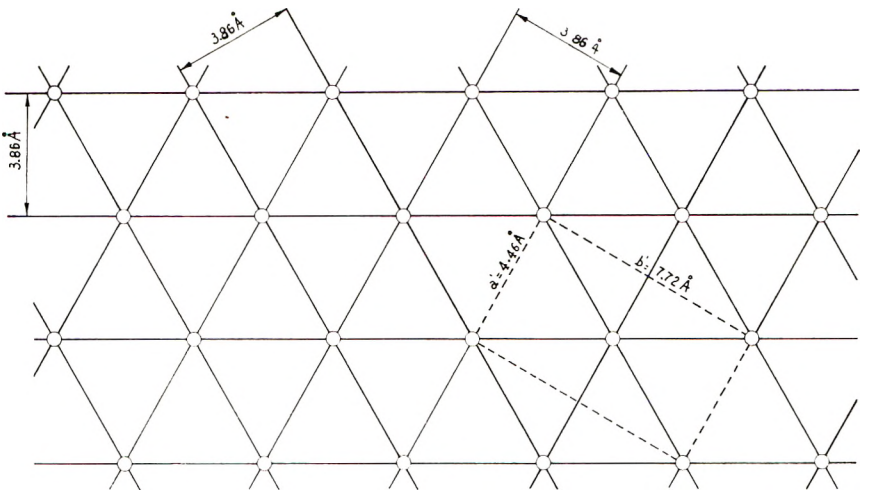

Fig. 7. Projection onto plane *ab* of hexagonal polyoxymethylene lattice.

cells, both orthorhombic, viz.: (I) $d_{(110)} = 4.04$ A., $d_{(020)} = 3.83$ A., $d_{(115)} = 2.67$ A., and $d_{(025)} = 2.60$A. This solution gives a cell with $a = 4.77$ A., $b = 7.65$ A., $c = 17.80$ A. A second possibility is (II) $d_{(020)} = 4.04$ A., $d_{(110)} = 3.83$ A., $d_{(025)} = 2.67$ A., and $d_{(115)} = 2.60$ A. This second solution gives a cell with $a = 4.34$ A., $b = 8.10$ A., $c = 17.80$ A.

A comparison between the observed and calculated data for every possible reflection of the two above cells excludes the second and confirms the first. Furthermore, since no reflection with an l index other than 5 or multiples of 5 has been found, it may be concluded that the cell of the new form of polyoxymethylene is orthorhombic, with $a = 4.77$ A., $b = 7.65$ A., $c = 3.56$ A. From these figures the volume of the elementary cell is 129.9 A.^{3}

The theoretical density ρ of orthorhombic POM is then calculated as follows. With 3 monomers per cell, $\rho_{calc.} = 1.15$ g./cc.; with 4 monomers per cell, $\rho_{calc.} = 1.54$ g./cc.; with 5 monomers per cell, $\rho_{calc.} = 1.92$ g./cc. The experimentally found density ($\rho_{expt.}$) of orthorhombic POM is 1.52 g./cc. and so fixes the number of monometric units in the elementary cell at four (for hexagonal POM $\rho_{calc.} = 1.49$ g./cc. and $\rho_{expt.} = 1.43$ g./cc.

For what concerns the space group it must be borne in mind that the following reflections are extinguished: (h00), where $h = 2n + 1$; (0k0),

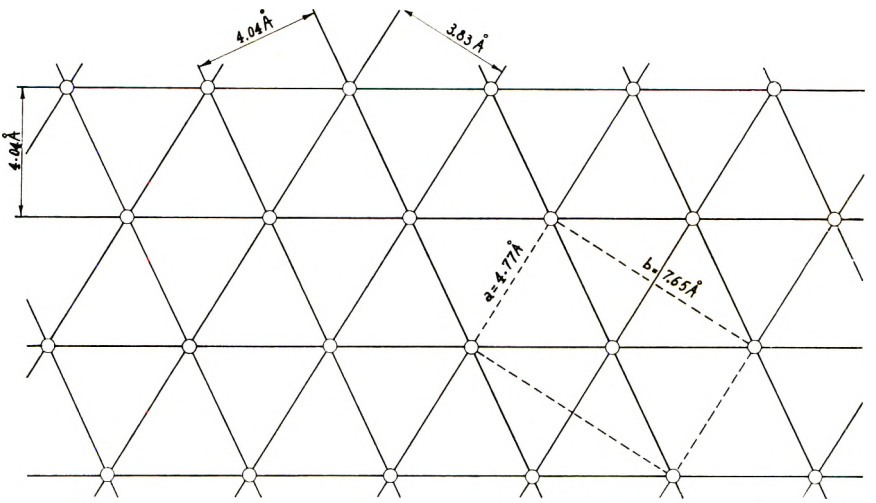

Fig. 8. Projection onto plane *ab* of orthorhombic polyoxymethylene lattice.

where $k = 2n + 1$; $(00l)$ where $l = 2n + 1$. These extinctions correspond to the three-dimensional space group $P2_12_12_1$, to which three two-dimensional space groups P_{gg} correspond.

Nevertheless, because of the uncertainty inherent in the findings of the powder spectra, in the following considerations we will discard any assumptions based on this space group.

Conformation of the Chain

The similarity of the spectra of orthorhombic and of hexagonal POM led to the hypothesis that the chains were parallel to the *c* axis and arranged in their projection on the *ab* plane at the four corners and at the center of the elementary cell. This lattice is slightly distorted, but very similar to that of hexagonal POM (Figs. 7 and 8).

This hypothesis is confirmed by the fact that the intensity of the (110) and (020) reflections is particularly high and that the first of these is also about twice as intense as the second.

The *c* axis therefore should contain one turn of the helical chain and two monomeric units. The shape of the chain has been calculated on the basis of the following assumptions: (*a*) the projection along the *c* axis of the C—O bond is equal to $c/4 = 0.89$ A.; (*b*) the length of the C—O bond is 1.43 A.; (*c*) the bond angles $\overset{\frown}{COC} = \overset{\frown}{OCO}$.

The solution of the calculation gives the following results, shown schematically in Figure 9: (*a*) the projection of the chain into the plane normal to its axis is a square having a side of length 1.12 A.; (*b*) the bond angles $\overset{\frown}{COC}$ and $\overset{\frown}{OCO}$ are 112°41′, (*c*) the distance of the atoms of the chain from the axis of the helix is 0.79 A.

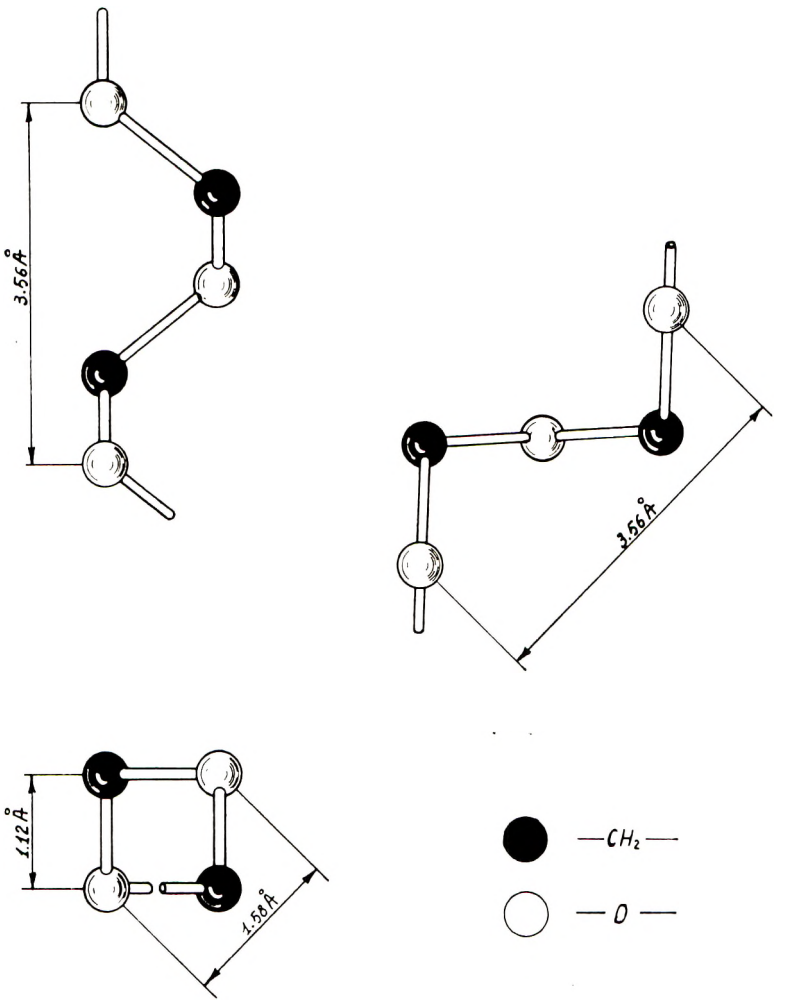

Fig. 9. Orthorhombic polyoxymethylene chain.

Projection of the Structure on the *ab* Plane

The orientation of the square projection of the chain, with respect to the *a* and *b* sides of the cell, is already defined by the absence of the (240) reflection. If the diagonals of the projection of the chain were parallel to the *a* and *b* axes, the (240) reflection should be very intense.

Only by the arrangement of the square projection with the sides parallel to *a* and *b* sides of the cell, can the experimentally found extinction of the (240) reflection be explained.

Figures 10 and 11 show schematically the structure factor of the (240) reflection for the two orientations mentioned above, with the positive zones crosshatched (origin according to *Pgg*).

As was seen above (Fig. 9), the carbon and oxygen atoms are arranged in

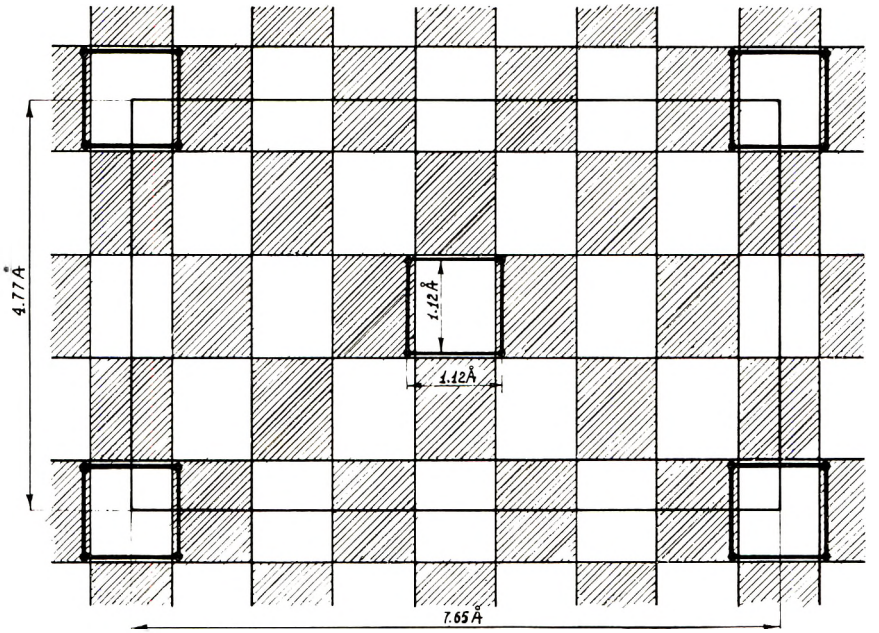

Fig. 10. Structure factor of the (240) reflection and square projection of chain with sides parallel to sides of cell.

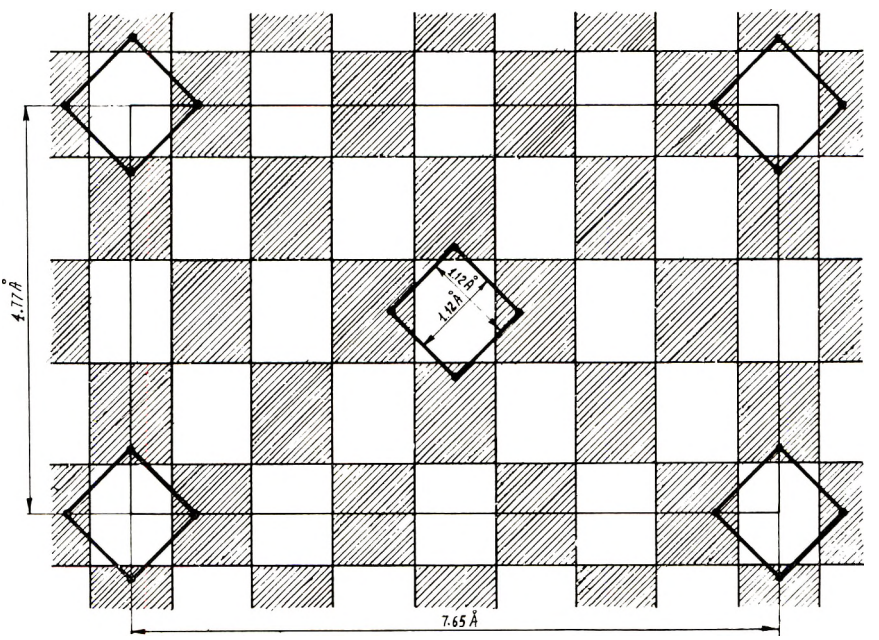

Fig. 11. Structure factor of the (240) reflection and square projection of chain with diagonal parallel to sides of cell.

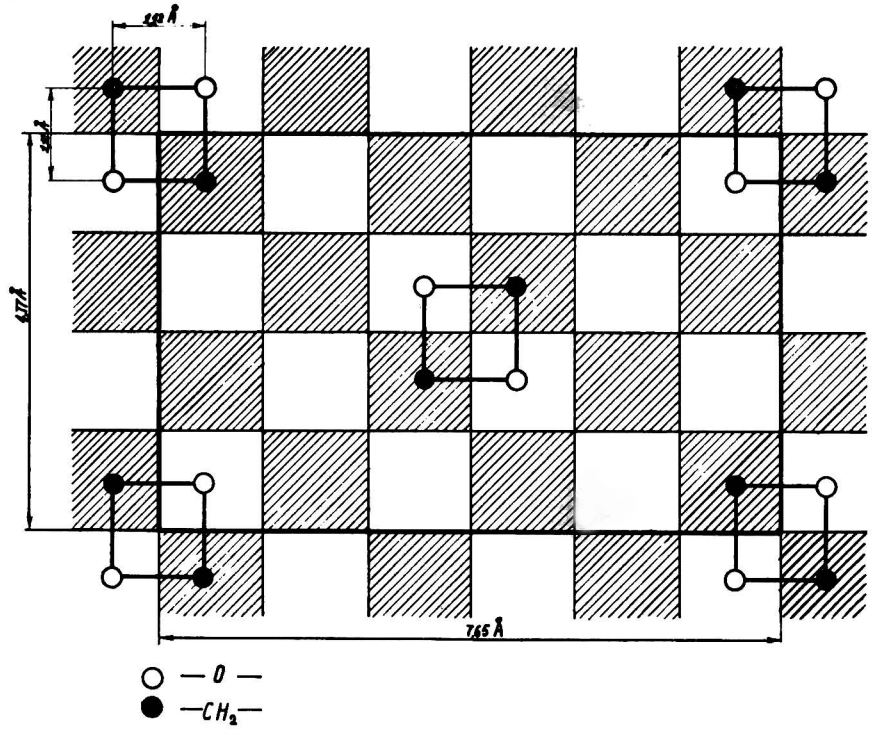

Fig. 12. Orthorhombic polyoxymethylene: structure factor of the (230) reflection; reflection $F\,(230) \neq 0$.

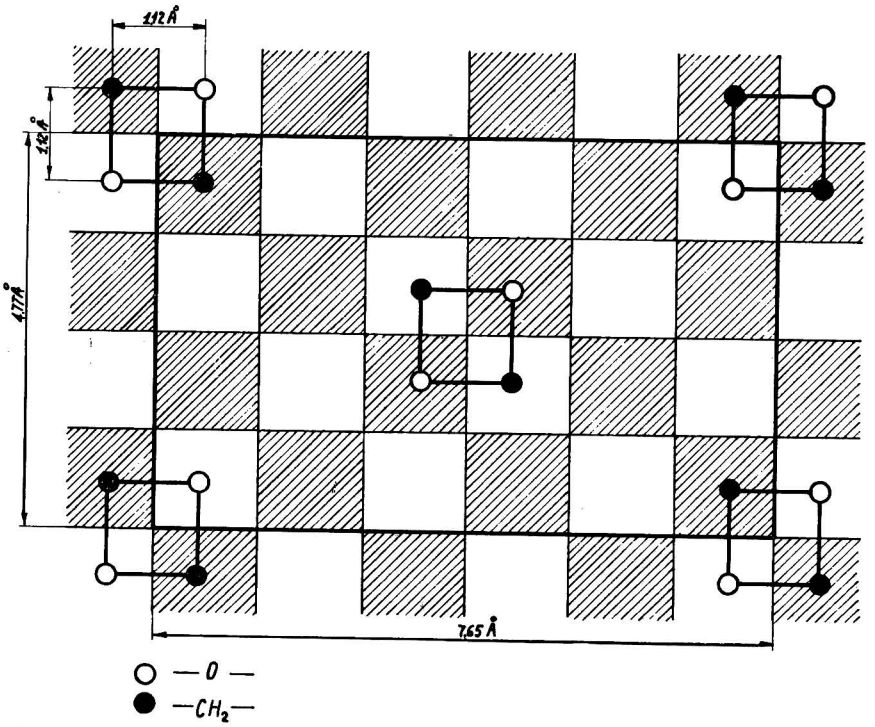

Fig. 13. Orthorhombic polyoxymethylene: structure factor of the (230) reflections; $F\,(230) = 0$ (origin of cell according to *Pgg*.)

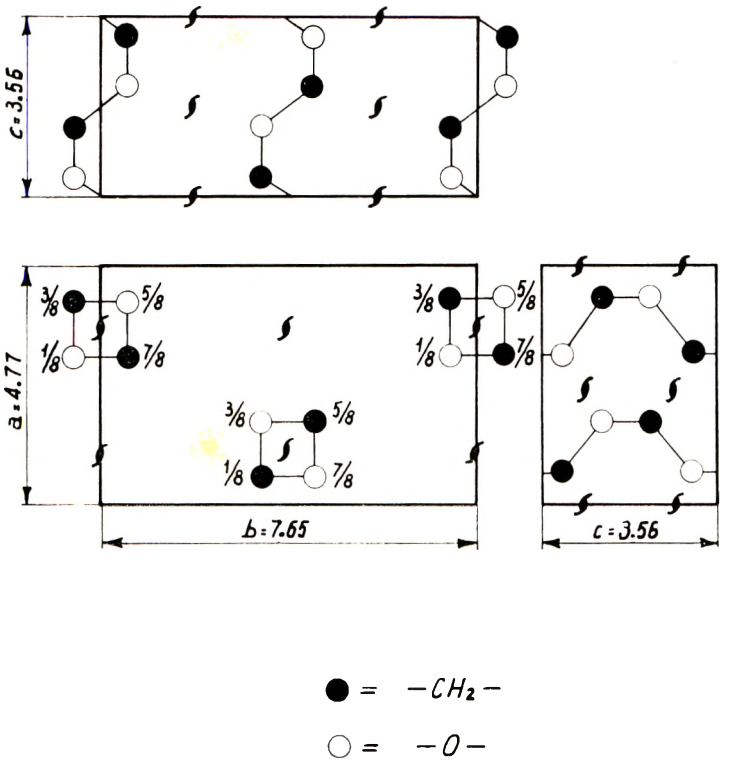

Fig. 14. Projections onto planes *ab*, *bc*, and *ac* of orthorhombic polyoxymethylene (origin of cell according to $P2_12_12_1$).

pairs in opposite corners of the square projection of the chain. The mutual orientation of the diagonals CC and OO in adjacent chains is automatically defined by the coordinates of the equivalent positions of the three-dimensional space group $P2_12_12_1$ and also by the corresponding two-dimensional space group Pgg.

Therefore, still on *ab* plane, we have the configuration shown schematically in Figure 12 (origin according to Pgg). However, even independently of any space group considerations, if the positions were as shown in Figure 13, extinction of the (230) reflection would occur, whereas in fact it is rather intense.

Calculation of Structure

It is sufficient to know the dimensions of the elementary cell, the coordinates of the atoms on *ab* plane and the space group to determine the missing parameters (the *z*-coordinates) which are necessary to complete the structure of orthorhombic POM. The same result may also be reached even without taking account of the space group simply by developing the projection described previously so as to obtain the most acceptable distances between the facing atoms of the adjacent chains. The three projections

of the structure onto the *ab*, *bc*, and *ac* planes are given schematically in Figure 14. The coordinates of the atoms are shown in Table I.

On the basis of the coordinates given above, calculations were made of the intensities ($I_{calc.}$) and of the structure factors ($F_{calc.}$) in order to compare them with the observed intensities and factors ($I_{obs.}$ and $F_{obs.}$). The data are given in Table II.

The $I_{obs.}$ correspond to the areas of the peaks on the spectrum obtained with the high-angle goniometer and CuKα radiation. The values given are the mean of those obtained with CuKα and FeKα radiation, taking into account the suitable angular correction coefficients.

TABLE I

Orthorhombic Polyoxymethylene: Atomic Coordinates Expressed as Fractions of *a*, *b*, and *c*

	x	*y*	*z*
C_1	0.367	0.073	0.875
C_2	0.867	0.427	0.125
C_3	0.633	0.573	0.625
C_4	0.133	0.927	0.375
O_1	0.133	0.073	0 625
O_2	0.633	0.427	0.375
O_3	0.867	0.573	0.875
O_4	0.367	0.927	0.125

The spectrum obtained with the FeKα radiation further permitted the separation from one another of certain peaks which were not sufficiently resolved by copper radiation. In those cases, where complete superimposition of a number of reflections in one peak occurred, the $I_{obs.}$ of the single reflections were deduced by subdividing the area of the peak on the basis of the $I_{calc.}$ of the reflections themselves.

For the calculated values we have employed an isotropic thermal factor $B = 2.3$. Comparing $F_{obs.}$ and $F_{calc.}$ we have a value:

$$R = \frac{\sum [|F_{(hkl)obs.}| - |F_{(hkl)\ calc.}|]}{\sum |F_{(hkl)obs.}|} = 0.16$$

From the values of $F_{obs.}$ and α of Table II, the three two-dimensional Fourier calculations (*hk*O), (O*kl*) and (*h*O*l*) shown in Figures 15, 16, and 17, respectively, were carried out, together with some three-dimensional elements.

These calculations were made with the kind cooperation of the Olivetti Electronic Calculation Center with the computer Elea 6001. The values of the coordinates of the atoms obtained from the above Fourier calculations are shown in Table III for one carbon and one oxygen only. The coordinates of all the others atoms correspond to those obtainable from the equivalent positions of the space group $P2_12_12_1$.

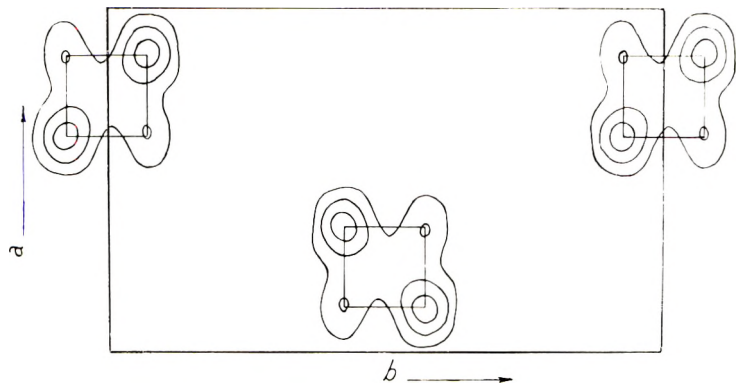

Fig. 15. Orthorhombic polyoxymethylene: two-dimensional Fourier projection, plane *ab*.

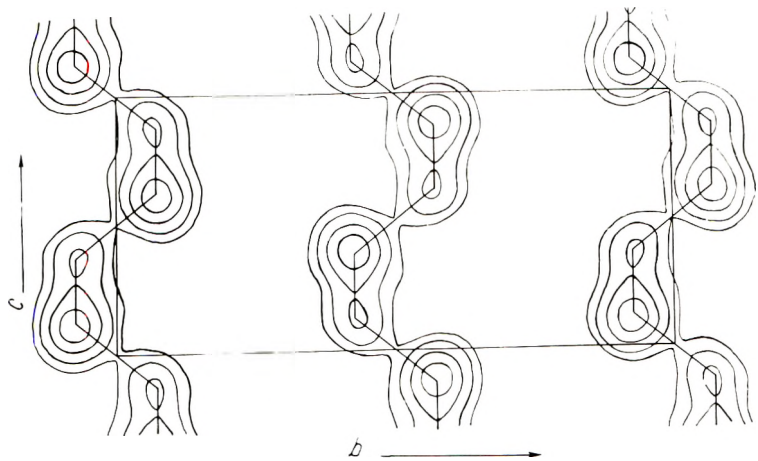

Fig. 16. Orthorhombic polyoxymethylene: two-dimensional Fourier projection, plane *bc*.

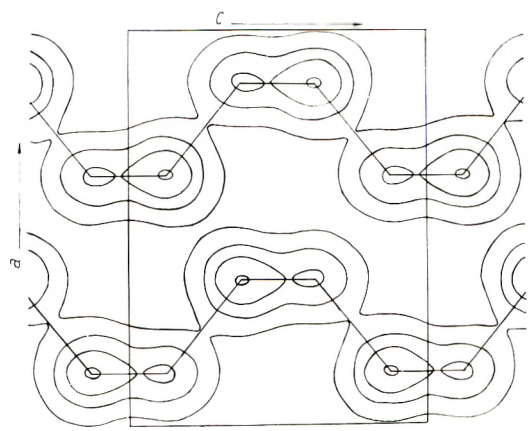

Fig. 17. Orthorhombic polyoxymethylene: two-dimensional Fourier projection, plane *ac*.

TABLE II

Orthorhombic Polyoxymethylene: Calculated and Observed Intensities I and Structure Factors F

hkl	2θ(CuKα)	$I_{calc.}$	$I_{obs.}$	$F_{calc.}$	$F_{obs.}$	α
010	11.55	0	0	0	0	—
100	18.59	0	0	0	0	—
110	21.98	1.600	1753	27.6	28.5	90°0′
020	23.23	557	623	24.5	25.4	0°0′
001	25.04	0	0	0	0	—
011	27.62	11	17	2.9	3.6	270°0′
120	29.95	24	8	4.6	2.6	90°0′
101	31.37	16	9	4.1	3.0	270°0′
111	33.55	407	440	15.4	15.8	151°18′
021	34.44	246	269	17.4	17.9	0°0′
030	35.19	0	0	0	0	—
200	37.65	3	3	2.9	2.9	180°0′
121	39.43	19	22	4.0	4.2	324°32′
210	39.57	8	9	3.6	3.7	180°0′
130	40.08	9	10	3.9	4.1	90°0′
031	43.65	12	39	5.0	8.9	270°0′
220	44.72	1	1	1.5	1.5	180°0′
201	45.76	123	166	16.9	19.3	270°0′
211	47.40	15	11	4.3	3.7	2°50′
040	47.53	7	6	6.1	5.1	180°0′
131	47.65	115	85	12.1	10.2	100°6′
002	51.40	0	0	0	0	—
140	51.46	5	5	3.9	3.9	90°0′
221	52.00	54	59	9.2	9.4	262°31′
230	52.55	11	11	5.9	5.7	180°0′
012	52.86	8	8	5.1	4.9	90°0′
041	54.44	53	53	13.6	13.3	0°0′
102	55.11	5	4	4.1	3.5	180°0′
112	56.52	17	15	5.7	5.3	180°0′
022	57.11	0	0	0	0	—
300	58.01	0	0	0	0	—
141	58.09	3	14	2.6	5.2	13°50′
231	59.08	0	0	0.7	0.6	27°8′
310	59.36	22	20	9.6	9.0	90°0′
050	60.50	0	0	0	0	—
122	60.64	2	9	2.1	4.5	180°0′
240	62.22	0	0	0.4	0	0°0′
320	63.26	2	2	2.7	2.7	270°0′
032	63.84	0	0	0	0	—
150	63.90	13	10	8.1	7.0	270°0′
301	64.14	1	1	2.3	2.1	90°0′
311	65.48	29	37	8.7	9.7	19°59′
202	65.52	0	0	0	0	—
051	66.55	1	1	2.0	1.7	270°0′
212	66.72	0	0	0.3	0	270°0′
132	67.06	38	32	10.3	9.2	180°0′
241	68.14	3	3	3.0	3.0	110°26′
321	69.28	1	1	1.6	1.4	46°3′
330	69.64	1	1	1.7	1.4	90°0′
151	69.76	19	14	7.5	6.4	51°27′
222	70.42	43	39	11.4	10.6	270°0′
042	72.62	0	0	0	0	—

(*continued*)

TABLE II (*continued*)

hkl	2θ(CuKα)	$I_{calc.}$	$I_{obs.}$	$F_{calc.}$	$F_{obs.}$	α
250	73.52	1	1	2.2	2.1	180°0′
060	74.41	12	8	12.6	10.4	180°0′
331	75.30	9	11	5.7	6.2	75°8′
142	75.80	0	0	0.5	0	0°0′
232	76.58	0	7	0	5.0	270°0′
160	77.48	0	0	0.6	0	90°0′
340	78.06	1	1	1.9	1.9	270°0′
251	79.06	0	0	1.1	1.1	96°30′
061	79.86	2	2	3.3	3.4	0°0′
400	80.54	10	11	12.2	12.7	180°0′
302	81.08	0	0	0	0	—
003	81.08	0	0	0	0	—
410	81.78	0	0	0	0	—
312	82.28	5	7	4.2	5.1	—
013	82.36	0	0	0.6	0	90°0′
161	82.98	0	0	1.0	0.8	65°34′
052	83.30	0	0	0	0	—
341	83.66	0	0	0.8	0.8	339°53′
103	84.12	0	0	0.9	0	270°0′
242	84.86	27	27	10.7	10.5	270°0′
420	85.22	5	5	6.6	6.5	180°0′
113	85.40	7	7	5.3	5.1	28°39′
322	85.86	0	0	0.7	0.8	180°0′
023	85.86	4	4	6.1	6.0	0°0′
401	85.96	0	0	1.5	1.3	90°0′
152	86.32	7	7	5.5	5.5	180°0′
260	86.50	0	0	1.0	1.1	0°0′
411	87.10	0	0	0.6	0	112°20′
350	88.08	2	7	4.2	7.7	270°0′
123	88.76	0	1	0.8	1.5	214°44′
070	89.70	0	0	0	0	—
421	90.57	7	7	5.8	5.6	171°6′
430	90.88	0	0	0.3	0	0°0′
332	91.78	14	15	7.9	8.1	0°0′
033	91.78	0	0	1.0	0	90°0′
261	92.00	8	8	6.2	5.9	92°21′
170	92.66	6	5	7.4	6.4	270°0′
203	93.10	5	4	6.8	5.9	90°0′
351	94.00	5	7	4.7	5.4	140°4′
213	94.14	0	0	0.8	0.8	357°11′
133	94.64	6	7	5.0	5.6	79°54′
071	95.10	0	1	0	2.7	90°0′
252	95.36	0	1	0	1.9	90°0′
062	96.18	0	0	0	0	—
431	96.84	0	0	0.9	0.8	92°18′
223	97.82	3	2	3.8	3.3	97°26′
171	98.10	4	3	4.3	3.6	355°42′
162	99.16	0	0	0.8	0.8	0°0′
440	99.22	1	1	2.3	1.8	0°0′
342	99.83	0	0	0.2	0	0°0′
043	99.84	4	5	6.1	6.6	0°0′
360	101.1	0	0	0.3	0	270°0′
270	101.7	0	0	0.1	0	0°0′

(*continued*)

TABLE II (*continued*)

hkl	2θ(CuKα)	$I_{calc.}$	$I_{obs.}$	$F_{calc.}$	$F_{obs.}$	α
402	102.2	0	0	0	0	—
143	102.9	0	0	0.6	1.6	166°10′
412	103.4	0	2	1.0	2.7	270°0′
233	103.8	0	0	0.1	0	333°14′
441	104.7	7	6	5.7	4.8	183°10′
422	107.1	1	1	1.3	1.2	90°0′
361	107.3	1	0	0.5	0	286°50′
271	107.4	0	0	0.7	0.8	180°24′
080	107.5	3	3	7.1	6.7	180°0′
500	107.7	0	0	0	0	—
262	108.3	2	2	3.1	2.9	270°0′
303	108.4	0	0	0.5	0	90°0′
510	109.0	4	4	6.3	5.8	270°0′
313	109.7	4	4	4.3	3.9	159°55′
450	110.1	0	0	0.1	0	0°0′
180	110.5	0	0	0.3	0	270°0′
352	110.6	5	5	4.9	4.5	0°0′
053	110.6	0	0	0.4	0	90°0′
072	111.8	0	0	0	0	—
243	112.3	1	1	1.5	1.5	249°34′
520	112.8	0	0	0.3	0	270°0′
081	113.2	1	1	2.7	2.7	180°0′
432	113.2	0	0	0.2	0	270°0′
323	113.4	0	0	0.3	0	133°55′
501	113.6	0	0	0.3	0	90°0′
153	113.9	3	3	3.8	3.4	128°33′
511	114.8	2	2	3.2	3.0	309°50′
172	115.0	0	0	0.3	0	0°0′
451	115.9	0	0	0.3	0	79°51′
181	116.1	0	0	0.3	0	122°50′
370	117.7	2	1	4.4	2.6	270°0′
521	118.8	0	0	0.3	0	155°32′
530	119.2	0	0	1.2	1.2	270°0′
333	119.9	2	1	3.1	2.3	104°54′
004	120.3	3	2	7.1	5.5	180°0′
280	120.5	0	0	0.6	0	0°0′
014	121.6	0	0	0	0	—
442	122.1	1	3	1.4	3.1	90°0′
104	123.8	0	0	0	0	—
371	124.0	5	4	3.9	3.5	182°56′
253	124.2	0	0	0.2	0	186°31′
460	124.5	5	5	6.3	5.6	0°0′
114	125.1	6	5	4.4	4.0	270°0′
362	125.2	0	0	0.3	0	0°0′
063	125.2	1	1	1.8	1.5	0°0′
272	125.6	0	0	0	0	90°0′
531	125.8	5	4	4.0	3.6	276°41′
024	125.9	0	0	0	0	—
281	126.8	5	4	4.0	3.5	86°40′
163	128.9	0	0	0.2	1.3	114°23′
540	129.2	0	0	0.3	1.8	270°0′
124	129.6	0	2	0.3	2.2	270°0′
090	130.1	0	0	0	0	—

TABLE III

Orthorhombic Polyoxymethylene: Comparison between Calculated Atom Coordinates and Coordinates Found by Fourier Method.

	x, A.		y, A.		z, A.	
	Theoretical	Experimental	Theoretical	Experimental	Theoretical	Experimental
C_1	1.75	1.74	0.56	0.54	3.11	3.13
O_1	0.63	0.63	0.56	0.55	2.22	2.20

As can be seen, the divergences are at the maximum of 0.02 A. and it is therefore difficult to decide whether they are really significant, since the maxima obtained with the Fourier calculations are somewhat flattened because of the high thermic factor.

Discussion of the Structure

For the solution of the structure of orthohombic POM we have at our disposal only powder spectra, which in themselves are not sufficient for a sure determination of the space group.

For this reason all the work relative to the formulation of the hypothesis of structure has been carried out for each single atom in a manner entirely independent of the conditions which would result from a knowledge of the space group. The method followed in the resolution of the structure of orthorhombic POM can be outlined as follows: (*a*) hypothesis of chains parallel to the *c* axis by analogy with the structure of hexagonal POM;

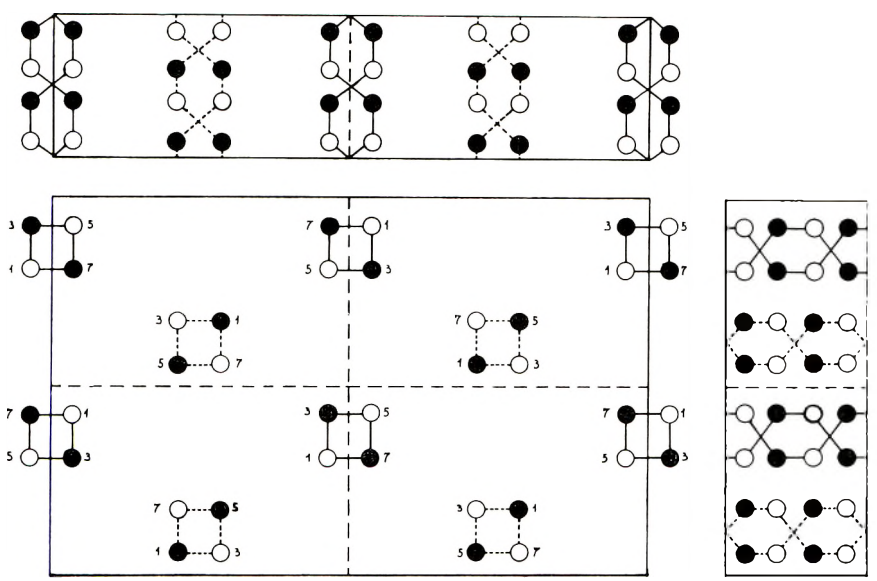

Fig. 18. Orthorhombic polyoxymethylene lattice with (--) left-handed and (——) right-handed chains; *a* and *b* doubled (case 1).

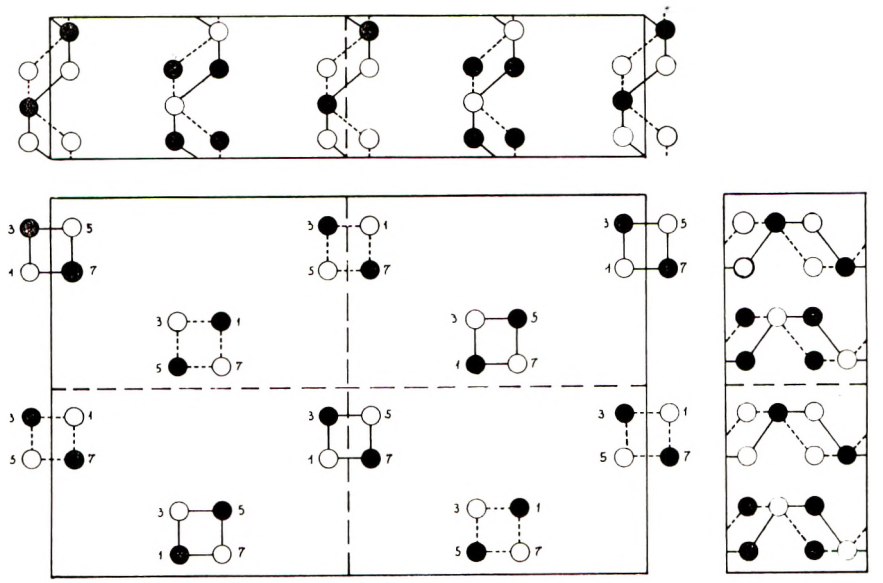

Fig. 19. Orthorhombic polyoxymethylene lattice with (--) left-handed and (——) right-handed chains; a and b doubled (case 2).

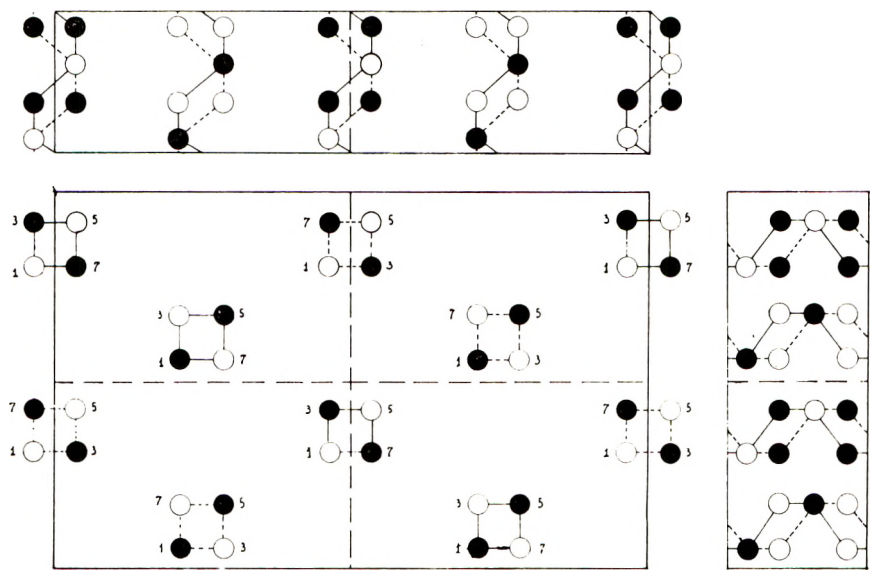

Fig. 20. Orthorhombic polyoxymethylene lattice with (--) left-handed and (——) right-handed chains; a and b doubled (case 3).

(b) determination of the form of the chain from a knowledge of the identity period, the bond lengths, and angles; (c) position of the sides of the square projection of the chain on the ab plane from the structure factor of the (240) reflection; (d) location of the carbon and oxygen atoms on the ab

projection by means of the structure factor of the (230) reflection; (*e*) determination of the *z*-coordinates by developing the chain along *c* so as to obtain the most acceptable distances between the faced atoms belonging to two adjacent chains.

In fact, we see that the structure shown schematically in Figure 14 is the only one which allows us to obtain a minimum distance of 3.48 A. between carbon and oxygen atoms of two adjacent chains. This is achieved only by

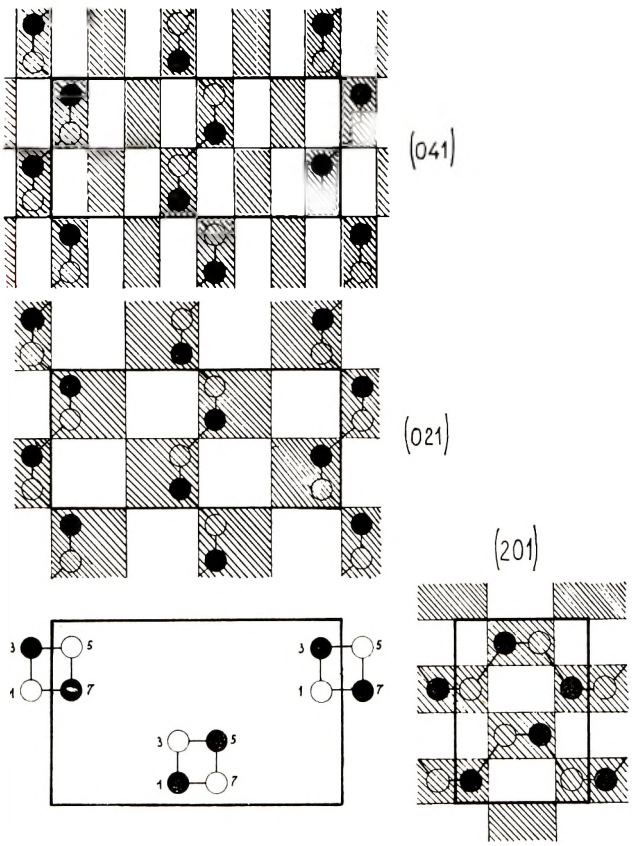

Fig. 21. Orthorhombic polyoxymethylene: projection of structure and structure factors of the (021), (041), and (201) reflections.

translating the *z*-coordinate of an atom by $c/2$ with respect to those of the two atoms of the adjacent chain facing it and superimposed upon themselves.

In this manner the configuration of each chain is automatically fixed by the four adjacent chains equal to each other.

The structure thus obtained belongs, in complete agreement also with the observed extinctions, to the space group $P2_12_12_1$ and has been confirmed by comparing the observed and calculated structure factors and also by the Fourier findings.

These results lead to a remarkable structural conclusion for a synthetic macromolecular substance: the lattice of the new orthorhombic form of POM must be made up of isomorphous chains, without the possibility of alternation or vicariance between right- and left-handed helices.

The structure of hexagonal POM also seems to lead to the same conclusions, but this will be discussed in another report. Crystal lattices built up only of isomorphous left- or right-handed helices have already been found by Natta and co-workers in the case of poly-*tert*-butyl acrylate and poly-5-methylhexene.[9]

An elementary cell built up of both right- and left-handed helices could be obtained in the case of orthorhombic polyoxymethylene by doubling the *a* and *b* axes of the cell and locating the chains according to the three possible lattices shown in Figures 18–20.

However, apart from any consideration about the space groups of these lattices, we note that their projections onto the *ac* and *bc* planes are in disagreement with the structure factors of the (021), (041), and (201) reflections, which impose in a unit cell the presence of isomorphous chains only (Fig. 21).

We wish to express our gratefulness to Prof. Silvio Bezzi, Director of the Instituto di Chimica Organica of the Padova University for preparing and supplying the orthorhombic POM samples and for his kind interest and authoritative survey to our work, and to Dr. Sabino Leghissa of the Montecatini for his continuous assistance and encouragement during the course of this work.

We thank the Centro Elettronico di Calcolo of the Olivetti Co. for its kind cooperation in the computation of structure factors and Fourier synthesis.

References

1. Staudinger, H., H. Johner, R. Signer, G. Mie, and I. Hengstenberg, *Z. physik. Chem.* **A126,** 425 (1927).
2. Hengstenberg, J., *Z. physik. Chem.*, **A126,** 435 (1927).
3. Hengstenberg, J., *Ann. Physik.*, **84,** 245 (1927).
4. Sauter, E., *Z. physik. Chem.*, **B18,** 417 (1932).
5. Sauter, E., *Z. physik. Chem.*, **B21,** 186 (1933).
6. Huggins, M. L., *J. Chem. Phys.*, **3,** 37 (1945).
7. Hammer, C. F., T. A. Koch, and J. F. Whitney, *J. Appl. Polymer Sci.*, **1,** 169 (1959).
8. Tadokoro, H., T. Yasumoto, S. Murahasi, and I. Nitta, *J. Polymer Sci.*, **44,** 266 (1960).
9. Natta, G., *Makromol. Chem.*, **35,** 93 (1960).

Synopsis

A new crystalline form of polyoxymethylene is described with an orthorhombic unit cell, space group $P2_12_12_1$, and lattice constants a = 4.77 A., b = 7.65 A., c = 3.56 A. The chains are helicoidal with the axis of the helix parallel to *c*. The period of identity of 3.56 A. comprises two monomeric units and one turn of the helix. The lattice of orthorhombic polyoxymethylene is made up of isomorphous helicoidal chains.

Résumé

On décrit une nouvelle modification cristalline du polyoxyméthylène à symétrie orthorhombique $P2_12_12_1$ dont les constantes du réseau sont a = 4.77 A, b = 7.65 A

et c = 3.56 A. Les macromolécules sont hélicoïdales et leurs axes sont parallèles à *c*. L'unité périodique est égale à 3.56 A; elle comprend deux unités monomériques par tour entier de l'hélice. Les cristaux sont formés de macromolécules isomorphes.

Zusammenfassung

Eine neue Form von Polyoxymethylen mit orthorhombischer Elementarzelle, Raumgruppe $P2_12_12_1$, Gitterkonstante a = 4.77 A., b = 7.65 A., c = 3.56 A. wird beschrieben. Die Ketten sind spiralförmig, mit der Schraubenachse parallel zu c angeordnet. Die Identitätsperiode von 3.56 A. enthält zwei CH_2O-Gruppen in einem Schraubengang. Das Gitter wird nur von Molekülen mit Rechts- oder Linksschraube gebildet.

Received December 13, 1961

JOURNAL OF POLYMER SCIENCE: PART A VOL. 1, PP. 985–992 (1963)

Experimental Data on Dilute Polymer Solutions. I. Hydrodynamic Properties and Statistical Coil Dimensions of Poly (*n*-Butyl Methacrylate)

R. VAN LEEMPUT and R. STEIN, *Laboratoire de Chemie générale, Université Libre de Bruxelles, Brussels, Belgium*

INTRODUCTION

It has now been fairly well established that the equations of Fox and Flory

$$[\eta]/[\eta]_\theta = \alpha^3 \tag{1}$$

$$(\alpha^5 - \alpha^3)/M^{1/2} = C\psi(1 - \theta/T) \tag{2}$$

do not correctly connect the hydrodynamic properties of polymer molecules with their unperturbed dimensions.

Kurata and Yamakawa[1] have recently developed a perturbation theory of the intrinsic viscosity, and together with the refinement of the Flory theory of the excluded volume effect carried out by Kurata, Stockmayer, and Roig,[2] this leads to two new equations

$$[\eta]/[\eta]_\theta = \alpha^{2.4} \tag{3}$$

$$(\alpha^3 - \alpha)[1 + (1/3\alpha^2)]^{3/2} = (4/3)^{5/2} C\psi(1 - \theta/T)M^{1/2} \tag{4}$$

In this and the following articles of this series, the authors intend to apply the two theories to the elucidation of the experimental results obtained with two linear flexible chain polymers, poly(*n*-butyl methacrylate) and poly(*n*-butyl acrylate) in a variety of solvents.

EXPERIMENTAL

Polymer, Solvents

The poly(*n*-butyl methacrylate) (PBM) was a sample obtained from the firm Polymer Consultants Ltd.

Six primary fractions were obtained from a 1% acetone solution through the addition of water until incipient phase separation and subsequent reduction of the temperature from 25°C. to 21°C.

The first three fractions were reprecipitated from a 0.4% acetone solution by the same procedure, giving 18 subfractions, five of which were selected for this investigation. These fractions were redissolved, centrifuged, and

reprecipitated, twice, to render them dust-free. They were vacuum-dried at room temperature until a constant weight was attained.

The reagent-grade solvents were distilled twice over molecular sieves under an inert atmosphere. Their measured densities are 0.8001 g./ml. and 0.7850 g./ml. at 25°C. for methyl ethyl ketone (MEK) and acetone, respectively.

The solutions were prepared gravimetrically: those used for light-scattering (LS) measurements were rendered free from suspended dust particles by centrifugation in capped tubes with Teflon joints in a field of 25,000 G over a period of 1 hr.

All measurements were carried out at 25°C.

Viscosity Measurements

We have used an Ostwald-type viscometer modified in order to maintain a constant overflow level. The mean rate of shear in the case of acetone was 300 sec.$^{-1}$. Kinetic energy corrections, of the order of 0.1%, were, nevertheless, applied. The flow times for MEK and acetone are 531.7 and 438.0 sec., respectively.

Osmotic Pressure Measurements

Osmotic pressures were measured statically in a modified Fuoss-Mead type osmometer with the use of No. 600 Cellophane (Sylvania Corp.) membranes with permeabilities in acetone of between 6×10^{-5} and 7×10^{-5} hr.$^{-1}$

The osmometer was immersed in a water thermostat at a temperature of 25.0 ± 0.002°C. Density corrections were applied in calculating the pressure. Details of the apparatus and measurements will be published in a subsequent paper.[11]

Light-Scattering Measurements

Angular scattering intensities were measured with a Cantow[3] photometer produced by the firm of Netheler and Hinz, Hamburg. Intensities were measured at 15 angles lying between 30° and 150° with the use of vertically polarized light at wavelengths of 546, 436, and 366 mμ.

The cylindrical measuring cell is furnished with two optically plane, parallel surfaces for the entry and the exit of the incident light beam, and with twin covers, to eliminate evaporation. It is placed, in a reproducible manner, in a thermostatic jacket which permits a regulation of the temperature in the cell to better than 0.1°C.

The refractive index increments were obtained with a Hilger and Watts differential refractometer using a 10-cm. cell equipped with a mercury-sealed cover. Particular attention was paid to the temperature regulation of the cell, permitting a constancy of ±0.002°C.

The values of dn/dc at wavelengths of 546, 436, and 366 mμ, respectively, are 0.1046, 0.1059 and 0.1064 in MEK and 0.1236, 0.1249, and 0.1257 in acetone.

Appropriate refractive index and Fresnel corrections were applied to all scattering measurements.

RESULTS AND DISCUSSION

All experimental results are collected in Tables I and II, completed by Figures 1 and 2.

TABLE I
Light-Scattering and Viscometric Measurements on Poly-(*n*-butyl Methacrylate) Fractions in Methyl Ethyl Ketone at 25°C.

Fraction	$\bar{M}_w \times 10^{-3}$	$A_2 \times 10^5$	$A_3 \times 10^3$	$\langle \bar{S}^2 \rangle_{LS}^{1/2} \times 10^8$	$[\eta]$
I-1	666	19.5	3.40	285	91.8
I-2	527	21.8	5.80	246	77.2
II-2	261	29.8	—	167	50.1
III-1	134	34.8	—	119	31.6
III-2	117	36.4	—	103	28.6

TABLE II
Light-Scattering, Osmotic and Viscometric Measurements on Poly-(*n*-butyl Methacrylate) Fractions in Acetone at 25°C.

	Light scattering				Osmotic pressure			
Fraction	$\bar{M}_w \times 10^{-3}$	$A_2 \times 10^5$	$A_3 \times 10^3$	$\langle \bar{S}^2 \rangle_{LS}^{1/2} \times 10^8$	$\bar{M}_n \times 10^{-3}$	$A_2 \times 10^5$	$[\eta]$	b
I-1	613	13.3	4.50	278	582	16.9	73.4	10
I-2	501	16.9	2.50	251	467	19.9	62.4	10
II-2	277	24.3	—	167	233	26.5	43.4	6
III-1	138	26.8	—	120	113	33.0	28.0	5
III-2	116	30.4	—	110	108	36.1	24.8	12

The results of angular scattering intensities measured in MEK and acetone were treated by the Zimm method. Values obtained from these diagrams were calculated by the method of least squares. Figure 1 shows typical plots of the values $(Kc/R_{\theta,v})_{\theta=0}$, against the concentration c of PBM for vertically polarized light of 436 mμ wavelength Values of the second virial coefficient A_2 have been calculated from the limiting tangents of these curves. In the case of the fractions of highest molecular weight I-1 and I-2, for which the range of concentrations measured was extended, a third virial coefficient, A_3, was taken into account.

For the sake of brevity, only the mean values of the results obtained for the three wavelengths have been reported here. The maximum deviations from the mean values obtained, for the different wavelengths are, respectively, 4% for the molecular weight, 8% for A_2, and 6% for the radius of gyration $\langle \bar{S}^2 \rangle_{LS}^{1/2}$. In the case of the molecular weight, agree-

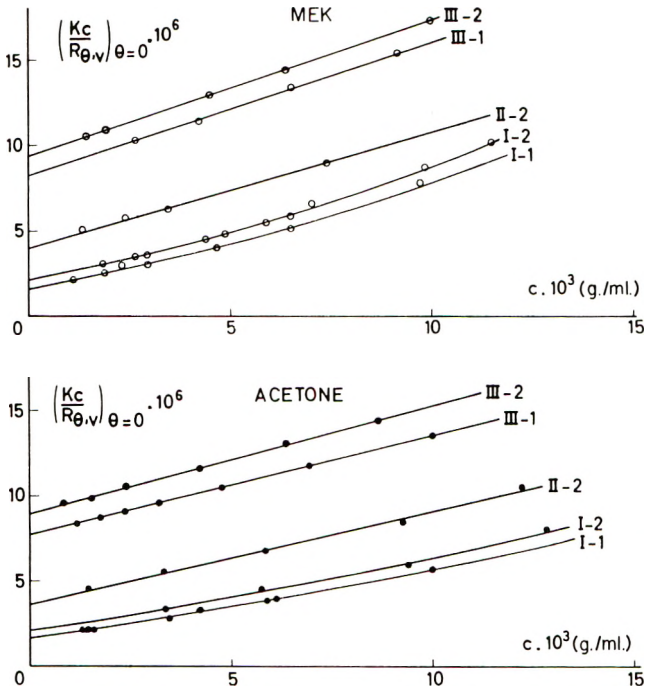

Fig. 1. Concentration dependence at zero angle of reduced scattered intensities at 436 mμ for PBM in MEK and acetone at 25°C.

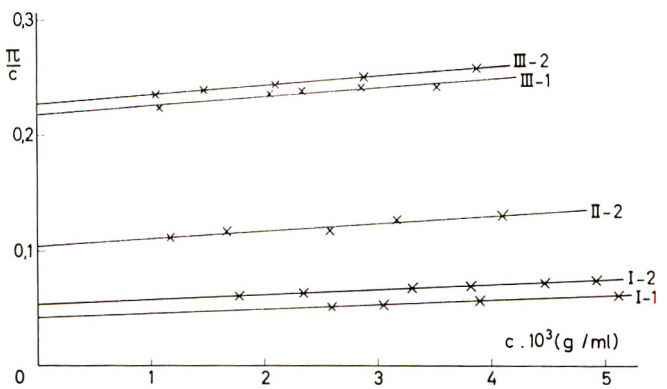

Fig. 2. Concentration dependence of the reduced osmotic pressure for PBM in acetone at 25°C.

ment between the results in the two solvents is good, and we have used the mean values in Table III and in all subsequent calculations.

In order to account for the heterodispersity of the samples, the molecular weights were measured osmotically in acetone as solvent.

A comparison of the number-average and mean weight-average molecular weights ($\bar{M}_n$ and $\bar{M}_w$) indicates fairly low degrees of heterodispersity for the fractions investigated.

The weight distribution of a polymer about its number-average molecular weight $\bar{M}_n$ may be represented by the expression[4]

$$W(M) = a^{b+1} M^b e^{-aM}/\Gamma(b+1) \tag{5}$$

where $\Gamma(b)$ is the gamma function, $a = b/\bar{M}_n$, and b is the parameter which characterizes the width of the distribution. This parameter may be deduced from the ratio of weight-average and number-average molecular weights:

$$\bar{M}_w/\bar{M}_n = (b+1)/b$$

As shown in Table II, the experimental values were relatively large. Nevertheless, heterogeneity corrections were applied to all our data.

Relations between $\bar{M}_w$, $[\eta]$ and $\langle \bar{S}^2 \rangle^{1/2}$

The observed relationships between the intrinsic viscosity $[\eta]$ and $\bar{M}_w$ for the PBM fractions in MEK and acetone, are of the type

$$[\eta] = KM^{\epsilon} \tag{6}$$

where K equals 1.00×10^{-2} and 1.79×10^{-2}, ϵ is 0.68 and 0.62 for MEK and acetone, respectively.

A heterodispersity correction factor of the type proposed by Matsumoto and Ohyanagi[5] has been applied, leading to the final expressions:

$$[\eta] = 0.97\, M^{0.68} \text{ for MEK} \tag{7}$$

$$[\eta] = 1.84\, M^{0.62} \text{ for acetone} \tag{8}$$

The relation between the radii of gyration, as determined by light scattering $\langle \bar{S}^2 \rangle_{LS}^{1/2}$, and $\bar{M}_w$ in the range of molecular weights investigated is expressed by the single relation, common to both solvents:

$$\langle \bar{S}^2 \rangle_{LS} = 1.90 \times 10^{-2} \bar{M}_w^{1.14} \tag{9}$$

This unique relationship is not predicted by the viscometric behavior of the PBM in the two solvents. It is now well established, both experimentally and theoretically,[6] that the dimensions determined by light scattering are true Z-averages only at the θ-point. They may be expressed in terms of a distribution function [eq. (5)] as follows:

$$\langle \bar{S}^2 \rangle_{LS} = \int \langle \bar{S}_i^2 \rangle\, M\, W(M) dM / \int M\, W(M) dM \tag{10}$$

In the case of a homogeneous fraction, the relation between $\langle \bar{S}^2 \rangle$ and M may be expressed as:

$$\langle \bar{S}^2 \rangle = CM^{1+\beta} \tag{11}$$

where β accounts for the expansion of the coil due to the excluded volume effect.

The value of β can be extracted from the relation:

$$\beta \cong (2\epsilon - 1)/3 \tag{12}$$

This approximation is based on the relationship between the hydrodynamic volume and the volume of the statistical coil, founded on the Flory theory. An alternative value of 2.43 instead of 3 could be used in the denominator on the right-hand side of eq. (12).

Expressing the relation of eq. (9) in terms of uniform (weight) averages, we obtain, again, the single relation:

$$\langle \bar{S}^2 \rangle_w = 1.32 \times 10^{-2} M^{1.16} \tag{13}$$

where the correlation factor is:

$$\langle \bar{S}^2 \rangle_w = \langle \bar{S}^2 \rangle_{LS} (b + 1)/(b + 2 + \beta) \tag{14}$$

The value of β adopted in eq. (14) was the mean value obtained from eqs. (7), (8), and (13), i.e., 0.12.

Chinai and Guzzi[7] obtain, for the same polymer, the relation $\langle \bar{S}^2 \rangle_{LS} = 0.135\ \bar{M}_w$ at 23°C. in MEK. A precise comparison between our values and those reported by these authors is difficult, as they do not report the heterogeneity of their samples. Their relation, however, implies an independence of the expansion factor, α, from the molecular weight, which is not substantiated by our results.

The values of Φ may be calculated, assuming Flory's equation:[8]

$$[\eta] = \Phi 6^{3/2} \langle \bar{S}^2 \rangle^{3/2} / M \tag{15}$$

for a homodisperse sample. This will be modified, in the case of a heterodisperse sample to:

$$[\eta]_{measured} = \Phi q 6^{3/2} \langle \bar{S}^2 \rangle_{LS}^{3/2} / \langle M \rangle_w \tag{16}$$

where q, the heterodispersity factor is given by:

$$q = (b + 1)[\Gamma(1 + \epsilon + b)/\Gamma(1 + b)][\Gamma(b + 2)/\Gamma(b + 3 + \beta)]^{3/2} \tag{17}$$

An inspection of the corrected values of Φ set out in Table III shows good agreement between the values obtained in the two solvents. The value, rather smaller than that predicted theoretically, could be ascribed to an accumulation of errors in the determination. A comparison with the

TABLE III
Calculated Values of $\langle \bar{S}^2 \rangle_w^{1/2}$, the Heterodispersity Factor q from Eq. (17) and Φ for PBM

		MEK			Acetone		
Fraction	$M_w \times 10^{-3}$	$\langle \bar{S}^2 \rangle_w^{1/2} \times 10^8$	q	$\Phi \times 10^{-23}$	$\langle \bar{S}^2 \rangle_w^{1/2} \times 10^8$	q	$\Phi \times 10^{-23}$
I-1	640	271	0.85	2.04	265	0.73	2.03
I-2	514	234	0.85	2.13	240	0.73	1.88
II-2	269	154	0.78	2.54	155	0.69	2.48
III-1	136	109	0.75	2.33	110	0.67	2.24
III-2	117	99	0.87	2.39	106	0.75	1.99
				2.29			2.12

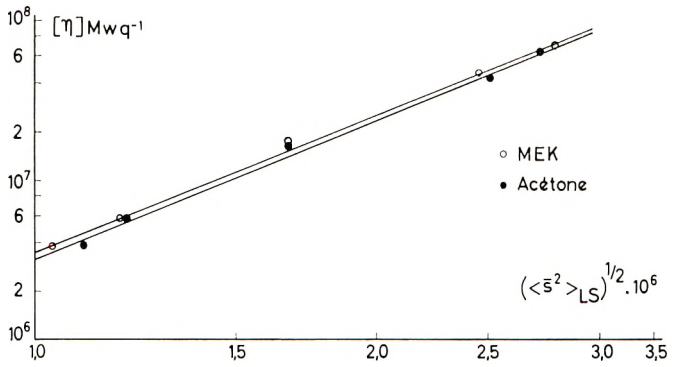

Fig. 3. Log–log plot of $[\eta]_{\text{measured}}Mq^{-1}$ against the light-scattering radius of gyration $\langle \bar{S}^2 \rangle_{LS}^{1/2}$.

collected values of Φ with respect to A_2 for a variety of systems quoted by Krigbaum and Carpenter[9] places these values in good agreement with the linear part of their smoothed curve.

We have obtained two relationships between A_2 and $\bar{M}_w$, being, respectively, in MEK and acetone:

$$A_2 = 0.025\bar{M}_w^{-0.36}$$

$$A_2 = 0.04\bar{M}_w^{-0.41}$$

These relationships have not been corrected for any dependence of A_2 on heterodispersity, due to the rather complicated relationships involved.[10]

We may now apply a test for Flory's relation, adopting a procedure proposed by Krigbaum and Carpenter,[9] which consists of plotting $[\eta]_{\text{measured}}\bar{M}_w/q$ against $\langle \bar{S}^2 \rangle_{LS}^{1/2}$ on a log–log scale (Fig. 3). Here q is the correction factor as determined in eq. (17). The slopes of the lines thus obtained are 2.83 in MEK and 2.87 in acetone, falling between the value of 3 proposed by Flory and that of 2.43 proposed by Kurata et al.

Measurements not reported here carried out on these fractions in four other solvents indicate expansion factors substantially lower than those reported by Chinai. A complete discussion of these results compared with those in a Θ solvent, will be presented in a forthcoming paper.[12]

References

1. Kurata, M., and H. Yamakawa, *J. Chem. Phys.*, **29**, 311 (1958).
2. Kurata, M., W. H. Stockmayer, and A. Roig, *J. Chem. Phys.*, **33**, 151 (1960).
3. Cantow, H. J., *Dechema-Monographien*, **27**, 124 (1956).
4. Schulz, G. V., *Z. physik. Chem.*, **B43**, 25 (1939).
5. Matsumoto, M., and Y. Ohyanagi, *J. Polymer Sci.*, **46**, 441 (1960).
6. Cassassa, E. F., *Ann. Rev. Phys. Chem.*, **11**, 477 (1960).
7. Chinai, S. N., and R. A. Guzzi, *J. Polymer Sci.*, **21**, 417 (1956).
8. Flory, P. J., and T. G. Fox, *J. Am. Chem. Soc.*, **73**, 1904 (1951).
9. Krigbaum, W. R., and D. K. Carpenter, *J. Phys. Chem.*, **59**, 1166 (1955).
10. Miyake, A., *J. Phys. Soc. Japan*, **15**, 883 (1960).

11. Van Leemput, R., and R., Stein, to be published.
12. Stein, R., and R. Van Leemput, *J. Polymer Sci.*, in press.

Synopsis

Viscometric, light-scattering, and osmotic pressure measurements were carried out on poly(*n*-butyl methacrylate) fractions in methyl ethyl ketone and acetone. Relationships between the limiting viscosity number, the average molecular weight, and the mean dimensions were obtained. Heterogeneity corrections were applied to all relationships, assuming a Schulz-type distribution. Values of Φ, calculated according to the Flory-Fox equation, were found to be 2.3×10^{23} and 2.1×10^{23} in MEK and acetone, respectively. No significant trend with molecular weight was noticed in the range investigated, though the dependence of $[\eta]$ on the mean radii of gyration is less than that predicted by the Flory theory.

Résumé

Des fractions de polyméthacrylate de butyle-*n* sont étudiées par des déterminations de viscosité, diffusion latérale de la lumière et pression osmotique dans la méthyl éthyl cétone et l'acétone. Les relations unissant l'indice viscosimétrique limite, la masse molaire moyenne et les dimensions sont présentées. Des corrections d'hétérogénéité ont été appliquées à toutes ces relations en supposant une distribution de Schulz. Les valeurs de Φ de l'équation de Flory-Fox sont respectivement $2,3 \times 10^{23}$ et $2,1 \times 10^{23}$ dans la méthyl éthyl cétone et l'acétone. Aucune variation significative de ce paramétre n'a été observée dans le domaine de masse molaire étudié, bien que la dépendance de $[\eta]$ en fonction du rayon de gyration de la pelote soit moindre que celle prévue par la théorie de Flory.

Zusammenfassung

Viskositäts-, Lichtstreuungs- und osmotische Messungen wurden an verschiedenen Poly-*n*-butylmethacrylatfraktionen in Butanon und Aceton durchgeführt. Nach Korrektur für Heterodispersität unter Annahme einer Schulz-Verteilung, wurden Beziehungen zwischen der Viskositätszahl, dem Molekulargewicht und der mittleren Grösse erhalten. Die Φ-Werte aus der Flory-Fox-Gleichung betragen in Butanon und Aceton 2,3 bzw. $2,1 \cdot 10^{23}$. In dem untersuchten Molekulargewichtsbereich wurde keine merkliche Änderung dieses Parameters beobachtet, obwohl die Abhängigkeit von $[\eta]$ vom Trägheitsradius des Knäuels geringer ist, als nach der Theorie von Flory zu erwarten wäre.

Received January 9, 1962

JOURNAL OF POLYMER SCIENCE: PART A VOL. 1, PP. 993–1003 (1963)

Fracture Processes in Polymeric Materials. IV. Dependence of the Fracture Surface Energy on Temperature and Molecular Structure

J. P. BERRY, *Research Laboratory, General Electric Company, Schenectady, New York*

The application of the Griffith fracture theory[1,2] to the data obtained from tensile tests on samples containing defects of known size gives a value for the energy required to produce unit area of surface as the defect increases in size. The fracture surface energies obtained from the results of such experiments on the glassy polymers poly(methyl methacrylate) and polystyrene, at room temperature, have values much greater than would be expected from the molecular structure of the materials.[3,4] It has been suggested that the discrepancy is due to the energy which is dissipated at the tip of the defect in effecting orientation of the molecules against the drag of viscous forces.[3] A similar discrepancy between the experimental and calculated surface energies is observed in steel, where an analogous plastic work process has been suggested to account for it.[5] Evidence in support of the orientation hypothesis in poly(methyl methacrylate) is found by examination of the fracture surfaces, which display interference color effects.[6,7]

A second factor which is important in determining the strength of glassy polymers is the size of the flaw inherent in the material.[4] This factor may be defined as the size of the equivalent Griffith crack, which, in a sample of the material with a given value of the product $E\gamma$ (Young's modulus $\times$ fracture surface energy), would cause it to fail at the observed value of the ultimate strength. Thus the inherent flaw size does not necessarily give the dimensions of a physical discontinuity in the sample, but rather those of an equivalent imperfection of given geometry. In polymers there is some indication that this parameter is related to the tendency of the material to craze,[4] i.e., to develop physical discontinuities at stress levels much below that required for failure. This effect is not at all well understood, and only recently has the nature of the discontinuities themselves been elucidated.[8] Since the crazing marks are generated by the application of stress, the "inherent flaw" refers to the effective size which these marks have attained by the time that failure is imminent. The flaws, in this case, are potential and do not exist as such in the unstressed sample.[4]

In view of the postulated importance of the viscous mechanism of energy dissipation, it is of interest to explore the effect of temperature and molec-

ular structure on the value of the surface energy obtained from the tensile experiments, since these factors would be expected to exercise a significant influence on the dissipative process and hence on the measured value of the surface energy. Such experiments have been carried out on poly(methyl methacrylate).

The results also provide further information on the crazing behavior of the polymer under extreme temperature conditions, and its relation to the size of the inherent flaw in the material.

TEMPERATURE EFFECTS

Apparatus

To avoid the numerous shortcomings of the air ovens normally used for temperature control in conventional tensile testing, it was considered desirable to devise a technique which would enable the experiments to be performed in a liquid thermostat. Furthermore, it was intended to make measurements at the temperature of liquid nitrogen, a condition which is rather difficult to realize in an air enclosure. Though no particular attempt was made, in the present series of experiments, to control the environment of the sample, the use of an essentially closed system, which would permit this is of obvious potential advantage. This feature has to be reconciled with the facility for rapid and easy changing from one sample to the next so that a series can be tested in a reasonable period of time. The apparatus which was devised to satisfy these requirements is described below.

The test cell unit is illustrated in Figure 1. A dumbbell sample, normally

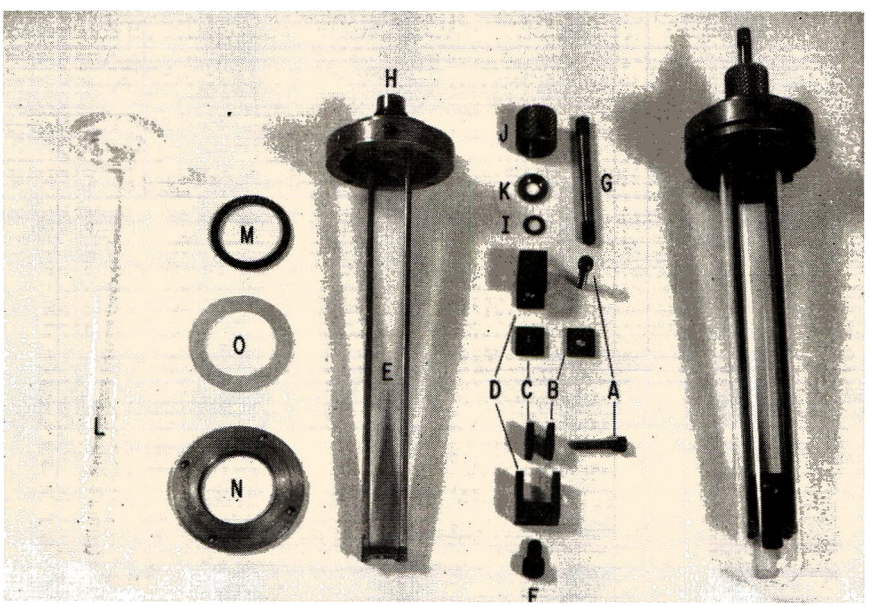

Fig. 1. The tensile test cell. The assembled unit is shown on the right.

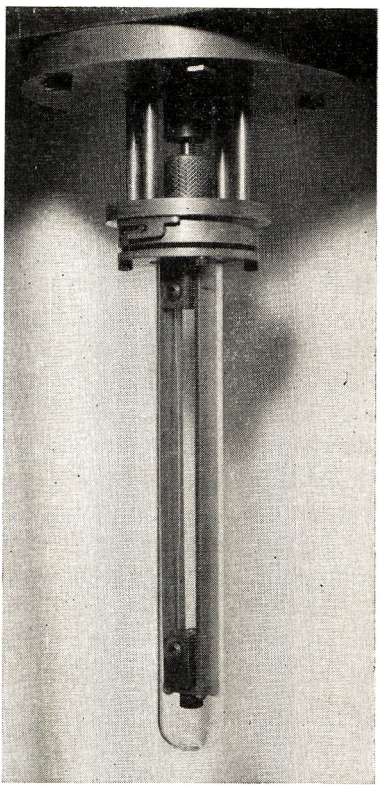

Fig. 2. The tensile test cell mounted on the testing machine.

6 × 1/2 in., is drilled at the ends to take the clamping screw A. To mount the sample, the end is inserted between the clamp faces B and C, of which the rear one (C) is tapped, and the "sandwich" so formed is placed in the clamp body D. The clamp screw A is inserted through the clearance holes in the clamp body, the clamp face B, and the sample, and passing through the tapped hole in C, is tightened to exert pressure on the sample. The clamp thus imposes both a friction grip, and also provides a positive locating pin which prevents slippage. The second clamp is applied in a similar way, and the sample with the clamps attached is then placed within the frame E. It is attached to the frame by means of the base screw F which passes through a hole in the bottom of the frame, and is screwed into the lower clamp. A pull rod G, passing through the collar H is screwed into the upper clamp. The rubber sealing ring I can then be used with the screwed cap J and washer K, to provide an effective seal at this point. The frame is enclosed within the flanged glass jacket L, a rubber ring M forming the seal between the flange and the collar H of the apparatus. The jacket is held in place by the ring N and is cushioned by the rubber ring O. The collar is provided with two pins which engage in a simple but effective bayonet fitting suspended below the crosshead of the tensile tester (Fig. 2). A connecting rod is attached to the pull rod of the test

cell by means of a screwed collar, and passing through the crosshead is connected to the normal load measuring device. Since the unit is suspended below the crosshead, it can be immersed, without difficulty, in a liquid thermostat placed between the vertical columns of the testing machine. The testing is then carried out by the normal procedures.

The design of the apparatus is such that the test cell moves with the crosshead, so that if the thermostat rests on the body of the machine, the cell will be immersed in the bath to different extents during the course of the experiment. With glassy polymers the ultimate extension is low, so that no difficulty arises from this cause, but with other materials it may be necessary to mount the thermostat on a support which will enable its position, relative to the crosshead, to be maintained constant.

In carrying out an experiment on a series of samples it is convenient to mount each sample in its own individual cell; the cells are then placed in the thermostat bath to attain thermal equilibrium. It is then a simple matter to bring a particular cell into position below the crosshead, attach it to the connecting rod, and perform the tensile experiment. In this way a number of samples can be tested successively without removing them at any time from the bath liquid, with greater speed and ease than is possible when operating the testing machine in a conventional manner. Also the closed cell in which the sample is held permits a much better control of the experimental conditions.

Experimental

The samples used in the study were cut from sheets of Plexiglas II UVA (Rohm and Haas) and defects were inserted in the manner described previously.[3] The dependence of the ultimate stress on the size of the defect was determined at a series of temperatures. By applying the Griffith fracture theory to the results, the value of the fracture surface energy at each temperature was obtained. A series of conventional uncracked samples was also studied so that the effective size of the inherent flaw in the samples could be obtained. The Young's modulus, required for the calculation, was determined under the same conditions.

The lowest temperature studied was that of liquid nitrogen. In view of the inertness of the thermostat liquid and the low temperature involved, the samples were placed in direct contact with the liquid nitrogen and the glass jacket was dispensed with. It was necessary to avoid the thermal shock which is incurred if the sample (at room temperature) is placed directly in the refrigerant, and an initial cooling period was allowed with the sample enclosed in the glass jacket. After 2 hr. the jacket was removed and the sample immersed in the liquid for a further 2 hr. before testing. For the temperature of −78°C. a solid carbon dioxide-methanol mixture was used, and a bath of melting ice gave a temperature of 0°C. A water thermostat was used for the temperatures of 25 and 50°C. Higher temperatures were not investigated because of the increasing tendency to gross

viscous flow in the samples, which would render invalid the application of the theory.

Results

The ultimate stress was calculated from the maximum on the force–elongation curve, taking the cross-sectional area of the sample at the site of the fracture plane. The tensile strength T so obtained was plotted against $1/c^{1/2}$, where c is the measured length of the defect in the sample. The slope of the best straight line through the points and the origin gave the value of the product $E\gamma$, where E is the Young's modulus and γ is the fracture surface energy, assuming the theoretical Griffith expression,

$$T = [2E\gamma/\pi c(1 - \nu^2)]^{1/2}$$

For the purpose of the calculation, it was assumed that the Poisson's ratio ν was constant over the temperature range studied.

Figure 3 shows the variation with temperature of the product $E\gamma$, Young's modulus E, and the derived fracture surface energy γ. The data for Young's modulus were obtained from the force–elongation curves of the uncracked samples, and agree with the results obtained in three point bending tests. The change in the tensile strength of uncracked samples with temperature is given in Figure 4, together with the product $E\gamma$ and the calculated size c_0 of the inherent flaw.

Discussion

It will be observed in Figure 3 that the parameter $E\gamma$, the Young's modulus E, and the fracture surface energy γ all increase with decreasing temperature. With regard to the last, the change is relatively slow in the vicinity of room temperature, but it increases rapidly as the temperature is reduced; at the lowest temperature studied, there is no indication of any

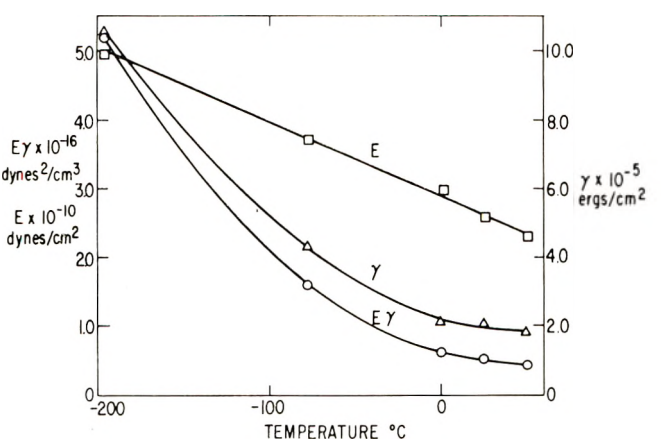

Fig. 3. The dependence on temperature of Young's modulus E, the fracture surface energy γ, and the product $E\gamma$ of poly(methyl methacrylate).

leveling off in its value. From the results obtained at room temperature it was concluded that the largest contribution to the value of the surface energy was due to the energy dissipated in an essentially viscous process in which the polymer molecules were moved from random configurations into a more or less ordered structure at the tip of the inserted defect.[3] The observation that the fracture surface energy maintains its high value, which in fact increases as the temperature is reduced, indicates that the dissipative mechanism is still operative at the lowest temperatures studied. This finding is perhaps surprising since the possibility of any significant extent of molecular motion would be considered rather unlikely at the temperature of liquid nitrogen.

The magnitude of the experimental surface energy is a function of both the effective "viscosity" of the system, and also the amount of material involved in the dissipative process. At room temperature, supplementary evidence for the proposed hypothesis is gained from examination of the fracture surfaces which display distinctive color effects. This observation indicates the presence of a structurally modified layer at the fracture plane and also provides an estimate of the thickness of the layer and hence the amount of material which is concerned. The fracture surfaces of tensile samples broken in liquid nitrogen are usually too rough for color effects to be detected, but such effects have been observed on the fracture surfaces of cleavage samples broken under these conditions. Thus it appears that at the low temperature molecular rearrangement is possible, to an extent comparable with that which occurs at room temperature.

This somewhat unexpected result is presumably related to the phenomenon of yielding in polymers, a process that results in a large local deformation, which is so great as to demand extensive molecular displacements, at temperatures considerably below the glass temperature. Recent work has indicated that the mobility of the polymer segments and hence the effective viscosity of the system is a function of both temperature and stress, such that the "viscosity" increases with decreasing temperature, but decreases with increasing stress.[9–11] Consequently, under conditions of low temperature and high stress, which obtain in the vicinity of the defect, molecular mobility may still be sufficient to permit orientation to occur. The amount of energy which is dissipated in this process will be a (presumably) complex function of the amount of material affected, temperature, stress, and time. From the experimental values of the surface energy it appears that the various opposing tendencies compensate to a large extent, so that the change with temperature (a factor of five) is small compared with the discrepancy which exists between the experimental and calculated values of the surface energy (a factor of about 500).[3]

At room temperature the fracture surface energy characteristics of polymers are similar to those of metals (steel).[3,5] In both, the observed value of the surface energy is much greater than that calculated from the molecular structure, assuming that the fracture process involves only the rupture of interatomic bonds. The difference is attributed to the energy dissipated

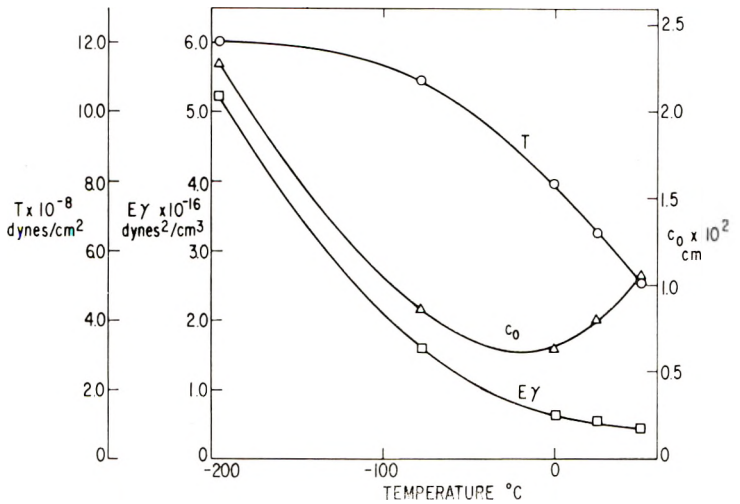

Fig. 4. The dependence, on temperature, of the tensile strength T, the inherent flaw size c_0, and the product $E\gamma$ of poly(methyl methacrylate).

at the tip of the defect in an irreversible manner. The dependence of the fracture surface energy on temperature has also been determined for zinc (+0.1% cadmium) and iron (+3% silicon).[12] In both of these materials the surface energy decreased as the temperature was reduced and approached the theoretical value at low temperatures. The difference between this behavior and that observed in poly(methyl methacrylate) is presumably related to the difference in the details of the mechanism of energy dissipation in the two classes of materials. In metals, plastic deformation occurs by slip across specific crystal planes, a mechanism which involves the motion of lattice dislocations. In polymers, the molecules are displaced from their random configurations and constrained to move into new positions. This motion takes place against the drag of viscous forces associated with the van der Waal's interactions between the molecules. Thus, although the process is related to self-diffusion in both instances, the force fields involved and the nature of the diffusing elements are quite different in their nature. Since the surface energies of the metals decrease as the temperature is reduced, it seems probable that the resistance to dislocation motion becomes so great that effectively no plastic deformation of the crystal lattice occurs at low temperatures.[13] At room temperature the extent of the deformation has been determined by x-ray diffraction studies of the fracture surfaces after different extents of etching.[5] However, such experiments have not been carried out on metals fractured at different temperatures, down to those at which, from the surface energy data, it would be concluded that no plastic deformation had occurred.

The tensile strength of uncracked samples of poly(methyl methacrylate) increases with decreasing temperature, but shows a tendency to approach a limiting value (Fig. 4). From the known variation in the product $E\gamma$, it

is possible to derive the change in the inherent flaw size c_0 with temperature. This parameter shows a minimum at about $-20°C.$, the value increasing as the temperature is raised or lowered from this value. It is believed that the inherent flaw size is related to the tendency of the material to craze,[4] but no quantitative studies of this latter phenomenon, over a wide temperature scale, have been made. However, it was noticed that the uncracked samples which had been tested in liquid nitrogen showed a much more severe extent of crazing, after fracture, than those tested at the higher temperatures. The force–elongation curves for such samples under these conditions displayed a leveling off, which occasionally became a distinct maximum, at the failure point. This effect is not to be attributed to macroscopic yielding of the sample, but rather to the onset of extensive crazing. In this respect the behavior of the polymer resembles that of polystyrene at room temperature, where similar features of the force–elongation curve are found, and where the acceleration in the crazing process near the failure point can be observed directly.[4] In this case also the samples, after fracture, show similar large extents of crazing. Again there is a qualitative relationship between the crazing tendency and the size of the inherent flaw, which supports the views already expressed. It might be considered that thermal shock was responsible, to some extent, for the increased extent of crazing observed in liquid nitrogen, and the correspondingly large value of the inherent flaw size calculated from the results obtained under these conditions. However, samples of the polymer which had been subjected to the cooling cycle and then allowed to return to room temperature by the reverse of that cycle showed no evidence of the characteristic random surface cracks usually associated with thermal shock. Also the crazing marks found in the sample after failure were characteristic of those produced by uniaxial tension, i.e., the marks were oriented in planes normal to the direction of the applied tensile stress.

MOLECULAR STRUCTURE EFFECTS

There is a close correlation between the structure of polymer molecules and the nature of their macroscopic viscoelastic responses. If the main contribution to the experimental value of the fracture surface energy is that dissipated in a viscous process, then changing the molecular structure should influence the amount of energy so dissipated and hence influence the measured value of the fracture surface energy. In particular, high degrees of crosslinking would be expected to inhibit large-scale molecular migration such as is believed to occur in the vicinity of a defect in a sample under stress. For this reason the study has been extended to include that of the behavior of copolymers of methyl methacrylate, and the tetrafunctional monomer, ethylene glycol dimethacrylate:

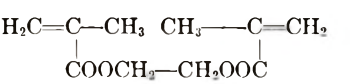

Materials

The methacrylate and dimethacrylate monomers, as supplied, contained a polymerization inhibitor (hydroquinone), which was removed by extraction with 5% aqueous sodium hydroxide. The monomer was then washed with water until all trace of alkali had been removed, dried overnight over anhydrous calcium sulfate, and finally passed through a column of activated alumina. The product was stored in the refrigerator in the dark until used.

Benzoyl peroxide was used as polymerization initiator.

A mold was constructed from two sheets of plate glass 8 in. square. They were held apart by a gasket of flexible polyethylene tubing and clamped externally by steel bars. The cavity so formed was approximately $7 \times 7 \times {}^1/_8$ in.

Attempts were first made to prepare a sheet of the homopolymer of the dimethacrylate. The peroxide (0.2 wt.-%) was dissolved in the monomer and the solution poured into the mold, which was then heated in an air oven at 100°C. After 30 min. the polymerized sheet had broken into small fragments, presumably because of the large density change on polymerization which induced sufficiently high stresses in the sample to cause it to shatter. Variations in the experimental procedure did little to alleviate the trouble and finally the attempt to prepare the completely crosslinked homopolymer was abandoned. The preparation of copolymers containing decreasing amounts of the tetrafunctional compound was then undertaken, and success was achieved with a copolymer containing 10 mole-% of the dimethacrylate monomer. This material was extremely brittle, and the

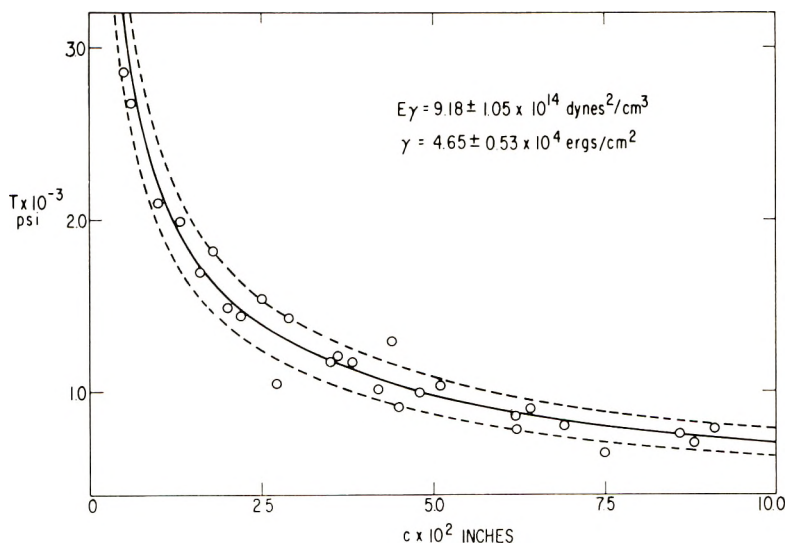

Fig. 5. The dependence of the tensile strength of a methyl methacrylate–ethylene glycol dimethacrylate copolymer on the size of the defect in the sample.

preparation of samples containing cracks of controlled size proved very difficult. The results of experiments conducted at 25°C. are summarized in Figure 5. They were obtained from a number of different sheets of material, and the relatively small extent of scatter is an indication of the reproducibility of the polymerization procedure.

Results

The position of the solid line in Figure 5 corresponds to a value for $E\gamma$ of 9.18×10^{14} dynes^2/cm.^{3}, and since the measured value of Young's modulus for the material is 1.97×10^{10} dynes/cm.^{2}, the surface energy is then 4.65×10^4 ergs/cm.^{2}. Experiments on uncracked samples of the copolymer gave a value for the tensile strength of 8100 psi, which, with the value for $E\gamma$ quoted above, yields a value for the size of the inherent flaw in the material of 1.81×10^{-3} cm.

Discussion

The value of the surface energy of poly(methyl methacrylate) at 25°C. is 2.07×10^5 ergs/cm.,^{2} and the size of the inherent flaw is 5.1×10^{-3} cm. Thus the induction of a comparatively small extent of crosslinking is sufficient to reduce the surface energy of the polymethacrylate by a factor of five, while the inherent flaw size is decreased by a factor of three. The fracture surfaces of the copolymer samples are very smooth and highly reflecting, but do not show any indication of interference color effects There is no evidence for the transition from low to high rates of crack propagation, such as occurs in the methyl methacrylate homopolymer,[6] either from observation of the moving crack or by examination of the resulting fracture surfaces. It has been suggested that this transition is due to a viscous or plastic process which occurs at the tip of a defect in the sample.[14] Thus, there are a number of points of evidence which indicate that such processes do not occur to the same extent in the copolymer as in the homopolymer, which supports the conclusions drawn from surface energy considerations. The reduction in the size of the inherent flaw would indicate that the copolymer is more craze resistant than the homopolymer. At present, however, there is no direct evidence to support this conclusion.

The observations reported in this paper support the hypothesis already presented concerning the factors which govern the strength and fracture properties of glassy polymers. Unfortunately, it is still not yet possible to provide any quantitative relationships between the variables studied and the effects on the results which they produce.

The author wishes to acknowledge the able technical assistance of Paul J. Krusic and Clark N. Adams, who carried out most of the experimental work.

References

1. Griffith, A. A., *Phil. Trans. Roy. Soc.*, **A221**, 163 (1921).
2. Griffith, A. A., *Proc. Intern. Congr. Appl. Mech. Delft*, 55 (1924).
3. Berry, J. P., *J. Polymer Sci.*, **50**, 107 (1961).
4. Berry, J. P., *J. Polymer Sci.*, **50**, 313 (1961).
5. Felbeck, D. K., and E. Orowan, *Welding J. Research Suppl.*, **34**, 570-s (1955).
6. Berry, J. P., *Nature*, **185**, 91 (1960).
7. Berry, J. P., *J. Appl. Phys.*, **33**, 1741 (1962).
8. Spurr, D. K., Jr., and W. D. Niegisch, *J. Appl. Polymer Sci.*, **6**, 585 (1962).
9. Lazurkin, L. S., *J. Polymer Sci.*, **30**, 595 (1958).
10. Binder, G., and F. H. Müller, *Kolloid Z.*, **177**, 129 (1961).
11. Robertson, R. E., *J. Appl. Polymer Sci.*, in press.
12. Gilman, J. J., *J. Appl. Phys.*, **31**, 2208 (1960).
13. Stein, D. F., and J. R. Low, Jr., *J. Appl. Phys.*, **31**, 362 (1960).
14. Stroh, A. N., *J. Mech. Phys. Solids*, **8**, 119 (1960).

Synopsis

The study of the influence of flaw size on the tensile strength of poly(methyl methacrylate) samples has been extended over the temperature range −190°C. to 50°C. The fracture surface energy increases with decreasing temperature, while the inherent flaw size of uncracked samples passes through a minimum at about −20°C. The fracture surface energy and inherent flaw size of a copolymer of methyl methacrylate and 10 mole-% of ethylene glycol dimethacrylate have been obtained at room temperature, by a similar method. These results are examined in the light of the hypothesis already put forward concerning the factors which govern the strength and fracture properties of glassy polymers.

Résumé

L'étude de l'influence de la forme de la rupture sur la force de rupture d'échantillons de polyméthacrylate de méthyle a été complétée dans la zone de température de −190°C à 50°C. L'énergie de surface de fracture augmente quand la température diminue, quand la forme inhérente de la rupture des échantillons non craquelés passe par un minimum aux environs de −20°C. L'énergie de surface de fracture et la forme inhérente de la rupture d'un copolymére de méthacrylate de méthyle et 10% en mole de diméthylacrylate d'éthyléne glycol a été déterminée de la même façon. Ces résultats ont été examinés en vue de l'hypothese déjà suggérée concernant les facteurs qui influencent la rigidité et les propriétés des polyméres vitreux.

Zusammenfassung

Die Untersuchung des Einflusses der Grösse der Defekte auf die Zugestigkeit von Polymethylmethacrylatproben wurde auf den Temperaturbereich von −190°C bis 50°C ausgedehnt. Die Bruchflächenenergie nimmt mit fallender Temperatur zu, während die charakteristische Defektgrösse ungevrackter Proben bei etwa −20°C durch ein Minimum geht. Die Bruchflächenenergie und die charakteristische Defektgrösse eines Copolymeren aus Methylmethacrylat und 10 Mol% Äthylenglykoldimethacrylat wurden nach einer ähnlichen Methode bei Raumtemperatur erhalten. Die Ergebnisse werden im Lichte der schon früher für die Faktoren, die Festigkeits- und Brucheigenschaften von Polymeren im Glaszustand bestimmen, entwickelten Hypothese diskitiert.

Received January 9, 1962

JOURNAL OF POLYMER SCIENCE: PART A VOL. 1, PP. 1005–1014 (1963)

Light-Scattering Studies on Sugar Beet Arabans

YOSHIO TOMIMATSU and K. J. PALMER,
Western Regional Research Laboratory, Albany, California*

INTRODUCTION

In a previous paper,[1] a discrepancy in the molecular weight of sugar beet araban by light scattering in two solvent systems, 2*M* NaCl and 1% (v/v) *N*,*N*-dimethylformamide (DMF), was reported. Endgroup analyses and sedimentation results led the authors to conclude that the higher molecular weight in salt was correct. The lower molecular weight in DMF was attributed to a multicomponent effect, i.e., preferential absorption of water by araban. This latter conclusion was based primarily on the assumption that araban was uncharged in solution. Further work on araban has confirmed the correctness of the molecular weight in salt but the assumption that araban is uncharged was erroneous, and the apparent low molecular weight in DMF can be explained on the basis of a charge effect in a low ionic strength solvent.

Molecular weight measurements on the araban acetate prepared for purification purposes indicated considerable degradation during deacetylation. This means that the original araban, as extracted from sugar beet pulp, probably is much larger than assumed from molecular weight measurements on the purified material.

Experimental

The starting material was crude araban extracted from sugar beet pulp.[2] Acetylation was carried out according to the procedure of Carson and Maclay.[3] Deacetylation was done in a threefold excess of 1*N* NaOH at room temperature. Since the primary purpose of this study was to resolve the discrepancy in molecular weight in the two solvent systems, 2*M* NaCl and 1% (v/v) DMF, no attempt was made to obtain a complete fractionation of the araban acetate on a charcoal column.[4]

Two main araban acetate fractions were prepared. In preparation of fraction I, the charcoal column was loaded with 26 g. of crude acetylated araban and eluted successively with 2l. of acetone, a 50–50 (v/v) mixture of acetone and chloroform, and chloroform. The araban acetate in the middle fraction was recovered (12.95 g.), dissolved in acetone and subjected to fractional precipitation with petroleum ether. The acetate remaining in

* A laboratory of the Western Utilization Research and Development Division, Agricultural Research Service, U.S. Department of Agriculture.

solution after the acetone: petroleum ether (v/v) ratio reached 200:91 was recovered (4.35 g.) and designated fraction I. Hydrolysis of 4.0 g. of fraction I yielded 2.36 g. of araban fraction I-A.

Fraction II was prepared from another sample of crude araban acetate. Crude acetate (50 g.) was dispersed in 2 l. of chloroform and 20 g. of charcoal (Darco G60) added in 1 g. increments with vigorous stirring. The mixture was allowed to stand overnight, then gravity filtered through a medium porosity, sintered-glass filter containing a layer of filter aid. The araban acetate was recovered from the filtrate (44 g.) and extracted with ten 100-ml. portions of methyl ethyl ketone (MEK). The araban acetate recovered (18 g.) from the combined extracts was designated fraction II. Two portions of fraction II (7.0 and 5.3 g.) were hydrolyzed to yield araban fraction II-A (4.0 g.) and fraction II-B (3.1 g.), respectively. Fraction II-B (1.13 g.) was reacetylated to yield 1.37 g. of araban acetate fraction II-B-1.

Light-scattering measurements were made with a slightly modified Brice[5] photometer. The calibration of this instrument has been described.[6,7] Specific refractive increments, dn/dc, were measured with a Brice[8] differential refractometer. For solvents containing intermediate salt concentrations, dn/dc was obtained by interpolating the values in water and 2M NaCl. Light-scattering measurements on the acetate were carried out in MEK. The solvent (EK 383) was treated with anhydrous $CaCl_2$ and redistilled daily.

Most of the scattering measurements were made by means of the dilution procedure, but for scattering data at extremely low concentrations, the Dintzis[9] procedure was used. A simple mixing device utilizing an ordinary vacuum-operated, windshield-wiper motor provided rapid mixing without wetting the stopper of the small ($1 \times 1 \times 5$ cm.) cell used in this procedure. The lightweight holder, constructed of Duraluminum, with suitable slots to hold the cell tilted at a slight angle over the center of rotation, was attached to the oscillating arm.

Concentrations were determined by dry weight determinations or by Δn measurements. For the Dintzis procedure, concentrations were calculated from the known initial volume of solvent, and the measured increment of added stock araban solution of known concentration. As a check, Δn measurements were made on the final solution. Measured and calculated araban concentrations of the final solutions checked within 1%.

Equilibrium dialysis studies were carried out with the use of dialysis tubing (Visking, 1/4-in. diameter) fitted over a piece of capillary glass tubing. A syringe was used to fill the system with 1% araban in 1% (v/v) DMF solvent (~5 cc.). The apparatus was placed in a bath containing a large volume of solvent (3 l.), the height of the liquid in the capillary being adjusted to a predetermined point to minimize changes in araban concentration. Possible changes in DMF concentration inside the dialysis bag were followed by appropriate Δn measurements.

Results and Discussion

Light-scattering results on the various fractions are summarized in Table I. The molecular weights of the three araban acetate fractions measured in MEK, when corrected for 39.0% acetyl,[10,11] give 54,400, 68,900, and 46,100 for fractions I, II, and II-B-1, respectively, as the molecular weights for the free araban. The values for I and II, corrected for acetyl, are appreciably higher than the measured values for the subsequently hydrolyzed fractions I-A and II-A, while the value for II-B-1, corrected for acetyl, is in essential agreement with the measured value, before reacetylation, for fraction II-B. These results suggest appreciable degradation upon deacetylation but none during acetylation. Degradation during deacetylation may reflect alkali sensitivity similar to that observed for Link's compound (polymethyl ester of methyl polygalacturonic acid) by Volmert,[12] who concluded that depolymerization of Link's compound in alkali ceases only upon complete deesterification. Andrews et al.[10] reported the presence of 5% galacturonic acid in a purified araban preparation from sugar beet chips. Although the location of galacturonic acid in the araban molecule is unknown, the acid groups must surely be esterified in araban acetate. These esterified galacturonic acid groups could produce enough depolymerization in the alkaline medium before complete deesterification to explain the observed results.

Andrews et al.[10] reported a molecular weight of 12,500 for their araban. Since this was a value calculated from a molecular weight determination on the acetate, differences in degradation during deacetylation cannot account for the low molecular weight observed by them. However, their value, determined by an isopiestic method, is a number-average molecular weight. If we apply the previously determined[1] mean $\bar{M}_w/\bar{M}_n$ of 1.6, our present

TABLE I
Light-Scattering Molecular Weights of Araban and Araban Acetate Fractions

Fractions	Solvent	λ, mμ	dn/dc[a]	MW[b]
Araban acetates				
I	MEK	546	0.0886	89,200
II	MEK	546	0.0886	113,000
II-B-1	MEK	546	—	75,500
Arabans				
I-A	2*M* NaCl	436	—	34,500
I-A	1% (v/v) DMF	436	—	19,900
II-A	2*M* NaCl	436	—	38,800
II-A	1% (v/v) DMF	436	—	16,200
II-B	0.01*M* Veronal buffer, 0.09*M* NaCl, pH 7.6	436	—	42,100

[a] Values entered in this column are the measured values for the particular fraction. Where no entries are made, previously determined[1] values are assumed, e.g., 0.130 and 0.142 for 2*M* NaCl and 1% (v/v) DMF solvents, respectively, at λ = 436 mμ.

[b] Fluorescence correction factors[1] have been applied.

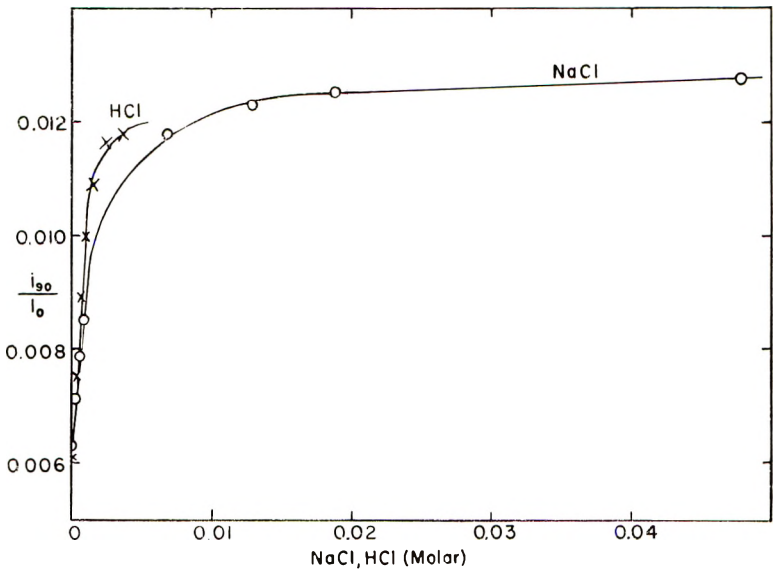

Fig. 1. Effect of added NaCl and HCl on the scattering from a water solution of araban fraction II-A (0.004 g./ml.) initial pH = 4.23; final pH for HCl system = 2.63.

result indicates a $\bar{M}_n$ of about 25,000, which is still twice the value reported by Andrews et al. The explanation for this discrepancy must be in the fact that the araban used in this study represents a much greater fraction of the total araban originally present in sugar beet pulp. Goodban and Owens[2,4] obtained a yield of 16.5% or over 80% of the arabinose content of the sugar beet pulp in their extraction procedure, while Andrews et al. obtained a yield of 5–6%. The more difficultly removed araban is probably enough higher in molecular weight to account for a factor of two in the observed number-average molecular weights.

The measured apparent molecular weights for araban fractions I-A and II-A both show the discrepancy reported previously in the two solvent systems, 2*M* NaCl and 1% (v/v) DMF. To account for a decrease in molecular weight from 34,500 to 19,900 for fraction I-A by preferential binding of water by araban, about 22% of the water molecules must be unavailable to DMF at 1% araban concentration.[13] This means that the effective DMF concentration in the sample system is increased by 28%. Equilibrium dialysis of a small volume of sample solution against a large volume of 1% (v/v) DMF should result in movement of DMF out of the dialysis bag into the solvent system. A change in n of 3.4×10^{-4} was expected from the measured dn/dc of 0.126 ml./g. for DMF. However, equilibrium dialysis experiments with I-A showed no change in n of the inside solution, even after 66 hr.

These experiments effectively eliminated the multicomponent effect in 1% (v/v) DMF solvent as the explanation for the discrepancy, and con-

sequently aggregation in 2*M* NaCl became suspect. The effect of ionic strength and pH on turbidity was followed by adding small increments of 0.1*M* NaCl or 0.1*N* HCl to a dialyzed water solution of araban fraction II-A. The results are shown in Figure 1.

The rapid increase in turbidity with the addition of NaCl can be explained either by aggregation in salt or decrease in interaction of a highly charged system when the ionic strength is increased. Only the latter explanation is consistent with the much greater rate of increase in turbidity with ionic strength when the pH is lowered concurrently. If the charge is due to the carboxyl ions of the galacturonic acid,[10] then the addition of HCl will decrease the charge and increase the ionic strength; both effects should increase turbidity. The NaCl curve of Figure 1 was carried out to sufficiently

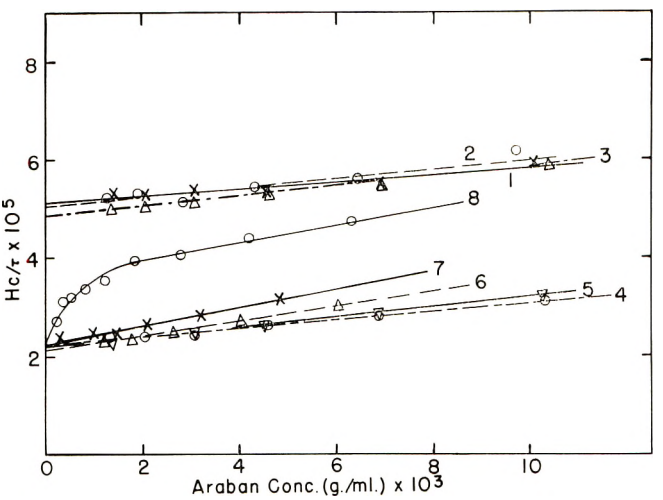

Fig. 2. Debye plots for araban fraction II-A: (*1*) in water; (*2*) in 0.5% (v/v) DMF; (*3*) in 1% (v/v) DMF; (*4*) in 2.0*M* NaCl; (*5*) in 0.1*M* NaCl; (*6*) in 0.01*M* NaCl; (*7*) in 0.004*M* NaCl; (*8*) in 0.0004*M* NaCl.

high ionic strength to show a definite leveling off at about twice the turbidity in water, which is about the ratio of molecular weights observed in 2*M* NaCl and 1% (v/v) DMF.

Titration of a dialyzed sample of fraction II-A, initial pH 4.57, with standard base, gave an equivalent weight of 4130 or about 10 acid groups per mole of araban of molecular weight 40,000. However, titration of the sample with standard acid indicated that at pH 4.57, an appreciable fraction of the carboxyl groups was present in the salt form. Although an accurate measure of total carboxyl could not be obtained, the best estimate was that at pH 4.57 the carboxyls were approximately half neutralized. This would be true for carboxylic acid with an equilibrium constant comparable to that for acetic acid. Sodium analysis on a dialyzed sample of fraction II-B, pH 4.72, gave 69.3 ppm sodium, or 12 moles carboxyls per mole araban of molecular weight 40,000. Since sodium is the only counterion present in

the system, this result is in agreement with the conclusion that the acid groups are half neutralized at pH 4.57.

Figure 2 shows results of a series of light-scattering experiments with araban fraction II-A in water, 0.5, and 1.0% (v/v) DMF, and various NaCl concentrations. Curves *1*, *2*, and *3* support the results of the equilibrium dialysis studies, i.e., there is no effect of DMF. The increased slopes of curves *6* and *7* over those of *4* and *5* indicate appreciable interaction between araban molecules at the lower ionic strengths. Curve *8* is most interesting, in that its general shape resembles that for charged molecules at very low ionic strength.[13-17] Extrapolation of the straight line portion of curve *8* leads to an apparent molecular weight of 24,600, while the intercept from the curved portion is essentially the same as that at higher ionic strengths.

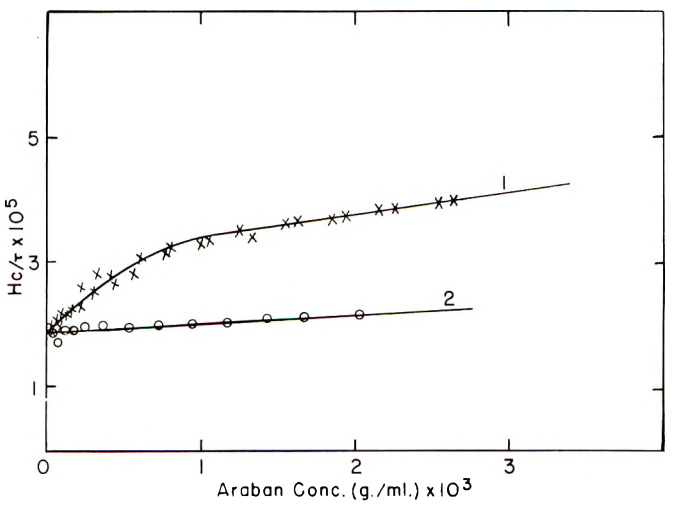

Fig. 3. Debye plots for araban fraction II-B (*1*) in $5 \times 10^{-4}M$ Veronal buffer, pH 7.6; (*2*) in $0.1M$ NaCl, $5 \times 10^{-4}M$ Veronal buffer, pH 7.6.

To verify the downward curvature at low concentrations, light-scattering measurements were carried out on fraction II-B, by means of the Dintzis procedure. Results in $5 \times 10^{-4}M$, pH 7.6, Veronal buffer (curve *1*) and in $0.1M$ NaCl, $5 \times 10^{-4}M$ Veronal, pH 7.6 (curve *2*) are shown in Figure 3. These results show that at the low ionic strength, downward curvature occurs at low concentrations, while no curvature is observed at an ionic strength of 0.1. Extrapolation of the straight line portion of curve *1* gives an apparent molecular weight of 27,000, while the curved portion extrapolates to the same intercept as curve *2*, or a molecular weight of 43,900.

The steep initial slope of the Debye plot of light-scattering data for highly charged macromolecules in low ionic strength solvent has been interpreted as an ordering effect due to strong electrostatic repulsion.[15] The subsequent leveling off of the Debye plot at higher macromolecule concentration is attributed to the growth of screening. In their treatment of the

light scattering of bovine serum albumin at pH 3.30 in low ionic strength solvent, Doty and Steiner[14] assigned an empirical relationship between macromolecule concentration and the distance of closest approach of the scattering centers to obtain a semiquantitative description of their experimental data.

Stigter and Hill[18,19] have developed statistical thermodynamic relationships for the Donnan membrane system which for low concentrations of charged colloid spheres connects the turbidity with macromolecular parameters, i.e., size and surface potential of the spheres and effective ionic strength of the solution.

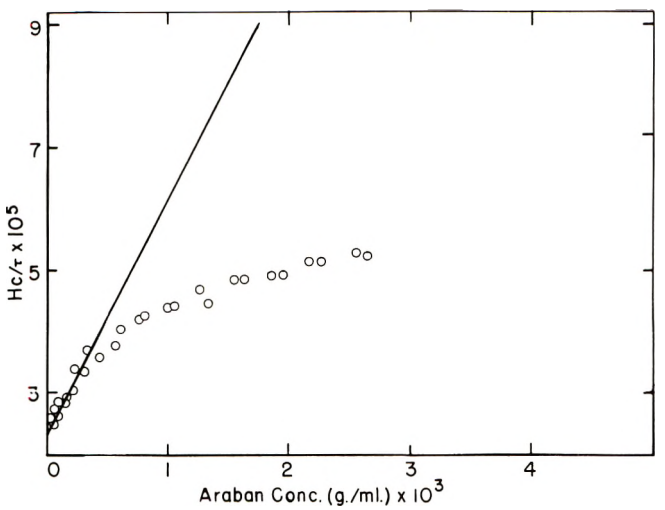

Fig. 4. Debye plots: (——) calculated by the method of Stigter and Hill for a spherical molecule of molecular weight 44,000, radius 45 A. and effective charge 10 in $5 \times 10^{-4}M$, pH 7.6, Veronal buffer; (O) experimental points of curve *1*, Fig. 3, corrected for fluorescence.

The theory[19] shows that for high ionic strength the electric repulsion becomes relatively unimportant. Under these conditions the initial slope of the Debye plot is related to the effective volume of the uncharged macromolecule. Thus, if it is assumed that araban has a spherical shape with molecular weight 44,000, the turbidity data on araban in $2M$ NaCl indicates a radius of 45 A. For low ionic strength, the initial slope is very sensitive to the electric charge.[18,20] For spheres with 45 A. radius, the araban data in $5 \times 10^{-4}M$ Veronal buffer, pH 7.6, gives an effective charge $Z = 10$ per molecule. On the other hand, titration and sodium analysis indicated a total charge of about 20. The difference is not unreasonable, and may in large part be due to the inadequacy of the solid sphere-diffuse double layer model assumed in interpreting the turbidity data.

The above information on radius and effective charge enables one, using the theory,[18,20] to estimate the limiting curvature of the Debye plot, which turns out to be very small and does not contribute significantly in the calcu-

lation of the Debye plot over the araban concentration range studied. The result is shown as the solid line in Figure 4, the circles being the experimental points of curve *1*, Figure 3, corrected for fluorescence. The discrepancy suggests an increase in ionic strength and/or a decrease in effective charge as araban concentration increases. Chloride, the most likely ionic impurity, could not be detected in the stock araban solution. A change in effective charge from 10 to 7.5 at 1.0×10^{-3} g./ml. araban will lower the calculated reciprocal intensity value to 4.54×10^{-5}, in agreement with the experimental value. Overbeek and Stigter[21] and Wall and Berkowitz[22] both reported that the effective charge of polyelectrolyte spheres decreases with increasing values of ka, where k is the reciprocal thickness of the ionic double layer and a is the radius. In the present case, ka increases from 0.33 at 1×10^{-5} g./ml. to 0.36 at 1×10^{-3} g./ml. araban. Although for these low values of ka the effective charge can be expected to decrease rapidly as ka increases, the change in ka noted above is not sufficient to decrease the effective charge from 10 to 7.5.

The discrepancy perhaps indicates the inapplicability of the virial expansion method used by Stigter and Hill. For high colloid concentrations and low ionic strength, the expansion converges slowly. Evaluation of additional terms is difficult. The less rigorous Donnan method gives closed expressions[23,24] which can also be applied when the colloid/salt ratio is not low. It was found that for $Z = 10$, the Donnan approach gives essentially the solid curve of Figure 4. Corrections for Debye-Hückel interactions[24] are small. This agreement is not surprising, since for low concentrations the Donnan and virial expansion methods approach the same limit.[19] At higher colloid concentrations, the Donnan method predicts that a plateau[23] is reached, as suggested in Figures 2–4 for our results on araban and as observed by others for different systems.[14,15] However, the quantitative aspects of the Donnan method, which pictures both colloid and small ions as point charges, are reliable only in very dilute solutions.

Although our experimental results for araban in low ionic strength solvent can not be accounted for by the Stigter-Hill theory, the similarity of the general shape of the Debye plot to others reported in the literature justifies the conclusion that the previously obtained molecular weight in 1% (v/v) DMF solvent was low because measurements were not carried out at sufficiently low araban concentrations to show the downward curvature observed in the present study.

We wish to thank A. E. Goodban for the preparation of fraction I, W. H. Ward for the titrations, H. C. Lukens for the sodium analysis, W. B. Maher and E. F. Potter for the chloride analysis, and D. Stigter for stimulating discussions and helpful suggestions in connection with the theoretical treatment.

Reference to a company or product name does not imply approval or recommendation of the product by the Department of Agriculture to the exclusion of others that may be suitable.

References

1. Tomimatsu, Y., K. J. Palmer, A. E. Goodban, and W. H. Ward, *J. Polymer Sci.*, **36,** 129 (1959).
2. Goodban, A. E., and H. S. Owens, *J. Am. Soc. Sugar Beet Technologists,* **9,** 129 (1956).
3. Carson, J. F., and W. D. Maclay, *J. Am. Chem. Soc.*, **68,** 1015 (1946).
4. Goodban, A. E., and H. S. Owens, *J. Polymer Sci.*, **23,** 825 (1957).
5. Brice, B. A., M. Halwer, and R. Speiser, *J. Opt. Soc. Am.*,**40,** 768 (1950).
6. Tomimatsu, Y., and K. J. Palmer, *J. Polymer Sci.*, **35,** 549 (1959).
7. Tomimatsu, Y., and K. J. Palmer, *J. Polymer Sci.*, **54,** S21 (1961).
8. Brice, B. A., and M. Halwer, *J. Opt. Soc. Am.*, **41,** 1033 (1951).
9. Timasheff, S. N., H. M. Dintzis, J. G. Kirkwood, and B. D. Coleman, *J. Am. Chem. Soc.*, **79,** 782 (1957).
10. Andrews, P., L. Hough, D. B. Powell, and B. M. Woods, *J. Chem. Soc.*, **1959,** 774.
11. Goodban, A. E., private communication.
12. Vollmert, B., *Makromol. Chem.*, **5,** 110 (1950).
13. Timasheff, S. N., and M. J. Kronman, *Arch. Biophys. Biochem.*, **83,** 60 (1959).
14. Doty, P., and R. F. Steiner, *J. Chem. Phys.*, **20,** 85 (1952).
15. Kronman, M. J., and S. N. Timasheff, *J. Phys. Chem.*, **63,** 629 (1959).
16. Witnauer, L. P., F. R. Senti, and M. D. Stern, *J. Polymer Sci.*, **16,** 1 (1955).
17. Harrap, B. S., and E. F. Woods, *J. Polymer Sci.*, **49,** 353 (1961).
18. Stigter, D., and T. L. Hill, *J. Phys. Chem.*, **63,** 551 (1959).
19. Stigter, D., *J. Phys. Chem.*, **64,** 838 (1960).
20. Stigter, D. *J. Phys. Chem.*, **64,** 842 (1960).
21. Overbeek, J. Th. G., and D. Stigter, *Rec. trav. chim.*, **75,** 543 (1956).
22. Wall, F. T., and J. Berkowitz, *J. Chem. Phys.*, **26,** 114 (1957).
23. Mysels, K. J., *J. Phys. Chem.*, **58,** 303 (1954).
24. Hill, T. L., *Discussions Faraday Soc.*, **21,** 31 (1956).

Synopsis

The discrepancy in the light-scattering molecular weight of sugar beet araban in two solvent systems, 2*M* NaCl and 1% (v/v) DMF, is explained as being due to a charge effect in the latter solvent. The previously reported explanation of a multicomponent effect in 1% (v/v) DMF, based on the assumption that araban is uncharged, is shown to be incorrect by equilibrium dialysis experiments. Titration and sodium analysis indicate a total charge of about 20 per araban molecule, while the limiting slope of the Debye plot of light-scattering data in low ionic strength solvent indicate an effective charge of 10. Attempts to explain the observed curvature in the Debye plot for araban in low ionic strength buffer on the basis of the Stigter-Hill method was unsatisfactory, probably due to the inadequacy of the solid sphere-diffuse double layer model for araban and/or the inapplicability of the Stigter-Hill virial expansion method at high ratios of macromolecule to salt in low ionic strength solvent. Molecular weight measurements on araban acetate prepared for purification purposes indicate considerable degradation during deacetylation but not during acetylation. This suggests that araban *in situ* has a molecular weight considerably greater than that observed for the purified araban.

Résumé

La différence dans les poids moléculaires obtenus par diffusion lumineuse de l'arabane de la betterave sucrière dans deux solvants, 2*M* NaCl et 1% (v/v) DMF, s'explique comme un effet de charge dans le dernier solvent. On a démontré par des expériences de dialyse à l'équilibre que l'explication qu'on a donné antérieurement d'un effet de plusieurs composants dans le DMF à 1% (v/v) et qui se basait sur le fait que l'arabane

n'est pas chargée est fausse. Une titration et la détermination du sodium montrent qu'il y a une charge totale égale environ à 20 par molécule d'arabane tandis que l'inclinaison limite dans le diagramme de Debye de diffusion lumineuse dans le solvant de faible force ionique donne une charge égale à 10. On a essayé sans succès d'interprèter l'inclinaison dans le diagramme de Debye pour l'arabane dans un mélange tampon à faible force ionique selon la méthode de Stigter-Hill. Ceci est probablement dû au fait que le modèle de sphère solide et de la double couche diffuse pour l'arabane et/ou le fait qu'on ne peut pas employer la méthode viriale de l'expansion selon Stigter-Hill pour des rapports élevés macromolécules/sel dans un solvant à faible force ionique. Des mesures de poids moléculaires des acétates d'arabane préparés à des fins de purification indiquent qu'il y a une dégradation considérable pendant la désacétylation et non en cours de l'acétylation. Ceci suggère que l'arabane a un poids moléculaire *in situ* beaucoup plus grand que ce qu'on observe dans l'arabane purifié.

Zusammenfassung

Die Diskrepanz zwischen dem Lichtstreuungs-Molekulargewicht von Zuckerrüben-Araban in den beiden Lösungsmittelsystemen, 2*M* NaCl und 1% (v/v) DMF, wird auf einen Ladungseffekt im letzteren Lösungsmittel zurückgeführt. Die früher gegebene Erklärung als ein Vielkomponenteneffekt in 1% (V/V) DMF, die auf der Annahme beruhte, dass Araban keine Ladungen trägt, erweist sich auf Grund von Gleichgewichtsdialyseversuchen als unhaltbar. Titration und Natriumanalyse ergibt eine Gesamtladung von etwa 20 pro Arabanmolekül, während die Grenzneigung im Debyediagramm der Lichstreuungsdaten in einem Lösungsmittel niedriger Ionenstärke eine effektive Ladung von 10 liefert. Ein Versuch, die beobachtete Krümmung im Debyediagramm für Araban in einem Puffer niedriger Ionenstärke auf Grundlage der Methode von Stigter-Hill zu erklären, war unbefriedigend, was wahrscheinlich auf das Nichtzutreffen des Modells: feste Kugel–diffuse Doppelschicht, für Araban und auf die Nichtverwendbarkeit der Virial-Expansionsmethode von Stigter-Hill bei hohem Verhältnis Makromolekül zu Salz im Lösungsmittel niedriger Ionenstärke zurückzuführen ist. Molekulargewichtsbestimmungen an Arabanacetat, das für Reinigungszwecke hergestellt wurde, sprechen für einen beträchtlichen Abbau während der Entacetylierung, aber nicht während der Acetylierung. Das Molekulargewicht des Arabans *in situ* ist daher bedeutend grösser als das am gereinigten Araban gemessene.

Received January 15, 1962

JOURNAL OF POLYMER SCIENCE: PART A VOL. 1, PP. 1015–1023 (1963)

Crosslinking of Natural Rubber by Dicumyl Peroxide in the Presence of Oxidation Inhibitors

J. SCANLAN and D. K. THOMAS,* *Rubber and Plastics Research Association of Great Britain, Shawbury, Shrewsbury, Shropshire, England*

It has been shown[1,2] that the crosslinking of natural rubber by dicumyl peroxide results from the combination of two rubber radicals produced by the abstraction of hydrogen from the rubber by cumyloxy or methyl radicals. The crosslinking efficiency is high (>90%) and none of the cumyloxy or methyl radicals are thought to enter the crosslinked network.[2] Braden and Fletcher[1] have studied the effect of conventional antioxidants upon the crosslinking reaction in natural rubber and have found that certain phenolic compounds, notably hydroquinone and pyrogallol, have an adverse effect upon the tensile strength and modulus of the product, while others, such as resorcinol or phenol, produced little change. Amine antioxidants also interfered with the crosslinking reaction. It is generally agreed that phenolic compounds inhibit oxidation of hydrocarbons by exchanging a hydrogen atom with the peroxy radical involved in the propogation step; the same level of agreement does not exist in the case of amines. Bickel and Kooyman,[3] Kuzminskiĭ,[4] and Shelton, McDonel, and Crano[5] are of the opinion that hydrogen abstraction from the amine group is involved, while Boozer and Hammond,[6] Walling and Hodgdon,[7] and Pedersen[8] have found evidence to the contrary. An alternative mechanism proposed by Boozer and Hammond involves the formation of a pi-complex between amine and free radical which reacts with another radical to yield stable products.

The present work reports a quantitative measure of the effect of a series of additives upon the crosslinking density in dicumyl peroxide–natural rubber cures and compares the reactivities with those in other reactions where these additives are found to inhibit free radical reactions. In the case of those compounds commonly used as antioxidants the results should assist in making the best choice for use in dicumyl peroxide cures.

EXPERIMENTAL

Preparation and Vulcanization of Stocks

A stock supply of natural rubber was extracted with acetone for 16 hours, dried *in vacuo*, and then loaded with 1.5 wt.-% of recrystallized dicumyl

* Present address: Royal Aircraft Establishment, Farnborough, Hampshire, England.

peroxide on a mill in the normal fashion; all experiments were carried out on samples of this material. Molecular weights were obtained by measurement of the limiting viscosity number in benzene at 25°C. and use of the relationship $[\eta] = 2.29 \times 10^{-7}\bar{M}_n^{1.33}$ found for masticated rubber by Mullins and Watson.[9] The additives were mixed into 15 g. portions of rubber and the molecular weight redetermined before use. Vulcanization was carried out at 140°C. and 1500 psi for 1 hr., in all cases a control specimen containing only dicumyl peroxide being included. Each experiment was performed in duplicate.

Equilibrium Volume Swelling

The volume of rubber in the swollen material at equilibrium was determined by immersing a strip of known weight in *n*-decane at 25 ± 0.02°C. for 48 hr. The strip was then removed from the decane, surface dried, and weighed in a stoppered bottle. Finally the strip was dried to constant weight *in vacuo*. From this final weight, the weight of decane in the swollen strip, and the densities of rubber (0.91) and decane (0.725) at 25°C., v_r, the volume fraction of rubber in the swollen vulcanizate is calculated.

Evaluation of Crosslink Density

The crosslink densities in the vulcanizates are obtained by using the correlation between crosslinking and equilibrium swelling established by Mullins[10] and Moore and Watson.[11] The elastic constant C_1, is related to v_r by the equation

$$-\ln (1 - v_r) - v_r - \mu v_r^2 = 2\ V_0 C_1 R^{-1} T^{-1}\ [v_r^{1/3} - (v_r/2)]$$

where V_0 is the molar volume of the swelling liquid and μ, the interaction constant for rubber–decane, has a value of 0.425. Corrections for chain entanglements and network flaws are given by

$$C_1 = (C_1^* + 0.78 \times 10^6)\ (1 - 2.3M_c/M)$$

where C_1^* is the corrected value of C_1, M_c is the molecular weight between crosslinks, and M is the initial molecular weight of the polymer. Finally C_1^* and M_c are related by

$$C_1^* = \rho RT/M_c$$

ρ being the density of the polymer.

RESULTS

The experimental results were analyzed by a simplified reaction scheme in which the free radicals produced from dicumyl peroxide are assumed to be identical in so far as their relative reactivities towards the rubber and additive are concerned:

$$\text{Peroxide} \xrightarrow{k} \text{R}\cdot \xrightarrow[k_2]{k_1} \begin{matrix}\nearrow \text{crosslinks} \\ \searrow \text{reaction with additive}\end{matrix}$$

R· representing either a cumyloxy, methyl, or rubber radical, and k, k_1, and k_2 the rate constants for peroxide decomposition, hydrogen abstraction from the rubber, and reaction of the radical with the additive, respectively, both the latter reactions being assumed first order in the reactants. Then the rate of formation of crosslinks is given by

$$dx/dt = {}^1/_2 k_1 \text{ [rubber][R}\cdot\text{]} = k_1' \text{ [R}\cdot\text{]}$$

and rate of removal of additive is given

$$-d[A]/dt = k_2 \text{ [A][R}\cdot\text{]}$$

Denoting by $[A_0]$ the initial concentration of A, we have

$$\ln[A_0]/[A] = k_2 x/k_1'.$$

If one molecule of additive can react with only one free radical and X_0 represents the final number of crosslinks formed per unit volume in the absence of additive

$${}^1/_2([A_0] - [A_f]) = X_0 - X_f$$

TABLE I
Rate Constant Ratios and Fractional Decrease in Crosslinking of Natural Rubber

Additive	Fractional decrease in crosslinking	$0.434(k_2/k'_1)$	$k_2/k_{2\text{phenol}}$
Phenol	0.11	12.3	1.0
Hydroquinone	0.24	31.6	2.6
Resorcinol	0.11	12.5	1.01
Pyrogallol	0.29	48.2	3.9
o-Cresol	0.19	23.4	1.9
2,6-Xylenol	0.28	46.5	3.8
α-Naphthol	0.49	162	13.2
β-Naphthol	0.15	26.8	2.2
2-Thionaphthol	0.42	132	10.7
N-Methylaniline	0.24	33.4	2.7
Dimethylaniline	0	—	—
α-Naphthylamine	0.25	47.3	3.8
Phenyl-β-naphthylamine	0.14	31.1	2.5
Diphenylamine	0.08	13.6	1.1
Dinaphthyl-*p*-phenylene diamine	0.12	48.1	3.9
Triethanolamine	0	—	—
Urea	0.02	1.0	0.08
Thiourea	0.03	2.0	0.16
Thioacetamide	0.28	27.7	2.3
Thioacetanilide	0.32	76.5	6.2
Thiobenzanilide	0.30	104	8.4

where f denotes a final value, and

$$-\ln [A_f]/[A_0] = -\ln \left\{1 - \frac{[A_0] - [A_f]}{[A_0]}\right\}$$

$$= -\ln \left\{1 - \frac{2(X_0 - X_f)}{[A_0]}\right\} = \frac{k_2}{k_1'} X_f$$

i.e.,

$$k_2/k_1' = -(1/X_f) \ln \left\{1 - 2(X_0/[A_0])\ [(X_0 - X_f)/X_0]\right\}$$

For any two additives A and B, the values of $(k_2/k_1')_A$ and $(k_2/k_1')_B$ and hence k_{2A}/k_{2B} can be obtained.

The experimental results are given in Table I as the fractional decrease in crosslinking $(X_0 - X_f)/X_0$ for 1 g. of additive per 100 g. of rubber and as the derived rate-constant ratios. Calculation shows that even with the most reactive of the additives used only a fraction is consumed during the reaction.

DISCUSSION

Among the additives tested the only ones which had no effect upon the crosslinking of natural rubber by dicumyl peroxide were dimethylaniline and triethanolamine; all the other materials produced a decrease, although it is doubtful whether the small effect shown by urea and thiourea could be regarded as detectably different from zero. It is significant that dimethylaniline and triethanolamine are the only additives used which did not possess an amine or phenolic hydrogen atom, and the immediate conclusion is that these compounds owe their inhibitory powers to the fact that in their phenolic or amine hydrogens they have atoms which can be

TABLE II
Efficiencies of Phenolic Compounds as Inhibitors of Oxidation and Polymerization Reactions Relative to that of Hydroquinone

Inhibitor	Oxidation of ethyl linoleate (45°C.)[a]	Autoxidation of animal fats (75°C.)[b]	Vinyl acetate polymerization (75°C.)[c]	Oxidation of gasoline (100°C.)[d]	Present work (140°C.)
Phenol	—	—	0.016	0.44	0.38
Resorcinol	0.016	—	0.029	1.00	0.40
Hydroquinone	1.00	1.00	1.00	1.00	1.00
Pyrogallol	3.00	1.57	3.20	10.6	1.52
α-Naphthol	0.56	0.57	—	14.2	5.12
β-Naphthol	0.077	—	—	1.88	0.84

[a] Data of Bolland and ten Have.[15]
[b] Data of Olcott.[16]
[c] Data of Jeu and Alyea.[17]
[d] Data of Lowry et al.[18]

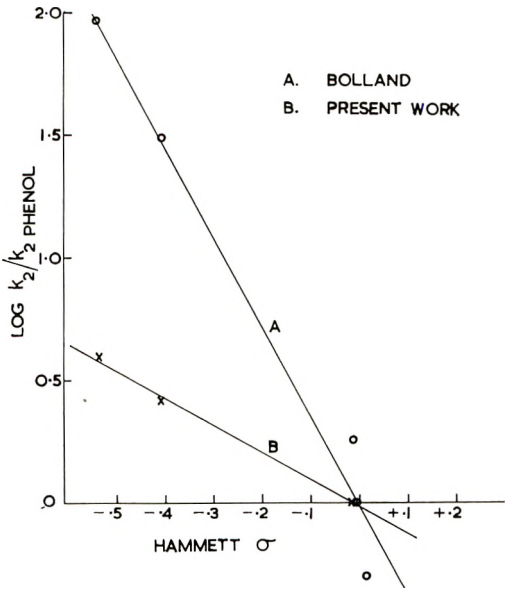

Fig. 1. Relationship of inhibitor efficiencies to Hammett function: (*A*) data of Bolland plotted according to Boozer and Hammond;[6] (*B*) present work.

more or less readily exchanged with the free radicals (cumyloxy, methyl, or polymer radicals) involved in the crosslinking reaction.

Phenolic compounds have found wide use as antioxidants, and many data are available relating to their effectiveness as inhibitors of oxidation. Only a small part of this work is of a quantitative nature, and the results obtained from the more comprehensive studies are shown in Table II; the data given for oxidation of animal fats and gasoline were obtained from a study of induction periods and may not be readily comparable to the remaining data from rate studies.

Boozer and Hammond[6] found that the log efficiencies for inhibition of oxidation of unsaturated hydrocarbons by a series of substituted phenols gave a good linear relationship with the Hammett σ values. The present results for the efficiencies of similar compounds as retarders of crosslinking show a similar relationship (see Fig. 1), although the number of compounds is rather small. The slope in this case is, however, considerably smaller than in the earlier work (-1.1 against -3.7). Thus the reaction rate is considerably less sensitive to the lability of the phenolic hydrogen atom in the present type of hydrogen abstraction than that by $RO_2\cdot$ radicals in inhibited oxidation. This appears to indicate that the radical involved is more reactive than the $RO_2\cdot$ radical. The linearity of the Hammett plot gives some indication that only one of the types of radical involved in the crosslinking is really important in reaction with the additives. It has also been found that hydroquinone reduces greatly the degradation of polyisobutene by dicumyl peroxide in which, as has been shown, only

TABLE III
Efficiencies of Amines as Oxidation Inhibitors Relative to Phenol

Inhibitor	Oxidation of cumene in chlorobenzene[a]	Oxidation of gasoline[b]	Present work (140°C.)
N-Methylaniline	—	—	2.7
Dimethylaniline			0
α-Naphthylamine	—	2	3.8
Phenyl-β-naphthylamine	—	—	2.5
Diphenylamine	2.1	2	1.1
Dinaphthyl-*p*-phenylenediamine	—	—	3.9
Triethenolamine	—	—	0
N,*N*′-Diphenyl-*p*-phenylenediamine	16	—	14.0

[a] Data of Hammond et al.[6]
[b] Data of Jeu and Alyea.[18]

cumyloxy radicals are active.[12] Since analysis of the products of dicumyl peroxide vulcanization of natural rubber also shows that the cumyloxy radical is the most active in hydrogen abstraction,[13] it is likely that reaction with this type of radical rather than with the more stable allylic type produced from the rubber accounts for the major part of the reduction in crosslinking. Such a conclusion justifies to a considerable extent the use of the simplified kinetic scheme for interpretation of the experimental results.

The data in the literature for the reactivity of amines as inhibitors are far fewer than those for the phenols. The meagre data available are shown in Table III.

The indications of the present work are that the presence of an amine hydrogen is essential for reaction with the free radicals involved in the vulcanization, and this provides oblique support for the hydrogen exchange mechanism of amine antioxidant action. In addition to direct measurements of inhibitory efficiency, the reaction between diphenylpicrylhydrazyl and aromatic amines has been investigated by Kuzminskiĭ,[14] who found that hydrogen transfer occurred between the free radical and the amine with no reaction with the *N*-disubstituted methylphenyl-β-naphthylamine. The ratio of reactivities between phenyl-β-naphthylamine and diphenylamine found was 4.5, comparable with the factor 2.4 in the present work.

In general the inhibitory power of the amines increases with the complexity of the aromatic groups attached to it, in accordance with the expected enhanced stability of the radicals formed by hydrogen abstraction. The activity of α-naphthylamine is, however, unexpectedly high compared with the disubstituted amines, suggesting steric hindrance in the latter compounds.

The reactivities of the other additives are generally in line with expectations on the basis of hydrogen abstraction, although the large difference in

reactivity between thiourea and thioacetamide is not expected at first sight and suggests that an appreciable proportion of the latter may exist in the tautomeric thiolimine form.

Choice of Antioxidant for Dicumyl Peroxide–Natural Rubber Vulcanizates

It is desired, of course, to choose an antioxidant which, while displaying good antioxidant properties, interferes as little as possible with the crosslinking reaction. The choice is made difficult by the paucity of reliable quantitative data on the relative efficiencies of antioxidants. Data for those compounds for which a comparison of inhibitory power in the autoxidation of hydrocarbons and in crosslinking by dicumyl peroxide is possible are given in Table IV; the relative reactivities refer to equimolar concentrations of the inhibitors, but the fractional decrease in crosslink density following the addition of 1 wt.-% of each is also given. In general, increased antixoidant activity goes hand in hand with an increased interference in crosslinking, but the measurements reported show a distinct advantage of the phenols in antioxidant efficiency for a given level of reduction in crosslinking. It should be pointed out, however, that this advantage is apparent in rate measurements and that the low concentrations of these powerful antioxidants, necessary to avoid excessive wastage of vulcanizing agent, may effect adversely the duration of the protective action. In addition, Shelton and Cox[19] have found that although phenolic antioxidants were more powerful than amines in gum stocks in line with the data on their effect in autoxidations, the difference was nullified or even reversed by carbon black; whether or not carbon black has a similar effect on the hindrance to crosslinking is not known.

TABLE IV
Efficiencies of Antioxidants as Retarders of Oxidation and Crosslinking

Antioxidant	Efficiency in		Reduction in crosslinking by 1%
	Autoxidation of hydrocarbons	Crosslinking by dicumyl peroxide	
Phenol	1	1	0.11
Resorcinol	0.50	1.0	0.11
Hydroquinone	31	2.6	0.24
Pyrogallol	94	3.9	0.29
o-Cresol	3.3	1.9	0.19
2,6-Xylenol	14.8	3.8	0.28
α-Naphthol	17.5	13.2	0.49
β-Naphthol	—	2.2	0.15
N-Methylaniline	1.2	2.7	0.24
Diphenylamine	2.1	1.1	0.08
N,N'-Diphenyl-*p*-phenylenediamine	16	14	0.44

The authors gratefully acknowledge a grant in support of this work from Hercules Powder Company (U.K.) Ltd. and the experimental assistance of Mr. A. T. Nevols.

References

1. Braden, M., and W. P. Fletcher, *Trans. Inst. Rubber Ind.*, **31**, 155 (1955).
2. Amberg, L. O., and W. D. Willis, *Proc. Intern. Rubber Conf., Washington, D.C., Nov. 1959*, 565 (1959).
3. Bickel, A. F., and E. C. Kooyman, *J. Chem. Soc.*, **1953**, 3211; *ibid.*, **1956**, 2215; *ibid.*, **1957**, 2217, 2415.
4. Kuzminskiĭ, A. S., and L. G. Angert, *Doklady Akad. Nauk. S.S.S.R.*, **82**, 747, (1952); *ibid.*, **96**, 1187 (1954).
5. Shelton, J. R., E. T. McDonel, and J. C. Crano, *J. Polymer Sci.*, **42**, 289 (1960).
6. Hammond, G. S., C. E. Boozer, C. E. Hamilton, and J. N. Sen, *J. Am. Chem. Soc.*, **77**, 3238 (1955).
7. Walling, C., and R. B. Hodgdon, *J. Am. Chem. Soc.*, **80**, 228 (1958).
8. Pedersen, C. J., *Ind. Eng. Chem.*, **48**, 1881 (1956).
9. Mullins, L., and W. F. Watson, *J. Appl. Polymer Sci.*, **1**, 245 (1959).
10. Mullins, L., *J. Polymer Sci.*, **19**, 225 (1956).
11. Moore, C. G., and W. F. Watson, *J. Polymer Sci.*, **19**, 237 (1956).
12. Thomas, D. K., *Trans. Faraday Soc.*, **57**, 511 (1961).
13. Thomas, D. K. unpublished results.
14. Angert, L. G., and A. S. Kuzminskiĭ, *J. Polymer Sci.*, **32**, 1 (1958).
15. Bolland, J. L., and P. ten Have, *Discussions Faraday Soc.*, **2**, 252 (1947).
16. Olcott, H. S., *J. Am. Chem. Soc.*, **56**, 2492 (1934).
17. Jeu, Kia-Khwe, and H. N. Alyea, *J. Am. Chem. Soc.*, **55**, 575 (1933).
18. Lowry, C. D., G. Egloff, J. C. Morrell, and C. G. Dryer, *Ind. Eng. Chem.*, **25**, 804 (1933).
19. Shelton, J. R., and W. L. Cox, *Ind. Eng. Chem.*, **46**, 816 (1954).

Synopsis

A number of phenols, simple and *N*-substituted aromatic amines, thioamides, and thioanilides which are known to inhibit free radical reactions have been introduced into dicumyl peroxide–natural rubber cures, and their influence upon the degree of crosslinking has been determined. A simple kinetic scheme allows a calculation of the relative reactivities of these additives and the values obtained are compared with those of other workers for the same additives but in different systems. It is concluded that the additives interfere with the crosslinking reaction by exchanging a hydrogen atom with the free radicals involved, and the sequence of reactivities is readily explained in terms of current theories for the effect of substituents upon the reactivity of organic compounds. Types of materials likely to be useful as antioxidants in dicumyl cures are discussed.

Résumé

Un certain nombre de phénols, d'amines aromatiques simples et *N*-substituées, de thioamides et de thioanilides qui sont connus pour leur pouvoir d'inhibition dans les réactions par radicaux libres, ont été introduits dans des vulcanisats de caoutchouc naturel au peroxyde de dicumyle, et on a déterminé leur influence sur le degré de pontage. Un schéma cinétique simple permet de calculer les réactivités relatives de ces additifs et les valeurs obtenues sont comparées à celles obtenues par d'autres auteurs pour les mêmes additifs mais dans des systèmes différents. On conclut que les additifs interfèrent avec la réaction de pontage en échangeant un atome d'hydrogène avec le radical libre concerné et on explique facilement le gamme des réactivités par les théories courantes do l'effet des substituants sur la réactivité des composés organiques. On discute de types de matériaux qui pourraient être également intéressants, comme antioxydants dans les vulcanisats dicumyles.

Zusammenfassung

Eine Anzahl von Phenolen, einfachen und *N*-substituierten aromatischen Aminen, Thioamiden und Thioaniliden, deren inhibierende Wirkung auf Reaktionen freier Radikale bekannt ist, wurden in Dicumylperoxyd–Naturkautschukmischungen eingebracht und ihr Einffuss auf den Vernetzungsgrad bestimmt. Ein einfaches kinetisches Schema erlaubt eine Berechnung der relativen Reaktivität dieser Additivs und die erhaltenen Werte werden mit den von anderen Autoren für die gleichen Additivs aber in anderen Systemen erhaltenen verglichen. Man kommt zu dem Schluss, dass die Additivs die Vernetzungsreaktion durch Austausch eines Wasserstoffatoms mit den auftretenden freien Radikalen stören; die Reaktivitätsreihe kann auf Grund der bekannten Theorien für den Einfluss von Substituenten auf die Reaktivität orgsnischer Verbindungen leicht erklärt werden. Stofftypen, die wahrscheinlich als Antioxydantien bei der Dicumylperoxydvulkanisation brauchbar sind, werden besprochen.

Received October 9, 1961
Revised November 27, 1961

JOURNAL OF POLYMER SCIENCE: PART A VOL. 1, PP. 1025–1039 (1963)

Grafting of Poly (methyl Methacrylate) to Granular Corn Starch

C. E. BROCKWAY and K. B. MOSER, *Research Center, A. E. Staley Manufacturing Company, Decatur, Illinois*

INTRODUCTION

Various reports in the literature indicate that graft and block copolymers of starch can be prepared by methods applicable to other natural and synthetic high polymers. The earliest reported grafting was that of Jones and co-workers,[1] who claimed graft copolymer by the persulfate-initiated polymerization of acrylonitrile in aqueous solution of starch, though they did not publish evidence of grafting. Grafting is also reported by the solution copolymerization of styrene and allyl starch,[2] by the initiation of mixtures of butadiene and styrene or acrylonitrile with starch solutions previously peroxidized by oxygen or ozone,[3] and by the action of ceric ion on starch solutions containing acrylic monomer.[4,5] Starch macroradicals, generated by cryolysis of starch solutions[6] or by mastication of dry starch in the presence of monomer,[7] have been reported to initiate polymerization of vinyl monomers, presumably to yield block copolymers.

Kargin and co-workers made a more detailed study of the products obtained by initiation of styrene[8] or methyl methacrylate[9] with peroxidized starch. Granular potato starch, in the dry form, in aqueous slurry or as starch solution was ozonized. The starch reacted most efficiently in slurry; peroxide groups, detected by iodometric titration, were introduced at a level of up to one per six anhydroglucose units of starch. Suspensions of peroxy-starch and monomer in water were heated at 60–90°C. for a few hours, sometimes in the presence of ferrous and pyrophosphate salts. Graft copolymer was isolated from the products by a combination of extraction and fractional precipitation with benzene as solvent for the polystyrene system, and ethylene dichloride for poly(methyl methacrylate). Of special interest is the observation[9] that graft copolymer containing as much as 92% of poly(methyl methacrylate) swelled only slightly without dissolving in ethylene dichloride, an effective solvent for the homopolymer of methyl methacrylate. Various physical properties of the grafts were measured, and the grafted side chains were isolated and characterized after acid hydrolysis of the starch chains.

Object of the present work, done mostly prior to the appearance of the Kargin publications,[8,9] was to find a relatively simple procedure for pre-

paring graft copolymers of starch, and to obtain evidence of grafting. By preliminary study of several polymerization techniques, the polymerization of monomer by peroxide–iron initiation in an aqueous slurry of granular starch was found to be simple and effective. Several monomers graft readily; but we worked chiefly with methyl methacrylate.

RESULTS

In a typical procedure a slurry of 100 parts of granular starch (dry basis) in 400 parts of water was deaerated and thereafter maintained under nitrogen. Monomer, activator, and initiator were added. With the onset of polymerization, usually in a matter of a few seconds after the initiator was added, a sharp temperature rise occurred. After stirring was continued for the desired time, the product was filtered, washed with water and dried in air. The product, a white powder, typically dried at room temperature to an equilibrium moisture content of 5–7%. Per cent conversion of monomer was calculated on the dry weight of the product recovered,

TABLE I
Various Starches, Various Monomer Levels[a]

Run	Starch[b]	Parts MMA	Polymerization time, hr.	Polymerization temp., °C.	Conversion, %[c]	PMMA in product, %[c]	Apparent grafting efficiency, %[d]
1	Unmodified	49	1.2	40–59	90	31	62
2	"	49	1.4	30–39	94	32	93
3	"	25	3.7	20–26	74	15	98
4	"	99	3.6	20–37	88	45	92
5	"	99	4.3	3–6	86	44	95
6	Acid-hydrolyzed	51	4.0	20–30	92	30	97
7	Oxidized	52	2.3	19–29	94	32	99
8	"	103	3.2	18–34	94	48	96
9	"	155	3.3	20–45	93	60	80
10	Waxy maize, unmodified	50	1.3	29–37	89	29	93
11	Unmodified	100[e]	2.1	20–33	99	50	91

[a] Recipe: granular starch, 100 parts (dry basis); water, 400 parts; ferrous ammonium sulfate hexahydrate, 0.33 parts; H_2O_2 (50%), 0.60 parts.

[b] For a description of the starches, see Experimental Section.

[c] Calculated from the known wt. of starch charges and the total weight of product obtained, both on dry basis.

[d] Defined as per cent of total polymer not separable by extraction. Values for runs 1 and 2 based on three successive extractions with ethylene dichloride and a final extraction with acetone. All other values based on a single extraction with ethylene dichloride.

[e] Twenty-five parts of monomer added at the start, the remainder added gradually during 1 hr.

TABLE II
Use of Various Initiators[a]

Run	Initiator		Activator		Conversion, %	PMMA in product, %	Apparent grafting efficiency, %[b]
	Type	Parts	Type	Parts			
12	H_2O_2 (50%)	1.20	None	—	0	—	—
13	"	3.00	None	—	0	—	—
14	"	0.60	$Na_2S_2O_4$	0.25	82	30	87
15	"	0.60	"	1.22	0	—	—
16	"	0.20	FAS[d]	0.33	100	33	94
17	Cumene hydroperoxide	0.45	FAS	0.90	99	33	66
18	*tert*-Butyl hydroperoxide	0.45	FAS	0.90	98	33	81
19	Azoisobutyronitrile	1.00	None	—	97	49	12[c]

[a] Recipe: unmodified starch (dry basis), 100 parts; water, 400 parts; MMA, 50 parts; temp., 30–40°C.; time, 4-5 hr.

[b] Based on a single extraction with acetone.

[c] Reduced to 7% by a second extraction.

[d] Ferrous ammonium sulfate hexahydrate.

assuming all starch and polymethyl methacrylate were retained in the solid product. The validity of this assumption was confirmed by examination of filtrate and washings from typical runs. In no instance was there any detectable amount of starch or polymer in the filtrate, with the exception of runs in which oxidized starch was used. In this instance, about 1% of carbohydrate material, based on the weight of starch used, was recovered from the filtrate. This is consistent with the typical observation that hypochlorite-oxidized starches contain a little oxidation product which is extractable by water at room temperature.

As a first approximation, it was assumed that the homopolymer of methyl methacrylate could be separated from starch and graft copolymer by extraction of the powdery solid product with a suitable solvent. Preliminary studies were made in which the product, containing about 5% of moisture, was tumbled at 50°C. for 24 hr. or more with three successive portions of ethylene dichloride and a final portion of acetone. This work demonstrated that all but a few per cent of the extractable polymer was removed on the first extraction. Hence, in most of the work only a single extraction was used; 20 parts (dry solids basis) of product was extracted with 100 parts of ethylene dichloride or acetone for a period of 16 hr. at 50°C. At the end of this period the solid readily settled from the solution, but a little remaining turbidity was centrifuged out prior to taking an aliquot of the mother liquor for the determination of the amount of solid extracted. In several instances the infrared spectra of the recovered solid

samples were compared with that for polymethyl methacrylate and found to be identical.

Apparent grafting efficiencies reported in Tables I and II are the percentages of total poly(methyl methacrylate) in the products that are not extractable by a single extraction using the above technique. Exhaustive extraction would give figures a few per cent lower than those reported in the Tables. In view of the uncertainties regarding the effectiveness of such extraction in removing homopolymer, however, more exhaustive extraction appeared pointless.

For example, there is the question of the effect of moisture content of the product on the extractability of ungrafted poly(methyl methacrylate). To check this point, a product was prepared at 50 parts of poly(methyl methacrylate) per 100 parts of unmodified granular starch by initiation with cumene hydroperoxide and iron. This product was dried to 27.4% moisture content, and various portions were then dried to different lower moisture levels. These products were then extracted with acetone and with ethylene dichloride by the procedure described above. Results are shown in Table III.

TABLE III
Extractability of PMMA as a Function of Moisture Content of Product[a]

	PMMA not extracted, %	
Moisture, %	Ethylene Dichloride	Acetone
27.4	43.3	64.7
19.0	54.9	66.6
8.0	75.0	72.8
3.7	76.4	74.4
0.9	83.1	74.6

[a] Recipe: unmodified starch/PMMA at 100/50; 20 g. (dry basis) solid extracted for 16 hr. at 50°C. with 100 ml. of solvent.

It is strikingly evident that increase in moisture content allows for extraction of more of the polymer. This may be due to a swelling effect of moisture in the starch-polymer particle which allows for more ready penetration by solvent or at least a more ready escape of polymer molecules. In any event our results underline the influence of extraction conditions on the apparent grafting efficiency. It should be noted that the values reported in Tables I and II for grafting efficiency are based on extractions of products containing about 5% moisture. It would appear, therefore, that the results in the tables are self-consistent, since higher moisture levels are required to change the apparent grafting efficiency significantly.

Evidence for Grafting

Typical methods for detecting and isolating graft copolymer include fractional precipitation,[10,11] turbidimetric titration,[12] elution,[13] and paper chromatography.[14] Only for relatively few systems, as, for example,

natural rubber and poly (methyl methacrylate),[15] have really satisfactory procedures been worked out. The study of Allen et al.[13] illustrates the difficulties sometimes encountered.

With two polymers as widely different in solubilities as starch and poly (methyl methacrylate), separation of graft copolymer ought to be relatively simple. Turbidimetric titration or fractional precipitation depend on the availability of a solvent which will dissolve both homopolymers and the graft. For this system, dimethyl sulfoxide is such a solvent. However, we were unable to find a satisfactory precipitating medium. We therefore resorted to extraction of solid mixtures with liquids which are solvents for poly(methyl methacrylate) but nonsolvents for starch.

Extraction of Granular Products. Microscopic examination of the product recovered from the polymerization shows that starch granules still retain their individual identity (Fig. 2). That crystallinity is still present is shown by the birefringence seen with polarized light. Extraction of such particles with a solvent such as ethylene dichloride ought to remove homopolymer of methyl methacrylate. Graft copolymer ought to be unextracted, not only because of its probable insolubility,[9] but because the starch moiety will probably still be bound into the structure of the granule. Infrared spectra of a number of the extracts (Tables I and II) showed indeed that, within the limits of sensitivity of the method, the soluble portion was homopolymer.

In spite of the uncertainty about the quantitative extent of grafting (Table III), the extraction of product prepared with *N, N'*-azobisisobutyronitrile (AIBN) supports the belief that extensive grafting has occurred in the other runs of Tables I and II. With AIBN initiation, all but 7% of the poly(methyl methacrylate) was removed as homopolymer by two extractions with ethylene dichloride. High conversion of monomer with little or no grafting has also been reported when AIBN is used to initiate methyl methacrylate in the presence of natural rubber, although benzoyl peroxide causes extensive grafting in the same system.[15,16]

Extraction of Precipitated Products. The run with AIBN suggests that there is little mechanical entanglement of the homopolymer of methyl methacrylate in the starch granule, since entanglement might prevent extraction of the homopolymer. Nevertheless it was of interest to extract product in which the granular structure had been disrupted. Such a product is available by first dissolving the granular product, followed by addition of a precipitant for all polymer components. In product so treated the graft polymer will no longer be bound by crystallinity or other intragranular effects.

Predissolved material was prepared as follows. The granular product was dissolved at 5% concentration in dimethyl sulfoxide by heating to 100°C. or less for a few minutes. The solution was poured while still hot into a large excess of vigorously stirred 95% ethanol, the precipitate filtered, washed by reslurrying in ethanol, air-dried, ground to a fine powder, then oven-dried. Recovery was practically quantitative. The moisture-free

TABLE IV
Extraction of Predissolved Products[a]

Run	Initiator	PMMA in Product, %	Fraction	Wt.-% of Product	Carbon, %	PMMA (calc.), %
7	H_2O_2/Fe	33	1st extract	46.4	49.4	32
			2nd "	12.3	47.7	21
			Residue	—	52.5	52
8	H_2O_2/Fe	50	1st extract	24.1	53.0	53
			2nd "	32.6	55.0	68
			Residue	—	50.5	39
9	H_2O_2/Fe	62	1st extract	18.5	53.9	61
			2nd "	68.6	53.4	58
			Residue	—	53.8	60
19	AIBN	49	1st extract	45.1	56.9	80
			2nd "	7.4	57.9	86
			Residue	47.0	44.4	0
Mixture of unmodified starch and PMMA	—	35	1st extract	38.6	58.8	92
			2nd "	3.3	60.6	100
			Residue	52.6	45.2	5

[a] A 20.0 g. portion of dried product was extracted with successive 400-cc. portions of ethylene dichloride.

product was then extracted with ethylene dichloride by a technique similar to that described for the granular product.

A different behavior during extraction was at once evident. The granular materials underwent no visible change during extraction, and settled rapidly from the solvent once the agitation was stopped. Predissolved samples, on the other hand, swelled appreciably, and separation from the mother liquor required centrifuging. In some instances, the mother liquor could not be completely clarified by centrifuging. Moreover, in contrast to the granular product, a second extraction dissolved a further very significant amount of material.

Typical samples of polymer recovered from solution in the mother liquors showed by infrared curves the presence of carbohydrate. In spite of the well-known difficulty in obtaining an accurate carbon analysis of starch by combustion (a control sample of starch was reported to contain 43.04% carbon), the calculated carbon contents of starch and poly(methyl methacrylate), 44.5% and 60.0%, respectively, suggest carbon analysis as a convenient means of obtaining approximate composition of the extracted polymer. This method was used for determining compositions listed in Table IV.

The data in Table IV constitute positive evidence for grafting. In the first place, starch, dextrins, and oxidized or hydrolyzed starches are virtually completely insoluble in ethylene dichloride. That very significant amounts

of carbohydrate occur in the ethylene dichloride-soluble fractions strongly suggests that starch is carried into dispersion by the attached polymethyl methacrylate. The solubility of graft copolymer containing at least 50% of starch is in contrast to the results of Kargin, who reported[9] that graft copolymer containing as much as 92% poly(methyl methacrylate) was insoluble in ethylene dichloride. Moreover, results obtained by extracting a physical mixture of starch and poly (methyl methacrylate) indicate relatively good separation of the two polymers. The fact that AIBN-initiated product allows much better separation than typical grafted products again illustrates that this initiator promotes polymerization with little or no grafting.

A curious trend is revealed in the extraction of runs 7 and 9, Table IV. Contrary to the figures in the table, the residue would be expected to have significantly lower PMMA content than the extracts. Moreover, contrary to the results from runs 8 and 9, the first extraction would be expected to remove a larger amount of material than the second. A possible explanation for these anomalous results is that between the time of preparation of the sample and its extraction, sufficient hydrogen bonding of the carbohydrates was established that solution of the grafted molecules could occur only slowly as the solvent penetrated and swelled the solid matrix.

Mechanism of Grafting

As in other systems in which grafting is accomplished via free radical reactions, the present process may be presumed to involve formation of radical sites on the backbone polymer. This may occur either by reaction of a radical from the initiator or transfer from a growing chain with the starch molecules. In either event, with hydrogen peroxide and ferrous iron, the well-known Fenton's reagent, the first step is undoubtedly formation of hydroxyl radicals.[17]

The possible steps in the grafting process are illustrated in eqs. (1)–(7):

$$H_2O_2 + Fe^{+2} \rightarrow HO\cdot + OH^- + Fe^{+3} \quad (1)$$

$$HO\cdot + M \rightarrow M\cdot \quad (2)$$

$$M\cdot + n\text{-}1M \rightarrow M_n\cdot \quad (3)$$

$$HO\cdot + \text{Starch—H} \rightarrow \text{Starch}\cdot + H_2O \quad (4)$$

$$M_n\cdot + \text{Starch—H} \rightarrow \text{Starch}\cdot + M_nH \quad (5)$$

$$\text{Starch}\cdot + M \rightarrow \text{Starch—M}\cdot \quad (6)$$

$$\text{Starch—M}\cdot + n\text{-}1M \rightarrow \text{Starch-}M_n\cdot \quad (7)$$

While either reaction (4) or (5) would produce the necessary radical site on the starch chain, the fact that relatively little grafting occurs when initiation is by AIBN indicates that transfer of poly(methyl methacrylate) radicals with starch occurs only to a minor extent if at all.

On the other hand, chain degradation of starch by attack of Fenton's reagent is well known. Brown[18] ascribed the effect to hydrolysis activated by the peroxide, but in the light of the known generation of the highly active hydroxyl radical by Fenton's reagent,[17] degradation involving abstraction of hydrogen by hydroxyl radical, followed by any of several possible paths leading to chain scission, seems much more plausible. We found in the present work that when starch slurry is treated at room temperature with the same levels of peroxide and iron as used to initiate polymerization (Table I), but in the absence of monomer, the reduced viscosity of the starch in 1 *N* aqueous KOH solution dropped to about a third of the initial value.

In this work we have not attempted to establish the specific position in starch at which grafting occurs. However, in view of the ability of hydroxyl radical to abstract hydrogen from any C—H link,[17] more or less random attack at all possible positions in the anhydroglucose ring seems probable.

Termination by combination of growing chain ends would be expected to lead to crosslinking. The fact that the grafted products are readily soluble in dimethyl sulfoxide is in harmony with the known tendency of methyl methacrylate to terminate chiefly by disproportionation.[19]

Acid Hydrolysis of Grafts

Selected samples of the granular grafted products were subjected to hydrolysis by refluxing for 2 hr. in a large excess of 1 *N* hydrochloric acid. Although the hydrophobic powder underwent no visible change during this treatment, the undissolved product recovered was found by material balance, solubility in ethylene dichloride, and infrared curves to be poly(methyl methacrylate). In most instances the infrared curves were identical with that of the authentic homopolymer except for slight peaks at 3.0 and 9.75μ which are typical of glucose or its polymers. The height of these peaks suggested a maximum carbohydrate content of about 5%, and probably much less in some instances. Extraction with water of ethylene dichloride solutions failed to remove the carbohydrate.

After hydrolysis, washing, and drying, the recovered polymers were readily and completely soluble in ethylene dichloride. In some instances the solutions were slightly turbid, but these were readily clarified by centrifuging. Solution viscosities were determined by standard techniques in ethylene dichloride at 30°C. In most instances a single determination was made at a concentration of 0.4 g./dl. The method of Hart[20] was used to estimate intrinsic viscosities, and from these the molecular weights were calculated on the basis of the constants published by Riddle.[21] The values so obtained are shown in Table V. These must, of course, be treated as only rough approximations. The presence of a little carbohydrate matter could by hydrogen bonding lead to an apparent molecular weight much higher than the actual value for the pure homopolymer. But, in any event the data suggests that the graft consists of extremely long side chains grafted at very widely spaced intervals.

TABLE V
Estimated Molecular Weights of PMMA Recovered By Hydrolysis of Starch

Run	$[\eta]$, 100 ml./g.	Mol. wt. $\times 10^{-6}$
3	0.79	0.27
4	3.0	1.5
5	2.9	1.4
6	2.3	1.0
7	3.1	1.6
8	4.0	2.2
9	3.3	1.7
10	2.1	0.9

Physical Characteristics of Grafted Starches

Typical products containing 50–100 parts of polymer per 100 parts of starch are white powders which are very free-flowing. Microscopic examination of the particles shows them to be similar in appearance to the untreated starch (Figs. 1 and 2). The particles still retain much of the birefringence characteristic of starch granules. The powders are quite hydrophobic, and the particles show no tendency to swell and no other

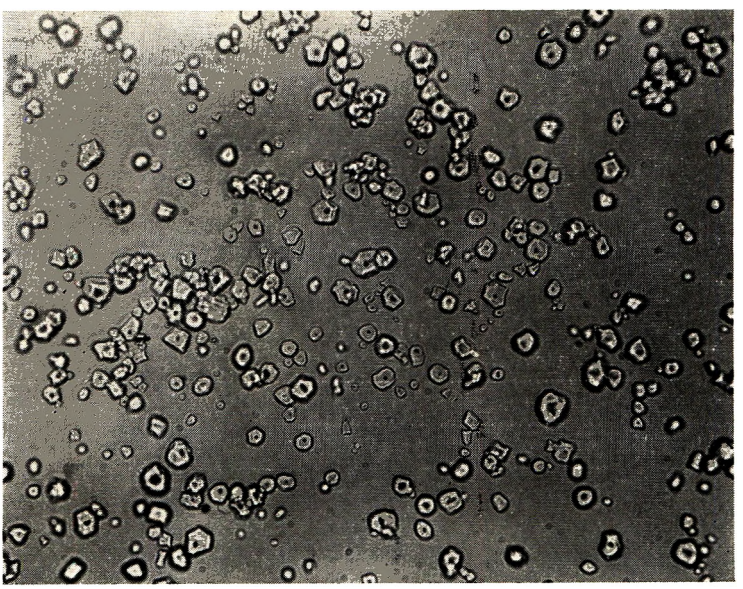

Fig. 1. Granular unmodified starch (PFP), 210×.

visible change after refluxing four hours in 5% aqueous slurry. Refluxing in 1*N* hydrochloric acid, which results in nearly quantitative removal of the carbohydrate component, leaves hydrophobic particles many of which retain a superficial appearance similar to that of the granular starch (Fig. 3). Products containing about equal parts of starch and poly(methyl methacrylate), for example run 11, were tested as to their

thermoplasticity. Excessively high mold pressures and temperatures were required to effect molding. No plastic flow could be realized at temperatures under 250°C., at which temperatures the product browned severely.

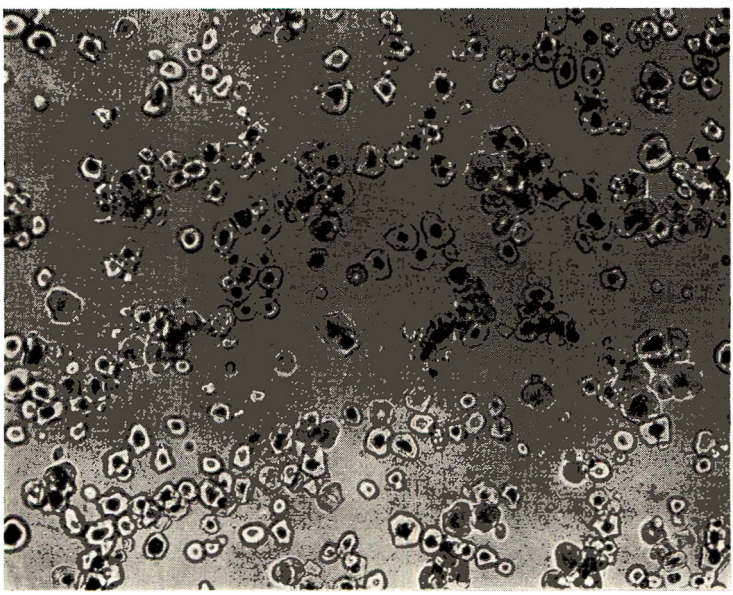

Fig. 2. Unmodified starch plus poly(methyl methacrylate) at 50/50 ratio (run 11), 210×.

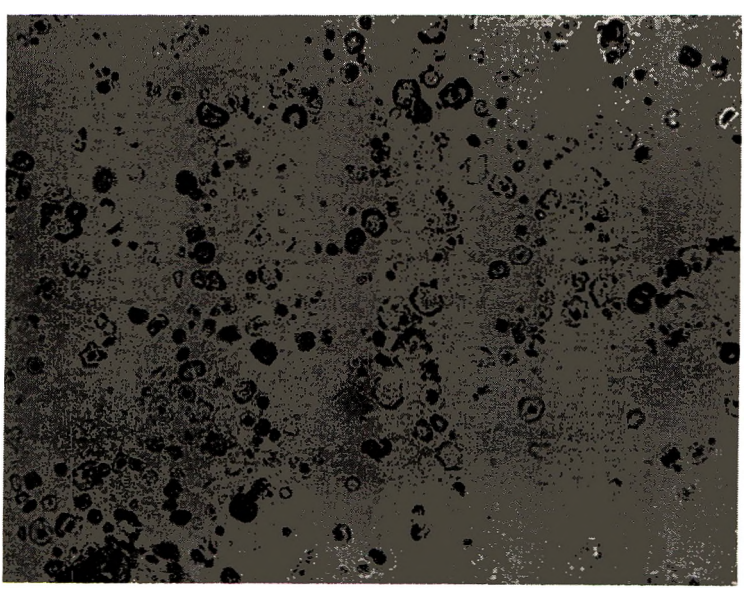

Fig. 3. Product of Fig. 2 after removal of starch by acid hydrolysis, 210×.

EXPERIMENTAL

Materials

Unless otherwise noted, inorganic chemicals were reagent grade or equivalent. The 50% hydrogen peroxide was obtained from duPont. Hydroperoxides were obtained from Hercules Powder Company. Dimethyl sulfoxide was used as received from Stepan Chemical Company.

Methyl methacrylate, from Rohm & Haas was alkali-washed to remove the hydroquinone. The washed material was stored at 40°F. until used. Allowance was made for the water content when weighing out material for runs.

All starches except waxy maize were commercial grades prepared by the A. E. Staley Mfg. Co. Waxy maize corn starch was obtained from American Maize Company. All these products were used in their granular form. Moisture content of each was determined; typical values were 8–10% water. After determination of moisture contents, the products were kept in tightly capped jars to avoid further change. Products were weighed on a dry basis for use in the various runs.

Procedures

Polymerizations. A 1-liter resin kettle was fitted with a paddle-type stainless steel stirrer, a reflux condenser, a thermometer, and an inlet for nitrogen. The starch, usually about 100 g. of dry substance, and 400 ml. of distilled water were charged. The vent from the reflux condenser was then fitted to a water aspirator, and the mixture was evacuated with stirring until it had boiled for 5–10 min. at or near room temperature. The vacuum was broken with nitrogen. Thereafter an atmosphere of nitrogen was maintained. Ferrous ammonium sulfate was added, then the methyl methacrylate. The temperature was adjusted to the desired point, then the hydrogen peroxide added. In typical runs there was a pronounced and rapid temperature rise, after which the temperature gradually dropped again. Ordinarily neither heating nor cooling was applied after the beginning of the reaction cycle. In some instances the viscosity increased markedly for the first few minutes and then gradually dropped again as stirring was continued.

After stirring for 2–3 hr., the mixture was filtered and the product thoroughly washed by slurrying with distilled water. The product was air-dried at room temperature overnight or longer. Its moisture content was determined by weight loss on heating at 110°C. From the net weight of the product and the known starting weight of the starch, the weight of poly(methyl methacrylate) and hence the conversion of monomer were determined.

Further details of the recipes and procedures are shown in Table I and II.

In a few instances the combined filtrate and washings were evaporated to dryness to determine if any polymer or carbohydrate was present. Only with oxidized starch was any product found in the filtrate and washings.

In one instance this amounted to carbohydrate to the extent of about 1% of the original charged starch. It should be particularly noted that all the poly(methyl methacrylate) was retained in the filtered product.

Typical products were white, free-flowing powders containing about 5% of moisture after air-drying at room temperature.

Extraction of Granular Products. An exhaustive extraction of the product of run 1 was carried out as follows. A 100-g. portion of dry, granular product and 500 ml. of ethylene dichloride were put into a 1-qt. crown-capped bottle. After rotation for 72 hr. in a 50°C. bath, the bottle was removed and allowed to cool. The solid product settled rapidly. The mother liquor was decanted, and 100 ml. of fresh ethylene dichloride was added. After shaking, settling, and decanting of this wash liquor, another 100 ml. of ethylene dichloride was used as a second wash. The combined mother liquor and washing were evaporated to dryness and the dry product was weighed. This extraction procedure was repeated twice more with fresh 500 ml. portions of ethylene dichloride, and then a final extraction was similarly carried out with 500 ml. of acetone.

For the remaining products the simpler procedure was used. In typical runs 20.0 g. (dry substance) of the starch–polymer product, containing about 5% of moisture, was put into a 1-qt. crown-capped bottle, 100 ml. of ethylene dichloride added, and the bottle rotated in a 50°C. bath for at least 16 hr. The bottle was removed, cooled, and the contents quickly transferred to a stoppered centrifuge bottle. After centrifuging to clarify, 20.0 ml. of the clear mother liquor was pipetted into a weighed drying pan. Most of the solvent was allowed to evaporate at room temperature. The final drying was for 1 hr. at 110°C. From the weight of dried solid, the solids content in the solution, and hence the fraction of polymer which had been extracted, were calculated.

Extraction of Pasted Grafts. The following is typical of the procedure used. A 30-g. portion (dry basis) of the product from run 11 and 850 ml. of dimethyl sulfoxide were heated to nearly 100°C. with stirring in a resin kettle. The powdery product dispersed to give a nearly clear solution at about 75°C. After 30 min. of stirring and while still hot, the mixture was poured with vigorous stirring into 1 gal. of 3A ethanol. The flocculant precipitate was filtered and then reslurried in methanol, filtered again, and then spread out to air-dry. After two days of air-drying the product was dried for six hours at 110°C. The dried product weighed 30.6 g. In most instances, the product was ground in a Wiley mill prior to the final oven-drying.

A quantity of 5.00 g. of product obtained as above was put in a 1-qt. bottle, 500 ml. of solvent was added, the bottle capped and tumbled for 16 hr. in a 50°C. bath. The mixture was then centrifuged, the mother liquor decanted, and the solid residue treated with a fresh 400 ml. of the extracting solvent. After mixing 20 hr. in the 50°C. bath, the product was removed and the solids separated by centrifuging. The mother liquors from the first and the second extractions were worked up separately.

Each was concentrated by evaporation to 100 ml. or less and the solid precipitated by the addition of excess 3A ethanol or Skellysolve F (paraffin solvent, mostly pentane). The precipitated solid was oven-dried for 4 hr. at 100°C. and then weighed. The twice-extracted solid residue was also dried and weighed. Appropriate samples obtained were submitted for infrared curves and for carbon-hydrogen analyses.

Acid Hydrolysis of Grafts. The following is a typical procedure. A 50-g. portion (dry basis) of the product of run 11, containing about equal parts of starch and poly(methyl methacrylate), was placed in a 2-liter resin kettle fitted with a reflux condenser, thermometer, and stirrer. There was added 1000 ml. of 1*N* hydrochloric acid. The mixture was stirred and refluxed for about 90 min. During this time, the powdery product remained hydrophobic and tended to float on the surface of the liquid. After cooling, the solid was filtered, washed thoroughly with water, and then oven-dried at 100°C. for 4 hr. The product was a fine, white powder weighing 24.5 g. Calculated weight of poly(methyl methacrylate) in the charge was 23.7 g. The product dissolved readily in ethylene dichloride to give a faintly turbid solution. A clear solution was obtained by taking up 10 g. of the product in 500 ml. of acetone and centrifuging at about 5000 rpm. Polymer was recovered by precipitation with 3A ethanol. After oven-drying for 4 hr. at 110°C. the polymer was readily for determination of reduced viscosity.

References

1. Jones, E. J., L. B. Morgan, J. F. L. Roberts, and S. M. Todd, Brit. Pat. 715,194 (1954).
2. Immergut, E. H., and H. Mark, *Makromol. Chem.*, **18–19**, 322 (1956).
3. Borunsky, J., Can. Pat. 549,110 (1957).
4. Mino, G., and S. Kaiserman, *J. Polymer Sci.*, **31**, 242 (1958).
5. Kimura, S., and M. Imoto, *Makromol. Chem.*, **42**, 140 (1960).
6. Berlin, A. A., and E. A. Penskaya, *Doklady Akad. Nauk S.S.S.R.*, **110**, 585 (1956).
7. Angier, D. J., R. J. Ceresa, and W. F. Watson, *J. Polymer Sci.*, **34**, 699 (1959).
8. Kargin, V. A., P. V. Koslov, N. A. Plate, and I. I. Konoreva, *Vysokomolekulyarnye Soedineniya*, **1**, 114 (1959).
9. Kargin, V. A., N. A. Plate, and E. P. Rebinder, *Vysokomolekulyarnye Soedineniya*, **1**, 1547 (1959).
10. Smets, G., and M. Claesen, *J. Polymer Sci.*, **8**, 289 (1952).
11. Blanchette, J. A., and L. E. Nielsen, *J. Polymer Sci.*, **20**, 317 (1956).
12. Melville, H. W., and B. D. Stead, *J. Polymer Sci.*, **16**, 505 (1955).
13. Allen, P. E. M., G. M. Burnett, J. M. Downer, and H. W. Melville, *Makromol. Chem.*, **38**, 76 (1960).
14. Hartley, F. D., *J. Polymer Sci.*, **34**, 397 (1959).
15. Allen, P. W., G. Ayrey, and G. G. Moore, *J. Polymer Sci.*, **36**, 71 (1959).
16. Angier, D. J., and D. T. Turner, *J. Polymer Sci.*, **28**, 270 (1958).
17. Vri, N., *Chem. Revs.*, **50**, 375 (1952).
18. Brown, W. R., *J. Biol. Chem.*, **113**, 417 (1936).
19. Bevington, J. C., H. W. Melville, and R. P. Taylor, *J. Polymer Sci.*, **14**, 463 (1954).
20. Hart, V. E., *J. Polymer Sci.*, **17**, 215 (1955).
21 Riddle, E. H., *Monomeric Acrylic Esters*, Reinhold, New York, 1954, p. 64.

Synopsis

Graft copolymers were prepared by the radical-initiated polymerization of methyl methacrylate in aqueous slurries of granular corn starch. High conversions of monomer were realized, giving products which were readily recovered by filtration. The products were free-flowing, white powders, which by microscopic examination looked much like granular starch. Grafting was demonstrated by extracting the granular products with ethylene dichloride, which in most instances removed only a minor part of the poly(methyl methacrylate). When azoisobutyronitrile was used for initiation, a high conversion of monomer resulted, but about 90% of the polymer was extractable with ethylene dichloride. Further evidence for grafting was obtained by extraction of predissolved product, prepared by dissolving the granular product in dimethyl sulfoxide, to destroy the structure of the starch granules, and precipitating with alcohol. The fractions soluble in ethylene dichloride contained significant amounts of carbohydrate. Similar treatment of product prepared with azoisobutyronitrile initiation or of physical blends of starch and poly(methyl methacrylate) gave much more efficient separation of starch from PMMA. Failure to obtain grafting with AIBN initiation suggests that grafting occurs mainly as a result of attack on starch by radicals generated by the reaction of hydrogen peroxide or organic hydroperoxide with ferrous iron. Acid hydrolysis of the products removed the starch. The PMMA so recovered typically had viscosity-average molecular weights of the order of 10^6, which suggests the grafts contained very long branch chains of PMMA attached at very infrequent intervals.

Résumé

Des copolymères greffés ont été préparés par polymérisation radicalaire du méthacrylate de méthyle dans une suspension aqueuse de farine granulaire de mais. On obtient un très haut degré de polymérisation donnant des produits qu'on retrouve facilement par filtration. Les produits sont des poudres très fines, qui, sous microscope, ressemblent fortement aux granules de l'amidon. Le greffage est démontré en extrayant les produits granulaires avec le chlorure d'éthylène, qui généralement ne solubilise qu'une petite fraction du polyméthacrylate de méthyle. Lorsqu'on utilise l'azoisobutyronitrile comme initiateur on obtient un haut degré de polymérisation mais environ 90% du polymère peut être extrait au chlorure d'éthylène. On obtient un autre argument pour le greffage quand on extrait les produits, dissous au préalable dans le sulfoxyde de diméthyle, afin de détruire la structure granuleuse de l'amidon et en précipitant ultérieurement à l'alcool. La fraction soluble dans le chlorure d'éthylène contient assez bien d'hydrate de carbone. Les traitements similaires des produits préparés avec l'azoisobutyronitrile ou des mélanges physiques de l'amidon et le polyméthacrylate de méthyle donnent des séparations de l'amidon et du polyméthacrylate de méthyle beaucoup plus efficientes. L'absence de greffage dans l'initiation à l'AIBN laisse suggérer que le greffage résulte surtout d'une ataque des radicaux qui sont formés par lar éaction du peroxyde d'hydrogène ou des hydroperoxydes organiques avec le fer ferreux sur l'amidon. Le PMMA ainsi obtenu à un poids moléculaire moyen, d'éterminé par la viscosité, de l'ordre de grandeur de 10^6; ceci laisse supposer que les polymères greffés contiennent des chaînes greffées très longues de PMMA qui sont attachées à des distances très irrégulières.

Zusammenfassung

Pfropfpolymere wurden durch radikal-gestartete Polymerisation von Methylmethacrylat in einem wässrigen Brei aus körniger Maisstärke dargestellt. Es wurde ein hoher Umsatz zu leicht durch Filtration abtrennbaren Produkten erzielt. Die Produkte waren fein verteilte weisse Pulver, die unter dem Mikroskop wie gekörnte Stärke aussahen. Die Aufpfropfung wurde durch Extraktion der körnigen Produkte mit Äthylendichlorid nachgewiesen, durch welche in den meisten Fällen nur ein geringer Anteil

des Polymethylmethacrylates entfernt wurde. Bei Verwendung von Azoisobutyronitril als Starter wurde zwar ein hoher Monomerumsatz erreicht, aber etwa 90% des Polymeren konnten mit Äthylendichlorid extrahiert werden. Ein weiterer Beweis für die Aufpfropfung wurde durch Extraktion eines vorgelösten, durch Auflösung der körnigen Substanz in Dimethylsulfoxyd zur Zerstörung der Struktur der Stärkekörner und Ausfällung mit Alkohol dargestellten Produktes erhalten. Die äthylendichloridlöslichen Fraktionen enthielten Kohlehydrat in grösserer Menge. Eine ähnliche Behandlung eines mit Azoisobutyronitrilanregung dargestellten Produkts oder von Mischungen von Stärke und Polymethylmethacrylat ergab eine viel wirksamere Trennung der Stärke von Polymethylmethacrylat. Das Ausbleiben der Aufpfropfung bei AIBN-Anregung spricht dafür, dass die Aufpfropfung hauptsächlich ein Ergebnis des Angriffs der Stärke durch Radikale aus der Reaktion zwischen Wasserstoffperoxyd oder organischen Hydroperoxyden und Eisen-II-ionen ist. Saure Hydrolyse der Produkte führte zur Entfernung der Stärke. Das zurückgewonnene Polymethylmethacrylat besass Viskositätsmittelwerte des Molekulargewichtes in der Grössenordnung von 10^6, was auf einen Gehalt der Pfropfpolymeren an sehr langen Polymethylmethacrylatketten in sehr grossen Abständen hinweist.

Received December 20, 1961
Revised January 15, 1962

JOURNAL OF POLYMER SCIENCE: PART A VOL. 1, PP. 1041–1048 (1963)

Molecular Weight Distribution in Polypropylene Glycol 2025

R. J. MORRIS, JR. and H. E. PERSINGER, *Research and Development Department, Union Carbide Chemicals Company, a Division of Union Carbide Corporation, South Charleston, West Virginia*

INTRODUCTION

Recent work by Case[1] has shown that polypropylene glycols with a number-average molecular weight of 700 can be fractionated effectively by countercurrent extraction between water and an organic solvent. High temperature vapor-phase chromatography has been applied by Shank[2] to the fractionation of polypropylene glycols up to 500 number-average molecular weight. Fractionation by molecular distillation was done by Havlik,[3] but only under very rigorous conditions. A brief investigation for suitable solvents for the countercurrent extraction technique was unsuccessful, and attempts to adapt the vaporization techniques to the higher homologs were not made because the vapor pressures of these higher homologs are too low to allow fractionation by the gas chromatographic or molecular distillation techniques without imposing very strenuous conditions.

EXPERIMENTAL

Materials

Samples. The polyglycol samples were labeled NIAX diol PPG 2025 from industrial production of the Union Carbide Chemicals Company, South Charleston, West Virginia.

Solvents. Acetone and diisopropyl ether were used as eluent and diluent, respectively, in the fractionation. Each of the solvents was technical grade originally, and both were purified by passing them through an activated alumina column identical to the one used in the fractionation procedure.

Spectroscopically pure carbon tetrachloride was used as a solvent in the near-infrared spectrometric analysis of each fraction for number-average molecular weight.

Chromatographic Column. The polymer was fractionated on a chromatographic column 1 in. in diameter and 12 in. long packed with 80 to 200 mesh chromatographic grade adsorption alumina (Fig. 1.) The

alumina was activated at 400°F. for 4 hr. Water adsorbed on the activated alumina was determined by the Karl Fisher titration,[4,5] and sufficient water was added to bring the adsorbed water concentration up to 4.0 wt.-%. After the addition of water, the adsorbant was mixed thoroughly and allowed to stand for 24 hr. to attain a homogeneous distribution

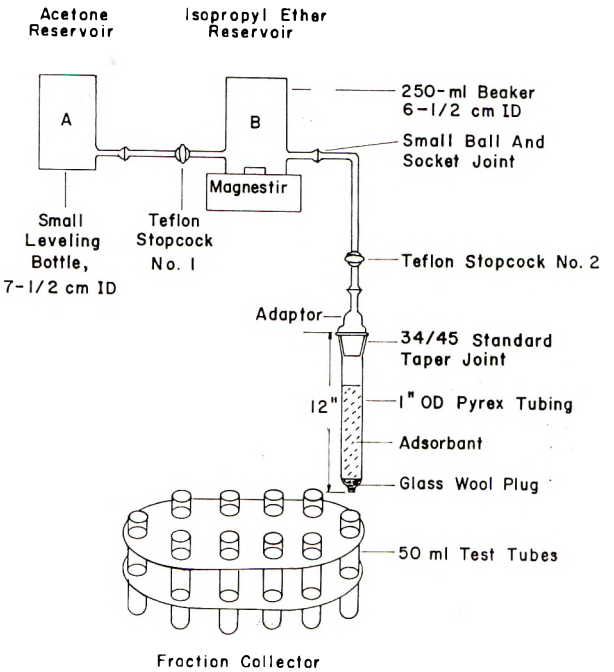

Fig. 1. Schematic diagram of fractionation apparatus.

Gradient Elution Apparatus. The apparatus used for the solvent gradient elution was basically like the cylindrical system described by Bock and Ling[6] as shown schematically in Figure 1. The reservoir diameters are critical, because they regulate the composition of the eluent. An automatic fraction collector was used in conjunction with the gradient elution system to facilitate handling the fractions so that continual operator attention is not required.

Procedure

Preparation of Column. A small glass wool plug was placed in the constricted end of the glass tube to support the adsorbant. Then 60 ± 1 g. of prepared adsorbant was placed in the tube and packed very carefully by running a Vibro-Tool up and down the column until there was no further settling of the adsorbant.

Fractionation. The fractionation apparatus was set up as shown in Figure 1 without the column or adapter. With stopcocks 1 and 2 closed, about 200 ml. of purified acetone was added to reservoir A and about 125

ml. purified diisopropyl ether to reservoir B so that the liquid levels were equal.

The sample solution was prepared by dissolving 1.0 g. of sample weighed to the nearest milligram in 20 ml. of diisopropyl ether.

The column was soaked by adding 50 ml. of diisopropyl ether. When the liquid level approached the top of the alumina, the sample solution was added; the sample container was then rinsed with 20 ml. of diisopropyl ether which was added when the liquid level again approached the top of the column. The column and adaptor were then attached to the elution apparatus, the magnetic stirrer started, and stopcocks 1 and 2 opened.

Because the first 100 ml. taken from the column contained only ether from the soaking, the solvent portion of the sample solution, rinse ether, and about 10 ml. of ether from reservoir B, it was collected in a graduate and discarded. Then 10-ml. fractions were collected in tared 50-ml. test tubes. Fraction size was controlled by adjusting the timing mechanism on the fraction collector to 2–3 min. The elution required about 90 min. to complete, and usually 28 fractions were collected.

Molecular Weight Determination. The test tubes containing the fractions were put in a vacuum desiccator under 2–5 mm. Hg pressure, absolute, at 25°C. to remove the acetone and diisopropyl ether solvents. It usually required 6–10 hr. for the fractions to attain constant weight. The final weight of each was then recorded, and the weight of each fraction was determined by difference from the original tared weight of the test tube.

The molecular weight was determined by near-infrared spectrophotometry; similar methods have recently been published.[7,8] The fractions were dissolved in spectroscopic grade carbon tetrachloride and scanned from 3.2 to 2.6 μ. The absorbance maximum near 2.88 μ is due to hydrogen-bonded hydroxyl and was used as the analytical wavelength.

EXPERIMENTAL RESULTS AND DISCUSSION

Adsorbant

When adsorption alumina is activated at 400°F as the manufacturers recommend, it is quite dry and holds the polyglycol molecules so tenaciously that even undiluted acetone will not elute all of the molecules from the column. However, if the water content is too high, all of the polymer comes through the column in the first few fractions and the fractionation is inefficient. The water content of the alumina must be adjusted to 4.0 wt.-% before a 2025 molecular weight polymer can be eluted satisfactorily. In effect, the water on the alumina reduces the adhesion of the polyglycol molecules to the adsorbant so that they can be eluted.

Gradient Elution Apparatus

Solvent gradient elution is an accepted technique in liquid chromatography for controlling eluent composition, but it is generally considered to

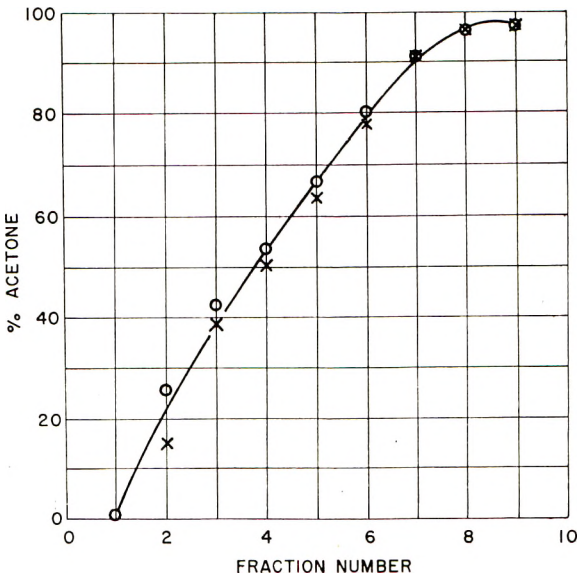

Fig. 2. Reproducibility of eluent composition: (×) original; (O) duplicate.

be a nonreproducible type of elution. We have found this not to be the case with the apparatus described above; the reproducibility of the eluent composition is shown in Figure 2. In order to obtain these data an elution was run without a sample and with 30 ml. fractions collected instead of the usual 10 ml. fractions. After the first elution, the apparatus was completely disassembled and the variables changed; the apparatus was then reassembled and the variables reset for the duplicate determination.

Molecular Weight Distribution Curves

The data from the fractionation as shown in Table I must be first plotted as an integral-type distribution curve because the fractionation is not so efficient as to separate discrete homologs. A typical integral distribution curve for polypropylene glycol 2025 is shown in Figure 3. If a differential-type distribution curve is desired, the data can be replotted from the integral curve; the differential curve corresponding to Figure 3 is shown in Figure 4. Superimposed on this experimental curve is the theoretical distribution of polypropylene glycol 2025 based on the calculations of Flory.[9]

Flory's theoretical treatment is postulated for idealized reaction conditions which we cannot presume to be present in actual practice. In the theoretical treatment, it is also assumed that the reaction rate remains constant throughout the reaction.

Experience has shown that a normal 2025 number-average molecular weight polypropylene glycol will have the type of distribution curve shown in Figure 4, probably due to deviations from Flory's ideal conditions. The

TABLE I
Typical Fractionation Data for Polypropylene Glycol 2025 (Sample Weight 1.0327 g.)

Fraction no.	Wt. fraction	Wt. %	Mol. wt.	Cumulative %
1	—	—	—	—
2	—	—	—	—
3	0.0052	0.5	—	—
4	0.0175	1.7	1210	2.2
5	0.0134	1.3	1350	3.5
6	0.0361	3.5	1500	7.0
7	0.0547	5.3	1590	13.3
8	0.0434	4.2	1630	17.5
9	0.0568	5.5	1660	22.0
10	0.0279	2.7	1700	24.7
11	0.0444	4.3	1740	29.0
12	0.1073	10.4	1810	39.4
13	0.0918	8.9	1880	48.3
14	0.1218	11.8	1900	60.1
15	0.0299	2.9	1940	63.0
16	0.0213	2.0	1980	65.0
17	0.0558	5.4	2000	80.4
18	0.0805	7.8	2030	88.2
19,20	0.0650	6.3	2060	94.5
21,22,23	0.0289	2.8	2090	97.3
24,25,26	0.0175	1.7	2220	99.0
27,28	—	—	—	—

distribution varies slightly for different samples of the polyglycol, but Figure 4 is generally typical.

The reason for this deviation, we believe, is the gradual decrease in reaction rate as the reaction proceeds to the later homologs. As the molecules grow larger, their decrease in reaction rate induces the propylene oxide molecules to add preferentially to lower molecular weight homologs.

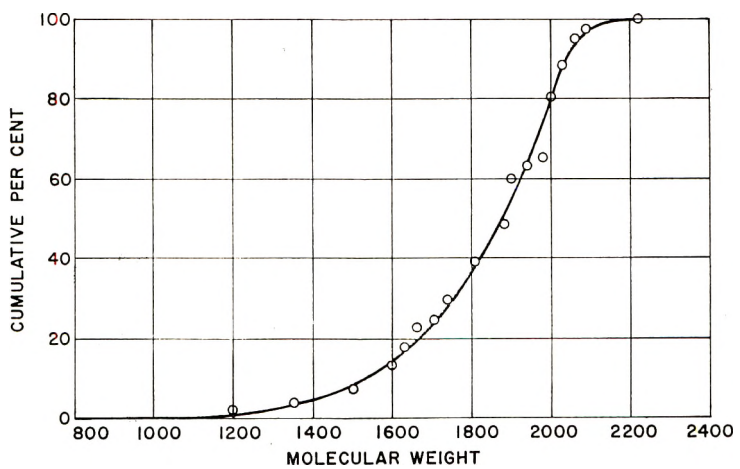

Fig. 3. Integral molecular weight distribution curve for polypropylene glycol 2025.

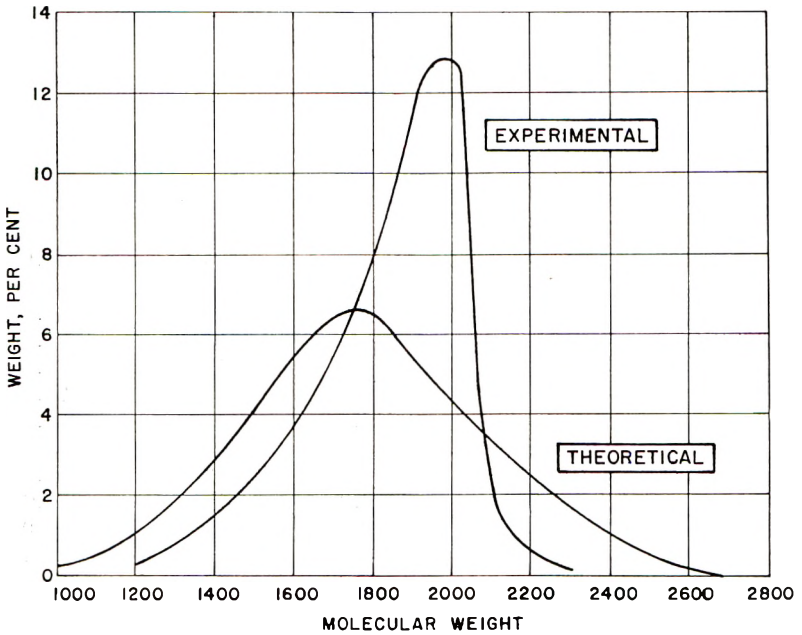

Fig. 4. Experimental vs. theoretical distribution curve for polypropylene glycol 2025.

This difference in reaction rates suppresses the formation of the very high homologs in the product because the propylene oxide molecules, which would under ideal conditions react with the higher homologs to make them even larger, instead react preferentially with the low molecular weight molecules. For this reason, the low molecular weight homologs become depleted. The experimentally determined distribution is consequently skewed from both the high and low molecular weights toward the center or average molecular weight.

PROOF OF METHOD

Inasmuch as the results which are obtained by this procedure are characteristic of a poor fractionation, it is necessary to prove that the fractiona-

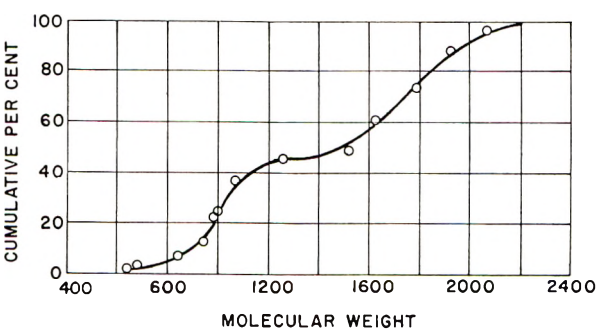

Fig. 5. Integral distribution curve for 50% polypropylene glycol 2025 and 50% polypropylene glycol 1025.

tion is capable of sufficient resolution that the demonstrated differences between the theoretical and experimental molecular weight distribution curves are valid. In order to establish the resolution of the fractionation, an equal mixture of polypropylene glycols with 1025 and 2025 molecular weights, respectively, was fractionated using the procedure described.

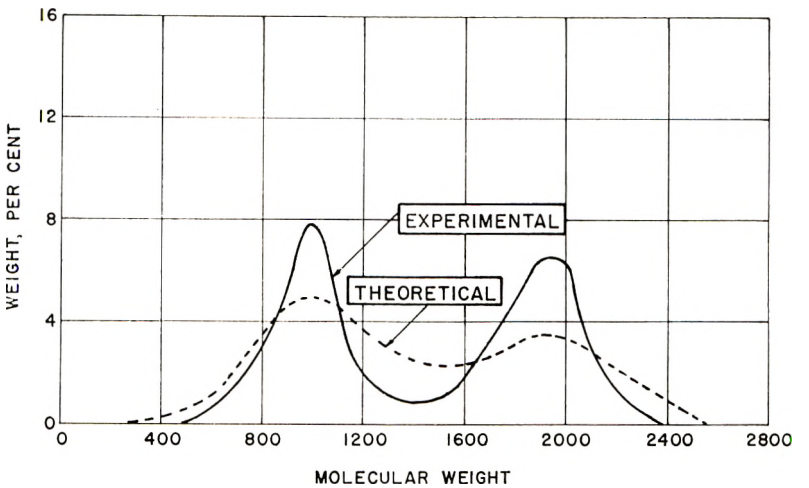

Fig. 6. Experimental and theoretical differential distribution curves for 50% polypropylene glycol 2025 and 50% polypropylene glycol 1025.

The results of this fractionation are shown in integral form in Figure 5 and in differential form in Figure 6. These figures clearly show that 1025 and 2025 molecular weight polymers of propylene oxide can be completely resolved and, therefore, the differences found between the experimental and theoretical distribution curves are within the capability of this fractionation.

The authors wish to express their appreciation to Messrs. A. C. Bowbeer, W. D. Dunn, W. W. Fink, and Dr. D. G. Leis for their help and cooperation during the development of this procedure.

References

1. Case, L. C., *J. Phys. Chem.*, **62**, 896 (1958).
2. Shank, J. T., Union Carbide Chemicals Company, South Charleston, West Virginia, private communication.
3. Havlik, A. J., and A. F. Hildebrant, paper presented at 134th National Meeting, American Chemical Society, Chicago, Ill., September 1958.
4. Fischer, K., *Angew. Chem.*, **48**, 394 (1935).
5. Bryant, W. M. D., J. Mitchell, D. M. Smith, and E. C. Ashby, *J. Am. Chem. Soc.*, **63**, 2924 (1941).
6. Bock, R. M., and N.-S. Ling, *Anal. Chem.*, **26**, 1543 (1954).
7. Burns, E. A., and R. F. Muraca, *Anal. Chem.*, **31**, 397 (1950).
8. Hilton, C. L., *Anal. Chem.*, **31**, 1610 (1959).
9. Flory, P. J., *J. Am. Chem. Soc.*, **62**, 1561 (1940).

Synopsis

The new applications of polypropylene glycols as chemical intermediates, particularly in the polyurethane field, have shifted emphasis from purely physical properties, such as density, viscosity, and volatility, to chemical properties, such as hydroxyl content, unsaturation, and molecular weight: Because much interest is also being shown in the uniformity of chain length, i.e., the "molecular purity" of the polypropylene glycol, methods were investigated for measuring this property. A liquid chromatographic procedure has been developed which will yield molecular weight distributions for polypropylene glycols in the 2025 number-average molecular weight range. The results approximate, but do not match, the values obtained by theoretical calculations. Details of the method and a typical distribution curve are presented.

Résumé

Les nouvelles applications des glycols polypropyléniques comme intermédiaires chimiques, spécialement dans le domaine des polyuréthannes ont fait dévier l'intérêt vers les propriétés chimiques telles que la teneur en hydroxyle, l'insaturation et le poids moléculaire, au lieu des propriétés purement physiques telles les densité, viscosité et volatilité. Etant donné qu'on montre également beaucoup d'intérêt pour l'uniformité de la longueur de chaîne, c'est à dire la "pureté moléculaire" du polypropylène glycol, on a étudié des méthodes pour mesurer cette propriété. On a développé un processus par chromatographie en phase liquide qui produira pour les glycols polypropyléniques des distributions de poids moléculaire d'environ 2025 comme moyenne en nombre. Les résultats approchent mais ne coincident pas avec les valeurs obtenues par des calculs théoriques. On présente les détails de la méthode et une courbe de distribution typique.

Zusammenfassung

Die neuartige Verwendung von Polypropylenglykolen als chemische Zwischenstoffe, besonders im Polyurethansektor, hat das Interesse von den rein physikalischen Eigenschaften, wie Dichte, Viskosität und Flüchtigkeit, zu chemischen Eigenschaften, wie Hydroxylgehalt, ungesättigter Charakter und Molekulargewicht verschoben. Da auch die Einheitlichkeit der Kettenlänge, d.h. die "molekulare Reinheit" von Polypropylenglykol, grosses Interesse besitzt, wurden Methoden zur Messung dieser Eigenschaft untersucht. Ein flüssigkeits-chromatographisches Verfahren wurde entwickelt, welches die Molekulargewichtsverteilung für Polypropylenglykole im 2025-Molekulargewichts-Zahlenmittelbereich liefert. Die Ergebnisse nähern sich zwar den theoretisch berechneten Werten, liefern aber keine volle Übereinstimmung. Einzelheiten der Methode werden beschrieben und eine typische Verteilungskurve angegeben.

Received December 14, 1961

JOURNAL OF POLYMER SCIENCE: PART A VOL. 1, PP. 1049–1053 (1963)

Radiation-Induced Cationic Polymerization of Ethylene

YONEHO TABATA and HIROSHI SHIBANO,
Department of Nuclear Engineering, University of Tokyo, and
HIROSHI SOBUE and KIYOSHI HARA,
Department of Industrial Chemistry,
University of Tokyo, Tokyo, Japan

Introduction

Radiation-induced polymerization of ethylene in the gasous state has been investigated by several workers.[1–5] Recently, solution polymerization of ethylene induced by ionizing radiation was also carried out by several investigators.[6,7] There has been no investigation of the radiation-induced polymerization of ethylene in the liquid state at low temperature. In this paper, the radiation-induced bulk polymerization of ethylene at −78°C. is reported.

Experimental

Ethylene monomer was purified by bubbling through 30% aqueous NaOH solution and 87% aqueous H_2SO_4 solution, and was dried by passage through a trap at −78°C. The polymerizations were carried out in 10 ml glass ampules by γ-rays from a Co^{60} source at −78°C. The ampule containing solid monomer was evacuated to 10^{-2}–10^{-3} mm. Hg. After irradiation, the ampule containing the irradiated monomer was sealed off at liquid nitrogen temperature and the unpolymerized monomer was evaporated at about −100°C. The experiments were carried out over the dose rate range of 4.9×10^4 to 1.04×10^5 r/hr. The effects of radical inhibitor and solvent on the polymerization were examined. The infrared spectra of the polymers obtained were also measured.

Results and Discussion

The relation between the polymer yield and irradiation time is shown in Figure 1. No induction period was observed in the liquid-state polymerization at −78°C. The relation between the polymer yield and irradiation dose under various dose rates is shown in Figure 2. These results indicate that the rate of polymerization is proportional to the dose rate for the liquid monomer at −78°C. It is well known that the rate of polymerization is proportional to the square root of the dose rate in a homogeneous

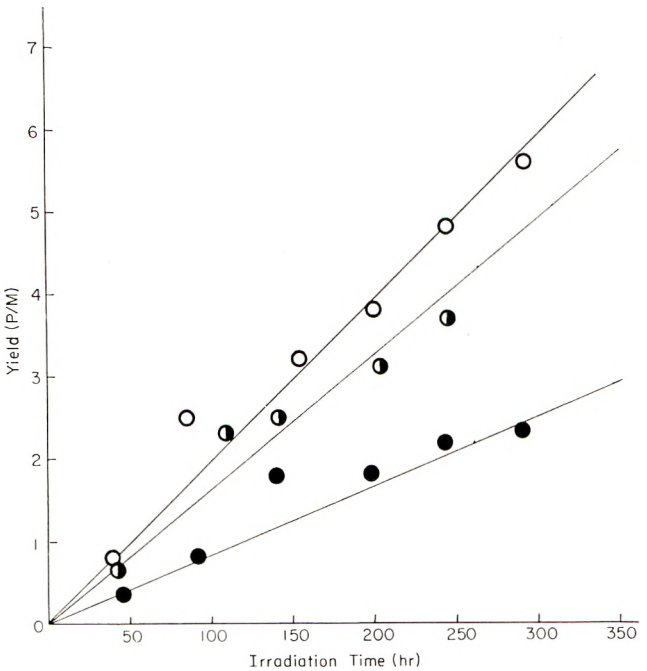

Fig. 1. Relation between the polymerization yield P/M (where P denotes mg. of the polymer obtained, and M is the volume of monomer in ml. at $-78°C$.) and irradiation time at various dose rates: (○) 1.04×10^5 r/hr.; (◑) 8.8×10^4 r/hr.; (●) 4.9×10^4 r/hr. Polymerization temperature $-78°C$.

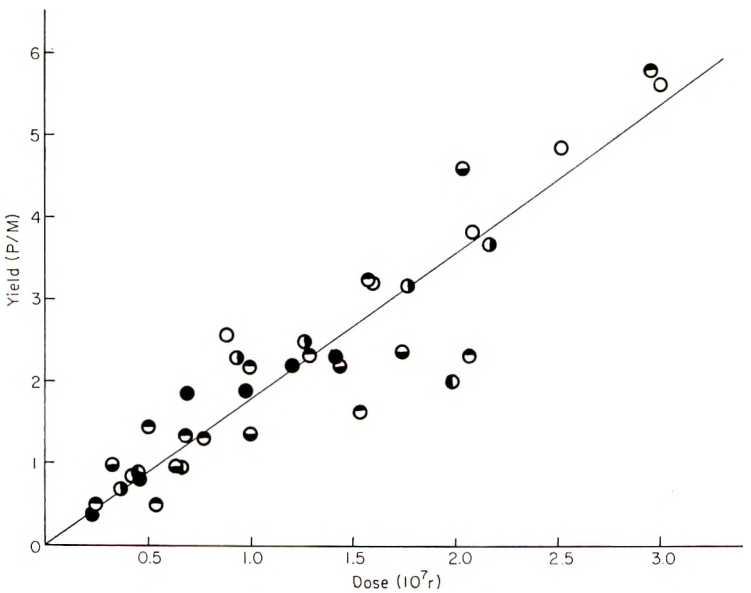

Fig. 2. Relation between the polymerization yield P/M and irradiation dose at various dose rates: (○) 1.04×10^5 r/hr.; (◑) 8.8×10^4 r/hr.; (◐) 8.0×10^4 r/hr.; (◒) 7×10^4 r/hr.; (◓) 6.4×10^4 r/hr.; (●) 4.9×10^4 r/hr.

TABLE I
Effects of Radical Inhibitor on Polymerization

Additive	Concn. of additive in ethylene monomer, %	Solvent	Irradiation dose, Mr	Relative yield
p-Benzo-quinone	0.75	CH_2Cl_2	5.2	1.11
Pyrogallol	0.63	None	8.3	1.27
	0.68	DMF	8.3	0.86
	0.58	None	8.3	1.15
DPPH	0.52	DMF	9.8	0.60
	0.49	DMF	8.2	1.62
	0.44	CH_2Cl_2	9.0	0.90
	0.57	None	7.9	0.84

radical polymerization and the rate is proportional to the first power of the dose rate in a homogeneous ionic one. These facts suggest that the polymerization of ethylene in bulk at −78°C proceeds by an ionic mechanism.

The effects of radical inhibitors on the polymerization are summarized in Table I.

It is apparent that the radical inhibitors had little effect on the polymerization. This also suggests that the polymerization proceeds by an ionic mechanism.

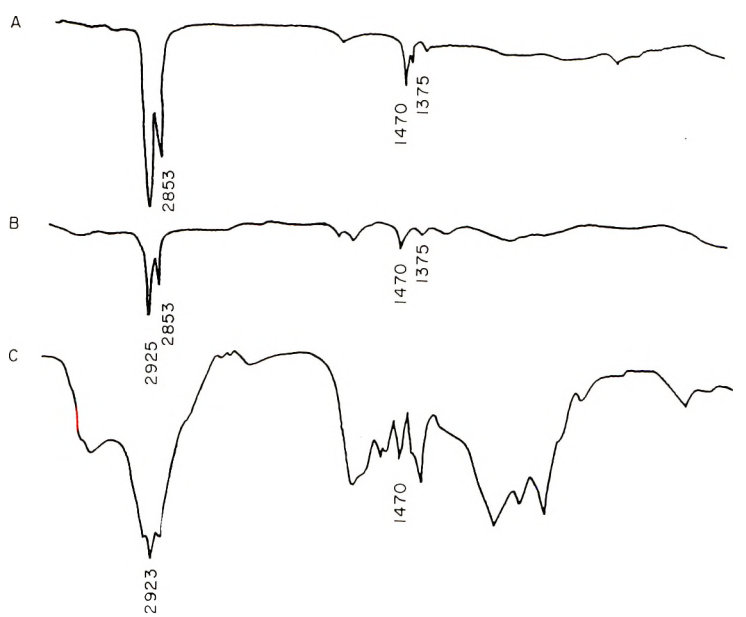

Fig. 3. Infrared spectra of the polymers obtained: (*A*) bulk polymerization, irradiation dose 2×10^7 r; (*B*) methylene chloride solution, irradiation dose 5×10^6 r; (*C*) isopropylamine solution, irradiation dose 10^7 r.

The effects of solvents on the polymerization of ethylene were examined at −78°C. It is generally found that methylene chloride accelerates a cationic polymerization, while amine solvents, such as dimethylformamide (DMF) and isopropylamine, accelerate anionic polymerizations. Polymerizations of ethylene were carried out both in methylene chloride and isopropylamine solutions. The infrared spectra of the products of the solution polymerizations are shown in Figure 3. It is apparent from these spectra that, though methylene chloride behaves purely as a solvent at a

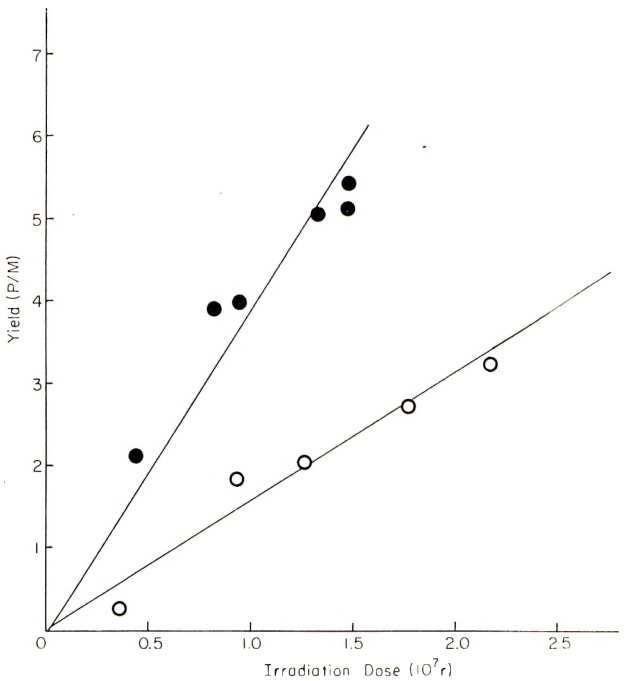

Fig. 4. The effect of methylene chloride on the polymerization: (●) methylene chloride solution (47 vol.-%), 8.0×10^4 r/hr.; (○) bulk, 8.8×10^4 r/hr.

relatively low irradiation dose below 10^7 r, isopropylamine reacts with ethylene cannot proceed in isopropylamine solution. A comparison of the rate of polymerization in ethylene chloride solution with that of the bulk polymerization at −78°C. is shown in Figure 4. It is evident from the figure that methylene chloride accelerates the polymerization of ethylene appreciably, suggesting a cationic mechanism for the liquid-state polymerization at −78°C.

It was concluded from the various experimental results described above that the polymerization of liquid ethylene at low temperature proceeds by a cationic mechanism.

References

1. Hayward, J., and R. Bretton, *Chem. Eng. Progr.*, **50**, 73 (1954).
2. Lewis, J. G., J. J. Martin, and L. C. Anderson, *Chem. Eng. Progr.*, **50**, 249 (1954).
3. Collinam, T., *J. Electrochem. Soc.*, **103**, 293 (1956).
4. Laird, R., A. Morrell, and L. Seed, *Discussions Faraday Soc.*, **22**, 126 (1956).
5. Hosaka et al., paper presented to 3rd Conference of Radioisotopes, Japan 1959.
6. Henly, E. J., and C. Chong, *J. Polymer Sci.*, **46**, 511 (1959).
7. Medvedev, S. S., A. D. Abkin, and P. M. Khomikovskiĭ, AEC Report 3894, Sept. 1959.

Synopsis

Radiation-induced polymerization of liquid ethylene was investigated at −78°C. No induction period was observed. The rate of polymerization was proportional to the first power of the dose rate. Radical scavengers did not inhibit the polymerization. On the other hand, methylene chloride accelerated the polymerization appreciably. It was concluded that the polymerization of liquid ethylene at low temperature proceeds by a cationic mechanism.

Résumé

La polymérisation de l'éthylène liquide induite par irradiation a été étudiée à −78°C. On n'a pas observé de période d'induction. La vitesse de polymérisation est proportionelle à la première puissance de la dose. Les capteurs de radicaux n'inhibent pas la polymérisation. D'autre part le chlorure d'éthylène accélère appréciablement la polymérisation. On en a conclu que la polymérisation de l'ethylène liquide à basse température procède par un mécanisme cationique.

Zusammenfassung

Die strahlungs-induzierte Polymerisation von flüssigem Äthylem wurde bei −78°C untersucht. Es wurde keine Induktionsperiode beobachtet. Die Polymerisationsgeschwindigkeit war der ersten Potenz der Dosisleistung proportional. Radikalfänger ergaben keine Inhibierung der Polymerisation. Andererseits wurde die Polymerisation durch Äthylenchlorid merklich beschleunigt. Es wurde gefolgert, dass die Polymerisation des flüssigen Äthylens bei niedriger Temperatur nach einem kationischen Mechanismus verläuft.

Received November 13, 1961
Revised December 23, 1961

JOURNAL OF POLYMER SCIENCE: PART A VOL. 1, PP. 1055–1068 (1963)

Crystal Structure Studies on the Polymorphic Forms of Nylons 6 and 8 and Other Even Nylons

DONALD C. VOGELSONG, *Carothers Research Laboratory, Textile Fibers Department, E. I. du Pont de Nemours and Company, Inc., Wilmington, Delaware*

INTRODUCTION

The crystal structure of polycaproamide (nylon 6) has been studied by several workers.[1–6] Holmes, Bunn, and Smith[6] have carried out the most detailed studies and shown that the lattice is monoclinic with four polymer chains passing through the unit cell. A second crystalline phase was shown to be present in certain nylon 6 fibers. From the x-ray photographs it was impossible, however, to decide conclusively the packing of the chains in this second form, called the β-phase.

More recently, Tsuruda, Arimoto, and Ishibashi[7] have shown that a second crystalline phase (pseudohexagonal) appears on treating drawn nylon 6 fibers with iodine–potassium iodide solutions. These authors and Ziabicki and Kedzierska[8] have shown that this new crystalline state can also be obtained by melt-spinning nylon 6 at very high speeds. Ziabicki[9] has recently discussed conversion of this pseudohexagonal phase to the normal monoclinic phase.

Several different chain packings have been proposed [6–8,11] to account for this second crystalline phase of nylon 6. Most of these, however, appear to be unacceptable, in that they propose structures with either incomplete amide hydrogen bonding or structures which possess large dipole–dipole repulsions. This would make the chain packing very unstable.

Schmidt and Stuart[10] and Slichter[11] have shown that x-ray patterns of normal drawn polycaprylamide (nylon 8) show a pseudohexagonal packing of the nylon chains. A second crystalline phase has also been reported[12] for nylon 8. X-ray pictures of this second modification of nylon 8 are indicative of a molecular packing similar to that present in normal monoclinic nylon 6. Because of the striking similarity of x-ray pictures of the polymorphic phases of nylons 6 and 8 (Figs. 1–4), it was felt that a detailed study of the structure of the second crystalline phase of nylon 6 would clear up some of the discrepancies existing in literature concerning this and the nylon 8 structure. The models proposed in this paper are consistent with the x-ray patterns and other experimental evidence. It is shown that the polymorphism results from a parallel and antiparallel packing of the polyamide chains for both nylons 6 and 8.

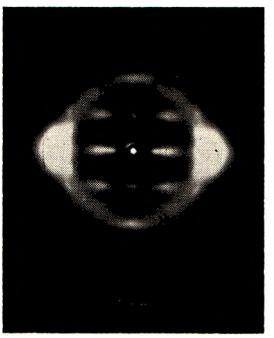

Fig. 1. Flat-plate x-ray diffraction pattern of nylon 6, α-phase. Fiber axis vertical.

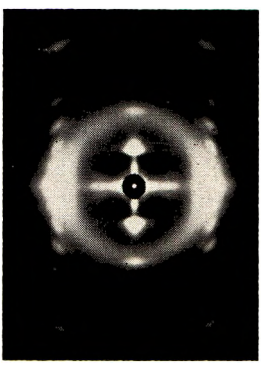

Fig. 2. Flat-plate x-ray diffraction pattern of nylon 6, γ-phase. Fiber axis vertical.

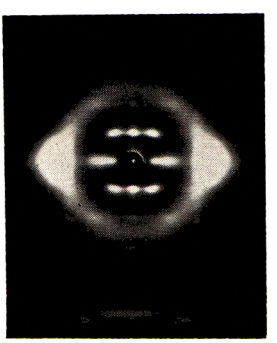

Fig. 3. Flat-plate x-ray diffraction pattern of nylon 8, α-phase. Fiber axis vertical.

EXPERIMENTAL

X-ray diffraction patterns were obtained with the use of nickel-filtered, copper Kα radiation. Flat-plate and cylindrical cameras were used. Sample-to-film distance was 5.0 cm. for both. Crystalline, drawn fibers of nylon 6 in the normal monoclinic state were soaked (taut) in aqueous 0.1M iodine and potassium iodide solutions overnight. The iodine was then washed out of the fibers via sodium thiosulfate and water. An x-ray

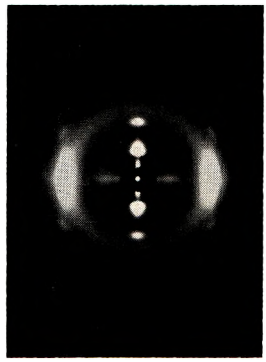

Fig. 4. Flat-plate x-ray diffraction pattern of nylon 8, γ-phase. Fiber axis vertical.

picture of the resulting fibers is shown in Figure 2. Preparation of the polymorphic phases of nylon 8 has been discussed elsewhere.[12] To increase crystallinity, all fibers were annealed taut at about 20°C. below their melting points for several hours. Reciprocal lattice coordinates were measured with the aid of the appropriate Bernal chart. Unit cell coordinates were calculated by standard reciprocal lattice methods.

The variety of shapes and sizes of the photographic sports of polymers makes it impossible to estimate directly the intergrated intensities, such as is done in most single crystal work. The method used in this research

TABLE I
Unit Cell Dimensions Determined From X-Ray Patterns

	Nylon 6 (monoclinic)[a]	Nylon 8 (monoclinic)	Nylon 6 (rhombohedral)[b]	Nylon 8 (rhombohedral)[b]
a, A.	9.56	9.8	4.79	4.79
b, A.	17.2	22.4	4.79	4.79
c, A.	8.01	8.3	16.7[c]	21.7[c]
β	67½°	65°	90°	90°
α	90°	90°	90°	90°
γ	90°	90°	60°	60°
No. of polymer chains passing through unit cell	4	4	1	1
Density, g./cm.³				
Calculated	1.23	1.13	1.13	1.09
Found	1.16	1.08	1.15[d]	1.07

[a] Data of Holmes et al.

[b] Although listed as rhombohedral, close examination of the diffraction pattern reveals that the lattice is slightly distorted from this symmetry. Evaluation of the Fourier transform for different models is affected very little by this lattice distortion.

[c] For the monoclinic lattices the fiber identity periods are the b axes; for the rhombohedral lattices, they are the c axes.

[d] This high density value is probably due to traces of iodine remaining in the fiber.

was to explore each spot separately with the aid of a Leeds and Northrup photometer. Peak intensities measured were then corrected for crystallite disorientation effects.[13] This gave a set of relative integrated intensities. The meridional intensities were obtained by oscillation and rotation of the fibers about an axis perpendicular to the x-ray beam. Under these conditions it was possible to calculate Lorentz polarization terms for the meridional diffraction spots. The many computations necessary for comparing calculated diffraction patterns from proposed models with the observed diffraction pattern were carried out on a Bendix computer.

RESULTS

Typical x-ray diffraction patterns of nylons 6 and 8 exhibiting the different polymorphic forms are shown in Figures 1–4. The diffraction spots can be indexed by the unit cells in Table I.

1. Structure and Molecular Packing of Monoclinic Nylons 6 and 8

Comparison of the unit cells listed in Table I indicates that the polyamide molecular chain packings are very similar for monoclinic nylons 6 and 8. The fiber identity period for nylon 8, 22.4 A., is the same as that found by Bunn and Garner[13] for nylon 6 10. This value is in good agreement with the theoretical value, 22.48 A., calculated for a planar chain with the accepted bond lengths and angles. The nylon 8 a and c coordinates, however, are slightly larger those values for the nylon 6 (Brill[1] gives these values for nylon 6 as 9.60 and 8.32 A., with an angle of 65° separating them) and indicates a "looser" packing of the chains for nylon 8 than nylon 6.

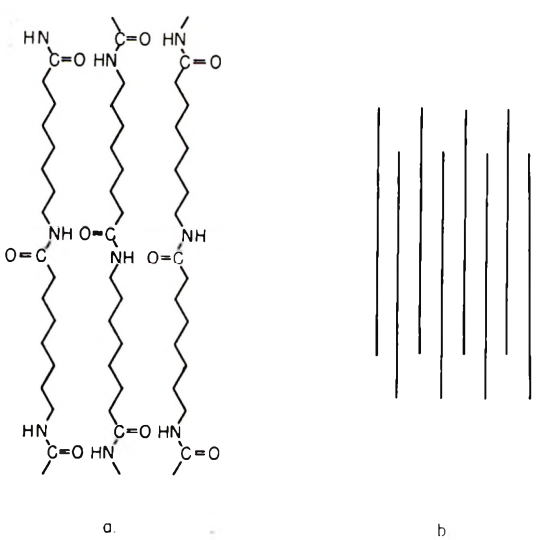

Fig. 5. Structure of nylon 8, α-phase: (a) schematic view of antiparallel chain structure; (b) several of the sheets as pictured in Fig. 5a viewed edgewise showing how the three-dimensional lattice is built up.

The NH—O hydrogen bonds are about 0.1 A. longer in the nylon 8 structure than in the nylon 6. Figure 5 shows the antiparallel chain packing proposed for nylon 8. Further proof of this structure by comparison of the intensities calculated from this model with the intensities observed in the x-ray pattern is not felt warranted in view of the work of Holmes et al.[6]

2. Structure and Molecular Packing of the Rhombohedral or Pseudohexagonal Phases of Nylons 6 and 8

The unit cells which can be used to index the diffraction spots in x-ray patterns of nylons 6 and 8 exhibiting this second crystalline phase are listed in Table I. Kinoshita[15] has recently studied the molecular packing of many different types of linear polyamides; and all of those exhibiting

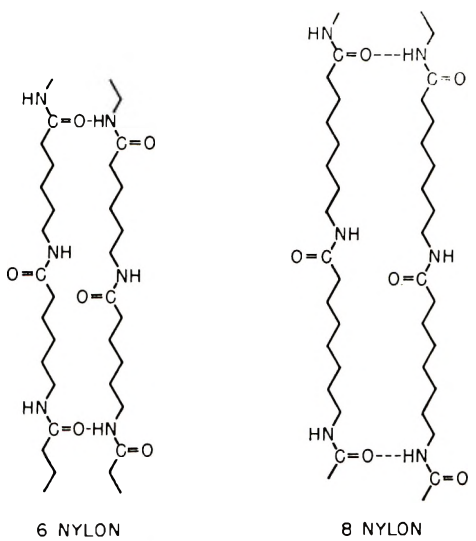

Fig. 6. Schematic view of parallel structure of nylons 6 and 8. Only 50% of the hydrogen bonds would be formed when the chains are fully extended.

this rhombohedral, or pseudohexagonal, packing of the chains have been termed γ-phase. This notation will be followed throughout the remainder of this paper. It is felt, though, that this phase is the same as the β-phase discussed in by Holmes et al.[6] and Ziabicki.[9]

Once having found unit cells which account for the geometric positions of diffraction spots in the x-ray patterns, the next step is to position the atoms within the unit cells. Several models have been proposed[6,7,9–11] for the molecular packing in the γ-phase of nylons 6 and 8. These models are all unacceptable, in that they propose either fully extended chains or require larger unit cells than found. The fiber identity periods listed in Table I for the γ-phase packings are shorter than those for the monoclinic phases, indicating a twist in the polyamide chains. The unit cells with

only one nylon chain passing through them indicate a parallel structure within the crystallite regions. In other words, all nylon chains run in the same direction. This differs from the monoclinic (or α-phase) packing, where alternate nylon chains run in opposite directions.

One question that must be answered, of course, is: Why is the fiber identity period shortened for the γ-phases? To answer this question, Figure 6 shows that when the nylon chains run in the same direction, only 50% of the NH—O hydrogen bonds can be made. The infrared work of Trifan and Terenzi[16] and others[7,15] has shown that for nearly all linear polyamides the hydrogen bonding is complete. Kinoshita[17] has recently proposed a model for the structure of nylon 7 in which the hydrogen-bonding requirements are satisfied by tilting the amide planes approximately 30° with respect to the fiber axis. Such a configuration is brought about by rotation around the C—C and C′—N single bonds of the groups

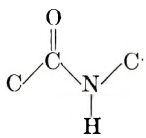

and would obviously cause a shortening of the fiber identity period.

Applying this concept of amide tilting to the structures of the γ-phase of nylons 6 and 8 shows that a reasonable model can be built which satisfies both the unit cell requirements and allows complete hydrogen bonding. Closer examination of this model, however, reveals that two equally probable nylon chain packings are possible. The first (Fig. 7) has the hydrogen-bonded amide groups lying near the 100 planes. Each nylon chain is thus hydrogen-bonded to two of its nearest neighbors, giving the

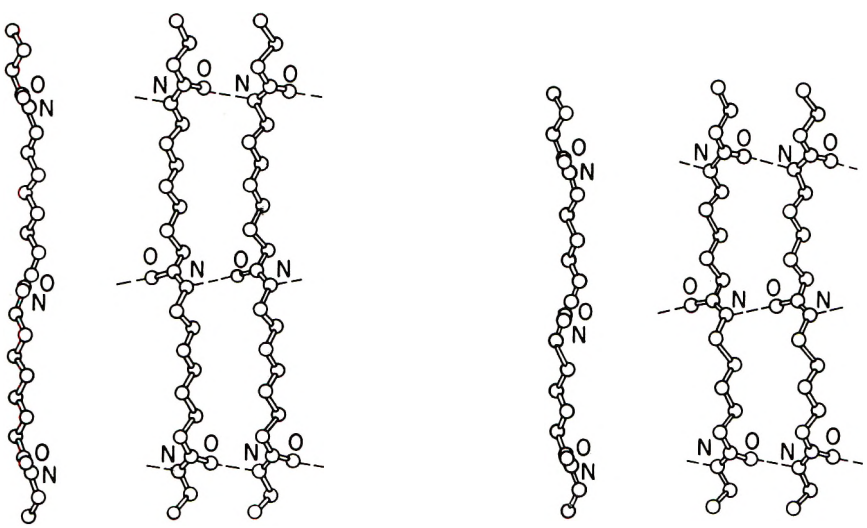

Fig. 7. Pleated sheet structure of (*a*) nylon 8, γ-phase; (*b*) nylon 6, γ-phase. Right: front views; left: side views.

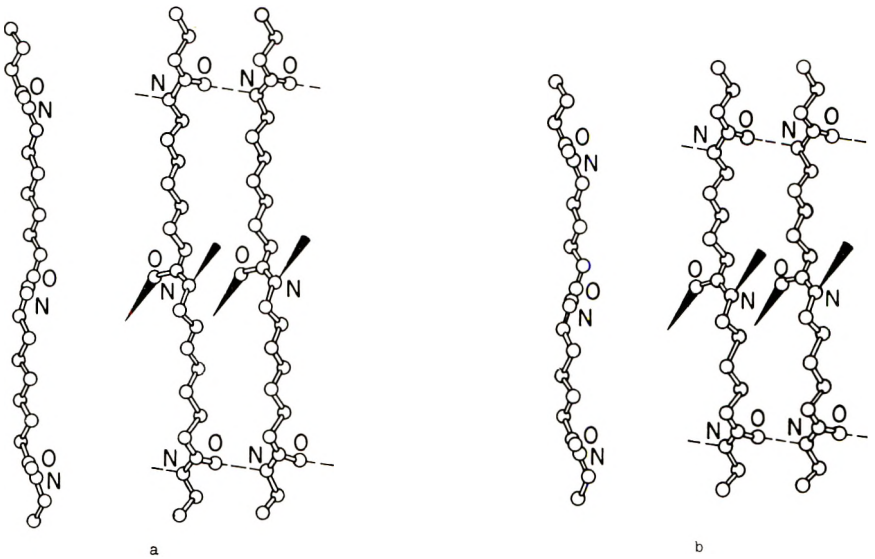

Fig. 8. Hydrogen-bonded amide groups alternate between and lie close to the 100 and 010 planes in (*a*) nylon 8, γ-phase; (*b*) nylon 6, γ-phase. Right: front views; left: side views.

appearance of a pleated sheet structure. The second (Fig. 8) is slightly different, in that as one progresses along a nylon chain the hydrogen-bonded planar amide groups alternate between the 100 and 010 planes. This can occur by slight rotations about the methylene groups. In this model each nylon chain is hydrogen-bonded to four of its neighbors. For both of these structures, the amide planes are tilted approximately 30° off the fiber axis. The carbonyl oxygen atoms all lie in planes perpendicular to the fiber axis. This would account for the increased intensity of the meridional diffraction spots of the γ-phase x-ray patterns over those of the monoclinic phase (see Figs. 1–4). In neither model, however, do the chains possess truly hexagonal symmetry. Thus, in the crystallographic sense, the term pseudohexagonal has been used.

In an effort to tell which of these two structures better represents the true molecular packing, coordinates of the heavy atoms for both of these models for γ-phase nylon 6 were measured. These were used to calculate intensities of the diffraction spots for comparison with the observed intensities. The coordinates were somewhat refined by a trial and error process. The calculated intensities are proportional to the square of the structure factor multiplied by Lorentz and polarization factors and by a temperature factor, $\exp\{-B(\sin\theta/\lambda)^2\}$, where $B = 10.0$ A^2. The scattering powers of C, O, CH_2, and NH were assumed to be in the ratio of 6:8:8:8 and were calculated by the analytical expression of Vand, Eiland, and Pepinsky.[18] A list of the atomic coordinates used in the final intensity calculations are given in Tables II and III. Carbon bond lengths and angles and the bond lengths and angles given by Corey and Pauling[19] for

amide groups in polypeptides were used. Normal van der Waal's contact radii between chains were also used. Because of the pseudohexagonal symmetry, each reflection of the type (hkl) is in most cases superimposed on corresponding reflections; the values of I_{calc} listed in Table IV comprise the sum of the contributions of such planes.

Of the two models listed in Table IV, the calculated scattering pattern of the one in which alternate amide groups of the nylon chain lie near the 100 and 010 planes appears to agree somewhat better with the observed. Other

TABLE II

Atomic Coordinates for Structure with Hydrogen Bonds Alternating Between 100 and 010 Planes

	X/a	Y/b	Z/c
C	+0.007	−0.011	+0.965
O	+0.000	+0.249	+0.978
CH_2	+0.202	−0.217	+0.893
CH_2	+0.086	−0.031	+0.814
CH_2	+0.145	−0.268	+0.745
CH_2	+0.008	−0.090	+0.666
CH_2	+0.118	−0.337	+0.597
NH	+0.101	−0.190	+0.517
C	−0.146	−0.087	+0.470
O	−0.398	−0.093	+0.483
CH_2	−0.111	+0.060	+0.390
CH_2	−0.113	−0.137	+0.317
CH_2	−0.211	−0.079	+0.241
CH_2	−0.183	−0.123	+0.166
CH_2	−0.309	+0.099	+0.092
NH	−0.158	−0.081	+0.017

TABLE III

Atomic Coordinates for Structure with Hydrogen Bonds All Lying Near 100 Planes

	X/a	Y/b	Z/c
NH	+0.125	+0.139	+0.989
C	−0.010	+0.015	+0.944
O	+0.008	−0.252	+0.959
CH_2	−0.196	+0.200	+0.868
CH_2	−0.057	+0.003	+0.791
CH_2	−0.172	+0.231	+0.717
CH_2	−0.041	+0.041	+0.638
CH_2	−0.189	+0.265	+0.563
NH	−0.020	+0.116	+0.488
C	+0.108	+0.242	+0.441
O	+0.091	+0.506	+0.451
CH_2	+0.271	+0.051	+0.365
CH_2	+0.133	+0.243	+0.286
CH_2	+0.300	+0.206	+0.214
CH_2	+0.209	+0.220	+0.134
CH_2	+0.314	−0.019	+0.003

reasons for believing this model more closely approximates the actual structure are: (*1*) This model better explains why the *a* and *b* axis of the unit cell are equal, and (*2*) hot-camera x-ray studies show that, as the temperature of the fiber is raised, at no time does the single intense diffraction spot split into two spots. (One would except for the other model that thermal expansion would be greater between the sheets, which are held together only by van der Waal's bonds, than between hydrogen-bonded chains.) This is true right up to the melting point. Cooling from the melt, however, leads to monoclinic nylon 6. In the case of nylon 8, heating either phase to the melt and then cooling produces only the γ-phase. The conclusions on the structures of the polymorphic phases of nylon 6 are directly applicable to the crystallite phase of nylon 8.

3. Structures of Other Even Nylons

Bamford, Brown, et al.[20] have shown that nylon 2 (polyglycine) is also polymorphic. Although one of these structures is described in terms of the β-structure of polypeptides, the present paper indicates that it might be a monoclinic packing similar to that of nylons 6 and 8. Crick and Rich[21] have shown that the structure of the second form of nylon 2 is helical. In this structure all chains are parallel, and each one has a three-fold screw axis. The chains pack in a truly hexagonal array, each chain being hydrogen-bonded to each of its six neighbors. This structure is similar to the model proposed for the γ-phases of nylon 6 and 8, but involves three chemical repeats (rather than two) for the identity period. Molecular models show that a two-residue helix for nylon 2 would be quite strained.

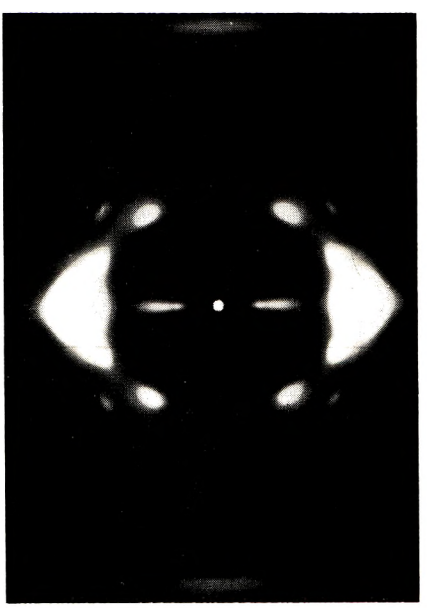

Fig. 9. Flat-plate x-ray diffraction pattern of nylon 4, α-phase. Fiber axis vertical.

TABLE IV
Comparison of Observed and Calculated Intensities

hkl	I_{obs}	I_{calc} (model proposed in Table II)	I_{calc} (model proposed in Table III)
100, 010, 110	286	286	286
1$\bar{1}$0, 210, 120	13.7	12	28.5
200, 020, 220	4.1	3.8	4.5
320, 230, 130, $\bar{1}$20, 2$\bar{1}$0	4.6	0.3	5.5
300, 030, 330	0	0	1
2$\bar{1}$0	0	0	0
1$\bar{3}$0	0	0	2
310	0	0	0.5
2$\bar{3}$0	0	0	0.5
101, 011, 111	67	79	171
211, 121, 1$\bar{1}$1	6.5	7	28.5
201, 021, 221	3.4	5.5	16.5
102, 012, 112	13.8	9.5	14.5
122, 212, 1$\bar{1}$2	0	5.5	2

(*continued*)

Drawn fibers of nylon 4 show monoclinic packing of the polyamide chains (Fig. 9). Unfortunately, much of the detail of the original x-ray pattern is lost in the reproduction. The unit cell determined from this pattern is: $a = 9.44$ A., $b = 12.1$ A., $c = 8.22$ A., $\beta = 64°$, indicating an antiparallel structure such as found for the monoclinic forms of nylons 6 and 8. The fiber identity period indicates fully extended chains. No evidence of a second polymorphic form has yet been found for nylon 4.

TABLE IV (*continued*)

hkl	I_{obs}	I_{calc} (model proposed in Table II)	I_{calc} (model proposed in Table III)
013 103 113	8.5	33.5	17.5
123 213 1$\bar{1}$3	3.3	3.5	3.5
104 014 114	7.8	5	20
124 214 1$\bar{1}$4	0	3	0
105 015 115	6.0	25.5	8.5
106 016 116	16	16	31.5
216 126 1$\bar{1}$6	3.5	3.5	10
206 026 226	4.1	8	8
107 017 117	7.5	14.5	32.5
002	20	15.5	25
004	5	6.3	9
006	1.5	4.5	5.5
008	1	2.4	3
0010	0.5	1.5	2
0012	1	2.3	5
0014	3	4	3.5
0016	0	0	0.3

Molecular models show that the structure proposed by Crick and Rich[21] for polyglycine II is also possible for the other even nylons. That this is not the structure of γ-phase nylons 6 and 8 is evidenced by the lack of the threefold screw symmetry in the x-ray diffraction patterns.

DISCUSSION

Polymorphism has been shown to be present in many of the even nylons. Unlike the polymorphic structures found for nylons 66 and 610,[14] which

result from a different stacking of sheets containing hydrogen-bonded polyamide chains, polymorphism in the even nylons results from the fact that the chains possess a sense of direction. A parallel and an antiparallel packing of the nylon chains is possible. Actual polyamide chain conformation present in these two phases is governed by amide hydrogen bonding between the chains. For example, in the antiparallel structure (alternate chains running in opposite directions), complete hydrogen bonding is possible for fully extended nylon chains. X-ray pictures of fibers in this state show the chains to be fully extended. In the parallel structure (all chains running in the same direction), complete hydrogen bonding is not possible for fully extended nylon chains. Hence, the nylon chains twist to satisfy this requirement. X-ray pictures of fibers in this state show that the crystal repeat, or identity period, along the fiber axis is shorter than one computes for fully extended chains.

Between nylons 6 and 8 there appears to be a transition between the thermodynamic stabilities of the polymorphic chain packings. Antiparallel chain packing appears to be the common form of nylons 4 and 6. Parallel chain packing appears to be the common form of nylons 8 and 10. Apparently, when sufficient flexibility is given to the even nylon chains by the addition of methylene groups, the twisted chain structure is favored. This is also borne out by the fact that when either phase of nylon 6 is melted, only the antiparallel phase results on cooling. When either phase of nylon 8 is melted, only the parallel structure results on cooling.

Note Added in Proof: H. Arimoto has recently published a paper (*Chem. High Polymers (Japan)*, **19,** 204, 212, 1962) in which a structure is hypothesized for γ-phase nylon 6. In this structure the parallel nylon 6 chains are hydrogen-bonded together to form pleated sheet-type planes. The sheets then pack together in the buildup of the three-dimensional lattice. Alternating sheets, however, contain antiparallel nylon 6 chains which would lead to a unit cell with more than one chain passing through it. Because the γ-phase nylon 6 x-ray diffraction pattern shows no evidence for such a large unit cell, it is felt the model proposed in the present paper better fits the experimental data.

References

1. Brill, R., *Z. physik Chem.*, **B53,** 61 (1943).
2. Broser, V. W., K. Goldstein, and H. E. Krüger, *Kolloid Z.*, **106,** 187 (1944).
3. Wallner, L. G., *Monatsch. Chem.*, **79,** 279 (1948).
4. Kordes, E., F. Günther, L. Büchs, and W. Göttner, *Kolloid Z.*, **119,** 23 (1950).
5. Okada, A., and K. Fuchino, *Chem. High Polymers (Japan)*, **7,** 122 (1950).
6. Holmes, D. R., C. W. Bunn, and D. J. Smith, *J. Polymer Sci.*, **17,** 159 (1955).
7. Tsuruda, M., H. Arimoto, and M. Ishibashi, *Chem. High Polymers (Japan)*, **15,** 619 (1958).
8. Ziabicki, A., and K. Kedzierska, *J. Appl. Polymer Sci.*, **2,** 14 (1959).
9. Ziabicki, A., *Kolloid Z.*, **167,** 132 (1960).
10. Schmidt, G. F., and H. A. Stuart, *Z. Naturforsch.*, **13a,** 222 (1958).
11. Slichter, W. P., *J. Polymer Sci.*, **36,** 259 (1959).
12. Vogelsong, D. C., and E. M. Pearce, *J. Polymer Sci.*, **45,** 546 (1960).
13. Franklin, R. E., and R. G. Gosling, *Acta Cryst.*, **6,** 678 (1953).
14. Bunn, C. W., and E. V. Garner, *Proc. Roy. Soc. (London)*, **A189,** 39 (1947).

15. Kinoshita, Y., *Makromol. Chem.*, **33**, 1 (1959).
16. Trifan, D. S., and J. F. Terenzi, *J. Polymer Sci.*, **28**, 443 (1958).
17. Kinoshita, Y., *Makromol. Chem.*, **33**, 21 (1959).
18. Vand, V., P. F. Eiland, and R. Pepinsky, *Acta Cryst.*, **10**, 303 (1957).
19. Corey, R. B., and L. Pauling, *Proc. Roy. Soc. (London)*, **B141**, 10 (1953).
20. Bamford, C. H., L. Brown, E. M. Cant, A. E. Elliot, W. E. Hanby, and B. R. Malcom, *Nature*, **176**, 396 (1955).
21. Crick, F. H. C., and A. Rich, *Nature*, **176**, 780 (1955).

Synopsis

Polymorphism present in the even nylons has been accounted for in terms of parallel and antiparallel packing of the polyamide chains. Hydrogen bonding appears to play the most important part in governing chain packing. For example, in the antiparallel structure (alternate chains running in opposite directions), complete hydrogen bonding is possible for fully extended planar zigzag nylon chains. In the parallel structure (all chains running in the same direction) complete hydrogen bonding is not possible for the fully extended nylon chains. Hence, the nylon chains twist to satisfy this requirement. This has been shown by interpretation of the x-ray diffraction pattern of γ-phase nylon 6. Between nylons 6 and 8 there appears to be a transition between the thermodynamic stabilities of the polymorphic chain packings. Antiparallel chain packing appears to be the common form of nylons 4 and 6. Parallel chain packing appears to be the common form of nylons 8 and 10. Apparently, when sufficient flexibility is given to the even nylon chains by the addition of methylene groups, the twisted chain structure is favored.

Résumé

Le polymorphisme présent dans les nylons à nombre pair d'atomes de carbone a été traité en termes de tassement parallèle et antiparallèle des chaînes de polyamide. Les liaisons-hydrogène semblent jouer le rôle le plus important dans le tassement des chaînes. Par exemple dans la structure antiparallèle (chaîne se dirigeant alternativement dans des sens opposés) la liaison par pont hydrogène est entièrement possible pour les chaînes en zigzag du nylon complètement étendues dans le plan. Dans la structure parallèle (toutes les chaînes dirigées dans le même sens) le liaison par pont-hydrogène n'est pas entièrement possible pour les chaînes de nylon complètement étendues. Dès lors, les chaînes de nylon se tordent pour satisfaire à cette exigence. Ceci a été montré par interprétation du réseau de diffraction des rayons-X pour du nylon-6 de phase gamma. Entre des nylons 6 et 8 apparait une transition entre les stabilités thermodynamiques des tassements de chaînes polymorphiques. Le tassement antiparallèle semble être la forme habituelle des nylons 8 et 10. Apparemment, lorsqu'on donne suffisamment de flexibilité aux chaîne de nylon à nombre pair d'atomes de carbone par addition de groupements méthylène, la structure de chaîne tordue est favorisée.

Zusammenfassung

Die bei geradzahligen Nylons auftretende Polymorphie wurde auf Grund der Parallel- und Antiparallelpackung der Polyamidketten erklärt. Wasserstoffbindung scheint die wichtigste Rolle bei der Festlegung der Kettenpackung u spielen. Zum Beispiel ist bei der antiparallelen Struktur (Ketten abwechselnd in der entgegengesetzten Richtung) eine vollständige Ausbildung der Wasserstoffbundung für völlig gestreckte, ebene Zick-Zack-Nylonketten möglich. Bei der Parallelstruktur (alle Ketten laufen in der gleichen Richtung) ist für völlig gestreckte Nylonketten keine vollständige Wasserstoffbindung möglich. Daher verdrehen sich die Ketten, um dieser Bedingung genüge zu leisten. Einen Beweis dafür lieferte die Auswertung des Röntgendiagramms der γ-Phase von

6-Nylon. Zwischen 6- und 8-Nylon scheint ein Übergang in der thermodynamischen Stabilität der polymorphen Kettenpackung stattzufinden. Antiparallele Kettenpackung scheint die gemeinsame Form für 8- und 10-Nylons zu sein. Offenbar wird bei genügender Flexibilität der geradzahligen Nylonketten durch zusätzliche Methylengruppen die verdrehte Kettenstruktur begünstigt.

Received January 17, 1962.

JOURNAL OF POLYMER SCIENCE: PART A VOL. 1, PP. 1069–1077 (1963)

Calculation of the Displacement Distance for a Three-Choice Cubic Lattice Chain

NOBORU TOKITA* and W. R. KRIGBAUM, *Department of Chemistry, Duke University, Durham, North Carolina*

The effect of short-range interactions upon the overall molecular conformation has been a problem of continuing interest to the polymer chemist. In brief, the rotation about a particular chain bond must take place in the force field created by near-by atoms or groups along the chain. The repulsive forces may be due to overlapping electron clouds or dipolar interactions, and they depend upon the particular structure of the neighboring group and upon the rotational positions of a limited number of the preceding chain bonds.

The early results of Benoit,[1] Kuhn,[2] and Taylor[3] expressed the mean-square unperturbed displacement length, $\overline{L_0^2}$, for a chain composed of N bonds of length b as:

$$\overline{L_0^2} = Nb^2[(1 - \cos\theta)/(1 + \cos\theta)(1 + \overline{\cos\phi})/(1 - \overline{\cos\phi})] \qquad (1)$$

Here θ is the valence angle and $\overline{\cos\phi}$ is an average calculated with the assumption that positive and negative values of the rotational angle ϕ occur with equal probability and in random sequence along the chain. Vol'kenshtein[4] proposed a simplified model in which only a limited number of rotational "states" of low energy (rotational isomers) were considered. Using this model he and his collaborators developed relationships for a number of the stereoisomeric forms, assuming no correlation between the successive rotations. Somewhat later Ptitsyn and Sharonov[5] considered the case in which the rotation about every other bond was correlated with that of its predecessor, thereby taking into account the interactions of large pendant groups on vinyl polymers. These developments are well treated in a book by Vol'kenshtein.[6] Finally, a number of authors have succeeded in treating model chains in which the rotation about each bond is correlated.[7–9]

One may take the view that the theoretical problem posed by short-range interactions is now solved, at least in principle. In practice one finds that the final result of these latter treatments is a set of matrix equations, and that considerable numerical calculation must be undertaken before conclusions can be drawn for any particular case. This is not an

* Present Address: U.S. Rubber Research Center, Wayne, New Jersey.

insuperable obstacle, and some very important practical results have been forthcoming. As examples one may cite the computations of Hoeve for polyethylene[10] and those of De Santis et al.[11] and Natta et al.[12] which predict the most stable helical conformation for crystalline stereoregular polymers. Nevertheless, we felt that it would be worth while to treat a less realistic model, one of sufficient simplicity that the problem of completely correlated rotations could be solved in a closed form analogous to eq. (1). This would facilitate a detailed comparison of the importance of the various factors which influence the chain conformation, and might have the practical result of diminishing the number of computations required for the exact treatment of a particular case of interest. The model we have chosen is a variant of the cubic lattice chain used by one of us in work on rubberlike elasticity.[13]

I. Theoretical Treatment

We will start from a simple model having a bond angle of 90° and three minimum potential positions around the bond axis; two of them correspond to the *cis* form, say +90° and −90°, and the other one the *trans* form, 180°. An orthogonal coordinate system is attached to each chain bond, so that the z-axis lies along the bond axis. The y-axis is located in the plane defined by this bond and the previous one. The x-axis forms a right-handed coordinate system with the y and z-axes, as shown in Figure 1. The direction of the rotation angle ϕ is measured in the direction counterclockwise from the *cis* structure.

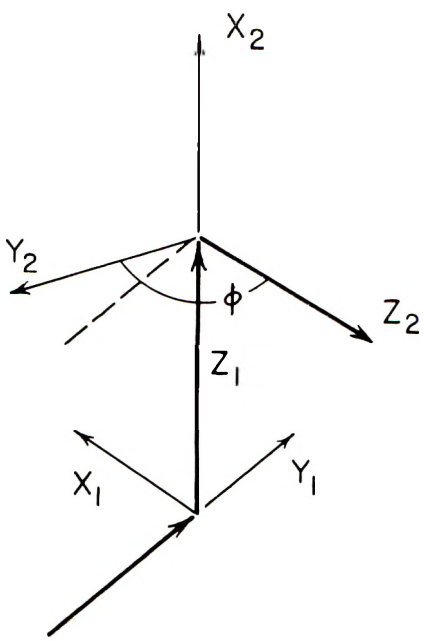

Fig. 1. An illustration of the chain coordinate system.

The transformation matrix T_K, which transforms the $(k + 1)$th coordinate system into the kth is given as follows:[14]

$$T_K = \begin{vmatrix} \cos\phi_K & \sin\phi_K & 0 \\ -\alpha\sin\phi_K & \alpha\cos\phi_K & \beta \\ \beta\sin\phi_K & -\beta\cos\phi_K & \alpha \end{vmatrix} \tag{2}$$

If the bond angle is 90° and the rotational angle ϕ is +90°, −90°, or 180°, we have three transformation matrices:

$$T^+ = \begin{vmatrix} 0 & 1 & 0 \\ 0 & 0 & 1 \\ 1 & 0 & 0 \end{vmatrix}, \quad T^- = \begin{vmatrix} 0 & -1 & 0 \\ 0 & 0 & 1 \\ -1 & 0 & 0 \end{vmatrix}, \quad T^\circ = \begin{vmatrix} -1 & 0 & 0 \\ 0 & 0 & 1 \\ 0 & 1 & 0 \end{vmatrix} \tag{3}$$

The mathematical method used here is an application of the matrix procedure developed by Hoeve.[9] With the transformation matrix described above, the end-to-end distance of a chain molecule can be represented in the following way:

$$L = (1 + T_1 + T_1T_2 + T_1T_2T_3 + \ldots + T_1T_2 \ldots T_{n-1})\begin{pmatrix} 0 \\ 0 \\ b \end{pmatrix}$$

Here $\begin{pmatrix} 0 \\ 0 \\ b \end{pmatrix}$ is the column vector representing the bond axis. The square L^2 is obtained by multiplying L^* by its transpose:

$$L^2 = (00b)(1 + T_1^* + T_2^*T_1^* + \ldots + T_{n-1}^*T_{n-2}^* \ldots T_1^*) \times (1 + T_1 + T_1T_2 + \ldots + T_1T_2 \ldots T_{n-1})\begin{pmatrix} 0 \\ 0 \\ b \end{pmatrix} \tag{4}$$

Since only the elements of the third row and third column of the matrix products contribute to the result, the operation, $T_2^*T_1^*$ may be replaced by its transpose T_1T_2. Hence the average value of eq. (4) can be described as follows:

$$\overline{L_0^2} = Nb^2(0, 0, 1)[E + 2(\bar{T}_\nu + \overline{T_{\nu+1}T_\nu} + \overline{T_{\nu+2}T_{\nu+1}T_\nu} + \ldots)]\begin{pmatrix} 0 \\ 0 \\ 1 \end{pmatrix} \tag{5}$$

where E is the unit matrix of order three and:

$$\begin{aligned} \bar{T}_\nu &= [1/(n-1)](\bar{T}_1 + \bar{T}_2 + \ldots + \bar{T}_{n-1}) \\ \overline{T_{\nu+1}T_\nu} &= [1/(n-2)](\overline{T_2T_1} + \overline{T_3T_2} + \ldots + \overline{T_{n-1}T_{n-2}}) \\ \overline{T_{\nu+2}T_{\nu+1}T_\nu} &= [1/(n-3)](\overline{T_3T_2T_1} + \ldots) \end{aligned} \tag{6}$$

If there exists a correlation between every pair of consecutive rotations, the a priori probability $a_{jk}(\nu, \nu + 1)$ that the rotational angles around bonds ν and $\nu + 1$ are $\phi_\nu^{(j)}$ and $\phi_{\nu+1}^{(k)}$, respectively, is given by:

$$a_{jk}(\nu, \nu + 1) = a_j(\nu)[C_{jk}(\nu, \nu + 1)]$$

and furthermore:

$$a_{jkl}(\nu, \nu + 1, \nu + 2) = a_j(\nu)C_{jk}(\nu, \nu + 1)C_{kl}(\nu + 1, \nu + 2), \text{ etc.}$$

Here $C_{jk}(\nu, \nu + 1)$ is an element of the transition probability matrix $[C]$. For the transition probability matrix in the present case we assume that there exist three minimum potential positions about the bond axis:

$$[C(\nu, \nu + 1)] = \begin{array}{c|ccc} & (+90°) & (180°) & (-90°) \\ (+90°) & c_1 & 1 - (c_1 + c_3) & c_3 \\ (180°) & (1 - c_2)/2 & c_2 & (1 - c_2)/2 \\ (-90°) & c_3 & 1 - (c_1 + c_3) & c_1 \end{array} \tag{7}$$

$$1 - (c_1 + c_3) = p, \quad (1 - c_2)/2 = q$$

By using the super matrix $[S]$ defined by Hoeve, the average value of products $\overline{T_{\nu+1}T_\nu}$, etc., may be obtained:

$$[S] = [C]\begin{vmatrix} T^+ & 0 & 0 \\ 0 & T^\circ & 0 \\ 0 & 0 & T^- \end{vmatrix} = \begin{vmatrix} c_1T^+ & pT^\circ & c_3 \\ qT^+ & c_2T^\circ & qT^- \\ c_3T^+ & pT^\circ & c_1T^- \end{vmatrix} \tag{8}$$

Each element of the super matrix $[S]$ is a three-by-three matrix defined by eq. (3). Furthermore, let the following matrices be defined:

$$[V] = (a_+T^+, a_0T^\circ, a_-T^-) \tag{9}$$

and

$$[X] = \begin{vmatrix} [E] \\ [E] \\ [E] \end{vmatrix}$$

where a_+, a_0, and a_- are the a priori probabilities for each rotational angle without any correlation, and $[E]$ is the three-by-three unit matrix.

Using the matrices shown in eqs. (8) and (9):

$$\overline{T}_\nu = [V][X], \quad \overline{T_{\nu+1}T_\nu} = [V][S][X], \quad \overline{T_{\nu+2}T_{\nu+1}T_\nu} = [V][S]^2[X], \text{ etc.}$$

Thus, eq. (5) can be restated in the following way:

$$\overline{L_0^2} = Nb^2(001)([E] + 2[V]|\mathbb{E} - [S]|^{-1}[X])\begin{pmatrix} 0 \\ 0 \\ 1 \end{pmatrix} \tag{10}$$

where $\mathbb{E}$ is the unit matrix of order $3 \times 3 = 9$.

The calculation of eq. (10) for three-choice model proceeds through use of the super matrix shown in eq. (8):

$$|\mathbb{E} - [S]| = \begin{vmatrix} (1 - c_1T^+) & -pT^\circ & -c_3T^- \\ -qT^+ & (1 - c_2T^\circ) & -qT^- \\ -c_3T^+ & -pT^\circ & (1 - c_1T^-) \end{vmatrix} \tag{11}$$

Equation (11) can be rewritten in another way, namely:

$$|\mathbb{E} - [S]| = \begin{vmatrix} T_{11} & T_{12} & T_{13} \\ T_{21} & T_{22} & T_{23} \\ T_{31} & T_{32} & T_{33} \end{vmatrix} = [T] \tag{12}$$

Furthermore, the inverse super matrix $|\mathbb{E} - [S]|^{-1}$ is defined as follows:

$$|\mathbb{E} - [S]|^{-1} = \begin{vmatrix} Q_{11} & Q_{12} & Q_{13} \\ Q_{21} & Q_{22} & Q_{23} \\ Q_{31} & Q_{32} & Q_{33} \end{vmatrix} = [Q] \tag{13}$$

There is, of course, one relation between eqs. (12) and (13):

$$[T][Q] = [Q][T] = 1 \tag{14}$$

The expression $[V]|\mathbb{E} - [S]|^{-1}[X]$ in eq. (10) is:

$$\begin{aligned} [V]\,|\mathbb{E} - S|^{-1}[X] &= [V][Q].[X] \\ &= |a_+T^+Q_{11} + a_0T^\circ Q_{21} + a_-T^-Q_{31}, \quad a_+T^+Q_{12} + a_0T^\circ Q_{22} \\ &\qquad + a_-T^-Q_{32}, \quad a_+T^+Q_{13} + a_0T^\circ Q_{23} + a_-T^-Q_{33}| \begin{pmatrix} E \\ E \\ E \end{pmatrix} \\ &= a_+T^+(Q_{11} + Q_{12} + Q_{13}) + a_0T^\circ(Q_{21} + Q_{22} + Q_{23}) \\ &\qquad + a_-T^-(Q_{31} + Q_{32} + Q_{33}) \\ &= a_+T^+[A] + a_0T^\circ[B] + a_-T^-[C] \end{aligned} \tag{15}$$

where $[A]$, $[B]$, and $[C]$ are the matrices shown below:

$$\begin{aligned} [A] &= |Q_{11} + Q_{12} + Q_{13}| \\ [B] &= |Q_{21} + Q_{22} + Q_{23}| \\ [C] &= |Q_{31} + Q_{32} + Q_{33}| \end{aligned}$$

As is evident from eq. (10), it is enough to know only the 3,3 component of eq. (15), namely:

$$\begin{aligned} ([V]|\mathbb{E} - [S][^{-1}]X])_{33} &= a_+(T^+[A])_{33} \\ &= +a_0(T^\circ[B])_{33} + a_-(T^-[C])_{33} \end{aligned} \tag{16}$$

and so we will proceed to calculate the values of matrices shown in eq. (14):

$$\left.\begin{aligned} T_{11}Q_{11} + T_{12}Q_{21} + T_{13}Q_{31} &= E \\ T_{11}Q_{12} + T_{12}Q_{22} + T_{13}Q_{32} &= 0 \\ T_{11}Q_{13} + T_{12}Q_{23} + T_{13}Q_{33} &= 0 \end{aligned}\right\}, \quad T_{11}[A] + T_{12}[B] + T_{13}[C] = E \tag{17a}$$

$$\left.\begin{aligned} T_{21}Q_{11} + T_{22}Q_{21} + T_{23}Q_{31} &= 0 \\ T_{21}Q_{12} + T_{22}Q_{22} + \quad \ldots &= E \\ T_{21}Q_{13} + \quad \ldots \qquad\quad &= 0 \end{aligned}\right\}, \quad T_{21}[A] + T_{22}[B] + T_{23}[C] = E \tag{17b}$$

$$\left.\begin{aligned} T_{31}Q_{11} + \ldots &= 0 \\ T_{31}Q_{12} + \ldots &= 0 \\ T_{31}Q_{11} + \ldots &= E \end{aligned}\right\}, \quad T_{31}[A] + T_{32}[B] + T_{33}[C] = E \tag{17c}$$

From eqs. (17), a linear matrix equation of third order, the unknown values of matrices $[A]$, $[B]$, and $[C]$ can be determined. For example, to find the value of matrix $[A]$, eq. (17c) is subtracted from eq. (17a):

$$|T_{11} - T_{31}|[A] + |T_{13} - T_{33}|[C] = 0 \qquad \therefore T_{12} = T_{32}$$

and so:

$$|T_{13} - T_{33}|^{-1}|T_{11} - T_{31}|[A] + [C] = 0 \tag{17d}$$

T_{22} (eq. (17a)) minus T_{12} (eq. (17b)):

$$|T_{22}T_{11} - T_{12}T_{21}|[A] + [T_{22}T_{13} - T_{12}T_{23}][C] = |T_{22} - T_{12}|$$

$$|T_{22}T_{13} - T_{12}T_{23}|^{-1}|T_{22}T_{11} - T_{12}T_{21}|[A] + [C] = |T_{12}T_{13} - T_{12}T_{23}|^{-1}|T_{22}T_{12}| \tag{17e}$$

Equation (17e) minus eq. (17d):

$$[L][A] = [|T_{22}T_{13} - T_{12}T_{23}|^{-1}|T_{22}T_{11} - T_{12}T_{21}| - |T_{13} - T_{33}|^{-1}|T_{11} - T_{31}|][A] = |T_{22}T_{13} - T_{12}T_{23}|^{-1}|T_{22} - T_{12}|$$

and so:

$$[A] = [L]^{-1}|T_{22}T_{13} - T_{12}T_{23}|^{-1}|T_{22} - T_{12}|$$

The results for the three matrix products are:

$$(T^{+}[A])_{33} = \{(c_1 - c_3)[2 - (c_1 + c_2 + c_3)]\}/[(1 - c_2)(1 - c_1 + c_3)]$$

$$(T^{\circ}[B])_{33} = \{(c_1 - c_3)[2 - (c_1 + c_2 + c_3)]\}/[(1 - c_2)(1 - c_1 + c_3)] + 1/[(1 - c_2)(c_1 + c_2 + c_3)]$$

$$(T^{-}[C])_{33} = \{(c_1 - c_3)[2 - (c_1 + c_2 + c_3)]\}/[(1 - c_2)(1 - c_1 + c_3)]$$

Equation (16) becomes:

$$([V][S][X])_{33} = a_{+}(T^{+}[A])_{33} + a_0(T^{\circ}[B])_{33} + a_{-}(T^{-}[C])_{33}$$

$$= (a_{+} + a_0 + a_{-})\{(c_1 - c_3)[2 - (c_1 + c_2 + c_3)]/[(1 - c_2) \times (1 - c_1 + c_3)]\} + a_0/[(1 - c_2)(c_1 + c_2 + c_3)]$$

Since $(a_{+} + a_0 + a_{-}) = 1$, the mean square displacement distance for three-choice model is:

$$\overline{L_0^2} = Nb^2\left(1 + 2\frac{(c_1 - c_3)[2 - (c_1 + c_2 + c_3)]}{(1 - c_2)(1 - c_1 + c_3)} + 2\frac{a_0}{(1 - c_2)(c_1 + c_2 + c_3)}\right) \tag{18}$$

II. Discussion of Results

To display the results in a more meaningful form, we conclude with a brief examination of the application of eq. (18) to some special cases.

A. When c_2 and a_0 are zero, this problem reduces to that of two choices. The transition matrix is then:

$$[C] = \begin{vmatrix} c_1 & c_3 \\ c_3 & c_1 \end{vmatrix} = \begin{vmatrix} \frac{1}{1+w} & \frac{w}{1+w} \\ \frac{w}{1+w} & \frac{1}{1+w} \end{vmatrix}$$

$$c_1 - c_3 = (1 - w)/(1 + w), \quad c_1 + c_3 = 1, \quad 1 - c_1 + c_3 = 2w/(1 + w)$$

Thus the average value, $\overline{L_0^2}$, becomes:

$$\overline{L_0^2} = Nb^2\left(1 + \frac{2(c_1 - c_3)}{1 - c_1 + c_3}\right) = Nb^2\left(\frac{1 + c_1 - c_3}{1 - c_1 - c_3}\right) = Nb^2\left(\frac{c_1}{1 - c_1}\right)$$

$$= Nb^2\left(1 + 2\,\frac{[(1 - w)/(1 + w)]}{[2w/(1 + w)]}\right) = Nb^2\left(1 + \frac{1 - w}{w}\right) = Nb^2\left(\frac{1}{w}\right)$$

B. When c_1 is zero and c_3 is 1, so that (+, +) or (−, −) sequences are forbidden and only the (+, −) and (−, +) sequences occur, the second

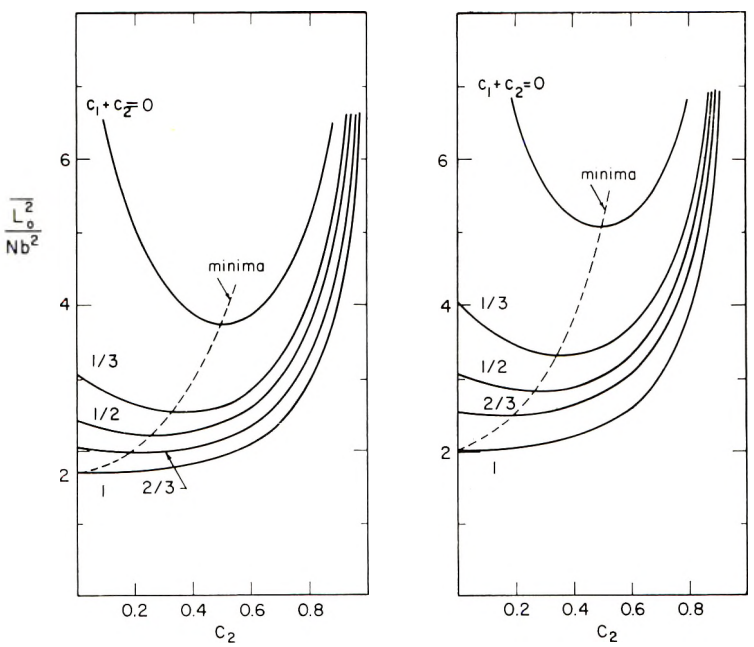

Fig. 2. ($\overline{L_0^2}/Nb^2$) ratios calculated for various values of the probability parameters.

term of eq. (18) is equal to −1 for any value of c_2. Hence the first and second terms cancel and only the third term remains. The a priori probability a_0, and transition probability c_2, then determine the value of $\overline{L_0^2}$.

C. If c_1 approaches 1, indicating that the number of (+, +) and (−, −) sequences increase compared with (+, −) and (−, +), the value of $\overline{L_0^2}$ approaches infinity unless $c_2 = 1$.

D. When c_1 and c_3 are equal, the probabilities of (+, +) or (−, −) and of (+, −) or (−, +) sequences are equal. The second term of eq. (18) then becomes zero and only the last term remains:

$$\overline{L_0^2} = Nb^2\{1 + [2a_0/[(1 - c_2)(c_1 + c_2 + c_3)]\}$$

This means that when the numbers of (+, +), (−, −), and (+, −) and (−, +) sequences are equal, these contributions to the end-to-end distance cancel, and only the (+, 0), (−, 0), and (0, 0) sequences are effective.

(*1*) Let c_1, c_2, c_3, and a_0 each equal $^1/_3$:

$$\overline{L_0^2} = Nb^2\{1 + [^2/_3/(^2/_3 \times 1)]\} = 2Nb^2$$

Hence, if the a priori probability a_0 and the transition probabilities all have the equilibrium distribution value $^1/_3$, the value of $\overline{L_0^2}$ is equal to that obtained on treating each pair as a unit of rotation.

(*2*) By taking the value of the a priori probability a_0 and the transition probability $(c_1 + c_3)$ as parameters, the values of $\overline{L_0^2}$ shown in Figure 2 were calculated. Here the value of c_2 is taken as a variable. Owing to the existence of the *trans* form, the average value of $\overline{L_0^2}$ is always larger than Nb^2.

This work was supported by a grant from the Carothers Laboratory, E. I. du Pont de Nemours & Company, Wilmington, Delaware.

References

1. Benoit, H., *J. chim. phys.*, **44**, 18 (1947).
2. Kuhn, H., *J. Chem. Phys.*, **15**, 843 (1947).
3. Taylor, W. J., *J. Chem. Phys.*, **16**, 257 (1948).
4. Vol'kenshtein, M. V., *Doklady Acad. Nauk. SSSR*, **78**, 879 (1951); *idem.*, *J. Phys. Chem. (U.S.S.R.)*, **26**, 1072 (1952).
5. Ptitsyn, O. B., and Yu. A. Sharonov, *Soviet Phys.-Tech. Phys.*, **2**, 2544, 2561 (1958).
6. Vol'kenshtein, M. V., *Configurational Statistics of Polymer Chains*, Academy of Sciences, U.S.S.R., Moscow, 1959.
7. Lifson, S., *J. Chem. Phys.*, **30**, 964 (1959).
8. Nagai, K., *J. Chem. Phys.*, **31**, 1169 (1959).
9. Hoeve, C. A. J., *J. Chem. Phys.*, **32**, 888 (1960).
10. Hoeve, C. A. J., *J. Chem. Phys.*, **35**, 1266 (1961).
11. De Santis, P., E. Giglio, A. M. Liquori, and A. Ripamonti, paper presented at the IUPAC Symposium on Macromolecular Chemistry, Montreal, July 27–Aug. 1, 1961.
12. Natta, G., P. Corradini, and P. Ganis, *J. Polymer Sci.*, **58**, 1191 (1962).
13. Krigbaum, W. R., and M. Kaneko, *J. Chem. Phys.*, **36**, 99 (1962).
14. Lifson, S., *J. Chem. Phys.*, **29**, 80 (1958).

Synopsis

The matrix procedure of Hoeve for the chain displacement length calculation is applied to a three-choice cubic lattice model. Although rotation about each link is correlated, the model is simple enough for the final result to be obtained as a closed algebraic expression. Certain special cases, resulting from particular assignments of the probability parameters, are examined.

Résumé

On a appliqué le procédé matriciel de Hoeve au calcul du déplacement longitudinal des chaînes pour un modèle de réseau cubique. Quoiqu'il y ait corrélation de rotation autour de chaque lien, le modèle est suffisamment simple pour que le résultat final puisse être obtenu sous forme d'une expression algébrique définie. On a examiné certains cas spéciaux, résultant de l'assignation particulière des paramètres de probabilité.

Zusammenfassung

Das Matrixverfahren von Hoeve zur Berechnung der Länge der Kettenverrückung wird auf ein kubisches Gittermodell mit dreifacher Wahlmöglichkeit angewendet. Obwohl die Rotation um jede Bindung in Korrelation gebracht wird, ist das Modell genügend einfach, sodass das Endresultat als ein geschlossener algebraischer Ausdruck erhalten werden kann. Gewisse Spezialfälle, die sich aus bestimmten Zuordnungen der Wahrscheinlichkeitsparameter ergeben, werden untersucht.

Received February 6, 1962.

JOURNAL OF POLYMER SCIENCE: PART A VOL. 1, PP. 1079–1086 (1963)

Photolytic Degradation of Poly(methyl Methacrylate)*

ROBERT B. FOX, LAWRENCE G. ISAACS, and SUZANNE STOKES,
Naval Research Laboratory, Washington, D. C.

INTRODUCTION

The photodegradation of vinyl polymers in the solid state has been studied quantitatively for only a few materials at temperatures where thermal degradation is not a significant process. Degradation in the absence of oxygen has received even less attention. Near 25°C., the photolysis of vinyl polymers in vacuum typically results in random scission of the polymer backbone by a radical process of short kinetic chain length. The low molecular weight products, which usually include small amounts of monomer, vary with the nature of the polymer. Quantum yields for chain scission in vacuum at about 25°C. have been reported for poly-α-methyl styrene)[1] and poly(methyl vinyl ketone),[2] and at higher temperatures for poly(methyl isopropenyl ketone)[2] and poly(methyl methacrylate) (PMMA).[3] Low quantum yields for chain scission in solution have been found for poly(methyl vinyl ketone),[4] polyacrylonitrile,[5,6] and poly(methacrylic acid).[7]

Poly(methyl methacrylate) is of particular interest, since at least at temperatures where thermal degradation is important, i.e., above 150°C., photolysis occurs by endgroup initiation and is accompanied by extensive depolymerization.[3] This polymer has also been photodegraded in air at room temperature by radiation from a low-pressure mercury lamp and the quantum yield for random chain scission determined.[8]

This report extends our earlier work[1] to films of PMMA photodegraded at room temperatures in both vacuum and air by the radiation from a medium-pressure mercury lamp. A study of the products of the photolysis allows some speculation in regard to the mechanism of the photodegradation of polymers containing ester chromophores.

EXPERIMENTAL

Materials

Methyl methacrylate, washed with dilute sodium hydroxide solution and water, was dried over Drierite and distilled under nitrogen. Heart

*Presented in part at the 140th meeting of the American Chemical Society, Chicago, Illinois, September 1961. This work was partially supported by the Aeronautical Systems Division, U. S. A. F.

cuts were degassed and bulk-polymerized at 60°C. to about 30% conversions in the presence of azobisisobutyronitrile (0.1 g. and 0.006 g./100 ml. of monomer) to yield two batches of PMMA having, after purification, $[\eta_0]$ = 1.58 and 4.54 dl./g., respectively. The polymers were isolated by precipitation with methanol and further purified by two reprecipitations with methanol from tetrahydrofuran solution, followed by drying in a vacuum oven at 70°C. for 60 hr. Tetrahydrofuran was refluxed with lithium aluminum hydride and distilled under nitrogen. Redistilled c.p. benzene was used in the viscosity measurements; c.p. methanol and spectroscopic grade methylene chloride were used as received.

Viscosity Measurements

Intrinsic viscosities were measured in benzene at 30°C. with Ubbelohde-type dilution viscometers having running times of about 170 sec. for benzene. From plots of η_{sp}/c against c for both blank films and highly degraded samples of PMMA, it was determined that the constant in the Huggins equation was unchanged for PMMA degraded to the extent reported here. Single-point determinations of intrinsic viscosity were therefore made on most degraded polymer samples. Viscosity-average molecular weights were calculated from the relation of Casassa[8] based on light-scattering measurements:

$$\log \bar{M}_v = (4.102 + \log [\eta])/0.73 \quad (1)$$

Apparatus

The irradiation cells have been described elsewhere.[1] A General Electric UA-3 medium-pressure mercury lamp was used as a radiation source. Mass spectrometric work was carried out with a Consolidated Electrodynamics Model 21–620 mass spectrometer. Ultraviolet spectra were obtained with a Perkin-Elmer Spectracord Model 4000 recording spectrometer.

Actinometry

Total output of the lamp from 2200 to 4400 A. was measured by uranyl oxalate actinometry,[9] and check runs were made for each series of exposures. On the basis of the spectral distribution of a typical UA-3 lamp[10] and the spectrum of a blank PMMA film (see Fig. 1) it was calculated that 3.5% of the incident radiation detected by the actinometer was absorbed by the film. In view of possible errors in the spectral distribution of the lamp, a high order of absolute accuracy is not claimed for the quantum yields reported here.

Procedure

Films were prepared in rectangular quartz or Pyrex dishes of known area from methylene chloride solutions of weighed amounts of PMMA. After evaporation of the solutions over a period of at least 24 hr., the films

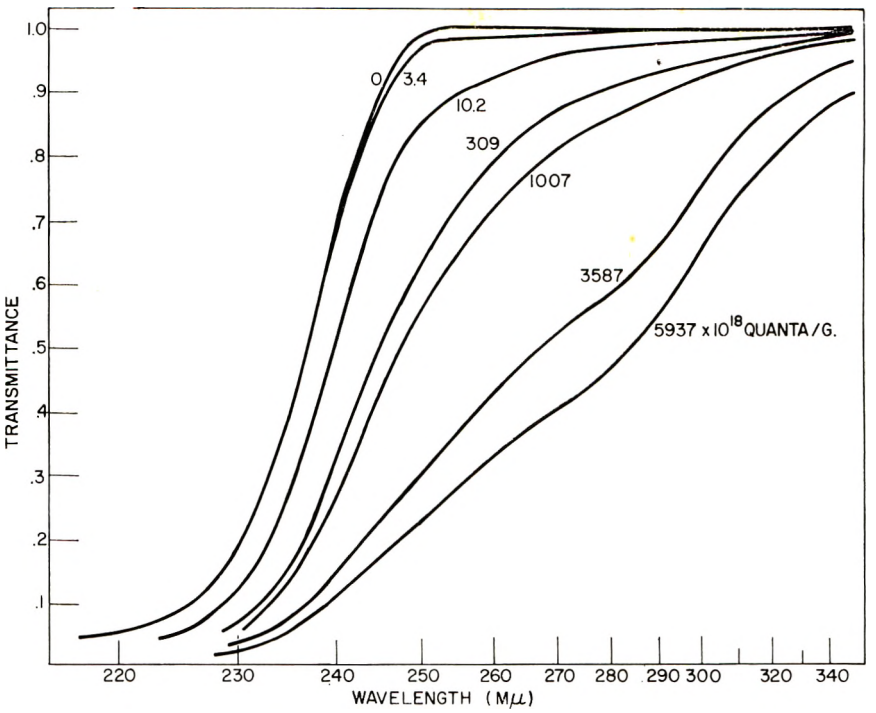

Fig. 1. Changes in the ultraviolet spectrum of PMMA during irradiation.

were maintained in a continuously pumped vacuum oven at about 2 mm. pressure for 16 hr. at 70°C., and for vacuum runs, on the vacuum line for an additional 2 hr. at room temperature before sealing off the cell for irradiation. Liquid nitrogen was used to condense volatiles formed during vacuum runs. Exposures in air were made in the same cell as the exposures in vacuum, but with the top of the cell removed. All exposures were made at ambient temperatures, 25 ± 3°C. After exposure, the films were dissolved in benzene and viscosities run as soon as possible; post-effects[11] were not studied.

The number of scissions per polymer molecule at a constant exposure was inversely and linearly related to film thickness up to thicknesses of 30 μ. In most of this work, film thicknesses were within 10% of 15 μ.

RESULTS AND DISCUSSION

Molecular Weight Changes

Ultraviolet irradiation of thin films of PMMA results in a rapid decrease in the viscosity-average molecular weight of the polymer and in the formation of very small amounts of volatile products. This behavior is characteristic of a polymer undergoing random scission without extensive depolymerization. Under such conditions it can be assumed that the number of scissions occurring in a polymer chain is proportional to the

number of quanta absorbed by that chain; the proportionality constant is the quantum yield for chain scission, Φ_s.

For a linear polymer having a number-average molecular weight $\bar{M}_{n_0}$ initially and $\bar{M}_n$ after a random cleavage process, the average number of scissions taking place in a polymer chain is given by $(\bar{M}_{n_0}/\bar{M}_n) - 1$. If $\bar{M}_v = \bar{M}_w$ and a "most probable" molecular weight distribution is assumed before and after degradation, the corresponding intrinsic viscosities can be used to give the number of scissions as $([\eta_0]/[\eta])^{1/\alpha} - 1$, where α is the exponent in the Mark-Houwink intrinsic viscosity-molecular weight relationship. The number of quanta absorbed per molecule of polymer is $It\bar{M}_{n_0}/A$, where I is the rate of absorption of radiation per gram of polymer, t is exposure time, and A is Avogadro's number. Therefore

$$\Phi_s = (A/\bar{M}_{n_0})\{([\eta_0]/[\eta])^{1/\alpha} - 1\}/It \qquad (2)$$

from which Φ_s can be evaluated for a single exposure or from the slope of a plot of the number of scissions per molecule against the number of quanta absorbed per gram of polymer.

These plots were linear up to absorptions in excess of 2×10^{19} quanta/g. In Table I are summarized the quantum yields for chain scission calculated from eq. (2), along with the standard deviations for each series of experiments under various conditions. Rates of irradiation in the second column are given in terms of quanta absorbed per unit area, since the films, although of constant thickness, varied slightly in both area and sample weight.

While the quantum yields for chain scission under the various conditions used here are close, certain differences are significant. The rate of degradation in air is lower than in vacuum, but a small amount of air is without effect, as shown by a comparison of the series run in the vacuums produced by an ordinary oil pump and by a mercury diffusion pump. It is unlikely that the air exposures are giving rise to crosslinking[12] which could result in misinterpretable viscometry. This conclusion is based on a comparison of the distribution of sedimentation constants determined by ultracentrifugation of PMMA samples before and after absorbing radia-

TABLE I
Quantum Yields for Chain Scission in PMMA Photolysis

Number of exposures	Rate of irradiation $\times 10^{-14}$, quanta/min./cm.^{2}	$[\eta_0]$, dl./g.	Pressure, μ	Quantum yield $\times 10^2$, scissions/quantum absorbed
6	5.29	1.58	2	4.0 ± 1.3
4	5.29	1.58	0.02	3.8 ± 0.8
4	4.93	1.58	0.02	3.9 ± 0.4
5	4.93	4.54	0.02	2.2 ± 0.6
4	6.26	1.58	1 atm. air	1.3 ± 0.4
3	6.26	4.54	1 atm. air	1.7 ± 0.1
6	7.40	1.58	1 atm. air	1.8 ± 0.6

tion in excess of 10^{20} quanta/g. in air; the sedimentation constants were unchanged.[13] Moreover, crosslinking has not been detected during degradation of PMMA in air by ionizing radiation.[14] Quantum yields for the scission of PMMA samples differing in molecular weight indicate that there is a slight dependence on molecular weight in vacuum exposures and that random scission processes, while predominating, may not be the only ones operating.

The quantum yield of 2.3×10^{-3} reported by Shultz[8] for the photodegradation of PMMA in air by 2537 A. radiation is somewhat lower than those given in Table I. Medium pressure mercury lamps such as the UA-3 radiate energy at wavelengths below 2537 A., and it is this radiation that will be absorbed to the greatest extent by PMMA. Since the photolytically active radiation under our conditions is of higher energy than that at 2537 A., it is likely that the rate of bond breaking would also be higher. Irradiation of PMMA through 2 mm. of Pyrex for a period far in excess of that required to produce extensive viscosity decreases with unfiltered radiation resulted in no detectable change in the sample.

Insight into the termination step in the photolysis of PMMA in vacuum is given by the effect of intensity, shown in Table II, on the scission of the polymer. Over a tenfold range of intensity, the extent of degradation is dependent only upon the total energy absorbed. In the photolysis of gases, this is generally interpreted to mean that the termination step is first order in respect to the radicals involved. In an amorphous solid, small reactive radicals might interact fairly rapidly, but the somewhat immobile polymer radicals resulting from homolysis of a chain are unlikely to recombine readily. Some sort of a disproportionation reaction is probably involved in the termination of PMMA radicals.

TABLE II
Effect of Intensity on the Photodegradation of PMMA in Vacuum

Rate of energy absorption, quanta/g./min.	Absorbed energy, quanta/g.	Scissions/polymer molecule
2.7×10^{17}	7.70×10^{18}	0.192
28.2×10^{17}	7.70×10^{18}	0.197

Spectral Changes

Figure 1 shows the progressive increase in absorption during the irradiation of PMMA in air. An almost identical series of changes is encountered in vacuum exposures. These exposures are mostly far in excess of those used to determine the quantum yields for chain scission. The band at 285 mμ observed by Shultz[8] is also seen in these spectra and is in the region usually associated with carbonyl chromophores. This absorption is in some way connected with the polymer chain itself rather than with a low molecular weight photolysis product, since quantitative reprecipitation of a degraded PMMA sample resulted in no change in the absorption spectrum.

Volatile Products

In addition to the usual photolysis products CH_4, H_2, CO, and CO_2, the major products from the photodegradation of PMMA in vacuum are methyl formate, methanol, and methyl methacrylate. A film of PMMA was heated 4 hr. at 110°C. and the volatiles collected; in addition to a small amount of residual solvent (methylene chloride), only methyl methacrylate was found. After irradiation (4.1×10^{18} quanta absorbed/g. polymer) at room temperature, the sample was again heated 4 hr. at 110°C. and the volatiles analyzed; quantum yields for methyl methacrylate, methyl formate, and methanol were 0.20, 0.14, and 0.48, respectively. The amount of monomer was approximately twice that found after the first heating, and only a trace of solvent was detected.

Methanol is undoubtedly a major photolysis product, since it was not found during the preliminary heating. Very likely, the methanol originates from photolysis of ester side groups of the polymer itself rather than from photolysis of methyl formate, since the absorption spectra of formate and polymer are similar and the concentration of formate in the film at any time must be small. Three major sources of monomer are possible: depolymerization, residual monomer, and monomer due to thermal degradation. The effect of irradiation on diffusion is unknown, but if all the monomer collected during irradiation is due to depolymerization after photolysis of the main chain, a maximum zip length of about five monomer units per scission is indicated. At 160°C., Cowley and Melville[3] found a kinetic chain length of at least 220 monomer molecules per quantum absorbed.

The formation of methyl formate with a quantum yield of about three times that for scission may mean that this product is associated with the act of chain-breaking. Although the prototype molecule of PMMA, methyl pivalate, has not been studied, photolysis of other esters[15,16] indicates two probable primary acts:

$$RCOOCH_3 \xrightarrow{h\nu} R\dot{C}{=}O + CH_3O\cdot$$

$$RCOOCH_3 \xrightarrow{h\nu} R\cdot + \cdot COOCH_3$$

which could account for the products found during photolysis of PMMA. It is noteworthy that the first of these reactions gives radicals which, if terminated with hydrogen atoms, lead to methanol and an aldehyde; the latter may account for the formation of the new absorption band at 285 mμ in the ultraviolet spectrum.

Mechanism

Only a plausible rationalization of the observed facts is possible at the present time. In vacuum, at least, it appears that at least two and possibly three primary photolytic processes are occurring simultaneously during the photodegradation of PMMA. Following absorption of energy

through the ester chromophore, a major reaction must be random homolysis of main-chain carbon-carbon bonds:

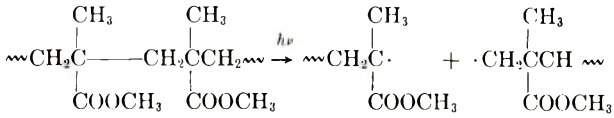

followed by stabilization of II and III by a reaction such as disproportionation to give $\cdot COOCH_3$ radicals and olefinically terminated polymer fragments. At the same time, photolysis of the ester side-groups could occur in either or both of two ways:

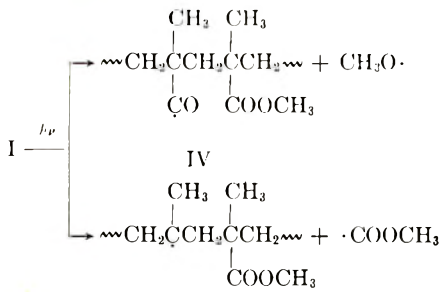

The radical IV in combination with a hydrogen atom leads to an aldehyde group on the polymer chain. It is possible that this group is a necessary precursor to a chain break.

Evidently, the mechanisms of photolytic and thermal degradation of PMMA have little in common. At least with PMMA, there appears to be a better analogy between radiolysis[11,14] and photolysis, since many of the products are similar and random scission is the predominating reaction. Little can be said regarding the role of oxygen in these processes other than that some inhibitory influence is exerted.

The authors wish to thank L. W. Daasch for carrying out the mass spectroscopic measurements and J. R. Lee, Jr. for aid in some of the experimental work.

References

1. Stokes, S., and R. B. Fox, *J. Polymer Sci.*, **56**, 507 (1962).
2. Wissbrun, K. F., *J. Am. Chem. Soc.*, **81**, 58 (1959).
3. Cowley, P. R. E. J., and H. W. Melville, *Proc. Roy. Soc. (London)*, **A210**, 461 (1952).
4. Guillet, J. E., and R. G. W. Norrish, *Proc. Roy. Soc. (London)*, **A233**, 153 (1955).
5. Jellinek, H. H. G., and I. J. Bastien, *Can. J. Chem.*, **39**, 2056 (1961).
6. Jellinek, H. H. G., and W. A. Schlueter, *J. Appl. Polymer Sci.*, **3**, 206 (1960).
7. Baxendale, J. H., and J. K. Thomas, *Trans. Faraday Soc.*, **54**, 1515 (1958).
8. Shultz, A. R., *J. Phys. Chem.*, **65**, 967 (1961).
9. Forbes, G. S., and L. J. Heidt, *J. Am. Chem. Soc.*, **56**, 2363 (1934).
10. General Electric Co., Tech. Publication LS-104 (1959).
11. Wall, L. A., and D. W. Brown, *J. Phys. Chem.*, **61**, 129 (1957).
12. Oster, G., G. K. Oster, and J. Moroson, *J. Polymer Sci.*, **34**, 671 (1959); J. C. Bevington, *J. Polymer Sci.*, **34**, 680 (1959).
13. Ford, T. F., and O. Nichols, private communication.

14. Shultz, A. R., *J. Polymer Sci.*, **35**, 369 (1959).
15. Ausloos, P., *Can. J. Chem.*, **36**, 383 (1958).
16. Wijnen, M. H. J., *J. Am. Chem. Soc.*, **82**, 3034 (1960); *Can. J. Chem.*, **36**, 691 (1958); *J. Chem. Phys.*, **27**, 710 (1957).

Synopsis

Thin films of poly(methyl methacrylate) (PMMA) at about 25°C. irradiated with a medium-pressure mercury lamp undergo random scission with a quantum yield of 0.039 and 0.017 scissions/quantum absorbed in vacuum and in air, respectively. Crosslinking in air was not observed. Quantum yields for scission were independent of intensity. Volatile products included methyl formate, methyl methacrylate, and methanol in quantum yields of 0.14, 0.20, and 0.48 molecules per quantum absorbed, respectively. During irradiation in either vacuum or air, the ultraviolet absorption of PMMA increases with a band at 285 mμ, attributed to carbonyl groups in the polymer itself. A mechanism for the photodegradation of PMMA is suggested.

Résumé

De minces films de polyméthacrylate de méthyle (PMMA) subissent une dépolymérisation statistique par irradiation à 25°C environ, à l'aide d'une lampe à mercure à moyenne pression; on trouve, respectivement sous vide et à l'air, un rendement quantique de 0.039 et 0.017 ruptures par quantum absorbé. On n'observe pas de pontage à l'air. Les rendements en ruptures par quantum sont indépendants de l'intensité. Les produits volatils comportent du formiate de méthyle, du méthacrylate de méthyle et du méthanol, avec un rendement quantique de 0.14–0.20 et 0.48 molécules par quantum absorbé respectivement. Pendant l'irradiation tant sous vide qu'à l'air, l'absorption d'U.V. du PMMA augmente dans la bande de 285 mμ. Elle est attribuée aux groupes carbonyles dans le polymère-même. On propose un mécanisme pour la photodégradation du PMMA.

Zusammenfassung

Dünne Filme von Polymethylmethacrylat (PMMA) erleiden bei der Bestrahlung mit einer Mitteldruckquecksilberlampe bei 25°C eine statistische Spaltung mit einer Quantenausbeute von 0,039 und 0,017 Spaltungen pro absorbiertes Quant im Vakuum bzw. unter Luft. Unter Luft wurde keine Vernetzung beobachtet. Die Spaltungsquantenausbeute war von der Intensität unabhängig. Als flüchtige Produkte traten Methylformiat, Methylmethacrylat und Methanol mit Quantenausbeuten von 0,14, 0,28 bzw. 0,48 Molekülen pro absorbiertes Quant auf. Während der Bestrahlung im Vakuum oder in Luft nimmt die Ultraviolett-absorption von PMMA in einer Bande bei 285 mμ zu, die Carbonylgruppen im Polymeren selbst zugeschrieben wird. Ein Mechanismus für den photochemischen Abbau von PMMA wird vorgeschlagen.

Received December 20, 1961

BOOK REVIEW

N. G. GAYLORD, Editor

Advances in Spectroscopy. Vol. II. H. W. THOMPSON, ed. Interscience, New York, 1961. 483 pp. $13.00.

Volume II of *Advances in Spectroscopy* is described on the jacket as "the second in a series of annual volumes." The quantity has not matched the publishers' optimism, but the quality has been maintained at a very satisfactory level. It has been characteristic of the articles in this series that they not only review the literature, but also review the subject. This is made possible by the high qualifications of the individual contributors, many of whom have been among those primarily responsible for the development of the areas about which they write.

A measure against which the review articles can be judged is the extent to which they enable someone knowledgeable in the broad field, but who has largely overlooked or ignored the specific area, to bring himself up to date quickly. This is well achieved, for example, in the reviews of atomic absorption spectroscopy, spectra of flames, x-ray spectroscopy, nuclear magnetic resonance, and refraction of gases in the infrared. In the first of these, A. Walsh discusses the theory of line widths and populations that suggests the employment of atomic absorption. He follows this with a consideration of experimental techniques and a critical evaluation of the method. A table gives a review of the literature of analytical applications. A. G. Gaydon emphasizes the structure of flames and variations of composition and of chemical reactions from one zone of the flame to another and the dependence on exact conditions. Several radicals found in flames are discussed, including their production and consumption. Of particular interest is the C_2 radical, which seems to be produced through a polymerization mechanism that has eluded discovery.

The review of x-ray spectroscopy by H. Friedman is very largely a discussion of the experimental techniques of x-ray fluorescence, evaluated with respect to the effects of the many parameters on the analytical sensitivity and accuracy. R. E. Richards discusses primarily the dynamics of nuclear magnetic resonance, placing emphasis on relaxation times and line widths. A thorough, clear development of the theory provides a sound basis for the discussion. The review by J. H. Jaffe of measurements of refractive indices for gases in the vicinity of infrared absorption bands, describes the history and progress of the field up to, but not including, his discovery of shifts of certain HCl lines that has caused a new flurry of activity in the theory of pressure broadening.

K. P. Norris has written on the infrared spectra of microorganisms. This chapter fits the pattern described above except that, due to the highly exploratory and empirical nature of the field, there is a lack of underlying unity. The strong contrast with other areas of infrared spectroscopy in interpretation of small differences in otherwise identical spectra makes the discussion valuable even to those not directly concerned with spectra of biological samples. The review of ultraviolet absorption spectra of proteins and related compounds by G. H. Beaven is a collection of very brief abstracts of the voluminous literature. Although this may prove very helpful as a first step toward searching the literature, more selection of important and convincing experimental demonstrations from the abundance of random results and speculative interpretations would be more valuable.

The other two chapters, by H. C. Longuet-Higgins and by W. Vedder and D. F. Hornig, are somewhat different in character. That entitled "Some Recent Developments in the Theory of Molecular Energy Levels," deals with vibronic energy levels when the Born-Oppenheimer approximation is inadequate, and specifically with the Jahn-Teller and Renner effects. The discussion assumes only that the reader has a good working knowledge of quantum mechanics; it is sufficiently complete that those who are concerned with such problems should be able to work their way through the details of the argument. The chapter by Vedder and Hornig, on the infrared spectra of crystals, treats the interactions of molecular vibrations with vibrations of adjacent molecules and with the field produced by the aggregate of other molecules constituting the crystal lattice. This subject has relevance in many fields, but the review assumes that the reader is familiar with group theory, normal coordinate calculations, and several aspects of crystallography. An appended classified, annotated bibliography and the many footnote references in the discussion should be very helpful.

R. P. Bauman

Polytechnic Institute of Brooklyn
Brooklyn, New York

ERRATUM

Molecular Orbital Calculation of Monomer Reactivity Ratios

(*J. Polymer Sci.*, **60**, 43–54, 1962).

By G. S. LEVINSON

Shell Development Company, Emeryville, California

On page 46, line 9, the equation should read

$$\Delta H^* = \bar{E}_R + \bar{E}_C + \delta E_R + \delta E_C = \bar{E}_R + \bar{E}_C + (a_1 + b_1)(\bar{E}_C - E_C^\circ)$$

On page 48, Table I, the values of β should read $\sqrt{0.05}$ for C (saturated) and $\sqrt{2}$ for O (unsaturated). For the nitrile group, the nitrogen parameters employed were $\alpha = 1$ and $\beta = \sqrt{2}$.